Master's thesis

NTNU
Norwegian University of Science and Technology
Faculty of Engineering
Department of Energy and Process Engineering

Øyvind Sekkesæter

Evaluation of Concepts and Systems for Marine Transportation of Hydrogen

Master's thesis in Mechanical Engineering
Supervisor: Jostein Pettersen, Øyvind Endresen (co-supervisor), Gerd Petra Haugom (co-supervisor)
June 2019

NTNU
Norwegian University of Science and Technology

Øyvind Sekkesæter

Evaluation of Concepts and Systems for Marine Transportation of Hydrogen

Master's thesis in Mechanical Engineering
Supervisor: Jostein Pettersen, Øyvind Endresen (co-supervisor), Gerd Petra Haugom (co-supervisor)
June 2019

Norwegian University of Science and Technology
Faculty of Engineering
Department of Energy and Process Engineering

NTNU
Norwegian University of
Science and Technology

Preface

This MSc thesis was written at the department of energy and process engineering (EPT) at the Norwegian University of Science and Technology (NTNU) from January to June 2019. The thesis was supervised by Professor II Jostein Pettersen (NTNU and Equinor), Øyvind Endresen (DNV GL) and Gerd Petra Haugom (DNV GL).

The search for alternative energy carriers is a highly relevant subject in a world where environmental issues are in the limelight. The shipping industry, among other sectors, is increasingly facing a regulatory pressure to adopt more environmental-friendly practices. This thesis has given me the chance to expand my knowledge in a wide field, encompassing elements from marine engineering, systems engineering, process engineering, and economics. It is my hope that this master thesis, among many other scientific works, will serve to aid planning of future energy-policy.

Jostein Pettersen has provided invaluable feedback and information throughout the entire time working on the project. I want to thank him for the enthusiasm he has shown for the thesis.
Gerd Petra Haugom and Øyvind Endresen has, already from the beginning of the project, made important contributions. I want to thank them for their time and insights.
Finally, I want to thank Alvar Mjelde (DNV GL) for preparing AIS-data used for modelling vessel energy-consumption during voyage.

Trondheim, 2019-06-10

Øyvind Sekkesæter

Problem Description

Reference is made to the specialization project report (Sekkesæter, 2018): "Hydrogen value chains and marine transport concepts", presenting high-level analyses of large-volume hydrogen transport schemes from Norway to Japan, where the hydrogen is transported in three alternative ways: (i) in liquefied form (LH_2), (ii) as liquefied ammonia (NH_3), or (iii) chemically bonded to an organic carrier liquid (LOHC). The analyses provide useful insight into large volume conversion and transport chains for hydrogen, but more detailed analyses with better modelling of energy conversion stages is needed. This includes conversion and processing into transportable products, marine transportation and propulsion systems, and energy conversion systems at the receiving terminal. Several assumptions and basis data need to be further developed and refined, including sensitivity analyses for relevant parameters. This also includes the basis for economic analyses and sensitivities for varying assumptions here.

The objective of the Master thesis is therefore to analyze concepts and systems for processing and marine transportation of hydrogen as an energy vector, comparing the various schemes and system designs for large-volume hydrogen shipment.

The work need to include an updated literature survey, establishment of updated basis of analysis and definition of cases, model developments for relevant subsystems and overall blocks, modelling, calculations and analyses, evaluation and discussions of results, and comparison of the studied transport solutions and extraction of key learnings.

Abstract

The transition to a more environmentally-friendly world necessitates an energy carrier which may enable large transfers of carbon-neutral energy from one place to another. Hydrogen is one such energy carrier and can be transported by various hydrogen carriers such as liquid hydrogen (LH_2), ammonia (NH_3), and Liquid Organic Hydrogen Carriers (LOHCs). Eco-friendly hydrogen can be produced directly from electrolysis or from reforming natural gas with carbon capture and storage.

The aim of this thesis is to analyse concepts and systems for processing and marine transportation of hydrogen as an energy carrier. Three different hydrogen carriers were examined: LH_2, NH_3, and LOHC. A model was developed to evaluate the performance of each hydrogen carrier on the basis of different technical and economic indicators. The model was applied to two different case scenarios in order to capture a wide range of circumstances for hydrogen transport.

All things considered, the results indicate that NH_3 is the hydrogen carrier most suited for large-scale marine transport of clean energy. The root cause for which is the high hydrogen density of NH_3, yielding a low fuel consumption for shipping. Moreover, the NH_3 transportation chain has the lowest energy consumption for processing, underscored by its high exergy-efficiency compared to that of LH_2 and LOHC.

Sammendrag

Et skritt på veien til en mer miljøvennlig verden er bruk av energibærere som muliggjør store overføringer av karbonnøytral energi fra ett sted til et annet. Hydrogen er en slik miljøvennlig energibærer, og kan transporteres av forskjellige hydrogenbærere som flytende hydrogen (LH_2), ammoniakk (NH_3) og flytende organisk hydrogenbærer (LOHC). Miljøvennlig hydrogen kan produseres direkte fra elektrolyse eller fra reformering av naturgass med karbonfangst og lagring.

Målet med denne oppgaven er å analysere maritime transportkjeder med hydrogen som energibærer. Forskjellige energikonverteringsprosesser for hver hydrogenbærer er tatt med i analysen. Tre forskjellige hydrogenbærere ble undersøkt: LH_2, NH_3 og LOHC. En modell ble lagd for å evaluere de forskjellige hydrogenbærerne på grunnlag av tekniske og økonomiske indikatorer. Modellen ble brukt til å undersøke to ulike case med forskjellige grensebetingelser for storskala hydrogentransport.

Alt tatt i betraktning viser resultatene at NH_3 er hydrogenbæreren mest egnet for maritim transport av ren energi i stor skala. Èn av årsakene til dette er den høye hydrogentettheten i NH_3 som gir et lavt drivstofforbruk for frakt. I tillegg har transportkjeden til NH_3 det laveste energiforbruket for energikonverteringsprosesser, noe som er understreket av sin høye eksergivirkningsgrad sammenlignet med LH_2, LOHC.

Executive Summary and Conclusion

Introduction

Environmental issues caused by the combustion of hydrocarbons are in the public spotlight. Private companies worldwide are increasingly facing regulatory pressure to take steps to reduce their emissions of greenhouse gases (GHGs), sulfur oxides (SO_x), and nitrogen oxides (NO_x). This is exemplified by the GHG strategy adopted by the International Maritime Organisation (IMO), which state that a 50% cut in GHG emissions is targeted in 2050, with a full de-carbonisation of shipping by 2100. Widespread adoption of green energy is not simple. There is a large global mismatch between where carbon-neutral energy may be feasibly produced, and where it may be consumed. Therefore, the transition to a more environmentally-friendly world necessitates an energy carrier which may enable large transfers of carbon-neutral energy from one place to another. Hydrogen is one such energy carrier, and may be transported by different hydrogen carriers such as liquefied hydrogen (LH_2), ammonia (NH_3), and liquid organic hydrogen carrier (LOHC). Environmentally-friendly hydrogen may be produced directly from electrolysis, or from reforming of natural gas with carbon capture and storage (CCS). Conventional energy carriers are compared with hydrogen carriers in Figure 1.

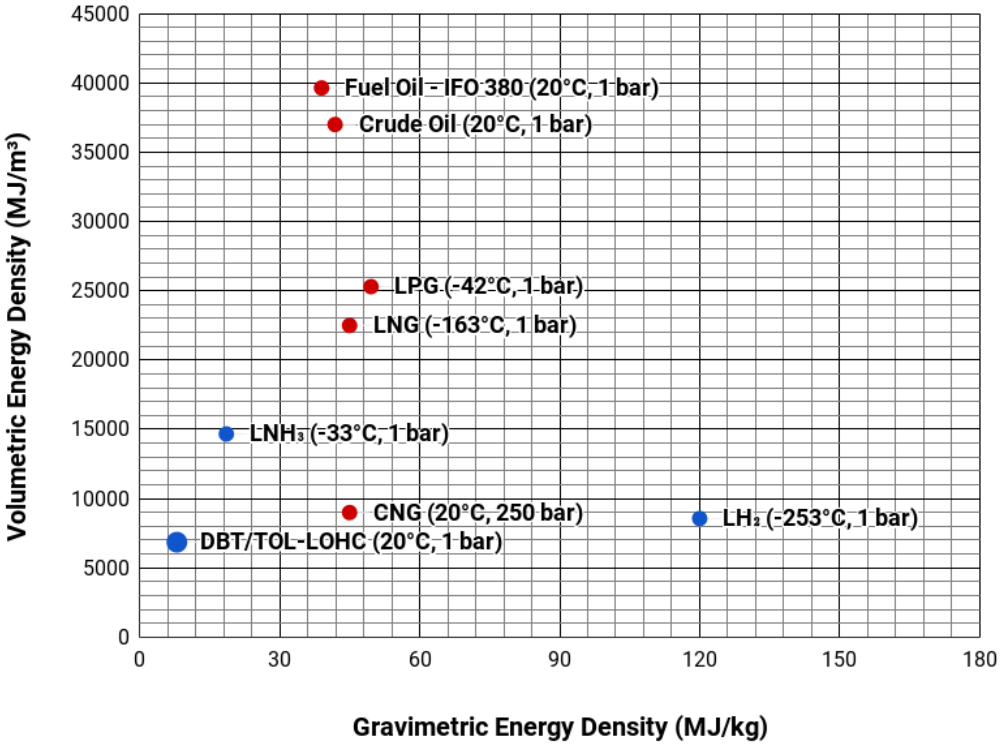

Figure 1: Comparison of energy content of different fuels both with respect to volume and mass. The energy density is taken to be the lower heating value (LHV) of each fuel. Liquid ammonia at -33°C and 1 bar is abbreviated as LNH_3. Alternate fuels are shown in blue and conventional fuels in red. Own work.

Generally, hydrogen carriers have a low volumetric energy density compared to conventional fuels which is an important drawback. The greatest benefit is naturally zero emissions of GHGs when combusted in an internal combustion engine (ICE) or consumed in a fuel cell (FC). Currently, the application of hydrogen as fuel is restricted to small niche markets such as rocket fuel. However, the Hydrogen Council and the International Renewable Energy Agency (IRENA) both predict a large market for hydrogen fuel in transportation and other industries by 2050[40][50].

Methodology

The aim of this thesis is to analyze concepts and systems for processing and marine transportation of hydrogen as an energy vector, comparing the various schemes and system designs for large-volume hydrogen shipment. Three different hydrogen carriers were examined: LH_2, NH_3, and LOHC. Two variations of LOHC hydrogen transportation chains were evaluated, the difference being the material used as a liquid organic carrier. Toluene (TOL) and dibenzyltoluene (DBT) are the evaluated LOHC materials. Their respective transportation chains will henceforth be referred to as TOL-LOHC and DBT-LOHC, respectively. Figure 2 shows a simplified representation of the transportation chain, involving each hydrogen carrier.

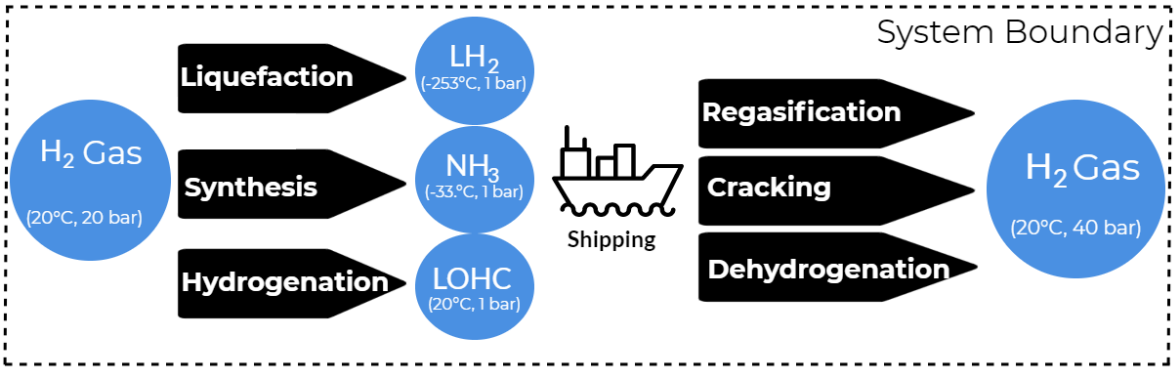

Figure 2: Simplified diagram of transportation chain. Reference made to Figure 6.4, 6.5, and 6.6 for more detailed diagrams. Each hydrogen carrier must go through different energy-conversion steps in order to store and release hydrogen.

Key assumptions made with respect to each transportation chain are as follows:

- *Exclusion of production and end-use*: Production and end-use of H_2 is out of scope for this study. Consequently, it is outside the system boundary.
- *Partial consumption of cargo*: At various energy conversion processes in each transportation chain (namely dehydrogenation, NH_3 cracking and LH_2 regasification) heat is required as an energy input. In all such cases, it is assumed that heat is drawn from the partial consumption of hydrogen cargo.
- *Zero-Emission Shipping*: Only concepts for zero-emission vessels (ZEVs) are used for marine transportation of hydrogen in all transportation chains. In this thesis, ZEVs are taken to be ships with no direct emissions of GHGs or sulphur oxides (SO_x), with minimal emissions of nitrogen oxides (NO_x). Emissions of NO_x is kept to a minimum by the use of selective catalytic reaction (SCR) systems.
- *Utilisation of Cargo as Shipping Fuel*: During shipping, the energy consumption of each ship is assumed to be covered by utilisation of cargo as fuel. Hence, enough cargo to power the cargo-ship for ballast voyage is left in the tanks after offloading cargo to export-destination.

Which hydrogen carrier is best-suited for bulk transport over large distances? Answering this question is difficult, as it depends on a wide variety of input-variables and boundary conditions. However, in the planning of future energy policy, it is necessary to not shy away from such challenges. In this thesis, a model has been developed to evaluate the performance of each hydrogen carrier on the basis of different technical and economical indicators. On a completely qualitatively basis, the complexity and technical maturity of each transportation chain has also been evaluated. A simplified schematic description of the model is shown in Figure 3.

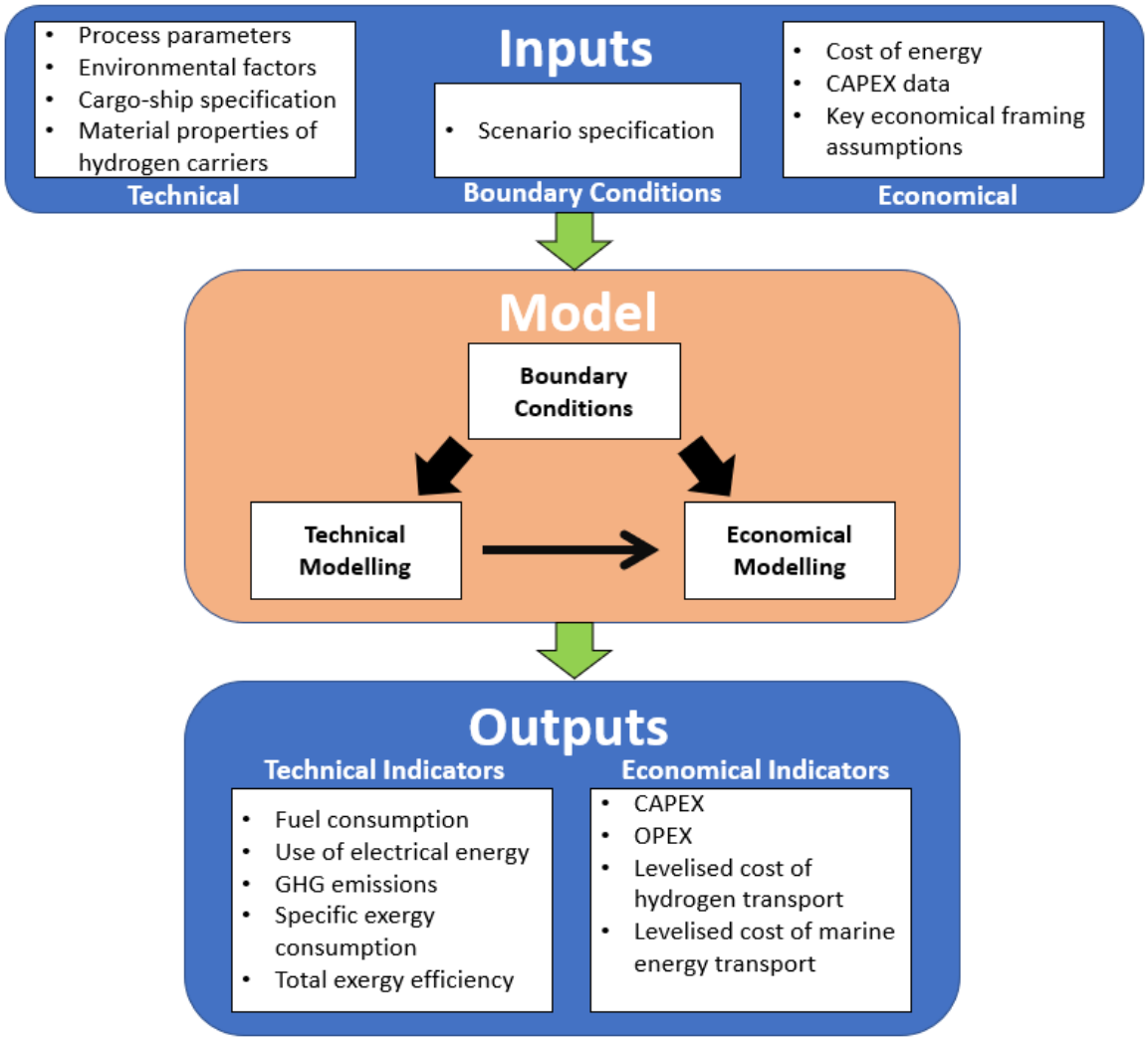

Figure 3: Simplified schematic description of model applied to assess different hydrogen carriers with regards to transportation.

The model was applied to two different case scenarios (see Figure 4), in order to capture a wide range of circumstances for hydrogen transport:

1. *Japan*: In a bid to diversify its sources of primary energy and reduce emissions of GHGs, Japan is set to become a future hydrogen society. In this scenario, it is assumed that 300,000 tons of hydrogen is transported to Japan annually.

2. *Svalbard*: As coal power is being phased out, Svalbard (more specifically Longyearbyen) will need an alternate way of producing power. In this scenario Svalbard is assumed to cover its energy demands from import of hydrogen.

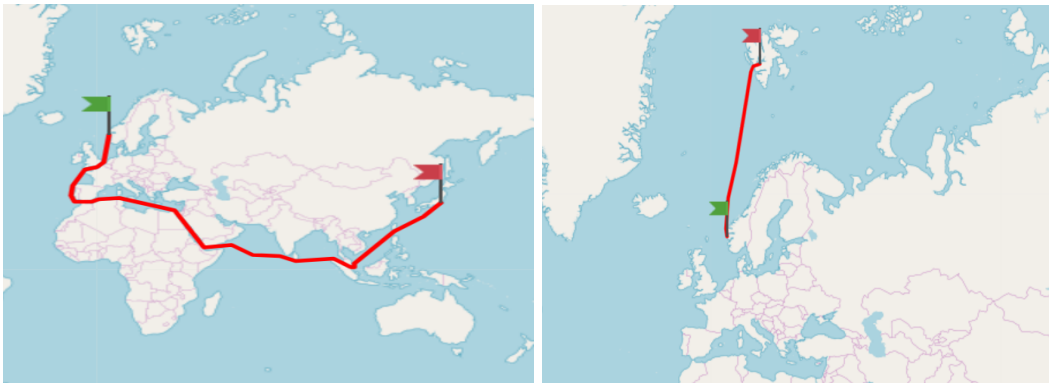

(a) Japan. *(b) Svalbard.*

Figure 4: Sea-routes for each scenario.

In each scenario, the export-site is set to be Kollsnes, Norway. Kollsnes is chosen a natural starting-point for hydrogen shipping due to its proximity to:

- Natural gas pipelines.
- Offshore reservoirs for CO_2 storage.
- Potential future offshore wind farms.

Results

Key results from the investigation is outlined and discussed below. Figure 5 shows the transportation efficiency of each transportation chain for both the Japan and Svalbard scenario. Transportation efficiency is an important technical indicator, which tells to which degree energy is lost as a result of transportation.

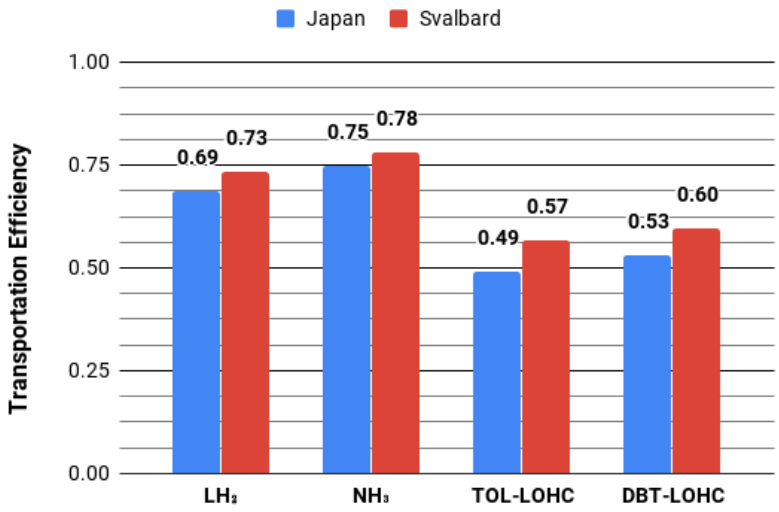

Figure 5: Transportation efficiency of each transportation chain. The transportation efficiency is a measure of exergy efficiency, and is based on both the fuel consumption and electrical energy use in each transportation chain. Reference is made to Section 6.4.1 for more details regarding transportation efficiency.

The Japan transportation chains have a lower efficiency than those of Svalbard, due to longer travelling distances. The NH_3 transportation chain is in both cases the most energy-efficient, with an efficiency of 0.78 and 0.75 for the Japan and Svalbard scenario respectively. The reason for this is that the energy-conversion processes of the NH_3 transportation chain is less energy-intensive compared to processes like H_2 liquefaction and LOHC dehydrogenation. Additionally, due to superior hydrogen density, the NH_3 transportation chain consumes less fuel for shiping, compared to other chains.

Arguably, the most central economic indicator is the Levelised Cost of Hydrogen Transport (LCoHT), since it takes into account both CAPEX and OPEX for the entire lifetime of each transportation chain. Figure 6 gives the LCoHT of each transportation chain.

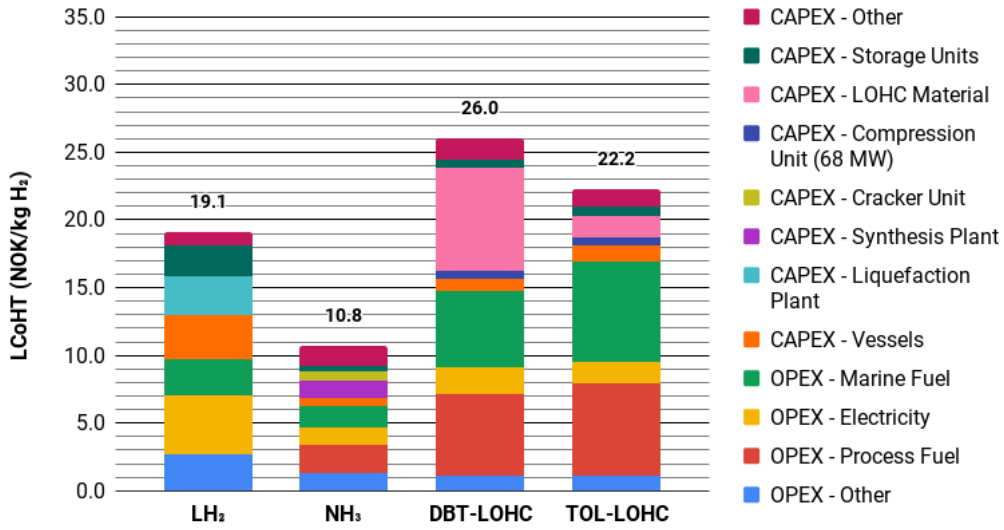

(a) Japan scenario.

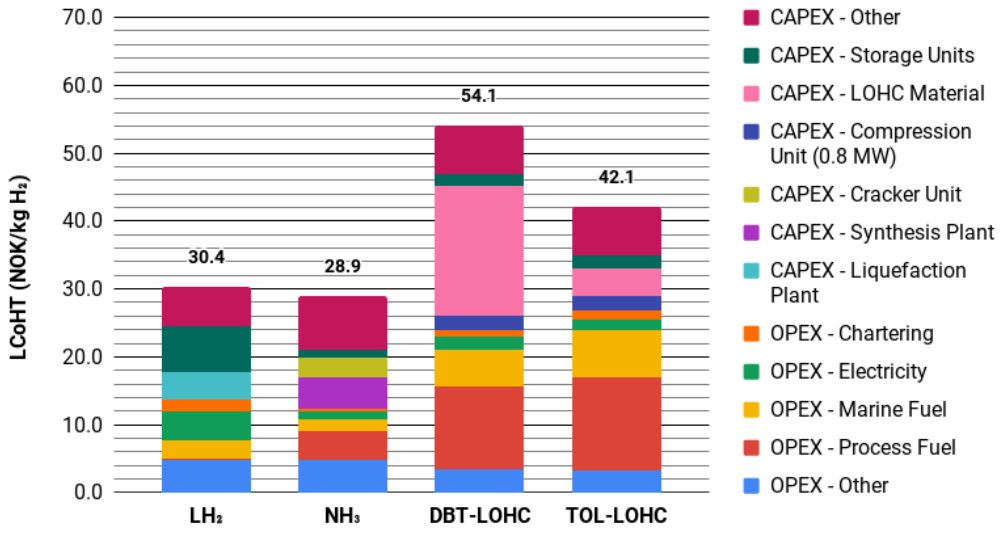

(b) Svalbard scenario.

Figure 6: Levelised Cost of Hydrogen Transport (LCoHT). The LCoHT gives the discounted cost of transporting 1 kg of hydrogen from Norway to each respective end-destination. See Section 6.5.3 for more details surrounding LCoHT.

The results indicate that the NH_3 transportation chain has an edge over the other systems as far economics is concerned. This is in part due to low OPEX costs, which may be tied to the NH_3 transportation chain's high transportation efficiency, as given in Figure 5. The high cost of DBT material, is a major reason for the high LCoHT of the DBT-LOHC chain. For both LOHC systems, OPEX on fuel consumption is very high. This is explained by a low hydrogen density, and the energy-intensive dehydrogenation process.

Inevitably, there are many uncertainties with regards to input parameters in the model. Key results from a sensitivity study which sough to identify the parameters that are particularly sensitive to the final results, is given below. Figure 7 shows the impact of changes in the cost of DBT. The effects of having available waste-heat for dehydrogenation at the export-destination, is also given.

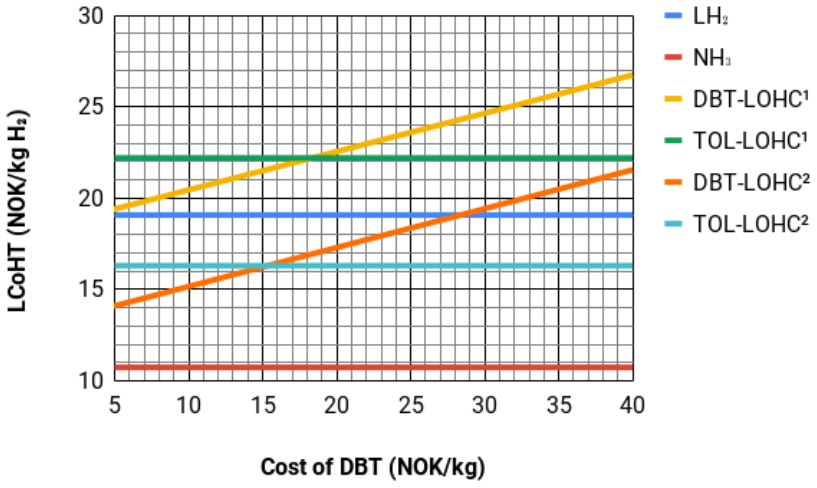

(a) Japan scenario.

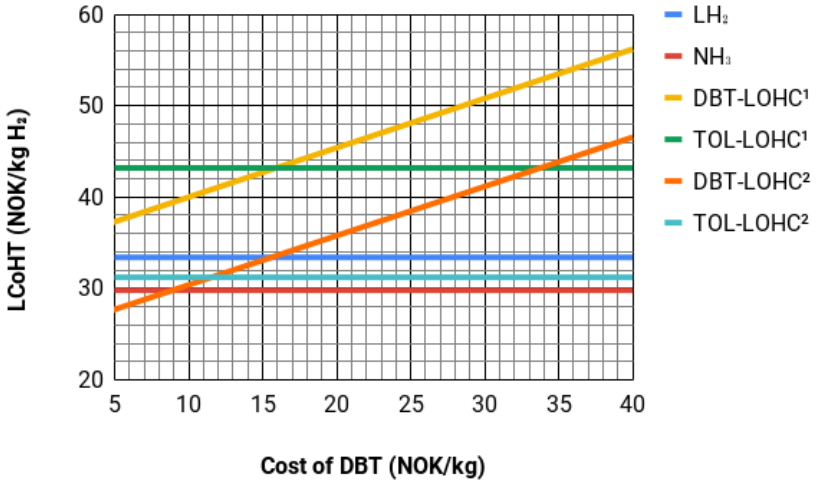

(b) Svalbard scenario.

Figure 7: Levelised Cost of Hydrogen Transport (LCoHT) vs. cost of DBT for each transportation chain. LCoHT is given for LOHC transportation chains with and without available waste heat for dehydrogenation.

[1]No available waste-heat for dehydrogenation at export-destination.

[2]Available waste-heat for dehydrogenation at export-destination. Reference to sensitivity-study in Section 11.1.

The LCoHT of the DBT-LOHC transportation chain is highly sensitive to the cost of DBT. Moreover, if waste heat for dehydrogenation is available at the export-destination of the LOHC transportation chains, the transportation costs are greatly reduced. In the Japan scenario, TOL-LOHC has a lower LCoHT than the LH_2 chain when waste heat is available for dehydrogenation. Moreover, DBT-LOHC has a lower LCoHT than TOL-LOHC when the cost of DBT is between 15-19 NOK/kg; depending on whether or not waste heat is available. At the most extreme, in the Svalbard scenario, the LCoHT of DBT-LOHC is lower than that of the NH_3 chain for a DBT cost of less than ≈9 NOK/kg. This is provided that waste heat for dehydrogenation is available.

Figure 8 shows the sensitivity of the chosen vessel cruising speed on the LCoHT of each transportation chain. The choice of cruising speed has a significant effect on the LCoHT of each transportation chain. Each transportation chain has a different optimal cruising speed, which depends on a trade-off between the amount of fuel consumed during shipping and the CAPEX of cargo vessels. In both scenarios, the optimal cruising speed of the LH_2 transportation chain is especially high - 14 kn and 13 kn for the Japan and Svalbard scenario respectively. This is due to the high cost of LH_2 cargo vessels which makes it more economical to have a high fuel expenditure, with a small no. of cargo vessels. Cruising speed has a relatively large impact on the LOHC transportation chains. This is because of the high fuel consumption for shipping, which is partly because of the low hydrogen density of TOL-LOHC and DBT-LOHC compared to LH_2 and NH_3. The NH_3 transportation chain is most insensitive to the choice of cruising speed, due to a relatively low fuel expenditure and CAPEX of cargo vessels.

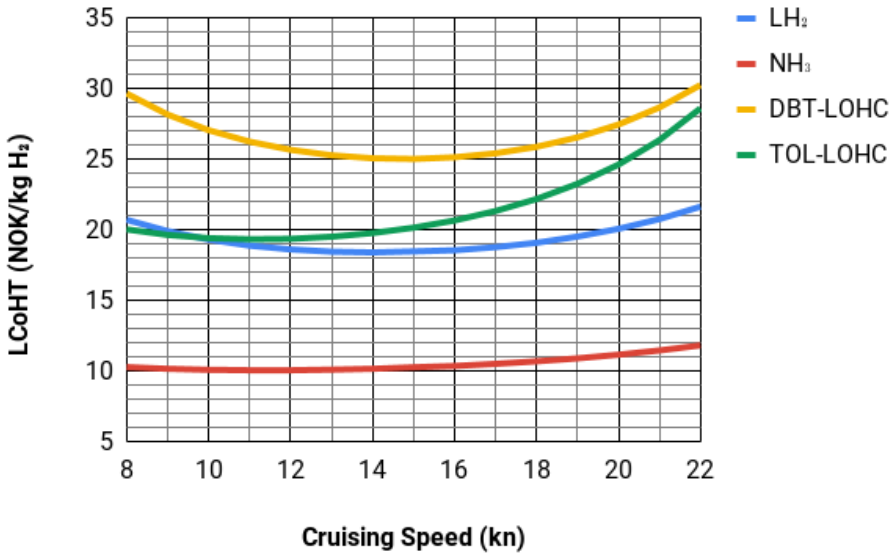

(a) Japan scenario.

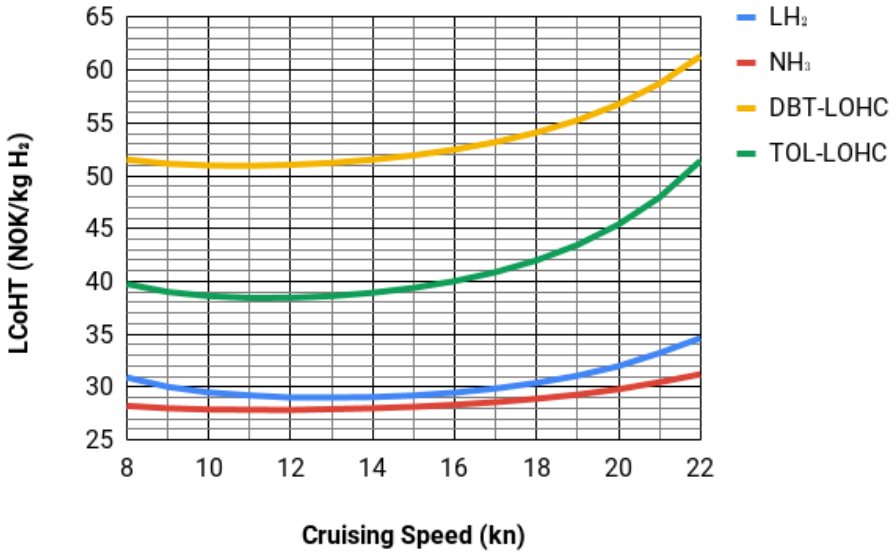

(b) Svalbard scenario.

Figure 8: Levelised Cost of Hydrogen Tansport (LCoHT) vs. cruising speed of each transportation chain. Choice of cruising speed has a large impact on the fuel consumption during shipping.

Conclusion

The relative strengths and weaknesses of each transportation chain is given in Figure 9. **For the Japan scenario**, NH_3 is found to be the highest-performing hydrogen carrier by a large margin. With the exception of complexity, NH_3 scored highest on a range of different technical and economic indicators. As an example, NH_3 has by almost half, a much lower transportation cost than LH_2 (which is the second-most cost-efficient hydrogen-carrier) on a mass basis. Sensitivity-analyses only revealed a very narrow and unlikely set of circumstances in which the other hydrogen carriers could compete with NH_3. **For the Svalbard scenario**, the NH_3 transportation chain still has the overall highest performance with respect to economical and technical indicators. However, the differences to other hydrogen carriers are much smaller. The TOL-LOHC transportation chain has lowest GHG emissions in part due to the assumption of zero grid GHG intensity in Longyearbyen. Moreover, the transportation cost of NH_3 is only slightly lower than that of LH_2. The sensitivity study exposed some circumstances in which LH_2 and DBT-LOHC may be more cost-effective than NH_3. These circumstances include; a very low cost of electricity in the Norwegian mainland, available waste heat for dehydrogenation and low cost of dibenzyltoluene, and a very high cost of fuel.

All things considered, the results indicate that NH_3 is the hydrogen carrier most suited for large-scale marine transport of clean energy. The root cause for which is the high hydrogen density of NH_3, yielding a low fuel consumption for shipping. Moreover, the NH_3 transportation chain has the lowest energy consumption for processing, underscored by its high exergy-efficiency compared to that of LH_2, TOL-LOHC, and DBT-LOHC.

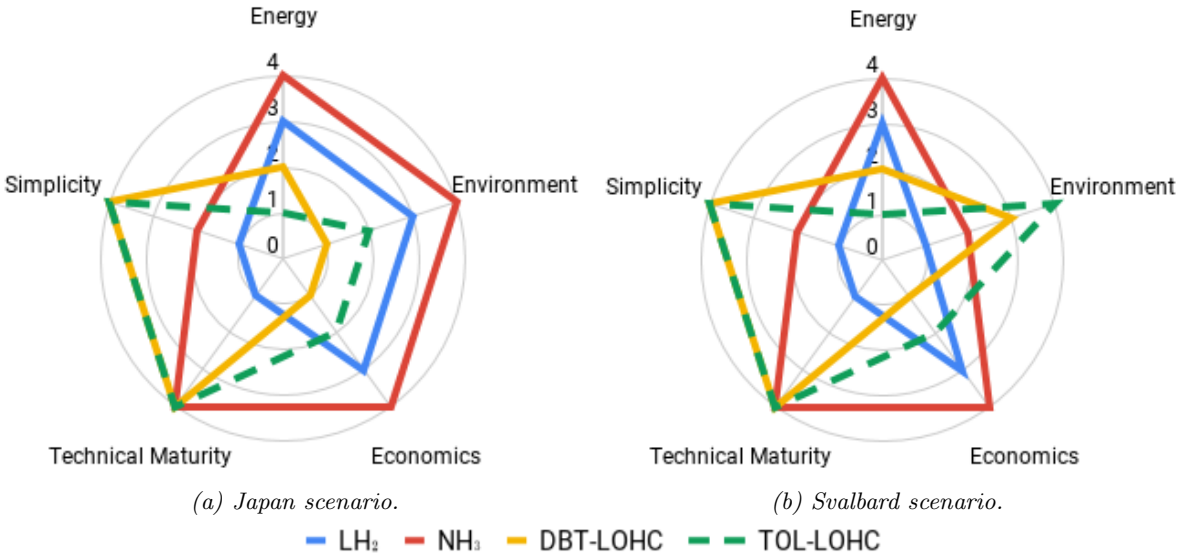

(a) Japan scenario. *(b) Svalbard scenario.*

(c) Legend.

Figure 9: Radar diagram showing the performance of each transportation chain with regards to energy, environment, economics, technical maturity, and complexity (given as "simplicity"). A score of 4 is indicative of the best performance.

Future Work

Further research is needed to fully evaluate the suitability of hydrogen carriers as means of transporting clean energy. A few areas are identified as follows:

- *More detailed modelling of NH_3 transportation chain*: The wide scope of this thesis, necessitated a high-level approach to modelling of several energy-conversion processes. NH_3 was identified as a very promising hydrogen carrier, and efforts should be made modelling its transportation chain with more detail. More detailed modelling of each energy-conversion step may reveal yet more insights.

- *Research into NH_3 cracking*: NH_3 cracking was identified to be a major obstacle for the implementation of a NH_3 transportation chain, due to low technical maturity. Projects should be directed towards increasing knowledge and operational experience of NH_3 crackers.

- *Other energy/hydrogen carriers*: Due to time-constraints, some potential hydrogen carriers were left out of the investigation. Methanol, which may be reformed to hydrogen at relatively modest temperatures and HydroSil are examples of other hydrogen carriers which play a part in future energy supplies. HydroSil is the trade-mark name of a recently developed liquid carrier material[25]. At the surface, HydroSil may seem to exhibit similar properties as LOHCs, however, there are substantial differences with regards to energy-conversion processes. Efforts should be made to evaluate the performance of other hydrogen carriers such as methanol and HydroSil with respect to marine transport.

- *Management of uncertainty*: Many input-variables in the applied model for each transportation chain has inherent uncertainty. Whether or not it is because input-parameters are based on future projections or are simply not known with 100% accuracy, implementation of a risk-managing method such as the Monte Carlo method allows these uncertainties to be taken account of in the final results.

- *Widening of scope*: Transport is only one part of the wider value chain of hydrogen. Widening the scope of study to encompass the whole value chain hydrogen including production and end-use would enable a more complete understanding of different hydrogen carriers.

Nomenclature

AHEAD	Advanced Hydrogen Energy Chain Association for Technology Development
ASU	Air Separation Unit
ATR	Auto-Thermal Reforming
BOG	Boil-off Gas
CC	Combined Cycle
CCS	Carbon Capture and Storage
CI	Compression-ignition
DBT	Dibenzyltoluene
EJ	Exajoule
FC	Fuel Cell
FCEV	Fuel Cell Electric Vehicle
GHG	Greenhouse Gas
GT	Gas Turbine
H_2-BOG	Hydrogen Boil-off Gas
ICE	Internal Combustion Engine
IMO	International Maritime Organization
IRENA	International Renewable Energy Agency
LH_2	Liquefied Hydrogen
LHV	Lower Heating Value
LNG	Liquid Natural Gas
LOA	Length Over-All

LOHC	Liquid Organic Hydrogen Carrier
MCR	Maximum Continuous Rating
mt	metric tons
NH_3-BOG	Ammonia Boil-off Gas
nm	nautical miles
NPV	Net Present Value
NSR	Northern Sea Route
ORC	Organic Rankine Cycle
PEMFC	Proton Exchange Membrane Fuel Cell
ppm	parts per million
PSA	Pressure Swing Adsorption
SCR	Service Continuous Rating
SEC	Specific Exergy Consumption
SI	Spark-ignition
SOFC	Solid Oxide Fuel Cell
TOL	Toluene
WHR	Waste Heat Recovery

Contents

Chapter 1

Introduction

Energy is an imperative element of life. In the past few decades, public awareness of the environmental issues originating from the combustion of hydrocarbons have accelerated the search for alternate fuels. Renewable sources are predicted to supply as much as 45% of all primary energy in 2050 [22]. Due to a large global mismatch between where renewable energy may feasibly be produced and where it may be consumed, the transition to renewable energy sources necessitates a way of transporting renewable energy over large distances. An energy carrier which may enable such large transfers of renewable energy from one region to another, with minimal losses, is hydrogen.

1.1 Background

Hydrogen in its pure form has many appealing properties which makes it an ideal energy carrier. Most importantly, regardless of whether it is consumed by combustion or a fuel cell, the only by-product is water. Thus, hydrogen is credited as a clean fuel if its production is zero-emission. Moreover, it has the highest mass energy density of all chemical fuels and have the potential to be produced cost efficiently. On the other hand, there are a few drawbacks concerning the use of pure hydrogen as a fuel. It poses many safety concerns including its inherent ability to ignite in air at a large span of concentrations. Therefore hydrogen must be handled with caution. The most significant drawback, however, is that the volumetric energy density of hydrogen is very low compared to other fuels. For example, hydrogen gas (H_2(g)) at 1 atm and 25 °C has a volumetric energy density of 10 MJ/m^3, compared to gasoline in similar conditions at 34,600 MJ/m^3. Liquefying hydrogen at -253°C yields a greatly improved volumetric energy density of 8,500 MJ/m^3 [107]. This is still, however, lower than for conventional carbon-based fuels such as liquid natural gas (LNG) with a volumetric energy density of 23,600 MJ/m^3.

Substantial research is focused on how to improve the volumetric energy density of stored hydrogen, while keeping the mass energy density high. Substances which are considered to be potential storage mediums for hydrogen are referred to as hydrogen carriers. Ammonia is one such hydrogen carrier due to its high hydrogen-content in liquid state. As a widely traded commodity, ammonia has a well-established and a globe-spanning infrastructure-network already in place. There are, however,

challenges related to its toxicity. Another promising hydrogen carrier is a group of organic liquids called liquid organic hydrogen carriers (LOHCs). Since they exist as a liquid in ambient temperature and pressure, LOHCs may be stored under standard conditions in contrast to other hydrogen carriers such as liquefied hydrogen and ammonia.

Adoption of hydrogen as a fuel necessitates a large world-wide hydrogen transportation network in which marine transport will play an essential role. It is therefore of great importance to find sustainable transport alternatives for ships. Environmental concerns have in recent years been raised regarding shipping's contribution to climate change, acidification, and eutrophication. Increased awareness of the consequences of global ship emissions have resulted in stricter regulation. The International Maritime Organization (IMO), a United Nations specialized agency, has adopted regulations to reduce emissions of both sulphur oxides and nitrogen oxides. In 2018 IMO adopted a strategy to reduce greenhouse gas (GHG) emissions from ships by at least 50% by 2050[49], and finally, 100% by 2100. Bearing this in mind, it is clear that future marine transportation is moving towards zero-emission.

1.2 Objective

Finding the most suited hydrogen carrier for large scale transportation of hydrogen is a challenging task dependent on numerous factors such as safety, complexity, technological maturity, the environment and economic feasibility. Major developments regarding hydrogen carriers have been made in the last decade, and more are likely to follow in subsequent years. At the time of writing, the following hydrogen carriers look to be the most promising:

1. LH_2
2. NH_3
3. LOHC

Using two different case scenarios, this report aims to conduct a comparative technical evaluation of these three hydrogen carriers with respect to large scale marine transportation chains. Accurate modelling of the transportation chains necessitates the development of concepts for hydrogen cargo ships and representations of land-based energy transformations. In the end, strengths and weaknesses of each hydrogen carrier should be established and understood.

1.3 Scope

The focal point of this thesis is the marine transport of hydrogen and associated energy transformations which take place to facilitate this. Consequently, the production of hydrogen and on-shore end-use is not covered by the thesis. The thesis concentrates on marine hydrogen transport from Norway to Svalbard and Japan. The results can therefore only be extrapolated with caution to different geographical regions and cases. Due to the extensiveness of the thesis objective, a high level approach is used for modelling.

1.4 Outline of Thesis

This thesis has been divided into three parts. Firstly, Chapter 2, 3, 4, and 5 will provide the basis for the subsequent analysis and discussion of hydrogen transportation chains. Chapter 6, 7 and 8 gives a detailed account of how each hydrogen transportation chain is modelled and concepts for marine hydrogen-transport are developed. Finally, Chapters 9, 10, 11, 12, and 13 presents a comparison between each transportation chain, followed by a discussion. Table 1.1 gives a more detailed description of the contents of each chapter.

Table 1.1: Overview of chapters.

Chapter	Content
2	Use of hydrogen as an energy carrier is a relatively new idea. However, its use as a feedstock in various industrial processes has been common practice for decades. Chapter 2 gives a brief description of the present day hydrogen market, and how it is likely to change in the future.
3	Chapter 3 is written about two case scenarios which present future cases for marine hydrogen transport.
4	Liquefied hydrogen (LH_2), ammonia (NH_3), and LOHC must undergo different processes in order to allow their function as hydrogen carriers. Chapter 4 gives theory behind the different energy transforming processes which are an important part of each hydrogen carrier's transportation chain.
5	Hydrogen has the potential to de-carbonise large sectors of the economy. Marine transportation is no exception. Chapter 5 describes how hydrogen and ammonia may be applied as a fuel in zero-emission vessels (ZEVs).
6	Chapter 6 gives the methodology on which the analysis of all hydrogen transportation chains is based.
7	Chapter 7 investigates many different concepts for zero-emission shipping of hydrogen. Each concept is evaluated technically and economically.
8	A detailed technical analysis of each hydrogen transportation chain is conducted in Chapter 8.
9,10	Chapters 9 and 10 compares the transportation chains from a technical and economical perspective, respectively. A wide range of different technical and economic are used.
11	Different sensitivities with respect to the performance of each hydrogen transportation chain is investigated in Chapter 11.
12	A final discussion based on preceding results will be the subject of Chapter 12. Key learning points are extracted and summarised.

Chapter 2

Present Hydrogen Market and Future Outlook

The hydrogen market is set to experience radical changes in coming decades. From being used primarily as a feedstock in various industrial processes, its ideal properties as an energy carrier may in the long term lead hydrogen to play a vital role in global energy markets. The driving momentum behind this transformation is hydrogen's potential to decarbonise large sectors of the economy such as transportation and power-production. This chapter gives a description of the hydrogen market today, and how it is likely to change in the future.

2.1 General

The use of hydrogen may be categorized as follows:

1. *Hydrogen as a feedstock*: Hydrogen has for decades been applied in various industrial processes such as ammonia synthesis.

2. *Hydrogen as an energy carrier*: Hydrogen may enable long-distance transfer of energy i.e. it may be converted to electricity, mechanical energy or heat.

Up until the time of writing, hydrogen has primarily been used as a feedstock and produced on-site of industrial complexes. However, this is set to change as hydrogen is adopted as an energy carrier.

2.2 Hydrogen Today

2.2.1 Demand

The hydrogen industry is well established. Hydrogen has been widely used as a feedstock in various industrial processes for a long time. The world currently produces and consumes more than 55 million tons of hydrogen annually [40]. On a lower heating value (LHV) basis, this is equivelant to 6.6 exajoules (EJ) ($= 6.6 \cdot 10^{18}$J $= 1833.33$ TWh of thermal energy). As a point of reference, the total daily energy consumption of the world is approximately 1 EJ [40]. This shows that present-day hydrogen production is significant. However, it is important to note that the vast majority of the produced hydrogen is used as a feedstock, and not an energy carrier. Moreover, hydrogen is almost exclusively transported by pipelines. Marine transport of hydrogen is (with very few exceptions) non-existent.

2.2.2 End-Use

Presently, the application of hydrogen as an energy carrier is limited to small niche markets, such as rocket propulsion fuel, and fuel cell electric vehicles (FCEVs). Therefore, hydrogen as an energy carrier make up a relatively insignificant proportion of total hydrogen consumption. For industrial processes, on the other hand, hydrogen demand is high. This point is highlighted by Figure 2.1, which shows the consumption of hydrogen by application. By far the largest application of hydrogen lies in the production of ammonia[40]. The refining industry also consumes a large proportion of hydrogen. Automotive fuel and rocket propulsion fuel are in the category "Processing" which makes up 5.3% of all hydrogen consumption. Most hydrogen is produced as part of an integrated plant. Therefore, hydrogen is usually not stored or transported across large distances.

Application	Description
Ammonia	Production of ammonia (for urea and other fertilizers).
Refining	For use in hydrocracking and hydrotreating (e.g., fuel desulphurization of petroleums).
Methanol	Production of methanol and derivatives.
Other Chemicals	Other chemicals (e.g., polymers, polyurethanes, fatty acids).
Processing	Automotive fuel, propulsion fuel, and semiconductor industry.

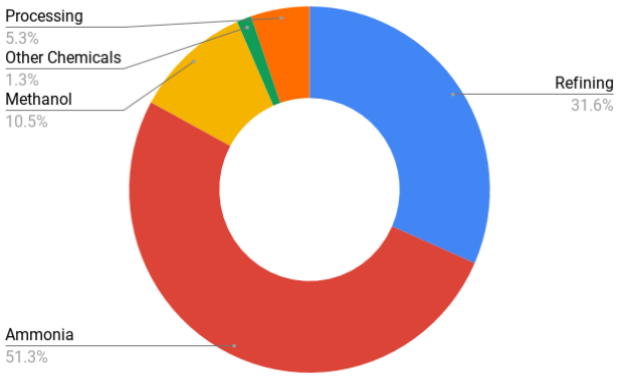

Figure 2.1: Percentage of global hydrogen demand by industry sector, out of a total annual demand of 50 million tons (2015 estimate). Adapted from [40].

2.3 Hydrogen in the Future

2.3.1 Demand

There is no unison agreement in professional circles as to what the demand for hydrogen will be in the future. The Hydrogen Council is a global group of leading energy, transport and industrial companies, that predicts a total hydrogen consumption of 49 EJ (=13,600 TWh) by LHV in 2050 excluding feedstock hydrogen[40]. This is equivalent to 408 million tons. The International Renewable Energy Agency (IRENA), on the other hand, predicts a more modest total hydrogen consumption of 6.5 EJ (=1805 TWh) by LHV [50], also excluding hydrogen consumption as feedstock in industrial processes - equivalent to 54 million tons. The big gap between estimated hydrogen consumption by Hydrogen Council and IRENA is indicative of the uncertainty with which actors anticipate global decarbonization and the means for achieving it. Both IRENA and the Hydrogen Council agree on one thing however: hydrogen will play an important role as an energy carrier in the future.

2.3.2 End-Use

As mentioned, the vast majority of the global hydrogen demand is currently derived from industrial applications. This is however likely to change in the future, as hydrogen plays an increasingly important role in energy markets. Figure 2.2 shows the anticipated consumption of hydrogen in 2050 by sector by the Hydrogen Council. Transport is the single largest area of application for hydrogen, followed up by industrial energy.

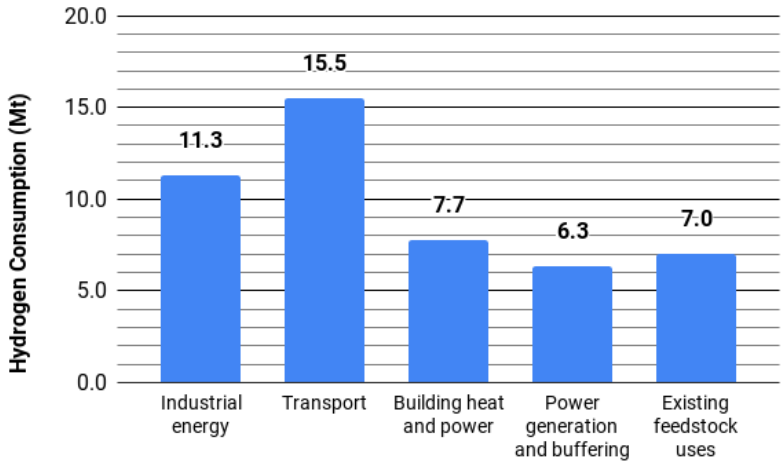

Figure 2.2: Potential of hydrogen in final energy supply by sector in 2050, as envisioned by the Hydrogen Council. Adapted from [40]. Given in units of million tons (Mt).

As far as transport is concerned, the Hydrogen Council envision that more than 400 million cars, 20 million trucks and around 5 million buses will be hydrogen-powered in 2050. Moreover, a quarter of all passenger ships and a fifth of locomotives on non-electrified tracks. Hydrogen-based synthetic fuels

will also power a share of all airplanes and freight ships [40].

In the future, hydrogen may have a multitude of different end-uses. These include:

1. *Transportation*: Some FCEVs are already commercially available, and more will be available in the future. Moving further on in time, hydrogen-powered large cars, buses, trucks, trains and forklifts will be commercialized and contributing to the increasingly high consumption of hydrogen in the transportation sector. Hydrogen also has much promise as a fuel for ships.

2. *Industrial energy*: In many industries, such as the aluminium- and fertilizer industries, high grade heat is required. Hydrogen may be used to provide this high-grade heat.

3. *Building heat and power*: Hydrogen may be blended into (or replace) natural gas in existing natural gas grid infrastructure to provide heat for buildings.

4. *Industry feedstock*: Large mounts of hydrogen is already applied (and will continue to do so) as feedstock in industrial processes such as refining, ammonia, and methanol production.

5. *Energy systems*: As energy systems worldwide rely on renewable energy, hydrogen could potentially play a growing role in the in the storage of renewable energy and storage. By 2030, 200 TWh could be generated in hydrogen power plants as a measure of decarbonisation[40].

A precondition for all the above end-uses of hydrogen is that an efficient method of hydrogen transportation is found.

Chapter 3

Hydrogen Transportation Scenarios

The main objective of the report is to evaluate different schemes for large-scale hydrogen shipping. In order to make the evaluation as generic as possible, two different framing scenarios for marine transport has been chosen. The two framing scenarios are based on hydrogen export to Svalbard and Japan. In both cases, hydrogen is exported from the western Norwegian mainland. This chapter gives details regarding each hydrogen transportation scenario.

3.1 Norway as an Exporter of Hydrogen

3.1.1 General

As a major energy exporter, Norway has great potential for becoming a future exporter of hydrogen. Norwegian export of natural gas amounted to approx. 120 billion Sm^3 in 2018. This is equivalent to a total energy of 1,240 TWh on a lower heating value (LHV) basis. If this natural gas was to be used in the production of hydrogen through steam-reforming or auto-thermal reforming (ATR) with carbon capture and storage (CCS), Norway could export hydrogen amounting to approximately 900 TWh(LHV)[75]. Natural gas aside, Norway also has the potential to produce a significant amount of hydrogen through other means. Hydrogen export could be based on renewable energy sources such as wind farms and hydroelectric resources through electrolysis plants. It is important to note, however, that the potential volumes of hydrogen from renewable sources is unlikely to match that produced from natural gas in the near future[37]. Given Norway's vast potential to produce hydrogen on a large scale, it is a natural point of departure for hydrogen shipping.

3.1.2 Export-Terminal

A number of factors need to be considered when selecting the location of a hydrogen export-terminal in Norway. Key criteria include:

1. Availability of natural gas for hydrogen production (via steam reforming or ATR).
2. Possibility of future hydrogen production by renewable energy, e.g. offshore wind farms.

3. Storage possibilities for CO_2.

4. Access to hydrogen markets.

Kollsnes (shown in Figure 3.1) in Hordaland county is chosen as the ideal location for the hydrogen export-terminal in Norway. Due to its proximity to the Norwegian continental shelf, there are ample opportunities for CO_2 storage from CCS. Natural gas pipelines transport gas from fields in the North Sea, most notably the Troll natural gas field, on-shore in Kollsnes for processing. Access to natural gas from offshore fields is precondition to produce a large amount of hydrogen via methods like steam reformation or ATR. There are also substantial wind resources near Kollsnes which might in the long term provide electricity for the production of hydrogen. Finally, since Kollsnes is located close to second largest city in Norway, Bergen, it is strategically located near a future potential Norwegian hydrogen market.

Figure 3.1: Picture of the gas processing plant at Kollsnes[74].

3.2 Japan

Lacking sufficient domestic energy sources, Japan currently imports 89% of its primary energy supply [51]. All of Japan's energy imports are currently fossil fuels (oil, LNG and coal). As a consequence of the Fukushima nuclear disaster in 2011 and consequent closures of nuclear power stations due to safety concerns, the share of nuclear power in the total primary energy supply of Japan has dropped from 11.2% in 2010, to barely 0.8% in 2016. This has increased Japan's reliance on fossil fuels. The primary energy supply by source for Japan is shown in Figure 3.2.

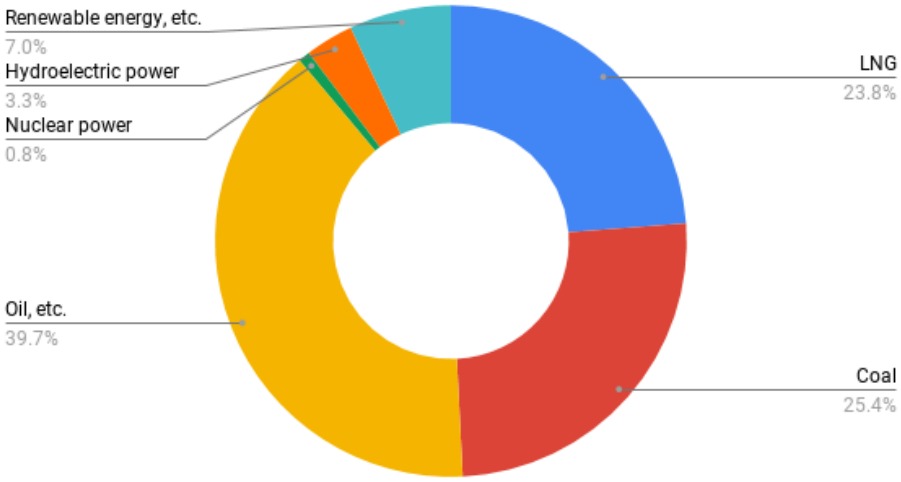

Figure 3.2: Primary energy supply by source in Japan, 2016 [51].

In a bid to diversify its sources of primary energy and reduce emissions of GHGs, Japan is set to become a future hydrogen society. As the Japanese government seeks to commercialise hydrogen power generation, its annual hydrogen procurement may reach as high as 5-10 million tons in 2030 [52]. This entails an ambition of achieving cost parity between hydrogen and other conventional fuels used for power generation such as LNG in the long term [43]. By 2030, the target is to reduce the price of hydrogen to 30 yen/Nm^3 ($\approx$ 21 NOK/kg). Consequently, Japan is a natural future consumer of hydrogen from Norway. HYPER, a joint research project undertaken by SINTEF and industry actors including Equinor and Kawasaki, aims to investigate feasibility for large scale hydrogen transport from Norway to global markets including Japan. Findings indicate that Norway has a large potential for large scale hydrogen export to Japan; especially when produced from natural gas with CCS[84].

3.2.1 Case Definition

In this scenario, it is assumed that 300,000 tons of hydrogen is to be transported to Japan annually from Kollsnes. More specifically, to the port of Yokohama in Japan which is a hub for a wider geographical area. The end-application of exported hydrogen is not limited to power generation, but may serve numerous purposes including as fuel for cars. The three most relevant route alternatives and their corresponding voyage distances are shown in Figure 3.3 and Table 3.1, respectively.

Table 3.1: Distance from Kollsnes to Yokohama, given in nautical miles (nm).

Choice of Route	Voyage Distance (nm)
Northern Sea Route (NSR)	6,500
Suez canal	11,600
Cape of Good Hope	14,900

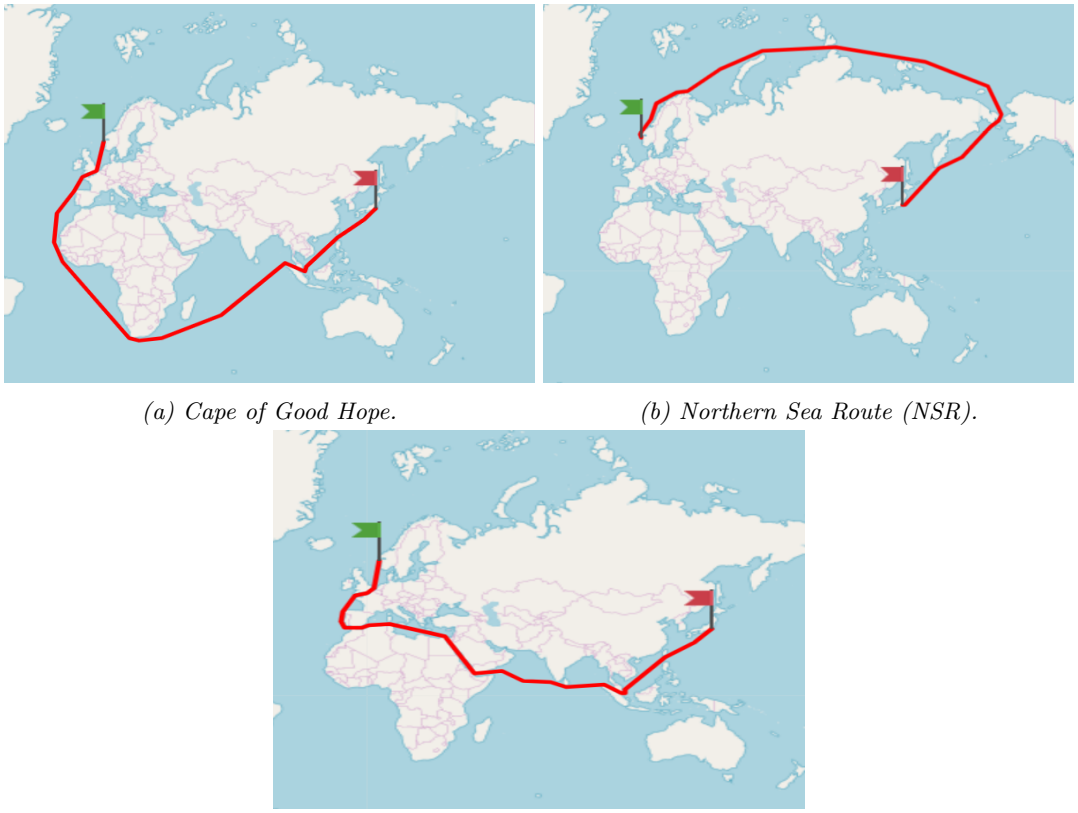

(a) Cape of Good Hope. *(b) Northern Sea Route (NSR).*

(c) Suez canal.

Figure 3.3: Different route-alternatives for sea-voyage from Kollsnes, Norway to Yokohama, Japan.

The north-west passage and Panama canal routes are disregarded, since they offer no advantages when compared to the NSR and Suez canal route, respectively. The NSR is the shortest route available for shipping between Kollsnes and Yokohama. However, there are also other factors than distance which determines the feasibility of each route. Even though climatic models unanimously predict that Arctic sea ice will continue to decline in the future, ships will most likely require an ice-breaking capability or the aid of an ice-breaker to fully navigate the NSR in 2040 - even during the relatively warm summer-months[98]. The Cape of Good Hope route, meanwhile, is significantly longer then the Suez route. Because of this, **the Suez canal is the route of choice for hydrogen transport to Japan**.

Table 3.2 shows the key parameters of the Japan transportation scenario.

Table 3.2: Key figures for the Japan transportation scenario.

Parameter	**Value**	**Unit**
Annual hydrogen export	300,000	tons/year
Mean thermal power of hydrogen export (LHV)	1140	MW
Voyage distance (one way)	11,600	nm
Cargo-vessel capacity	160,000	m^3
Internal cost of hydrogen as fuel	21	NOK/kg H_2

A few points are worth noting:

- The annual hydrogen export of 300,000 tons per year covers a sizeable portion of Japan's ambition to import 5-10 million tons by 2030.
- Cargo ships with capacity of 160,000 m^3 is common in the global LNG trade and facilitates the transport of large amounts of energy. Therefore, it is appropriate for this scenario.
- The assumed fuel cost of hydrogen only applies internally in the transportation chain and gives the economic cost of consuming hydrogen for shipping and energy transformation processes.
- Ordinarily, a toll must be paid for transiting the Suez canal. Suez canal toll is neglected in this thesis.

3.3 Svalbard

Svalbard is a Norwegian archipelago located in the arctic. Due to the island's remoteness, it is not connected to the mainland Norwegian electricity grid. Longyearbyen, the largest settlement of Svalbard, has long been dependent on a power station fuelled by locally extracted coal. However, as the future of local mines looks uncertain and the Norwegian government intends to reduce Longyearbyen's carbon footprint, alternative energy sources have been investigated. On contract with the Norwegian Ministry of Petroleum and Energy, THEMA Consulting group and Multiconsult has conducted a feasibility study addressing Longyearbyen's future energy supply [96]. Many energy supply solutions were investigated including systems based on electric power transmission, LNG and renewables. Statkraft, a large producer of renewable energy, has also considered several energy transport solutions to Svalbard[87]. With the premise that excess wind power in Finmark could be used to generate hydrogen for export to Svalbard, Statkraft evaluates five different alternatives including compressed hydrogen (CH_2) at 350 bar, liquefied hydrogen (LH_2), and ammonia as a hydrogen carrier. The report concludes that ammonia as a hydrogen carrier is an alternative which should be investigated more carefully.

3.3.1 Case Definition

In this scenario, the power consumption of Svalbard is covered by hydrogen import from Kollsnes on the Norwegian mainland. In 2017, the total consumption of electricity in Longyearbyen was 43 GWh [96]. In addition, the demand for district heating was 70 GWh of thermal energy. If one considers a scenario where all electricity and district heating needs are covered by a hydrogen power plant one may estimate the amount of hydrogen needed to be imported to be approximately 3390 tons per year. By imposing a time buffer of one month per year, in case of an interruption in supply, the total amount of exported hydrogen should amount to 3700 tons per year. In this scenario, it is assumed that the total electricity demand of Longyearbyen will remain static. Seasonal changes in Longyearbyen's energy demand is not taken into account for simplification. Figure 3.4 shows the sea route from Kollsnes to Longyearbyen. A hydrogen bunkering vessel (capacity of 5,000 m^3) serving a future maritime market for hydrogen fuel along the Norwegian coast is assumed to transport hydrogen from Kollsnes to the port of Longyearbyen. One such bunkering vessel (for LH_2) has already been designed by a consortium of companies including DNV GL, Equinor, Wilhelmsen and Moss maritime[94].

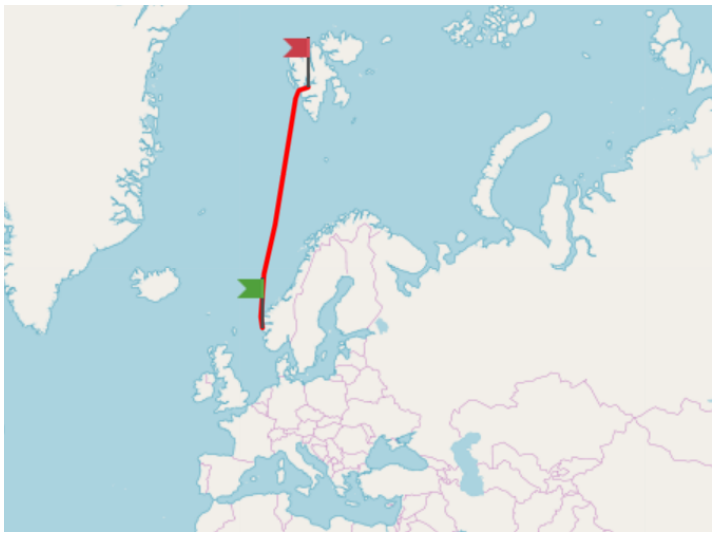

Figure 3.4: Graphical depiction of sea route from Kollsnes to Longyearbyen.

Table 3.3 shows the key parameters of the Svalbard transportation scenario.

Table 3.3: Key parameters for the Svalbard transportation scenario.

Parameter	**Value**	**Unit**
Annual electricity consumption in Longyearbyen	43	GWh
Annual district heating energy consumption in Longyearbyen	70	GWh
Annual hydrogen export	3,700	tons/year
Mean thermal power of hydrogen export (LHV)	14.1	MW
Voyage distance (one way)	1,100	nm
Cargo-vessel capacity	5,000	m^3
Charter rate	5	% of (Ship CAPEX)/year
Internal cost of hydrogen as fuel	42	NOK/kg H_2

A few points are worth noting:

- The annual quantity of hydrogen export is fixed by Longyearbyen's demand for energy. In this scenario, hydrogen is being exclusively applied as fuel for a combined heat and power (CHP) station upon arrival at the export-destination.
- Cargo-transport is assumed to be undertaken by a hydrogen-bunkering ship which is chartered for hydrogen transport to Svalbard from Kollsnes. Its chartering rate of 15% of (Ship CAPEX)/year is based on real-life chartering rates of different types of cargo-vessels.
- The assumed fuel cost of hydrogen is 42 NOK/kg H_2 which is twice that in the Japan scenario. The difference in fuel cost for hydrogen is attributed to economies of scale. The Svalbard scenario incurs higher costs related to smaller capacities of processing plants units.

Chapter 4

Hydrogen Carriers and Processing

The application of hydrogen as an energy carrier make necessary an efficient way to transport it practically over great distances in bulk. This is not possible to achieve without the use of a hydrogen carrier. Presently, compressed hydrogen and liquefied hydrogen (LH_2) are the most common hydrogen carriers in use commercially. This is however, set to change as more hydrogen carriers are developed - chief among which is ammonia and different liquid organic hydrogen carriers (LOHCs). This chapter gives a description of each hydrogen carrier along with the necessary energy-conversion processes that follow.

4.1 Overview of Prospective Carriers

Hydrogen carriers store hydrogen in some other chemical state apart from as free hydrogen molecules at standard conditions. Much research is underway to identify novel hydrogen carriers, both solid and liquid, to play a role as a storage medium for hydrogen.

The hydrogen carriers under consideration in this thesis are:

1. Liquefied hydrogen (LH_2).
2. Ammonia (NH_3) in liquid state.
3. LOHCs based on:
   (a) Dibenzyltoluene (DBT-LOHC).
   (b) Toluene (TOL-LOHC).

Figure 4.1 compares the energy content of hydrogen carriers with that of conventional fuels.

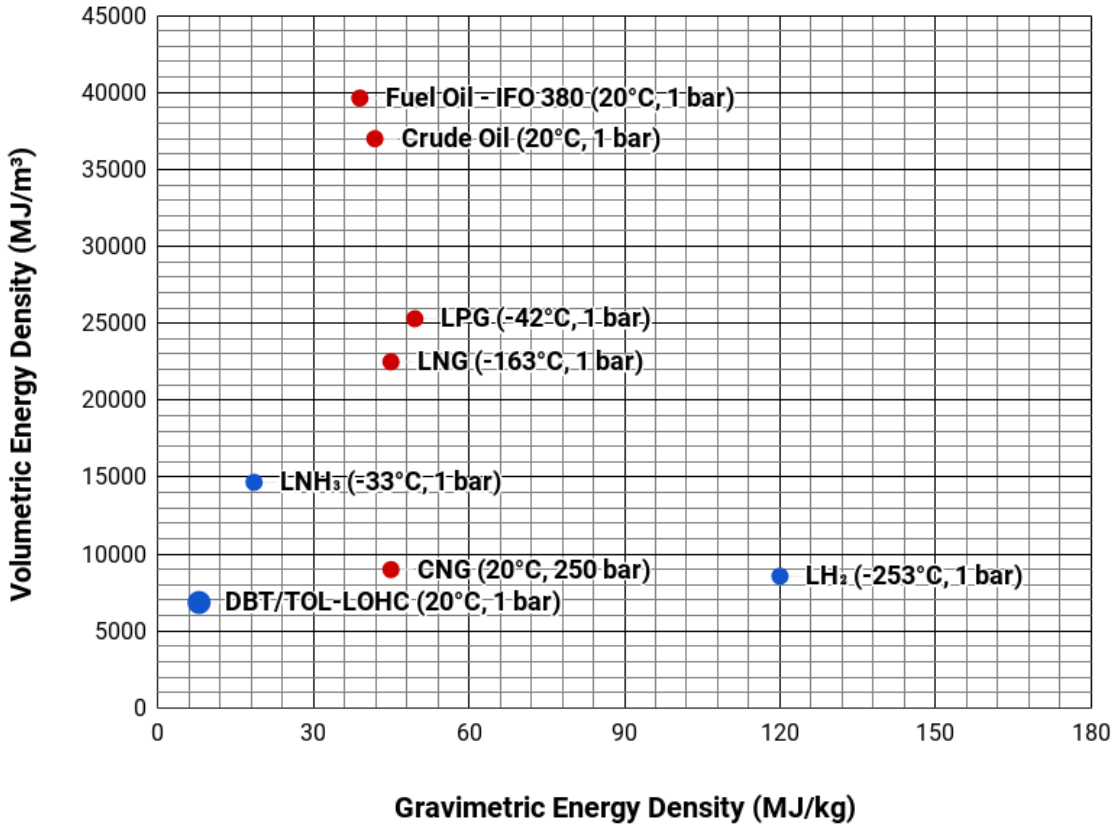

Figure 4.1: Comparison of energy content of different fuels both with respect to volume and mass. The energy density is taken to be the LHV of each fuel. Hydrogen carriers are shown in blue and fuels based on hydrocarbons in red. Own work.

Figure 4.1 highlights one of the most important drawbacks of using hydrogen as an energy carrier: all hydrogen carriers (LNH_3, LH_2, LOHC) have a significantly lower volumetric energy density compared to conventional fuels such as LNG and fuel oil (IFO 380). It also shows that ammonia (LNH_3) has a higher volumetric energy density than LH_2 and LOHC. On the other hand, LH_2 exhibit a very high gravimetric energy density more than twice that of LNG. In relation to maritime applications however, hydrogen's favourable gravimetric energy density may be of limited value since the volumetric energy density is of higher importance. It is important to note that if one includes the storage system of each fuel in Figure 4.1 (and not exclusively the fuel itself), the gravimetric and volumetric energy density will be reduced - especially so for LH_2[68].

Each hydrogen carriers have different physical and chemical properties. Hydrogen density, one of the most important physical properties of each hydrogen carrier is given in Figure 4.2.

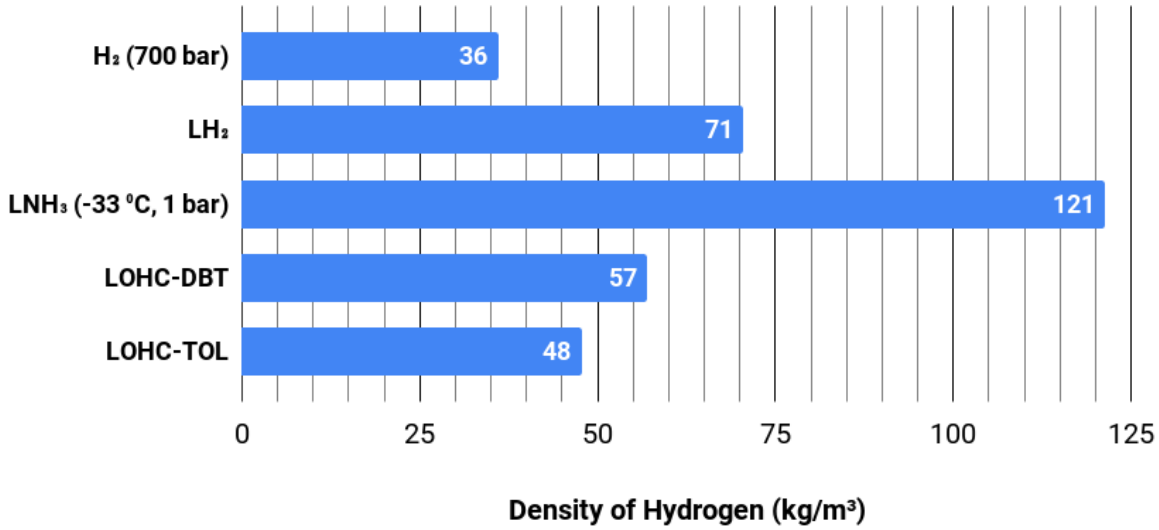

Figure 4.2: Hydrogen density of different hydrogen carriers. Compressed hydrogen at 700 bar is included even though it is not the subject of this investigation.

LOHC-TOL (hydrogenated toluene) has the lowest hydrogen density of all the hydrogen carriers considered. Ammonia (LNH_3), on the other hand, has by far the highest hydrogen density.

Ammonia may be kept as a liquid at a variety of different temperatures and pressures. These pressure and temperature combinations are often designated as fully pressurised (20 bar and 20°C), semi-refrigerated semi-pressurised (8 bar and -10 °C), or fully refrigerated (1 bar and -33°C)). Fully refrigerated ammonia has a slightly higher hydrogen density compared to fully pressurised or semi-pressurised semi-refrigerated ammonia. In this thesis, ammonia is assumed to be kept liquid as fully refrigerated. **Henceforth, fully refrigerated(-33°C, 1 bar) liquid ammonia will be known as LNH_3.** Table 4.1 summarises the storage conditions of each hydrogen carrier considered in this thesis.

Table 4.1: Storage conditions of different hydrogen carriers.

Hydrogen Carrier	**Temperature(°C)**	**Pressure(bar)**
LH_2	-252.8	1
Liquid Ammonia (fully refrigerated)	-33.3	1
LOHC-DBT	20.0	1
LOHC-TOL	20.0	1

4.2 LH_2

A pure form of hydrogen, LH_2 has long played a role as a fuel in small niche markets such as for submarines and rocket propulsion. The reason for which is LH_2's favourable mass energy density and potential integration with a fuel cell (FC) system. Concept vehicles such as the BMW H2R has also applied LH_2 as a fuel. In order to facilitate use of LH_2 as an energy carrier, it must undergo two basic processes before use: liquefaction and regasification.

4.2.1 Liquefaction

LH_2 is produced by the cooling and liquefaction of hydrogen feed gas from ambient conditions to a temperature of approximately -253°C. Hydrogen liquefaction processes is usually performed in two refrigeration steps: precooling and cryogenic cooling[14]. Precooling is performed to an intermediate temperature of approximately -190°C, with liquid nitrogen acting as a refrigerant. Cryogenic cooling between -190°C and -253°C is achieved through the use of helium or hydrogen as a refrigerant.

Hydrogen has two isomers known as ortho- and parahydrogen which play an important role when considering liquefaction. Ortho- and parahydrogen are defined by their nuclear spin orientation. At standard conditions, hydrogen consists of 75% ortho-hydrogen and 25% para-hydrogen in equilibrium state[34]. However, LH_2 has an equilibrium composition of 99.8% para-hydrogen. Since ortho to para conversion is exothermic, complete conversion should ideally take place during liquefaction. Otherwise, a large fraction of the liquid will evaporate during storage due to spontaneous conversion. A catalyst must be integrated in the liquefaction process in order for the ortho to para hydrogen conversion to take place at an acceptable rate.

The theoretical work for liquefaction of hydrogen from standard temperature and a pressure of 20 bar, is approximately 3.0 kWh/kg, shown by the light blue dashed line in Figure 4.3. In Figure 4.3, exergy efficiency of liquefaction is defined as the ratio between the specific work for an ideal hydrogen liquefaction process, ω_{ideal}, and the specific energy consumed by the real process ω_{real}. Exergy efficiency is expressed in Equation 4.1.

$$\eta_{ex} = \frac{\omega_{ideal}}{\omega_{real}} \tag{4.1}$$

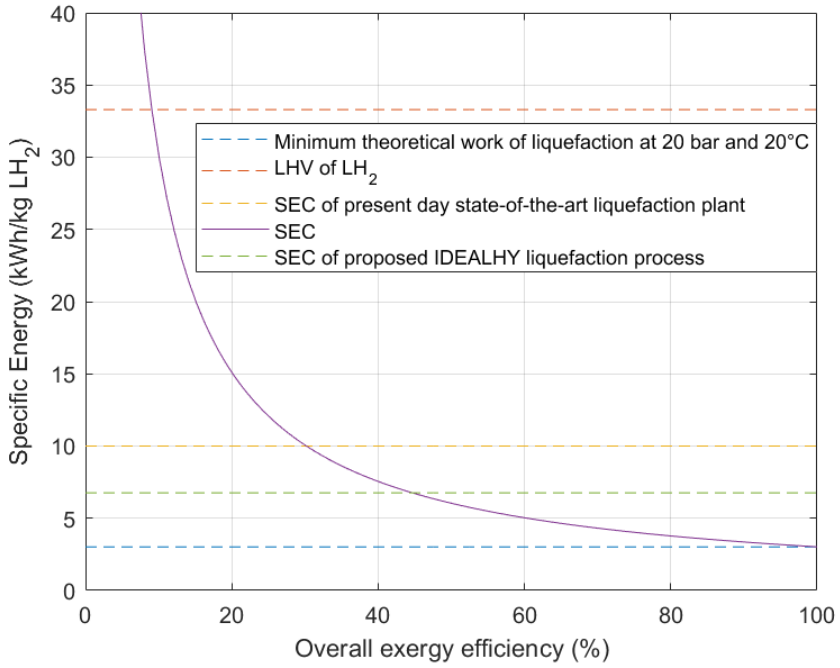

Figure 4.3: Specific Energy Consumption (SEC) of hydrogen liquefaction based on exergy efficiency. Own work.

Currently, a state-of-the-art hydrogen liquefaction plant with capacity for 5 tons LH_2 per day (tpd) consume about 10 kWh per kilogram output of LH_2[58]. This corresponds to a 30% exergy efficiency assuming that the feed hydrogen pressure is taken to be 20 bar. It is expected, that as liquid hydrogen is commercialized further as an energy carrier, significant gains in terms of exergy efficiency will be achieved in H_2 liquefaction processes. This is due to the fact that use of liquid hydrogen has largely been reserved for niche applications such as aerospace in the past, where there are few economic incentives for improving efficiency. In recent years, many studies have focused on improving the specific energy consumption (SEC) of liquefaction processes. One such study is IDEALHY[88], which has proposed a liquefaction process (shown in Figure 4.4) in which the SEC is reduced to 6.76 kWh/kg LH_2 (44% exergy efficiency) or 20.2% as a percentage of the lower heating value (LHV) of LH_2 with a plant capacity of 50 tpd. As a point of reference, a typical large natural gas (NG) liquefaction plant consumes $\approx$ 8% of the feed gas on a LHV basis [18], which corresponds to an exergy efficiency of approximately 45%. IDEALHY and other novel designs for hydrogen liquefaction processes are however, limited by economic viability and technological maturity[14]. From Figure 4.4, one may see that the propoesed IDEALHY process is very complex - 16 heat exchangers and 21 units of rotating machinery is needed.

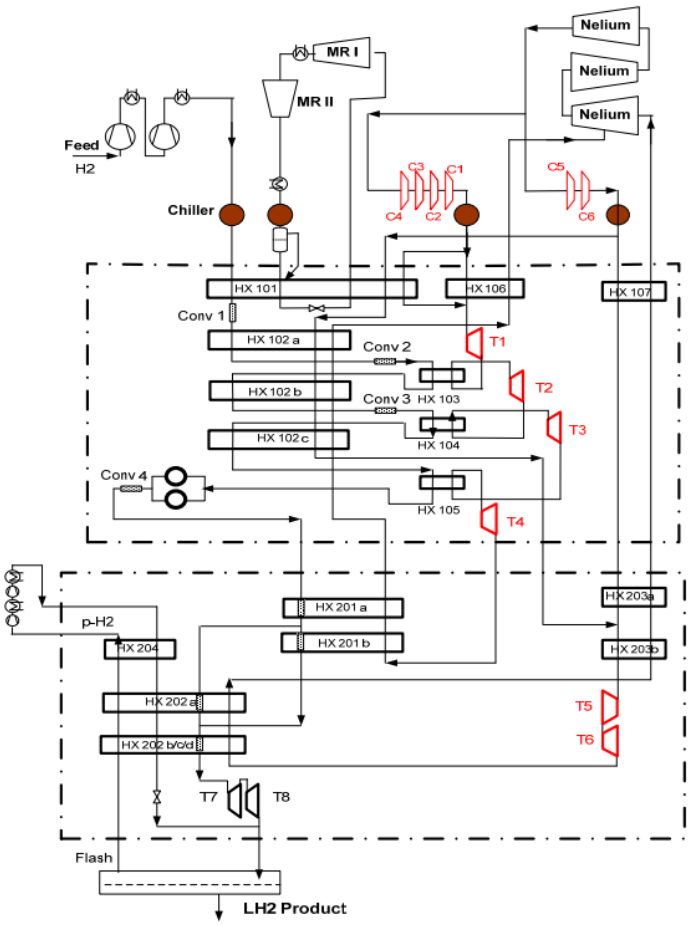

Figure 4.4: Process flow diagram of the IDEALHY process[88].

Until now, several industrial scale hydrogen liquefiers have been built and operated worldwide; especially in North America, Europe and Japan. In 2009, the worldwide hydrogen liquefaction capacity was 355 tpd [58], and has increased since then. Most recently built liquefiers have been dimensioned for capacities of around 5 tpd. This is however set to change as demand for LH_2 is increased because larger plants have large benefits with respect to specific costs of LH_2 as shown in Figure 4.5. The increasing demand for LH_2 is anticipated as a result of the increased usage of hydrogen as an energy carrier. Construction of the first large hydrogen liquefaction plant dedicated to hydrogen energy markets, by industrial gas company Air Liquide, commenced in 2019[2]. The liquefaction plant is to supply LH_2 to be used as fuel for the 40,000 fuel cell electric vehicles (FCEVs) anticipated to be deployed in California by 2022. Its capacity will be 30 tpd.

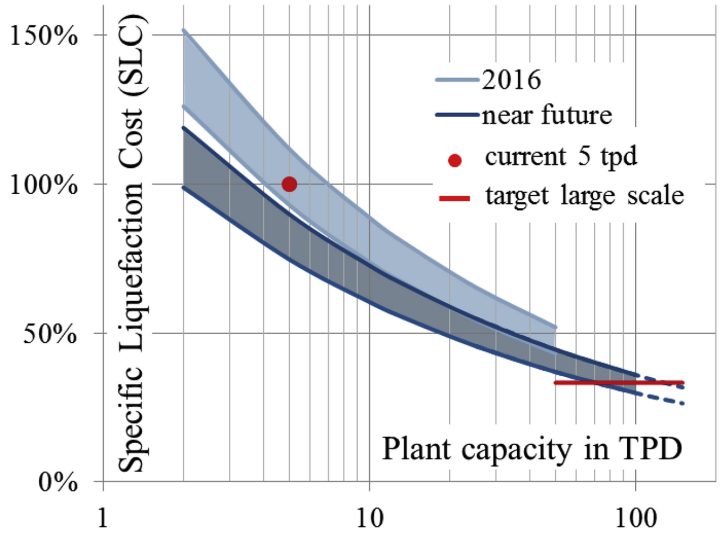

Figure 4.5: Relationship between hydrogen liquefaction capacity and specific costs associated with liquefaction[14].

An important point of information is that increased energy-efficiency in the liquefaction process does not necessarily lead to a reduced specific cost of liquefaction (SLC)[75]. This is due to the fact that capital expenditure (CAPEX) costs of liquefaction plants may become so high as to impact the total plant lifecycle costs to a large degree. It is therefore reasonable to assume that the optimum energy efficiency of liquefaction will not converge to the theoretical highest energy efficiency.

4.2.2 Regasification

Regasification is the process of turning a cryogenic fluid back to gaseous form. Currently, LH_2 regasification is not a common process in industry. Regasification plants have however, played an integral part of the LNG-infrastructure for decades and it is believed that LH_2- and LNG-regasification bear many resemblances[60]. A vital process in the LNG-industry, regasification evaporates LNG to become natural gas before utilisation in various applications such as power-generation. LNG regasification terminals operating today use a variety of different methods to vapourise LNG. Three of the most relevant methods technologies are described below.

By far the most prevalent technology used in LNG terminals operating today are open rack vapourisers heated by seawater, shown in Figure 4.6.

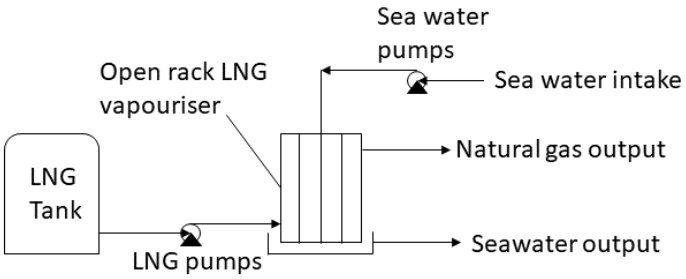

Figure 4.6: Working principle behind an LNG open rack vapouriser. Own work.

As many as 95% of LNG terminals worldwide use open rack vapourisers heated by seawater[1]. Since this technology relies on seawater as the primary heat source, it is effective only if seawater temperatures are above 5°C. The open rack vapouriser must be able to handle large temperature gradients (from -161°C to 5°C for LNG, and -253°C to 5°C for LH_2). This imposes strict demands on the materials used. Preventive measures must also be taken to deal with the corrosive nature of seawater. Since cold sea water is usually discharged directly into the ocean during regasification, local marine life may be affected depending on location.

Combustion heat vapourisers do not use sea water for LNG combustion. Instead, LNG is heated by the action of natural gas combustion; LNG flows through tube bundles that are submerged in a water bath heated by natural gas combustion. Exhaust gases emitted by the burner is fed directly through the water bath in order to provide heat. The principals of a combustion heat vapouriser is shown in Figure 4.7.

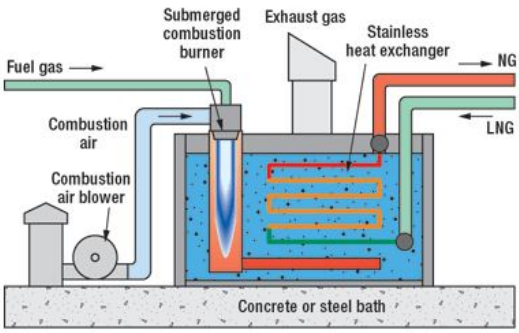

Figure 4.7: Working principle behind an LNG combustion vapouriser[77].

The biggest drawback of the LNG combustion vapouriser is the fact that the burner requires fuel amounting to approximately 1.5-2.0% of the energy content of the LNG (LHV)[1]. With reference to Table F.1, the heat of vapourisation for LNG and LH_2 is at a similar level. However, H_2 has a higher energy mass density, which suggests that LH_2 would require a lower percentage of total energy content (LHV) for regasification than LNG. Combustion vapourisers enables rapid load fluctuations as far as

regasification is concerned, creating flexibility in accordance with natural gas demand.

Ambient air vapourisers use heat energy from the ambient air to vapourise LNG. A series of surface heat exchangers make sure that air cools as it travels down and exits the bottom of the vapouriser. Air flow is controlled through the natural convection of cold, dense air, or by air fans. The principal operation behind an ambient air vapouriser is shown in Figure 4.8

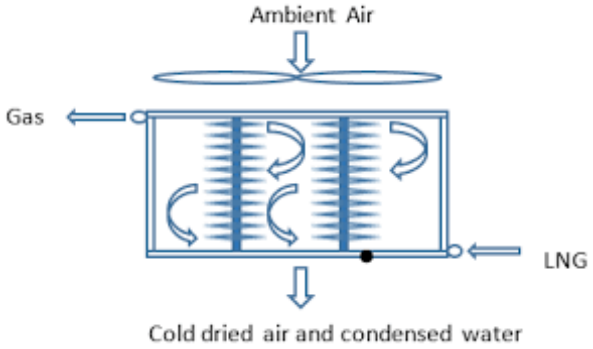

Figure 4.8: Working principle behind an LNG ambient air vapouriser[1].

Ambient air vapourisation is most suitable for areas with warmer ambient temperatures and where only small capacity LNG regasification is needed. In cooler climates, an additional heating system for the air is needed for effective operation. Since the heat capacity of air is much less than that of water, ambient air regasification requires more space and a larger number of vapourisers than both combustion heat and open rack vapourisers.

No LH_2 regasification terminals in operation today were found in a literary search. A pilot project in Japan, will see an LH_2 import terminal be built by 2020 by Kawasaki Heavy Industries in cooperation with Iwatani[104] . However, it is unclear whether or not this terminal will include regasification facilities, or will simply store LH_2 for transport further down the transportation chain.

4.3 Ammonia

Ammonia is a compound of nitrogen and oxygen with formula NH_3. Approximately 140 million tonnes of ammonia are produced annually. It is the second most traded industrial chemical in globally, and is used in a diversified set of industrial sectors, chief among which is agriculture as a fertiliser[99]. In the future however, ammonia might not only serve as an important product in agriculture, but also as an important energy carrier.

4.3.1 Nitrogen Production

Production of ammonia necessitates a source of nitrogen. In terms of cost and energy consumption, nitrogen production is the cheapest and least energy intensive process of all the modules that make up ammonia production[99]. Conventional nitrogen plants use the separation of air to produce nitrogen, hence they are called air separation units (ASUs). Currently, the two most important technologies for air separation are cryogenic air separation and pressure swing adsorption (PSA).

Cryogenic air separation consists of many steps. Firstly, air is compressed to approximately 8 bar, and re-cooled to ambient temperature with removal of water and CO_2 through molecular sieve absorbers. The air is then partially liquefied in a heat exchanger by residual gases. The mixture will at this stage consist of an oxygen-rich liquid and nitrogen-rich gas. Finally, the mixture is fed to a distillation column where pure nitrogen is the top product, and an oxygen-rich mixture as the bottom product. A distillation column may have a three-column design in order to reduce argon content of the nitrogen top product[99]. However, this implies higher capital costs for the ASU. Figure 4.9 shows a simplified diagram for a cryogenic ASU.

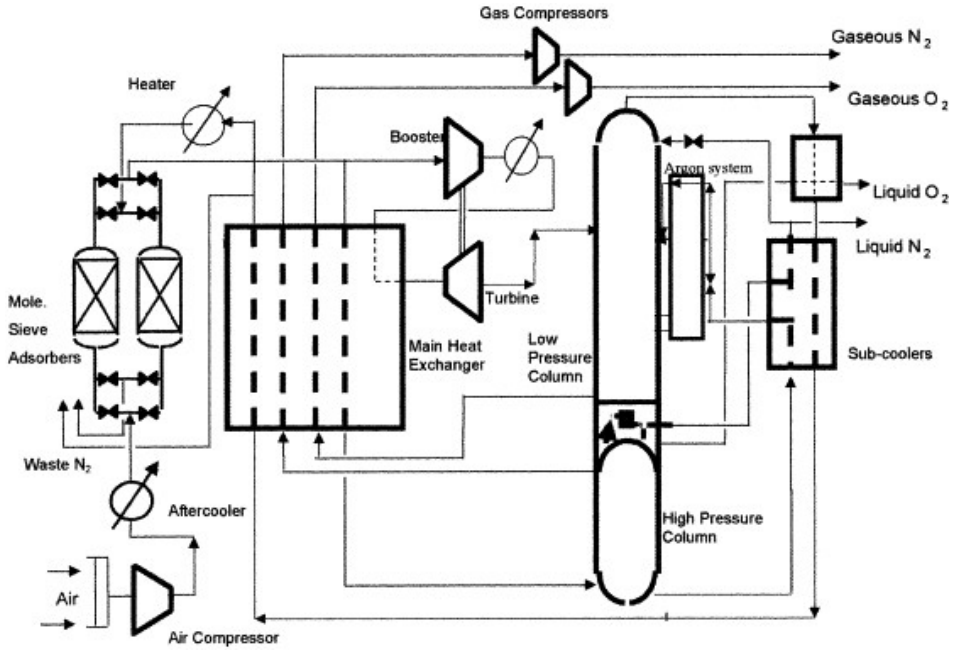

Figure 4.9: Simplified flow diagram for a cryogenic air separation unit[16].

Energy consumption in this process stems from compressors and coolers and is reportedly approximately 0.11 $kWh_e/kg\ N_2$[99]. The nature of a cryogenic ASU is such that it benefits from economies of scale to a large degree. Consequently, for applications involving large production levels, cryogenic air separation is presently most competitive ASU technology. Production range from cryogenic air separation units is from 7.5 - 63,000 tons N_2/day.

Pressure swing adsorption (PSA) plays an important role for small scale nitrogen production. PSA is characterised by four steps: pressurisation, adsorption, depressurisation and desorption. Figure 4.10 shows a simplified diagram of the process.

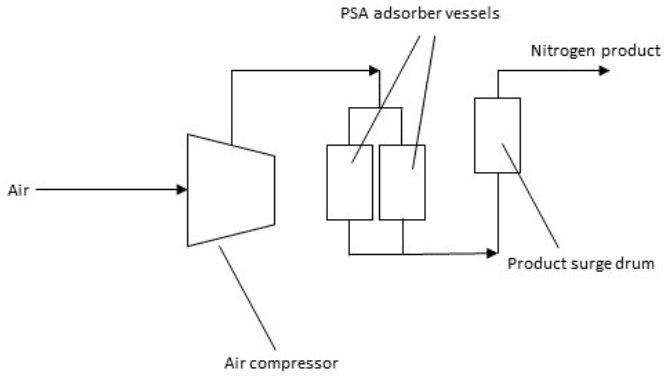

Figure 4.10: Simplified flow diagram for pressure swing adsorption air separation unit[16].

With reference to Figure 4.10, air is first compressed, before entering the adsorber vessels. The basic principle of air separation by PSA, is that high pressure oxygen binds more strongly to the adsorbent than the other constituents of air. The two adsorber vessels work in conjunction; while flow is entering one of the vessels, the other will desorb oxygen at lower pressures leaving behind a pure nitrogen product[16]. The product surge drum serves to smooth out variations in pressure and composition of the flow. A critical parameter of air separation PSA is the contact time in the adsorber vessels. A large contact time will increase the purity of the product. However, it will negatively affect production rates. This is the main reason for why PSA ASUs do not achieve as high a production rate as cryogenic ASUs with equivalent levels of purity. Production rates for high-purity N_2 are typically in the order of 150 tpd of N_2[99].

4.3.2 Ammonia Synthesis

The Haber-Bosch process is by far the most common way in which ammonia is made. It is technologically very mature, and used in ammonia plants worldwide. Nitrogen and hydrogen must be mixed in appropriate proportions, compressed and reacted together to form ammonia in the Haber-Bosch process. Nitrogen and hydrogen do not react with each other spontaneously at standard temperature and pressure, but reacts spontaneously at high temperatures and pressures in the presence of a catalyst. This is largely because of the strong triple-bond present in the nitrogen molecule. Even though there are many different configurations for ammonia synthesis plants, all plants have the same underlying process: mixed hydrogen and nitrogen gas (called "syngas") is compressed and converted to ammonia over a catalyst in a reactor. A mixture of hydrogen gas and nitrogen gas reacts over a promoted iron catalyst at temperatures of 400-500°C and pressures 100-250 bar[71] as shown in Equation 4.2.

$$N_2 + 3\,H_2 \rightleftharpoons {}_2NH_3 \tag{4.2}$$

A central part of any Haber-Bosch process is the ammonia synthesis loop, shown in Figure 4.11.

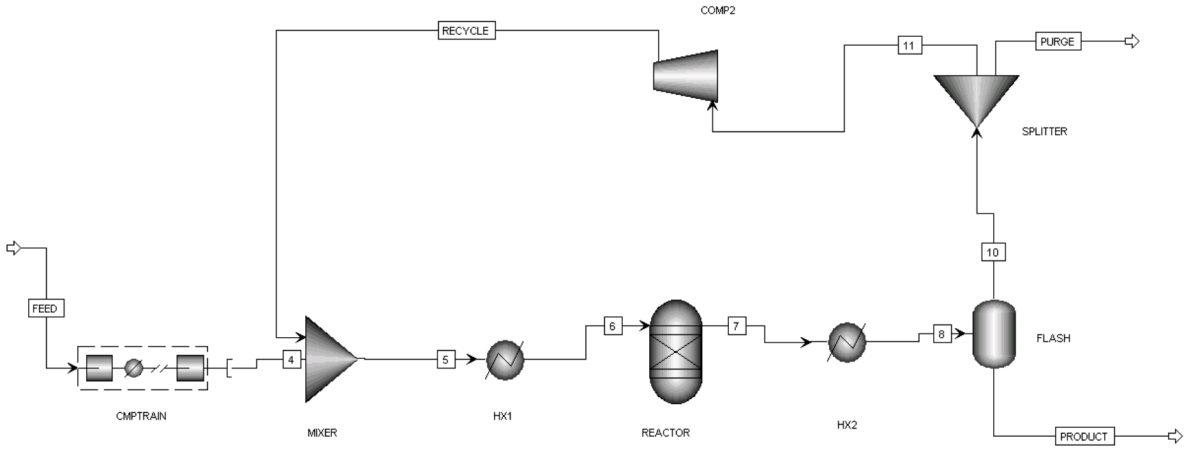

Figure 4.11: Simplified flow diagram for an Haber-Bosch ammonia synthesis loop[71].

Firstly, syngas enters a compressor train where pressure is raised to the required reaction pressure which ranges from 150-250 bar in most modern ammmonia plants. Inter-cooling between compressor stages is used to minimize compressor-work. Since the catalysts may become deactivated from sulphur compunds in the syngas, the syngas has a very high purity requirement. A purge stream is necessary due to the presence of small quantities of argon in the nitrogen stream from the ASU[99]. Because of the thermodynamic and kinematic constraints in the reaction, conversion rates per reactor pass tends to be around 20% in conventional Haber-Bosch loops. Consequently, a recycle stream is needed to avoid wasting expensive synthesis gas. Pressure drop in the loop normally amounts to around 6%[71], hence the need for a recycle compressor to bring syngas back to reactor pressure. Ammonia is separated from syngas in a flash drum, where it is forwarded to storage as a liquid. A mixer re-combines the recycled gas with feed syngas. Even though the recycling compressor has high mass flow input compared to the syngas compressors, the vast majority of work is done by the syngas compressors due to the high pressure increase[99]. Assuming that syngas is compressed from an initial pressure of 1 bar, the total power requirement of ammonia synthesis has been estimated to be approximately 0.64 $kWh_e/kg\ NH_3$ with a reactor pressure of 150 bar[71]. For initial feed pressure of 1 bar N_2 and 20 bar H_2, the electrical energy demand was simulated to be 0.26 $kWh_e/kg\ NH_3$ (1.47 $kWh_e/kg\ H_2$) using Hysys. More details are given in Appendix A.2.1.

One proposed alternative to the conventional Haber-Bosch ammonia synthesis process is electrochemical ammonia synthesis. Through the use of an electrolyser, ammonia may be produced from either hydrogen and nitrogen, or water and nitrogen. The latter option has the potential of bypassing the costly process of producing hydrogen from either natural gas or water electrolysis. Moreover, these solid state processes may allow operation at much lower temperatures and pressures than the conventional Haber-Bosch process. Electrochemical ammonia synthesis is however still technologically immature, and currently the attained rate of reaction is magnitudes away from being possible to commercialise. Figure 4.12 shows the principal behind electrochemical ammonia synthesis.

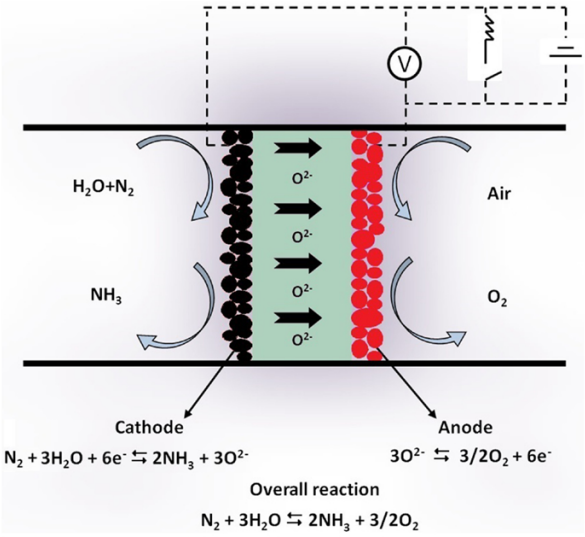

Figure 4.12: Principal behind electrochemical ammonia synthesis with nitrogen and water[31].

A key benefit with electrochemical ammomnia synthesis is that it is more flexible with regards to power inputs, making it easier to integrate intermittent renewable power sources such as wind turbines.

4.3.3 Ammonia Cracking

The dissociation of ammonia into nitrogen and hydrogen gas is an endothermic reaction usually conducted at high temperature in a process called cracking. The ammonia cracking process is shown in Equation 4.3), and is the reverse of NH_3 synthesis [107].

$$2\,\mathrm{NH_3} \rightleftharpoons \mathrm{N_2} + 3\,\mathrm{H_2} \tag{4.3}$$

The theoretical energy requirement of ammonia dissociation is 46.22 kJ/mol, equivalent to 0.75 kWh/kg NH_3 of thermal energy (14.5% of LHV). A mixture containing 75% hydrogen, and 25% nitrogen (as well as leftover ammonia) is the product. Ammonia cracking is not a new concept, but has been used in the metallurgical industry where it is used for the production of controlled atmospheres for heat treatment[81]. It is a catalytic reaction, and in the past, nickel heterogeneous catalysts have been widely employed for ammonia cracking; requiring a temperature in excess of 900°C for near-complete ammonia conversion. However, as the the use of catalysts in the process is optimised in the future, conversion temperatures below 500°C will be possible through the use of catalysts such as ruthenium [32].

Figure 4.13 shows the equilibrium conversion of ammonia at different temperatures and a pressure of 1 atm. It shows that the equilibrium conversion is higher as temperature increases. However, there will still be trace amounts of ammonia left even at very high temperatures.

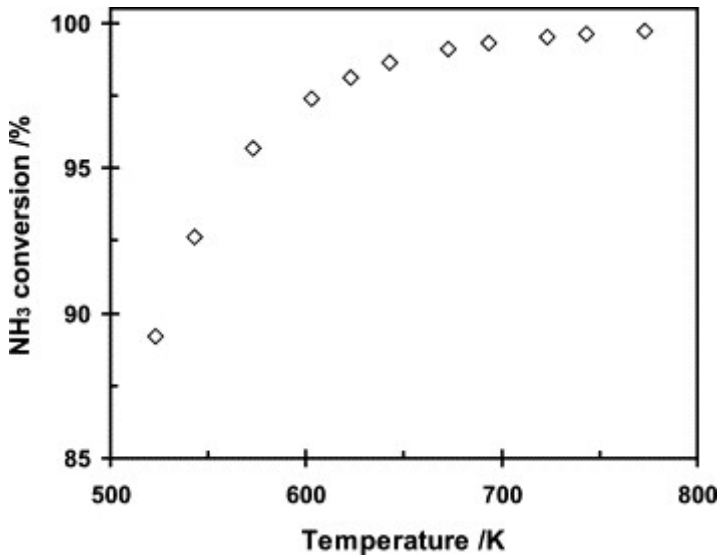

Figure 4.13: Equilibrium conversion of ammonia at different temperatures and 1 atm[106].

In the cracking reaction, it is possible to utilise waste heat from the gas products (N_2 and H_2) to heat up ammonia to the required temperature in the cracking reaction vessel. A principal diagram of the ammonia cracking process in shown in Figure 4.14.

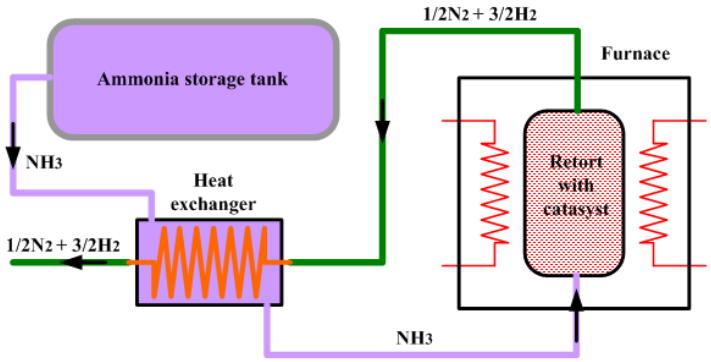

Figure 4.14: Principal behind ammonia cracking[24]. Waste heat from gas products is used to raise the temperature of ammonia before reaction.

Small ammonia cracking plants are in operation at low pressures. For large scale application the technology has been used in heavy water production. The Arroyito heavy water production plant in Argentina had a capacity to crack more than 3,000 tpd of ammonia. Plant and catalyst company Haldor Topsoe was the supplier for the Arroyito plant. No other suppliers are currently known [35].

The generation of hydrogen by the decomposition of ammonia results in a gas with 75% hydrogen and 25% nitrogen by volume. There are also still traces of ammonia which have not been converted as mentioned. The total conversion of NH_3 to N_2 and H_2 at 900°C and 40 bar is reportedly 99.5% [35]

using a conventional nickel catalyst. Depending on the application of the hydrogen product hydrogen, the purity of hydrogen must be increased. This is especially the case for proton-exchange membrane fuel cells (PEMFCs), where any residual ammonia could potentially contaminate the fuel cell by the permanently degrading of the electrolyte. That is why the purity standard for mobile PEM fuel cells (ISO14687-2) for use in fuel cell electric vehicles (FCEVs), sets a maximum concentration of 0.1 parts per million (ppm) of ammonia. Unless nitrogen gas is removed from the mixture, it will impose a significant energy penalty if the gas is to be compressed. Therefore, only 100 ppm of nitrogen gas is allowed. As a consequence, ammonia decomposition units for mobile PEMFCs must be equipped with the means for purification (removal of nitrogen in and of trace amounts of ammonia mixture).

Purification of hydrogen gas generated from ammonia decomposition has been the subject of much research in recent years. Removal of NH_3 and N_2 from the product stream may be achieved in one step, using a metallic membrane as shown in Figure 4.15. Membranes through which only H_2 molecules may permeate, are used to capture pure hydrogen from the ammonia decomposition products which include NH_3, N_2, and H_2. The retentate gases, including hydrogen which has not been absorbed by the membrane, are fed to a burner which provides thermal energy for the cracking process. The total energy consumption in an integrated ammonia cracking and purification facility has been estimated to 1.41 kWh/kg NH_3[32]. This includes a 86% recovery of H_2 in the cracker unit, with the remainder undergoing combustion in the burner.

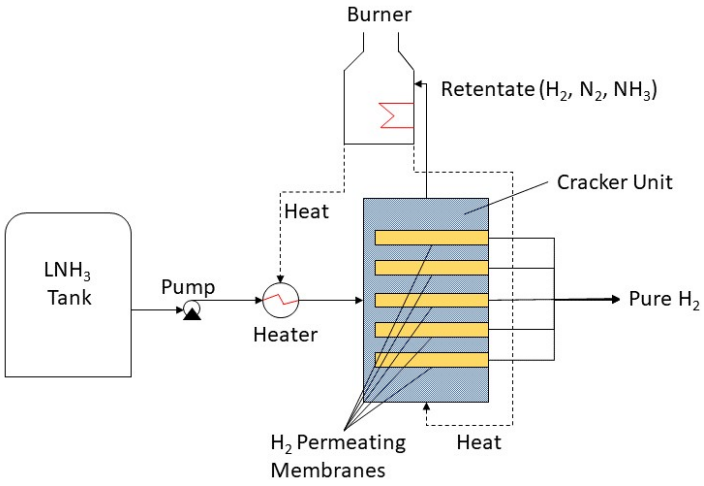

Figure 4.15: Integrated ammonia cracking with separation and purification of hydrogen through metal membranes. Adapted from [32].

The Commonwealth Scientific and Industrial Research Organisation (CSIRO), an Australian research agency, has developed a vanadium-based membrane to produce pure hydrogen from the product mixed gas in ammonia cracking [91]. Palladium-based membranes are also in use today. However, their application is limited due to the high cost of palladium.

Pressure swing adsorption (PSA) has applications for both air separation (as previously mentioned)

and hydrogen purification. PSA is a more technically mature way for hydrogen purification, compared to membrane separation and may be used to remove N_2 so that pure hydrogen is the product. PSA technology for removal of nitrogen from a N_2/H_2 gas mixture is based on the binding of N_2 gas molecules to adsorbent material. The ease at which N_2 molecules are bound to adsorbent material depends on many factors such as the choice of adsorbent material and the partial pressure of N_2 gas in the mixture. Adsorption is carried out at high pressure (typically 10 bar to 50 bar) until the equilibrium loading capacity is reached. Regeneration follows and is achieved by lowering the pressure inside the PSA vessel resulting in a respective decrease in equilibrium loading. Consequently, the nitrogen gas molecules on the adsorbent material are desorbed and the adsorbent material is regenerated [93]. Tail-gas consisting of hydrogen and nitrogen gas is released during regeneration. PSA units may be integrated with an ammonia cracking unit, where the tail-gas from the PSA system is burnt to provide heat for NH_3 decomposition. The hydrogen recovery rate is the ratio of the quantity of hydrogen from the feed that is recovered in the product. Commercial H_2 PSA purification systems have H_2 recovery rates between 80% and 90% for purities higher than 99.9% H_2 [38]. Removal of trace amounts of NH_3 in the product stream may be efficiently achieved prior to the PSA process by bubbling the H_2/N_2 gas mixture through water (scrubbing) due to the high solubility of NH_3 in water[32].

4.4 Liquid Organic Hydrogen Carrier (LOHC)

Through the formation of chemical bonds, hydrogen may be combined with various organic compounds to produce liquid organic hydrogen carriers (LOHCs). LOHCs are liquids or solids with low-melting points that can be reversibly hydrogenated and dehydrogenated. LOHC compounds retain their initial structure when hydrogen is released. LOHCs have hydrogen storage capacities ranging from 5.8 to 7.3 wt% [105]. A number of different materials have been proposed as potential LOHC materials. These include toluene, N-ethyl carbazole, dibenzyltoluene, formic acid, and naphthalene. However, research suggests that dibenzyltoluene (DBT) and toluene (TOL) are the LOHC materials with highest potential [105][73]. TOL and DBT are consequently the LOHC materials considered in this study.

4.4.1 Hydrogenation

During hydrogenation the hydrogen molecules are chemically bound to the liquid carrier by an exothermic catalytic reaction. This reaction is often realised at elevated temperatures and pressures. A generic hydrogenation reaction is shown in Equation 4.4.

$$\mathrm{H_0LOHC} + n\mathrm{H_2} \longrightarrow \mathrm{H}_n\mathrm{LOHC} \tag{4.4}$$

In Equation 4.4, $\mathrm{H_0LOHC}$ represents an arbitrary LOHC material. Before hydrogenation, both unloaded LOHC ($\mathrm{H_0LOHC}$) and hydrogen must be pressurised and heated to the required hydrogenation temperature and pressure. By recirculating hydrogen, all available hydrogen is bound to the LOHC material. After hydrogenation, the loaded LOHC stream is brought to ambient conditions, by cooling and decompression. Since the hydrogenation reaction takes place at an elevated pressure, prior to decompression, the product stream is saturated with hydrogen. Therefore, hydrogen is released during decompression. If not collected, approximately 0.1 wt% of the hydrogen is lost because of this[73]. Figure 4.16 shows a flow sheet of an arbitrary hydrogenation process.

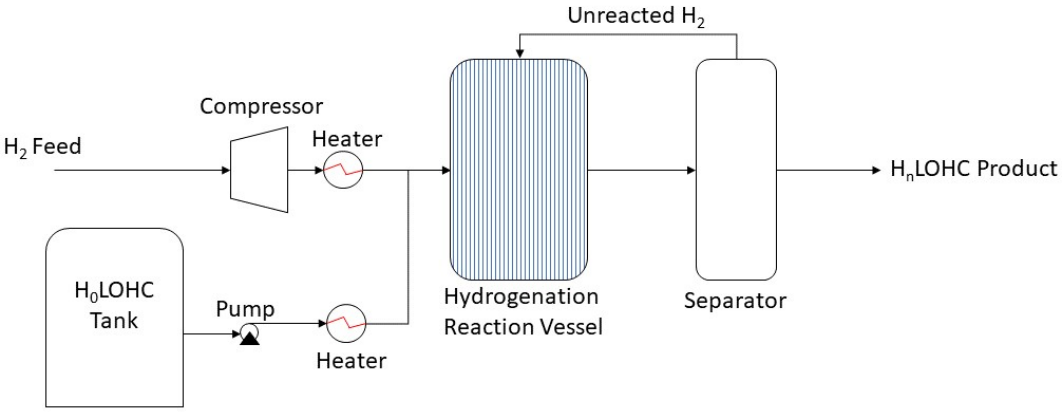

Figure 4.16: Sketch showing the working principle behind hydrogenation. Adapted from [73].

The conditions of the hydrogenation reaction depends on the LOHC material used. Table 4.2 shows the conditions necessary (in the reaction vessel) for TOL and DBT. Reaction enthalpy is also given.

Table 4.2: Hydrogenation reaction conditions for DBT and TOL[73].

LOHC Material	**Temperature(°C)**	**Pressure(bar)**	**Reaction Enthalpy (kJ/mol H_2)**
DBT	150	50	-65.4
TOL	200	20	-68.3

Heat is released at 150°C and 200°C for DBT and TOL respectively during hydrogenation. This waste heat stream could potentially be utilised, although this may be difficut due to its low grade. Also, a higher pressure is required for the hydrogenation of DBT, when compared to that of TOL. This gives the DBT hydrogenation an energy-penalty with respect to TOL. In both cases a catalyst is required for the reaction.

A literary review found only one LOHC hydrogenation plant in operation commercially in the USA. The system made by the German company, Hydrogenious, generates hydrogen using solar power and uses a small DBT hydrogenation plant to enable storage of hydrogen[85]. The highest-capacity hydrogenation plant offered by Hydrogenious (StoragePLANT 5000) has a capacity of 0.45 tons per hour, or 3.6 tpd [42]. As part of a pilot project, a small TOL hydrogenation plant will be built in Brunei and be operational by 2020 [90]. This hydrogenation plant will enable hydrogen export to Japan, and its construction will be the first time a hydrogenation plant is built separate from a dehydrogenation plant. The capacity of the pilot plant will be approximately 0.6 tpd [90].

4.4.2 Dehydrogenation

Dehydrogenation is the reverse reaction from hydrogenation, as shown in Equation 4.5.

$$H_nLOHC \longrightarrow nH_2 + H_0LOHC \tag{4.5}$$

The loaded LOHC stream is heated to the specific dehydrogenation reaction temperature and hydrogen is released in the reaction vessel. Unlike hydrogenation, dehydrogenation takes place at ambient pressure. Since the reaction is endothermic, the reaction vessel must be heated in order for the reaction to continue. The heat necessary for the dehydrogenation reaction to carry on may be provided by burning a fraction of the H_2 product stream. This is shown schematically in Figure 4.17. The product stream is cooled down-stream of the reactor before being separated in a vapour-liquid separation unit where H_0LOHC is removed from the hydrogen gas.

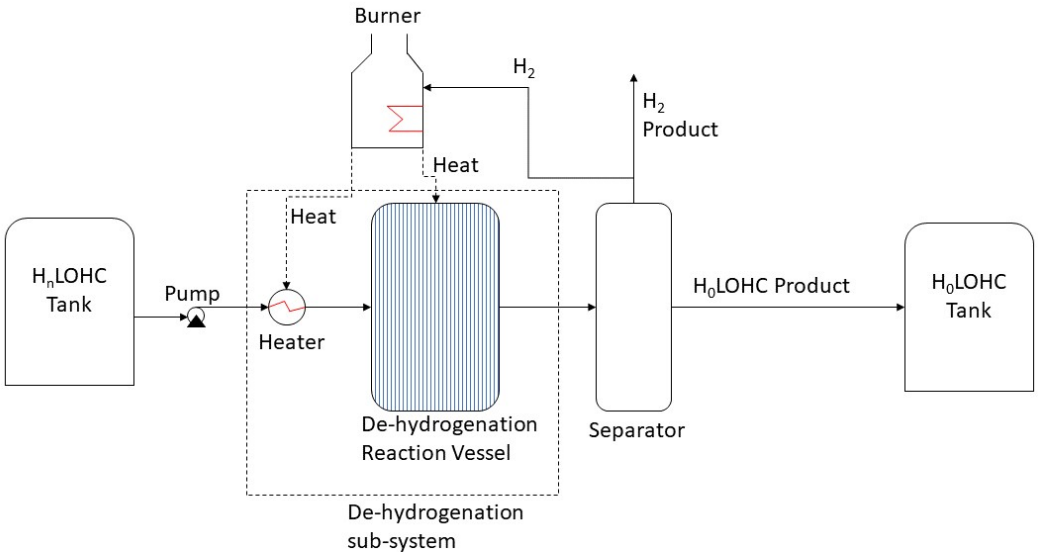

Figure 4.17: Sketch showing the working principle behind dehydrogenation. Adapted from [73].

Table 4.3: Dehydrogenation reaction conditions for DBT and TOL[73].

LOHC Material	**Temperature(°C)**	**Pressure(bar)**	**Reaction Enthalpy (kJ/mol H_2)**	**Conversion(%)**
DBT	310	1	65.4	97
TOL	320	1	68.3	95

As can be seen from Table 4.3, dehydrogenation of loaded TOL (TOL-LOHC) requires a slightly higher energy input than that of loaded DBT (DBT-LOHC). Moreover, the equilibrium conversion of TOL-

LOHC dehydrogenation is slightly lower than that of DBT-LOHC. Effectively, this implies that more of the TOL-LOHC will be transported back to the site of hydrogenation.

DBT dehydrogenation plants are currently offered commercially by Hydrogenious, under the trademark "ReleaseBOX". The ReleaseBOX 250 is the dehydrogenation plant offered with highest capacity of 0.18 tpd, no higher capcity plants are under development[41]. A pilot TOL dehydrogenation plant will be built in Japan and be operational by 2020[90]. This plant will enable import of hydrogen from Brunei, and will have a capacity of approximately 0.6 tpd.

Similarily to H_2 product gas from NH_3 cracking, H_2 gas produced from dehydrogenation needs to be purified. This is the case, irrespective of carrier material, for both TOL-LOHC and DBT-LOHC [8] [3]. Since LOHCs are liquid hydrocarbons, evaporation of the carrier molecule to gas phase, and consequentially, chemical conversion into by-products may introduce impurities to the output H_2 gas[3]. Product H_2 gas from dehydrogenation may be purified using similar methods to that of output H_2 gas from NH_3 cracking, explained in Section 4.4.2.

Chapter 5

Hydrogen and Ammonia as Future Marine Fuels

Use of hydrogen as an energy carrier has the potential to de-carbonisation large sectors of the world economy. The maritime industry is no exception. International Maritime Organisation (IMO) has adoped a resolution to cut CO_2 emissions by 50% by 2050, when compared to 2008[49]. If this ambition is to materialise, both pure hydrogen and hydrogen-carriers such as ammonia and LOHC is set to play a key role onboard ships producing power for propulsion and auxiliary needs. This chapter describes how H_2 and NH_3 may applied as fuels for green shipping.

5.1 Prospective Zero-Emission Ship Powering Options

Today, diesel engines provide the the principal mean of marine propulsion. Diesel engines may be categorised into: slow speed two stroke, medium speed two stroke, and high speed four stroke engines. The type of diesel engine used onboard a ship depends to a large degree on the design and operational profile of the ship. Dual-fuel and tri-fuel engines running on heavy fuel oil (HFO), natural gas (NG), and marine diesel oil (MDO) has also become common in liquid natural gas carriers (LNGCs). However, due to the inherent pollution problems of such carbon-based fuels (in relation to sulphur oxides (SO_x), nitrogen oxides (NO_x), CO_2 and particulate matter (PM)), a number of alternative fuels and propulsion systems have been proposed. Different alternative propulsion methods and fuels with zero tank-to-propeller GHG emissions are shown in Figure 5.1.

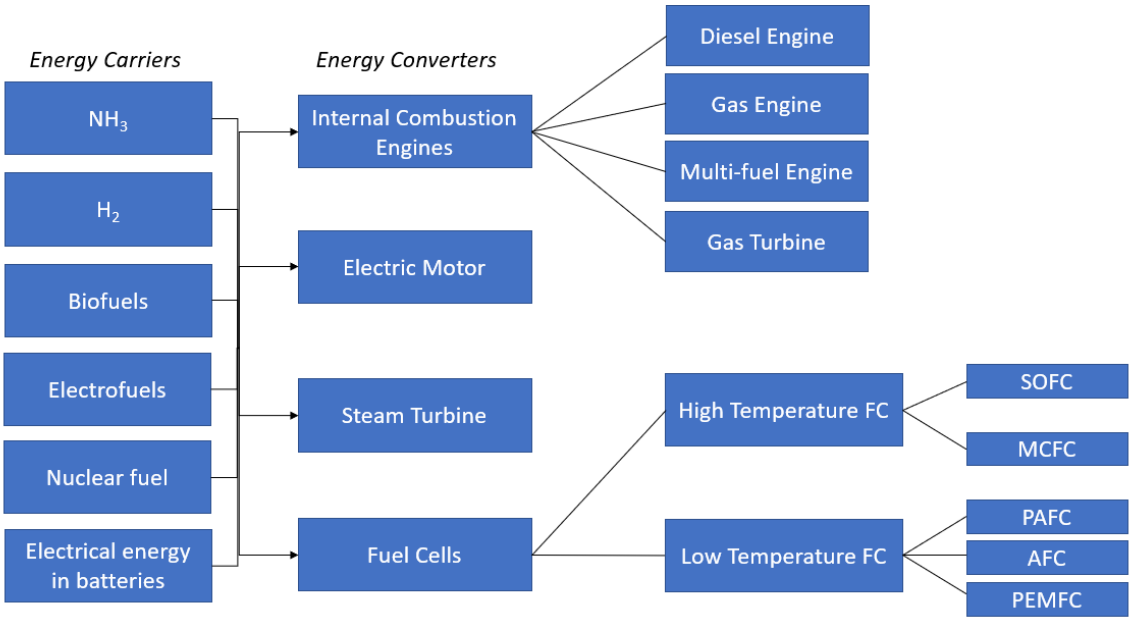

Figure 5.1: Alternative fuels and converters for zero-emission of GHGs. A combination of different energy converters (such as fuel cell and battery hybrid) is also possible.

Electrofuels (also known as e-fuels or synthetic fuels) is a term for carbon-based fuels such as diesel and methane, which are produced from CO_2 and water using electricity as the source of energy. CO_2 may be sourced from various industrial processes, the air, or seawater [23]. Even though CO_2 is a combustion product of electrofuels, electrofuels are carbon-neutral if they are produced from renewables, nuclear power or with CCS. A big advantage with electrofuels is the fact that they require little or no modification to already existing fuel infrastructure, including internal combustion engines (ICEs)[13].

Biofuels are derived from converting biomass (biological material) into liquid or gaseous fuels. They involve many different feedstocks and conversions, which ends up producing energy carriers such as diesel, methane and ethanol. Similarly to electrofuels, biofuels also release GHGs into the atmosphere during combustion. However, since CO_2 released during the combustion of biofuels is considered to be part of the CO_2 that otherwise would have been in circulation through natural cycles, biofuels are considered carbon-neutral.

This thesis is focused on propulsion systems utilising ammonia and hydrogen fuels. Different prime movers for ship propulsion systems utilising ammonia and hydrogen as fuels are described below.

5.1.1 Fuel Cells

Conversion of chemical energy to electrical energy takes place in a fuel cell (FC). Both batteries and FCs are electrochemical devices. The main difference is that in a battery, the electricity-producing reactants are regenerated in the cell by a recharging process, whereas in FCs producing reactants are

constantly supplied from an external source. There are many types of fuel cells, where the difference is mainly determined by the type of electrolyte being used. Moreover, the type of electrolyte being used has a large impact on the operating temperature of the FC. For this reason, fuel cells may be classified into high-temperature fuel cells, and low temperature fuel cells[59].

High-temperature FCs operate at temperatures greater than 600°C. This high temperature allows reforming reactions such as conversion of ammonia[32] into hydrogen and nitrogen to take place at the FC anode over a catalyst such as nickel or ruthenium. This is a significant advantage of high-temperature FCs as they do not necessarily rely on pure hydrogen for electricity generation. In addition, high-grade waste heat is produced in high-temperature FCs. This high-grade heat may be utilised for various purposes including combined cycle (CC) for power generation. Also, if loaded LOHC is used as a hydrogen carrier fuel onboard the ship, dehydrogenation could be achieved using waste heat from the FC system. On the other hand, there are disadvantages associated with the high operating-temperature of high-temperature FCs. There are challenges related to the selection of materials to withstand such high temperatures for an extended period of time, and long start-up times. Two examples of high-temperature fuel cells are Molten Carbonate (MCFC), and Solid Oxide (SOFC).

Low-temperature fuel cells typically operate below 250°C[59]. At these temperatures, ammonia cracking (or other reforming reactions) does not happen spontaneously at the anode. Therefore, these FCs require an external supply of pure hydrogen. Additionally, since they are operating at low temperatures, they produce low-grade heat. This heat is ordinarily too low-grade to be used for regeneration. Precious metal catalysts such as platinum are needed for electricity generation. On the other hand, low-temperature FCs exhibit fast start-up times due to their relatively low operating temperature. They also suffer fewer materials problems, and have several safety benefits owing to the low temperatures. Moreover, low-temperature fuel cells also have a tendency to exhibit a higher tolerance for cyclic operation[27]. Alkaline (AFC), Phosphoric acid (PAFC) and Proton Exchange Membrane (PEMFC), are all examples of different low-temperature fuel cells.

Solid Oxide fuel cells (SOFCs) and Proton Exchange Membrane fuel cells (PEMFCs) have been identified as among the most promising FC types for marine use by DNV GL and the European Maritime Safety Agency (EMSA)[27]. These fuel cell types will therefore be the object of further investigations in this thesis. Table 5.1 summarises the differences between SOFCs and PEMFCs.

Table 5.1: Comparison between SOFC and PEMFC. Partly adapted from [27].

Item	**FC Type**	
	Solid oxide (SOFC)	Proton exchange membrane (PEMFC)
Temperature (°C)	500-1000	50-100
Electrical Efficiency	60% (85% w/ heat recovery)	50-60 %
Relative Cost	High	Low
Lifetime	Moderate	Moderate
Maturity	Moderate	High
Electrolyte	Porous ceramic material	Humidified polymer membrane
Anode	Nickel yttrastabilised zirconia composite	Carbon support w/ platinum particles
Cathode	Strontium-doped lanthanum manganite	Carbon support w/ platinum particles
Advantages	High efficiency	Good cycling performance
	Possible heat recovery	Less strict material requirements
	Possible ammonia cracking at anode	Tolerance to load variations
	Tolerant to H_2 impurities	
Challenges	Slow start-up	Expensive platinum catalyst
	Strict material requirements	Sensitive to H_2 impurities
	Intolerance to load variations	

Both SOFCs and PEMFCs have been the subject of studies looking into FCs for maritime use. However, only PEMFCs have been used commercially so far, most notably in German Type 212A class submarines with modules from 30-50 kW each[27]. The German Alsterwasser passenger ship has been using a PEMFC system with power output 96 kW since 2008. While SOFCs have not yet been used commercially for marine applications (to the writer's knowledge), several projects have looked into the use of SOFCs in ships. This includes the SchiBZ project which aim to develop scalable, containerised SOFC systems for auxiliary power supply of commercial ships up to 500 kW.

5.1.2 Internal Combustion Engines

Internal Combustion Engines (ICEs) is a well-understood technology which has provided a reliable form of marine propulsion and auxiliary power generation for many decades in shipping. Today's marine ICEs are primarily diesel engines on heavy fuel oil (HFO) and marine gas oil (MGO), with many low-speed 2-stroke diesel engines achieving thermal efficiencies in excess of 50% under optimal conditions [23]. With the introduction of alternative fuels such as ammonia and hydrogen, however, design of new ICEs will have to adapt to accommodate a change in combustion properties from conventional fuels. There are a number of fuels which may be used in ICEs which are carbon-neutral. Table 5.2 shows different combustion properties of ammonia and hydrogen, compared with conventional diesel fuel and natural gas.

Table 5.2: Combustion properties of ammonia and hydrogen, compared with diesel and natural gas. Based on data from [56] and [83].

Properties	**Fuel**			
	Ammonia	Hydrogen	Diesel	Natural Gas
Chemical formula	NH_3	H_2	C_8 to C_{25}	C_1 to C_3
Flammability limit in air (%volume)	16-25	4-75	3-19	5-15
Adiabatic flame temperature (°C)	1800	2110	2082	1950
Laminar burning velocity in air (m/s)	0.07	2.91	0.7-1.5	0.36
Auto ignition temperature (°C)	650	585	363	580

As shown in Table 5.2, each fuel has different combustion properties which needs to be taken account of in the engine-design. This entails that current conventional engine designs will need to be changed in order to accommodate combustion of ammonia and hydrogen.

The hydrogen engine is not a new concept, but has been the subject of research for more than a century. Spark-ignition (SI) engines running on gasoline, may easily be converted to running on hydrogen. Conventional compression-ignition (CI) engines on the other hand, which usually run on diesel, cannot easily be converted to running on hydrogen [20]. This is largely due to the high auto ignition temperature of hydrogen compared to diesel, as seen in Table 5.2. A possible solution to this is to have the engine running on a dual-fuel mixture of hydrogen and diesel. Until now, no CI engine has been developed based on hydrogen's specific combustion properties. It is clear that such an engine would need a higher compression-ratio (than conventional CI engines) for the hydrogen to auto ignite. Hydrogen-fueled SI engines have however been developed, reaching a thermal efficiency of approximately 45% [102][36]. Even though hydrogen-fueled engines produce no GHGs, NO_x emissions are an issue due to hydrogen's high flame temperature. Operating the engine in lean mode, achieves reduced NO_x emissions[20]. Development of hydrogen-fueled internal combustion engines (H_2-ICE), has to some degree been restricted to the automotive sector so far. Car makers such as BMW and Ford have manufactured several demonstration models [20].

Similarly to H_2-ICE, ammonia-fueled engines (NH_3-ICE) have have a long history[57]. Both SI and CI engines have been operated with ammonia in the past. However, as a result of ammonia's low flame velocity and high auto ignition temperature, it has been found necessary to use combustion promoters such as gasoline, diesel or hydrogen along with ammonia [76]. Since hydrogen has zero carbon emissions when combusted and may be produced by the thermal decomposition of ammonia inside the engine, it is a particularly promising combustion promoter. Experiments have shown that even small amounts (approx. 3% H_2-NH_3 ratio) by mass added to air-ammonia mixture is effective to speed up combustion in order to keep an ICE running smoothly[30]. Production of NO_x in the engine is significant for a large span of ammonia-to-air ratios, necessitating a method of NO_x abatement. Moreover, experiments with ammonia-fueled SI engines, report a peak thermal efficiency of approx. 32%[101]. CSIRO gives the best case thermal efficiency of an ammonia combustion engine as 40%[32]. These thermal efficiencies are however only applicable to engines dimensioned for road transport. In

the maritime industry, ammonia has also received attention as a potential future fuel. The marine engine manufacturer MAN B&W recently launched a dual fuel engine running on either LPG (with pilot oil ignition) or HFO. Reportedly, relatively minor adjustments need to be taken to turn the engine into one running on ammonia with a quoted thermal efficiency of approx. 50%[64].

The gas turbine is another power-generating device which may be used for propulsion onboard a ship. Currently, commercially available gas turbines with bottoming cycles for merchant ships may have a peak thermal efficiency of 43%[79]. For partial loads, thermal efficiency of gas turbines drops significantly. Consequently, many ships with gas turbine propulsion have additional power generation options such as diesel engines. If gas turbines are used in a combined cycle with steam turbines, the total thermal efficiency may approach close to that of low-speed diesel engines. Application of ammonia and hydrogen as fuel in gas turbines is still in its early stages. However, hydrogen gas turbines are considered to be more technically mature than ammonia-fueled gas turbines[75]. The main challenge with regards to ammonia-fueled gas turbines is the very high associated emissions of NO_x [64]. A selective catalyst reduction (SCR) system is currently the best way of removing NO_x from exhaust gases. Another challenge is the low flame velocity of ammonia which contributes to a low combustion efficiency. Gas turbines fueled by hydrogen gas is also under development. The main motivation for this development so far, has been to integrate gas turbines with coal gasification combined cycles with carbon capture and storage (CCS).

5.1.3 Steam Turbine

The steam turbine has to a large degree been replaced as the prime mover on merchant-vessels since the 1950s, and have been replaced by diesel engines [70]. They may, however, still be found on some specialised ship types such as LNG carriers and coal carriers. The most important reason for the steam turbines loss of market share to diesel engines is due to its comparably low thermal efficiency. Both ammonia and hydrogen may undergo combustion in boilers to provide thermal energy for steam.

5.1.4 Electric Motors

All electric propulsion systems on-board ships require an electric motor to convert electric energy into mechanical energy. Marine electric motors typically operate at a high efficiency of 96-97% [62]. Conventionally, electric motors have been applied in diesel-electric propulsion systems which have a long history in ship propulsion. However, they will also find their use in electric propulsion systems which are not powered by diesel, but rather alternative fuels such as ammonia and hydrogen. For ship propulsion based on FCs, electric motors are a necessity. For energy converters including NH_3-ICE and H_2-ICE, electric motors are not necessarily needed as these energy converters output mechanical energy.

5.2 Waste Heat Recovery Systems

Inevitably, all propulsion machinery produce waste heat lost to the environment. Waste heat recovery (WHR) systems are devices implemented in ship power plants in order to recover some of the thermal energy otherwise lost. WHR systems may be categorised as follows[9]:

1. *Heat-to-heat*: Recovery of waste heat from ship machinery for fulfilling onboard heat demand. This is currently common practice on ships. Waste heat is used to generate steam which is then distributed to different users on the ship, for instance fuel heating, HVAC and freshwater generators.

2. *Heat-to-power*: Recovery of waste heat from ship machinery for generating mechanical power. Heat-to-power recovery is less common on ships than heat-to-heat recovery as it requires higher grades of heat in order to be economically feasible[82].

There are many different WHR technologies available. Turbochargers are driven by exhaust gas and may increase the efficiency of a reciprocal ICE by forcing extra compressed air into the combustion chamber. Power turbines utilise the engine exhaust gas to produce mechanical power directly. Power turbines and turbochargers are however only applicable to internal combustion engines.

Rankine cycles are also important with regards to ship WHR technologies. Conventional Rankine cycles operate by generating high-pressure steam which undergoes expansion in a turbine - generating mechanical power. For some applications, especially when only low-temperature waste heat is available (less than 250°C), it is advantageous to use Organic Rankine Cycles (ORC) [9]. The working process is similar to that of the conventional Rankine cycle, but different working mediumes are used.

The potential of WHR systems to turn waste heat into useful work, depends on both the magnitude of the waste heat stream, and its temperature(see Table C.1). Consequently, the potential for WHR depends to a large degree on the type of energy converter (i.e. ICE, FC etc.). The marine engine manufacturer MAN Diesel & Turbo reports that it may increase the total efficiency of its slow-speed marine diesel engines by approximately 5% using WHR systems[66]. Similarly, gas turbines may be used in combination with steam turbines in bottoming cycles to increase overall efficiency. Although steam turbines for propulsion has become obsolete to in most vessel-types today, Mitsubishi Heavy Industries reports that using a re-heat WHR system, its energy conversion efficiency may be raised by 15%[69]. As far as fuel cells are concerned, PEMFCs do not produce high grade heat suitable for WHR. However, through a co-generation process, the combined electrical conversion efficiency of SOFCs may be raised by 25%[27].

Besides heat-to-power WHR systems, heat-to-heat WHR is of particular importance for systems using hydrogen and ammonia as fuel. With reference to Section 4.3.3 and 4.4.2, cracking of NH_3, and dehydrogenation of DBT/TOL-LOHC (and regasification of LH_2 to a lesser extent) are endothermic reactions which require heat. A WHR system may easily be used to provide necessary thermal energy for these reactions, given that the source of heat is of appropriate magnitude and sufficiently high-grade.

5.3 Demonstrational Projects

Although alternate fuels such as hydrogen and ammonia are still in their infancies with respect to their use as fuels, several projects - both commercial and for research are taking place. A few selected projects where hydrogen and ammonia are applied as marine fuels are described below. Also outlined are projects which investigate marine transport of hydrogen.

5.3.1 Application as Fuel

In 2019, the Norwegian Public Roads Administration and the shipping company, NORLED, signed an agreement which will lead to the construction of the world's first operational hydrogen-electric ferry in 2021. The ferry will operate as part of the national road-network and at least 50% of the ferry's power requirement will be sourced from hydrogen fuel. The ferry will have a capacity of up to 299 passenger and 80 cars and hydrogen will be stored as liquid hydrogen (LH_2) inside the fuel tanks. While compressed hydrogen might also have been a competitive form of hydrogen for the vessel, LH_2's scalability for use in larger ships was decisive for the selection [97]. PEMFCs will produce electricity for the ship's electric propulsion system.

The cruise ship company, Viking Cruises, is planning to build the world's first cruise ship powered by LH_2 and fuel cells[95]. The ship's length overall (LOA) is 230m, with an onboard capacity of 1400 people. As part of the project, LH_2 bunkering vessels to supply fuel to the cruise ship are also looked into. A major benefit of using hydrogen as fuel for cruise-ships is its compatibility with fuel cells, which provide power with minimal noise.

Ship-design firm C-JOB sees ammonia as a sustainable and clean fuel for shipping[19]. The ability to be used directly in both FCs and ICEs is a major benefit for NH_3 as fuel. Technical feasibility and cost effectiveness of an ammonia tanker fueled by its own cargo (as depicted in Figure5.2) will be the subject of study in a project lead by C-JOB. The project aims to build a pilot propulsion system using ammonia as a fuel in combination with FC or NH_3-ICE prime movers[12].

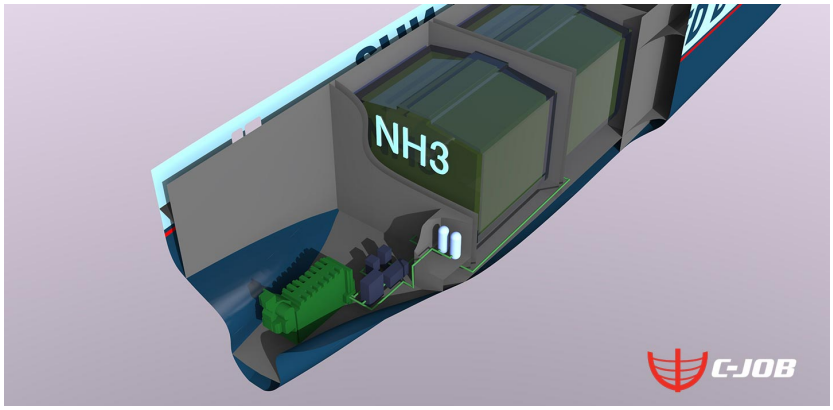

Figure 5.2: Graphical depiction of a NH_3 tanker fueled by its own cargo[19].

5.3.2 Marine Transport of Hydrogen

A pilot project in Japan run by Advanced Hydrogen Energy Chain Association for Technology Development (AHEAD), will transport approximately 210 metric tons of hydrogen (equivelant to powering 40,000 FCEVs) to Japan annually, from 2020 [90]. The hydrogen will be produced in Brunei, using steam-reformation of methane. An LOHC storage system, using toluene as the storage medium, will enable the hydrogen to be carried at ambient pressure and temperature in cargo ships. Necessary infrastructure such as a hydrogenation and dehydrogenation plants will be constructed in Brunei and Japan, respectively.

Another pilot project in Japan (HySTRA) will see the world's first dedicated small-scale hydrogen cargo ship being built by Kawasaki [54], shown in Figure 5.3. The ship will have a tank capacity of ($1250m^3 \times 2$), and will carry LH_2 sourced from the gasification of brown coal in Australia. The ship will use conventional diesel engines for propulsion and auxiliary power. A hydrogen liquefaction plant and receiving terminal will be built in Australia and Japan respectively. The intent is to build a full scale $160{,}000m^3$ LH_2 ship using experience from the pilot project in the long term.

Figure 5.3: Graphical depiction of the small-scale LH_2 cargo ship by Kawasaki [54].

Chapter 6

Methodology for Modelling of Transportation Chains

Which hydrogen carrier is best-suited for bulk marine transport of clean energy over large distances? Answering this question is difficult as it depends on a wide variety of input-variables and boundary conditions. However, in the planning of future energy policy, it is necessary to not shy away from such challenges. In this thesis, a model has been developed to evaluate the performance of each hydrogen carrier on the basis of different technical and economical indicators. This chapter gives a brief description of this model, along with all technical and economic indicators used.

6.1 Systems Theory

Systems theory aim at analysing objects with the intent of understanding, modifying or predicting their structure and behaviour [21]. Whether it concerns transportation chains, technical systems such as a ship's propulsion systems, or ecological systems, systems theory look at the object of study separated from its environment and search for solutions to enhance its performance. The search is primarily shaped by a unique problem definition. Therefore, systems in study are generally different from one another, as they depend on both the problem definition and sometimes on the person performing the analysis. Each system may be regarded as consisting of a number of elements. Separated from the rest of the world by system boundaries, the parts outside the system is called the environment or surroundings. Mutual relationship exists between each elements with each other and with each respective element's environment. Interactions between a system's elements with the environment occur through input or output of for example material or energy. Figure 6.1 shows the generic concepts of the systems theory approach to problem-solving, exemplified by marine transport of oil from an offshore rig to an on-shore refinery.

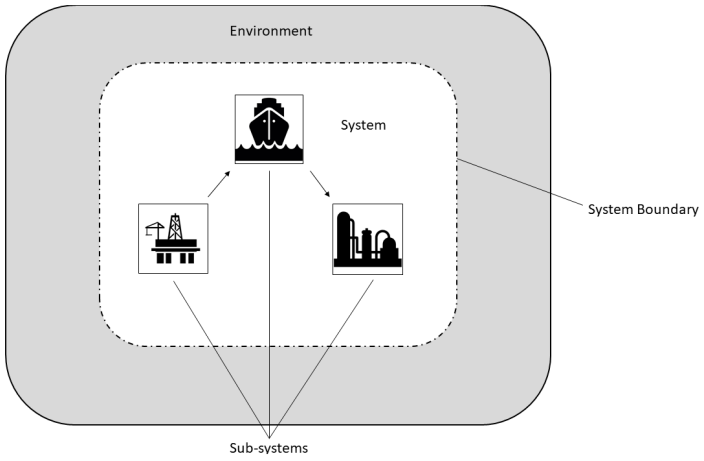

Figure 6.1: Depiction of general concepts within systems theory. Own work.

Normally, a system may be divided into several sub-systems considered part of a larger system. Hence, there can be many system levels where elements are found at the lowest level. The environment consists of elements that have any relationship to the system but are not part of it [21]. For instance, a marine engine may be considered a system. The engine interacts with its environment, the ship, by converting chemical energy to mechanical energy. However, the marine engine may also be perceived as a sub-system of the engine room, which in turn is an important sub-system of the vessel. Extending the system boundaries further, the ship may be considered part of a larger transportation chain. In this thesis, various system boundaries are used to study marine transportation chains of hydrogen.

6.1.1 Blackbox Approach

The blackbox approach is an important principle within systems theory. It focuses on the external relationships, starts from the system as a whole and does not look at the internal elements and relationships. By solely concentrating on the external relationships of the system with its environment it studies the interactions between these relationships to understand the behaviour of the system [21]. The advantage of the blackbox approach is found in the elimination of the internal details of the system. The blackbox approach is used widely in this thesis to simplify systems, and is illustrated in Figure 6.2.

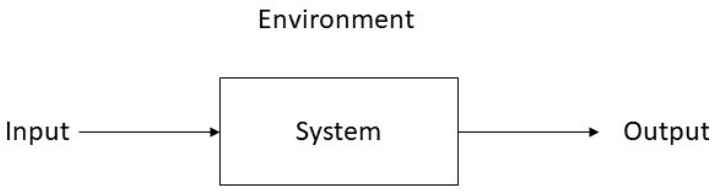

Figure 6.2: Graphical depiction of the blackbox approach.

6.2 System Boundaries and Overview of Transportation Chains

The fundamental premise of each transportation chain is that pure hydrogen at an initial state of 20 bar and 20°C is transported by various energy-conversion processes, until reaching a final state of 40 bar and 20°C at the end-destination. Production of hydrogen and its end-use is deliberately left out of each system, as this thesis' primary focus is to evaluate the transportation methods. The key assumptions made in the system modelling may be summarised as follows:

1. *Exclusion of production and end-use*: Production and end-use of H_2 is out of scope for this study. Consequently, it is outside the systems boundary.

2. *Consumption of cargo*: At various energy conversion processes in each transportation chain (namely dehydrogenation, NH_3 cracking and LH_2 regasification) heat is required as an energy input. In all such cases, it is assumed that heat is drawn from the consumption of hydrogen cargo.

3. *Pure hydrogen*: A major premise for the hydrogen transportation chains is that pure hydrogen is obtained at the final export destination. Since both the H_2 product output from the NH_3 and loaded LOHC has impurities, steps need to be taken to remedy this.

4. *Zero-Emission Shipping*: Only concepts for zero-emission vessels (ZEVs) are used for marine transportation of hydrogen in all transportation chains. In this thesis, ZEVs are taken to be ships with no direct emissions of GHGs or sulphur oxides (SO_x), with minimal emissions of nitrogen oxides (NO_x). Emissions of NO_x is kept to a minimum by the use of selective catalytic reaction (SCR) systems for propulsion systems using ICEs.

5. *Utilisation of Cargo as Shipping Fuel*: During shipping, the energy consumption of each ship is assumed to be covered by utilisation of cargo as fuel. Hence, enough cargo to power the cargo-ship for ballast voyage is left in the tanks after offloading cargo to export-destination.

6. *Energy conversion efficiency of ship propulsion*: Vessels are assumed to operate propulsion machinery at constant energy conversion efficiency at all times during the voyage.

7. *Use of electric energy*: For energy conversion processes which require an input of electric energy, electric energy is assumed to be drawn from the grid. Depending on the location at which electric energy is needed, electric energy is drawn from the Norwegian mainland grid, Svalbard grid or Japanese grid. The quantity of electric power used from the grid is deemed to be on a scale such that no improvements of grid infrastructure or capacity is necessary.

A description of all evaluated hydrogen transportation chains and associated system boundaries will follow. Diagrams showing the different schemes is shown in Figure 6.4, 6.5, and 6.6. Figure 6.3, shows the legend of these diagrams.

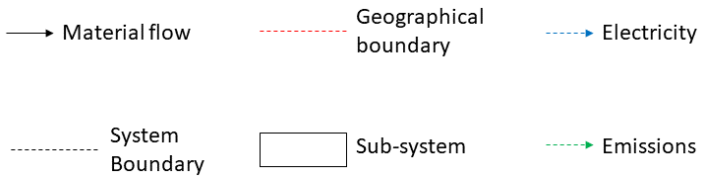

Figure 6.3: Legend to flow-charts.

6.2.1 LH_2

H_2 gas at ambient temperature and a pressure of 20 bar is fed into a liquefaction plant. The liquefaction plant is operated within the same parameters as projected by the IDEALHY project [88], and use electricity from the Norwegian electric grid. The end-product of the liquefaction process is liquefied hydrogen (LH_2) at a temperature of -253°C and atmospheric pressure. The LH_2 stream is then transferred to an on-shore transit storage tank, where all H_2 boil-off-gas (H_2-BOG) is re-liquefied so that there are no hydrogen losses. After a transit waiting period, LH_2 is loaded onto an LH_2 tanker. High amounts of H_2-BOG will be generated during the loading operation and returned to the on-shore storage tank for re-liquefaction using a vapour return line. The LH_2 tanker utilises cargo as fuel during both laden and ballast voyage, either as H_2-BOG or LH_2 pumped from cargo tanks. When the LH_2 tanker arrives at the export destination, LH_2 cargo is offloaded into transit storage tanks. A vapour return line facilitates re-liquefaction of H_2-BOG during the offloading operation. Enough cargo is left in the cargo tanks of the LH_2 tanker to power the ship during ballast voyage and for tank cooling purposes (similar to the *heel* of LNG tankers). During transit storage, H_2-BOG is re-liquefied in the tanks. After the transit storage period, liquid hydrogen is pressurised by pumps to a pressure of 40 bar before regasification. In the Japan-scenario, it is assumed that an open-rack seawater vapouriser. For the Svalbard-scenario, on the other hand, an air vapouriser is used. Cold ambient temperatures in Svalbard necessitates the consumption of hydrogen cargo in order to raise the temperature sufficiently. After regasification, hydrogen gas at 40 bar and ambient temperature is the end-result.

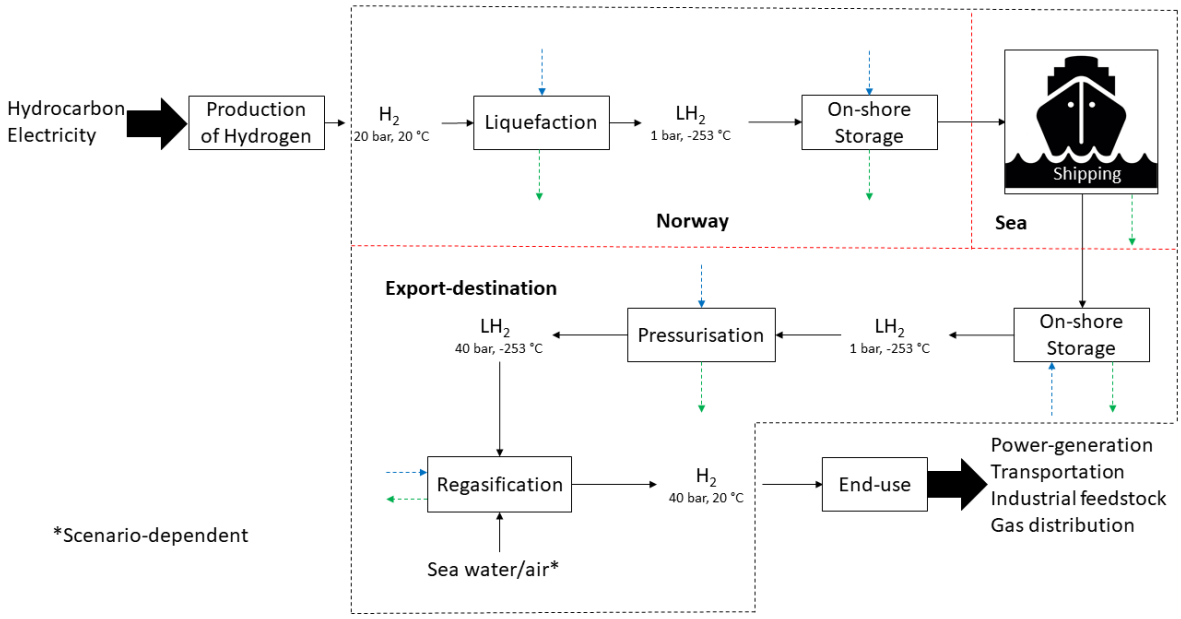

Figure 6.4: Flow-chart showing the system boundaries and steps associated with the LH_2 transportation chain.

6.2.2 NH_3

The NH_3 transportation chain requires a source of nitrogen gas. A cryogenic air separation unit (ASU) produces pure nitrogen gas with an end-state of 8 bar. Nitrogen at 8 bar and H_2 gas at 20 bar is fed into an all-electric Haber-Bosch ammonia synthesis plant, where liquid ammonia (LNH_3) is produced. Refrigerated on-shore storage-tanks are used for storage of LNH_3, before it is loaded onto the ammonia tanker as cargo. The ASU, synthesis plant and the refrigerated tanks draw power from the Norwegian electric grid. The ammonia tanker uses its own NH_3 cargo as fuel for producing propulsion and auxiliary power during laden and ballast voyage. When arriving at the receiving terminal in Japan, LNH_3 is offloaded from the ammonia tanker to an on-shore refrigerated transit storage tank. Enough cargo-fuel for powering the NH_3 tanker for the return ballast voyage is left in the cargo tanks after offloading. Pumps pressurise LNH_3 to a pressure of 40 bar before cracking. A cracking plant located nearby decomposes ammonia into nitrogen and hydrogen gas. The hydrogen gas is then purified through a pressure-swing adsorption (PSA). Trace amounts of NH_3 is removed by scrubbing. The products from the PSA process is pure hydrogen gas at 40 bar, and a low-pressure tail-gas mixture consisting of H_2 and N_2. The tail-gas is fed into the NH_3 cracker and provides thermal energy necessary for the decomposition of the ammonia.

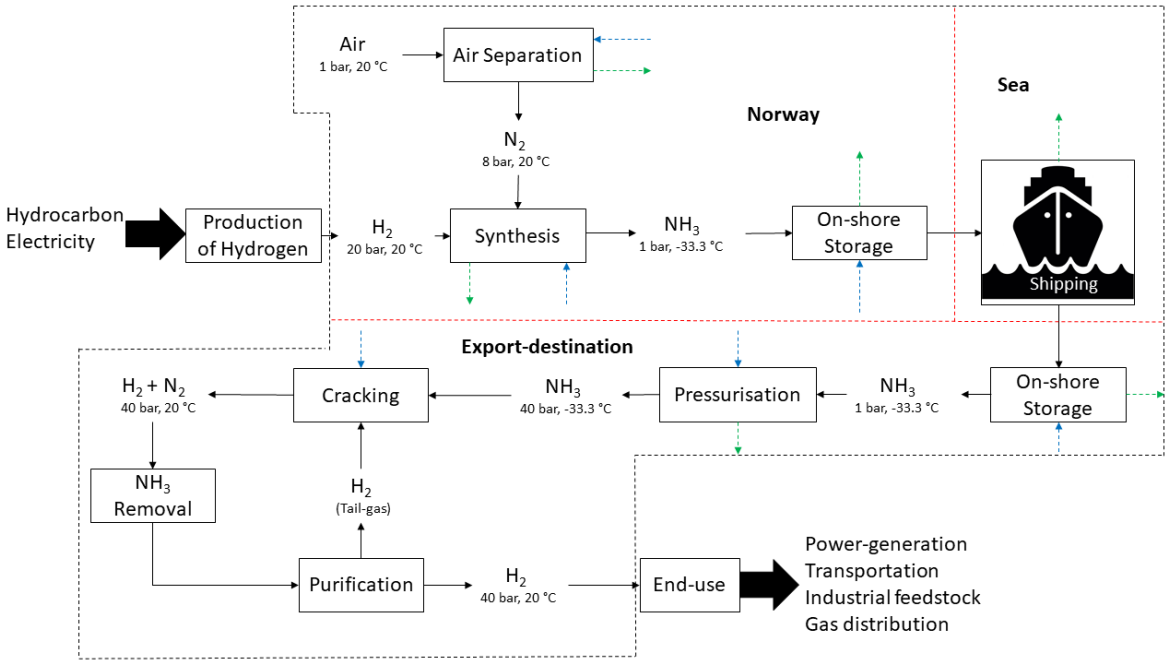

Figure 6.5: Flow-chart showing the system boundaries and steps associated with the NH_3 transportation chain.

6.2.3 LOHC

Hydrogen gas undergoes a hydrogenation reaction with an LOHC material (DBT/TOL) to form a liquid organic hydrogen carrier (DBT/TOL-LOHC) in a hydrogenation plant. Depending on the LOHC material used, hydrogen needs to be compressed to a pressure of 50 bar (DBT) or not at all (TOL) before hydrogenation. The hydrogenation plant is located in Norway and draws power from the Norwegian electric grid. The hydrogenation plant produces low-grade waste heat which is not exploited in the model. After transit storage near the export terminal, DBT/TOL-LOHC is shipped in ambient conditions in an LOHC tanker. The LOHC tanker is fuelled by hydrogen from its own DBT/TOL-LOHC cargo during both laden and ballast voyage. Therefore, enough cargo for powering the ship during ballast voyage is left after offloading cargo at the end-destination. At the receiving terminal, LOHC is offloaded from the ship and stored in tanks before undergoing dehydrogenation at a dehydrogenation plant. After dehydrogenation, the LOHC tanker is re-loaded with DBT/TOL for transportation back to Norway. H_2 gas product from dehydrogenation is purified by a PSA system, where the H_2 tail-gas is used to provide thermal energy for dehydrogenation. Since hydrogen gas at 1 bar is the product of the dehydrogenation reaction, it needs to be compressed to a pressure of 40 bar.

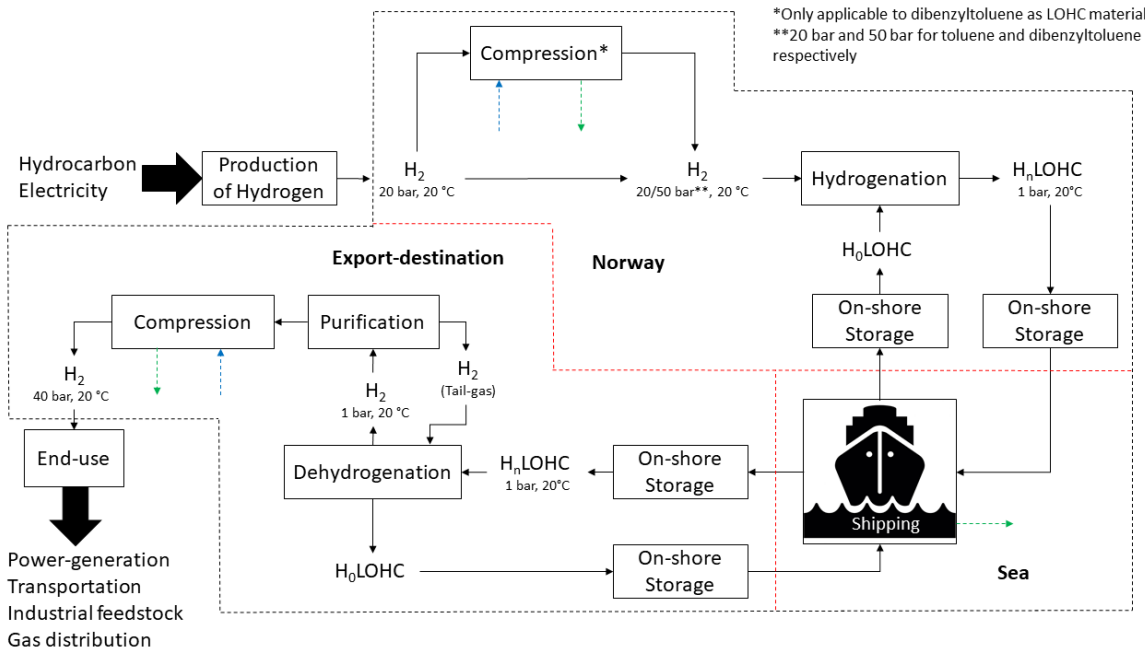

Figure 6.6: Flow-chart showing the system boundaries and steps associated with the LOHC transportation chain. H_nLOHC represents loaded LOHC, while H_0LOHC represenst unloaded LOHC.

6.3 Modelling of Transportation Systems

As a way of analysing the transportation systems shown in Figure 6.4, 6.5, and 6.6, a model is used. The model evaluated the performance of each hydrogen carrier by the calculation of different technical and economical indicators as shown in Figure 6.7. The model is primarily written in Microsoft Excel, with supplement usage of Matlab for the more complex calculations.

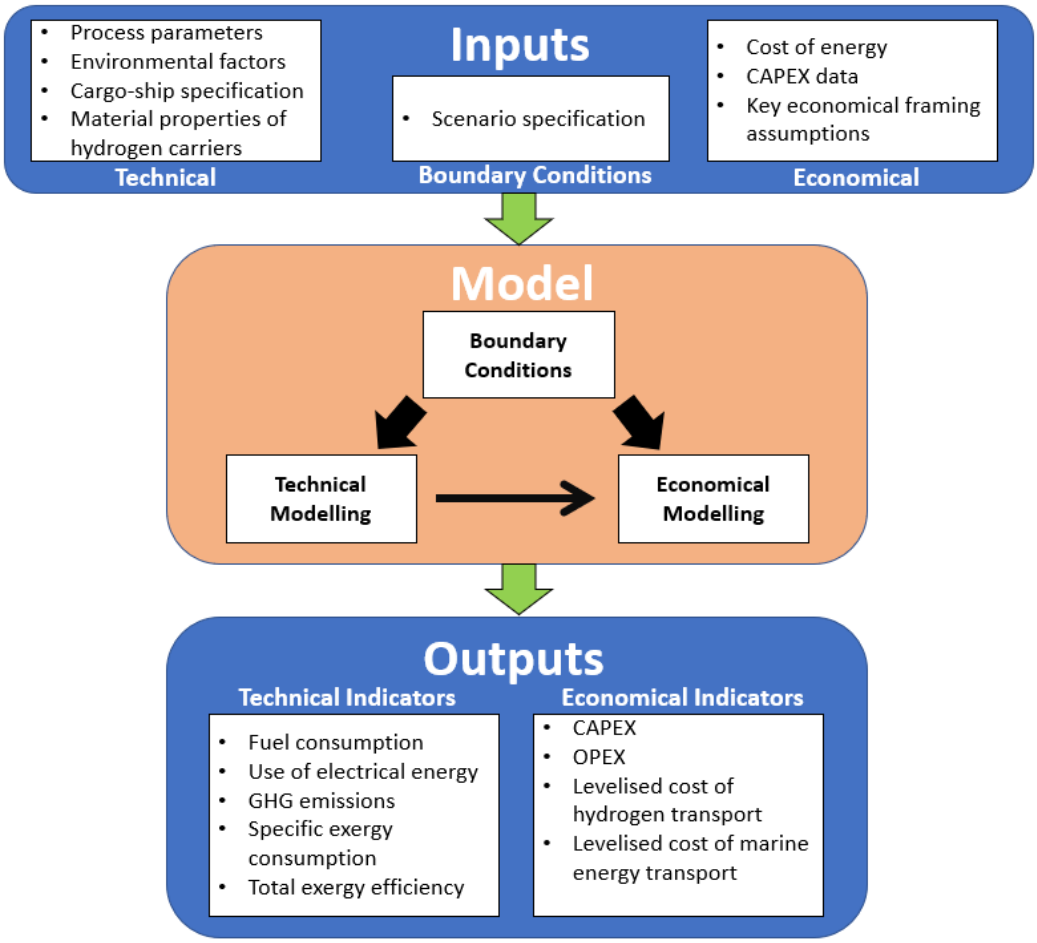

Figure 6.7: Simplified schematic description of model applied to assess different hydrogen carriers with regards to transportation.

The input variables to the model may broadly be defined as follows:

- *Technical parameters*: Parameters which provide the basis for calculation of technical indicators. Includes items such as energy usage in energy-conversion processeses, grid GHG intensity and material properties of hydrogen carriers.
- *Economical parameters*: Parameters which provide the basis for calculation of economical indicators. Primarily restricted to cost of grid electricity use, cost of fuel, and CAPEX data.

- *Boundary conditions*: Parameters which are scenario-specific e.g. is unique for a particular scenario.

The model processes the input parameters, outputting technical and economical indicators for each given hydrogen carrier and scenario. Section 6.4 and 6.5 describes the technical and economic indicators used in the thesis.

6.4 Technical Indicators of Transportation System

In order to assess each transportation chain from a technical perspective, a set of technical indicators are used. These indicators relate to the energy, the environment, maturity and complexity of each hydrogen transportation chain.

6.4.1 Energy

Energy consumption at different stages in each transportation chain may be categorised by the following:

1. *Electric energy*: For energy conversion processes which require an input of electric energy, electric energy is assumed to be used from the grid. Depending on the location at which electric energy is needed, electric energy is drawn from the Norwegian mainland grid, Svalbard grid or Japanese grid.

2. *Thermal energy*: For endothermic energy conversion processes which require an input of heat, heat is assumed to be derived from the combustion of cargo in each case. Thus, unlike electric energy, thermal energy is derived internally in the system. Likewise, in the ship sub-system, energy for propulsion and auxiliary purposes is assumed to be derived from the consumption of cargo.

Since a transportation system inherently involves a flow of mass from one destination to another, energy consumption for each transportation chain is given as power consumption in Chapter 8. The unit notation used for electrical power is MW_e, whereas MW is used for thermal power.

Specific Exergy Consumption

The specific exergy consumption (SEC) is a measure of the consumed exergy per kg delivered H_2 in each transportation chain. It is calculated using Equation 6.1.

$$e_{SEC} = \frac{\sum_{i=1}^{n} E_{in,i}}{3.6 \cdot \dot{m}_{del}} \tag{6.1}$$

$E_{in,i}$ = Rate of exergy input in process i (MW).
$\dot{m}_{del}$ = Delivered mass flow to end-destination (kg H_2/s).
e_{SEC} = Specific exergy consumption (SEC) per kilogram delivered H_2(kWh/kg H_2).

Transportation Efficiency

The transportation efficiency is a measure of the exergy efficiency of each transportation chain. It is given in Equation 6.2.

$$\eta_{tran} = \frac{e_{out}}{e_{in}} = \frac{e_{H_2}}{e_{SEC} + e_{H_2}} \tag{6.2}$$

e_{H_2} = Specific chemical exergy of hydrogen (kWh/kg H_2)).
η_{tran} = Transportation efficiency.
e_{out} = Delivered exergy to export-destination (kWh/kg H_2).
e_{in} = Total exergy input to transportation chain (kWh/kg H_2).

6.4.2 Environment

Due to the framework in which each transportation chain operates, emissions of GHGs are only taking place indirectly as a consequence of use of electric power from the grid. Appendix E gives estimates for the GHG emissions associated with the use of electric power from the Norwegian mainland grid, Svalbard grid, and Japanese grid. Using these estimates, CO_2 emission flows are calculated.

The total GHG emissions of a transportation chain for the duration of a year is calculated by Equation 6.3.

$$\dot{m}_{CO_2} = \frac{\sum_{i=1}^{n} E_{el,i} \cdot t_{op}}{3.6} \cdot \frac{GHG_{int}}{10^9} \tag{6.3}$$

The specific carbon emissions (SCE) is the CO_2 emissions per kg of H_2 delivered in each transportation scenario. It is given by Equation 6.4.

$$SCE = \frac{\dot{m}_{CO_2} \cdot 10^9}{m_{del,annual}} \tag{6.4}$$

SCE = Specific carbon emissions (gCO_2/kg H_2)
$E_{el,i}$ = Rate of electric energy input in process i (MW_e).
t_{op} = Annual operating time (s).
GHG_{int} = GHG intensity factor (gCO_2/kWh_e).
$m_{\dot{CO_2}}$ = Total rate of CO_2 emissions ($ktonCO_2$/year).
$m_{del,annual}$ = Mass of H_2 delivered annually to export-destination (kg H_2/year))

6.4.3 Technical Maturity

A mature technology is a technology that has been used and operated for a significant amount of time, so that most of its initial faults and inherent problems have been eliminated or reduced by technology development. Advances in a mature technology only happen at a slow speed, incrementally. For relatively immature technologies however, advances are often rapid and diverse. One method of describing the maturity of a technology is by the use of technology readiness levels (TRLs). The TRLs were initially developed by NASA and adopted by various industries as a scheme to determine the technical maturity of new technologies. Table 6.1 gives a proposed TRL scale used by the EU Research and Innovation programme *Horizon 2020* [39]. The scale consists of a ranking from 1-9, where 1 represents concepts that are scarcely developed and 9 represents technology that is fully developed and operational. This TRL scale is adopted in the study.

Table 6.1: TRL Scale[39].

TRL	**Development Stage Completed**
Research	
1	Basic principles observed
2	Technology concept formulated
3	Experimental proof of concept
Development	
4	Technology validated in lab
5	Technology validated in relevant environment (industrially relevant environment in the case of key enabling technologies)
6	Technology demonstrated in relevant environment (industrially relevant environment in the case of key enabling technologies)
Deployment	
7	System prototype demonstration in operational environment
8	System complete and qualified
9	Actual system proven in operational environment (competitive manufacturing in the case of key enabling technologies; or in space)

Technological Maturity is a key parameter for determining a technology's readiness for implementation.

6.4.4 Complexity

The complexity of the different cases of hydrogen transport considered in this investigation depends on the applied technology. The following factors are considered when evaluating complexity:

1. The number of process units required.
2. The process energy consumption.
3. Need for special procedure or resources.

Table 6.2 gives a scale from which the complexity of different hydrogen transport processes is judged in this study [55].

Table 6.2: Complexity scale[55].

Complexity designation	Low	Moderate	High	Very High
Needs	No particular need for special procedure or special resources.	Some need for special procedure or special resources.	Relying on extraordinary resources and experts.	Relying on extraordinary resources and expertise. Innovation.
	Few process units required compared to the other cases.	Moderate number of process units required.	Moderate/High number of process units required.	High number of process units required compared to the other cases.
	Low energy consumption and small amount of process waste.	Moderate energy consumption and large amount of process waste.	Moderate/high energy consumption and large amount of process waste.	High energy consumption and large amount of process waste.

6.5 Economical Indicators of Transportation System

All economic analyses made in this thesis are made on the basis shown in Table 6.3.

Table 6.3: Key economic assumptions.

Parameter	**Value**	**Unit**
Construction Period[1]	5	years
Operating Time	25	years
Discount Rate	6	%
Annual operating days	355	days/year
Fixed OPEX	2.5	%/CAPEX per year

[1]Ships are assumed to have a construction time of two years.

The reference year is set to be 2024. All future cash flows are therefore assumed to be discounted back to 2024. Construction is assumed to be starting in year 2025, lasting until 2029. Operation time is from 2030 to 2055. Since the scope of this thesis exclusively focuses on transportation of hydrogen, rather than production and end-use, all economic analysis is made on the basis of cost, not profit. Several economic indicators are used in this thesis to assess the economic performance of each hydrogen transportation chain. These economic indicators are given below.

6.5.1 OPEX

Operating expenditure (OPEX) is funds used for running each element of the transportation system. In Figure 6.4, 6.5, and 6.6, each element is represented by a box. In this study OPEX may be categorised into:

1. *Fixed OPEX*: Includes items such as direct labour costs, administrative costs, operating and maintenance costs, insurance, class and taxes. It is assumed in this study that fixed operating costs of each element is equivalent to 2.5% of its CAPEX.
2. *Variable OPEX*: Costs related to the consumption of fuel and use of grid electricity for each transportation chain.

Table 6.4 and 6.5 shows the basis on which variable OPEX is calculated from.

Table 6.4: Internal cost of hydrogen as fuel.

Scenario	**Cost (NOK/kg H_2)**
Japan	21
Svalbard	42

Table 6.5: Assumed cost of electricity. Based on current prices of electricity in Norway and Japan, including taxes.

Grid	**Cost (NOK/kWh$_e$)**
Norway (mainland)	0.7
Japan	1.2
Svalbard (Longyearbyen)	0.7

It is important to note that **the *internal cost of hydrogen as fuel* is the cost of consuming hydrogen cargo internally in each transportation chain**. It is therefore not necessarily directly related to the market-price of hydrogen.

6.5.2 CAPEX

Capital Expenditure (CAPEX) is funds used to buy or improve capital assets such as ships, buildings or equipment. In this study, the capital expenditure includes the construction and installation costs for each capital asset. CAPEX is based on figures available in litterature, such as the H21 Report[35], and are given in Appendix H.

Economies of Scale

It is normal for a unit of capacity in a large plant to cost less than that of a small plant. This property may be attributed to economy of scale. In this study the rule of six-tenths shown in Equation 6.5 is used as a scaling method for estimating CAPEX of the transportation chains.

$$C_B = C_A \left(\frac{S_B}{S_A} \right)^m \tag{6.5}$$

Where m is the scaling factor and C_A and C_B is the CAPEX of plants with size S_A and S_B respectively. In this investigation, m is set to be 0.7.

6.5.3 Levelised Cost

Levelised costs are the discounted lifetime costs of ownership and operation of different capital assets, often expressed on the basis of energy or mass. In the context of this thesis, levelised cost is expressed a measure of the economic cost per mass unit of hydrogen transported from Norway to the end destination. It is calculated in accordance with Equation 6.6, and includes all elements which are part of each hydrogen transportation chain.

$$LCoHT = \frac{Total\ Lifetime\ Cost}{Total\ Lifetime\ Mass\ Output} = \frac{\sum_{t=1}^{n} \frac{CAPEX_t + OPEX_t}{(1+r_D)^t}}{\sum_{t=1}^{n} \frac{m_{del,t}}{(1+r_D)^t}} \tag{6.6}$$

Equation 6.7 gives the levelised cost on an energy basis. The application of Equation 6.7 is exclusively for calculating costs associated to shipping in this thesis. Hence, costs related to items like buffer storage and on-shore energy conversion plants are excluded. The energy unit used is million British thermal unit (MBtu) to allow easy comparison with cost of LNG shipping, which is often expressed on an MBtu basis.

$$LCoMET = \frac{Total\ Lifetime\ Cost\ of\ Shipping}{Total\ Lifetime\ Energy\ Output\ of\ Shipping} = \frac{\sum_{t=1}^{n} \frac{CAPEX_{t,shipping} + OPEX_{t,shipping}}{(1+r_D)^t}}{\sum_{t=1}^{n} \frac{E_{del_{shipping},t}}{(1+r_D)^t}} \tag{6.7}$$

LCoHT	= Levelised Cost of Hydrogen Transport (NOK/kg H_2).
LCoMET	= Levelised Cost of Marine Energy Transport (NOK/MBtu).
$CAPEX_t$	= Total capital expenditure of transportation system in year t (MNOK) .
$OPEX_t$	= Total operational expenditure of transportation system in year t (MNOK).
$OPEX_{t,shipping}$	= Total operational expenditure of cargo vessels in year t (MNOK).
$CAPEX_{t,shipping}$	= Total capital expenditure of cargo vessels in year t (MNOK).
r_D	= Discount rate.
n	= Economic lifetime of transportation chain (years).
$E_{del_{shipping},t}$	= Energy (on a LHV basis) delivered by cargo-ships in year t (MBtu).
$m_{del,t}$	= Mass of hydrogen delivered in year t (kg).

Chapter 7

Analysis and Optimisation of Marine Transport Alternatives

The application of H_2 and NH_3 as marine fuels is in its infancy. New concepts for marine propulsion, some of which with energy-converters unprecedented in commercial shipping, need to be developed. This section proposes new propulsion systems for cargo-vessels carrying LH_2, NH_3, and LOHC. These propulsion systems are evaluated from a technical and economical perspective, and the ones deemed to be the most promising are implemented in the model.

7.1 General

Some of the options for propulsion systems of zero-emission-vessels (ZEVs) were described in Section 5.1. The next step is to show to show how these systems may be implemented on-board cargo-ships loaded with the hydrogen-carriers LH_2, NH_3, and DBT/TOL-LOHC. Of particular interest is the use of both hydrogen boil-off gas (H_2-BOG) and ammonia boil-off gas (NH_3-BOG) for providing propulsion power. There are many factors when choosing an appropriate propulsion system for hydrogen cargo ships. Economics, which is one important factor, is discussed in Section 7.5. Furthermore, in Appendix B.1 the delivered power - speed characteristics of appropriately sized vessels are found. Given approximate operational profiles (produced in Appendix B.2), the ship's total energy consumption during voyages (in both the Japan and Svalbard scenario) is modelled in Section 7.4.

7.2 Propulsion Alternatives

There are numerous options with respect to the methods of power generation onboard zero-emission-vessels (ZEVs). **The following discussion will exclusively cover propulsion systems using ship cargo as fuel**. Thus, various systems applying LH_2, NH_3, and DBT/TOL-LOHC as fuel will be evaluated. Although the propulsion systems for each ship-type will exhibit similarities, there will be differences owing to the fact that different energy carriers are carried as cargo. **For simplicity, all propulsion systems are assumed to be electric**. Consequentially, for all propulsion systems, electric motors are used for driving the propeller.

7.2.1 Overview of Energy Converters

In this thesis, the following energy converters are evaluated with respect to their application in zero-emission vessels (ZEVs):

1. Solid oxide fuel cell (SOFC)
2. Proton exhange membrane fuel cell (PEMFC)
3. Hydrogen-fueled Internal Combustion Engine (H_2-ICE)
4. Ammonia-fueled Internal Combustion Engine (NH_3-ICE)
5. Hydrogen-fueled Gas Turbine (H_2-GT)
6. Steam Turbine (ST)

Assumed energy conversion efficiencies and other properties for each energy converter are shown in Table 7.1.

Table 7.1: Technical comparison of different energy converters. Based on [65], [27] and [75]

.

Item	**Energy Converters**				
	SOFC	PEMFC	H_2-ICE/NH_3-ICE	H_2-GT	ST
Peak conversion efficiency[1]	0.60	0.60	0.50	0.35	0.30
Peak Comb. Cycle/Re-heat efficiency gain	0.25	0.00	0.05	0.10	0.10
Partial Load Efficiency	High	High	High	Low	Low
Tolerance to load variations	Low	Medium	High	High	High
Maturity	Low	Medium	High	High	High
Lifetime	Low[2]	Low[2]	High	High	High
Relative cost	High	Medium	Low	Medium	Low

[1]Thermal-to-electrical energy on a LHV basis.
[2]Due to need for stack replacements.

A few points are worth noting regarding each energy-converter:

- Both SOFCs and PEMFCs run on hydrogen. However, due to SOFCs' high operating temperature, NH_3 cracking may take place internally on the anode of the fuel cell.
- It is unclear whether or not H_2-ICE/NH_3-ICE energy converters are able to reach a thermal efficiency of 50%, without operation in a diesel-type engine with pilot fuel ignition. It is assumed that both H_2-ICE and NH_3-ICE are run in spark-ignition (SI) engines similar to current LNG gas engines. Consequently, no secondary pilot fuel is required for ignition unlike many two-stroke low-speed dual fuel engines available on the market today.
- Inevitably, unintended combustion of lubrication oil in ICEs will lead to production of particulate matter (PM) and other emissions [7]. Emissions resulting from combustion of lubrication oil is neglected in the thesis.
- GTs are assumed to be run on hydrogen, since ammonia-fueled gas turbines are at a very premature stage of their development [75]. Hydrogen gas turbines are referred to as H_2-GT.
- Boilers for ST propulsion systems are assumed to be fueled by either H_2 or NH_3, with no difference in performance.
- ICEs, GTs and STs all produce mechanical power. The scope of investigation only covers electric propulsion systems. It is therefore assumed that a generator is attached to all these energy converters. Hence, their conversion efficiency refers to their ability to produce electrical power and includes the addition of a generator.
- In the following discussions, no distinction is made between TOL-LOHC and DBT-LOHC (both are referred to as LOHC). This is because they exhibit very similar properties with regards to their function as fuel.
- Application of loaded LOHC as shipping fuel necessitates the addition of a dehydrogenation system, which produces H_2 and unloaded LOHC.

Table 7.1 shows the assumed peak conversion efficiency of all energy converters evaluated in this thesis. Arguably, the conversion efficiency of the entire propulsion system (henceforth referred to as the final energy conversion efficiency) is more interesting. The final energy conversion efficiency must take into account factors such as the auxiliary power for the fuel supply system and use of waste heat or consumption of cargo in order to provide thermal energy for LOHC dehydrogenation or NH_3 cracking. Appendix C and D describes how the final energy conversion efficiency is calculated for all of the propulsion alternatives which will be described in following sections.

7.2.2 LH_2 Tanker

The LH_2 tanker is flexible when it comes to propulsion machinery, allowing the use of many different types of prime movers. Alternatives for ZEV propulsion are shown in Table 7.2.

Table 7.2: LH_2-fueled ZEV propulsion systems. With respect to efficiencies given in Table 7.1, final conversion efficiencies are lower. Reference is made to Appendix D for details regarding calculation of final energy conversion efficiency.

Propulsion System Name	**Energy Converter**	**WHR System**	**Final Energy Conversion Efficiency**
LH_2-SOFC	SOFC	Combined Cycle	0.80
LH_2-PEMFC	PEMFC		0.56
LH_2-ICE	H_2-ICE	Combined Cycle	0.51
LH_2-GT	H_2-GT	Combined Cycle	0.41
LH_2-ST	ST	Re-heat	0.38

Figure 7.1 shows a principal sketch of the propulsion systems evaluated for the LH_2 tanker.

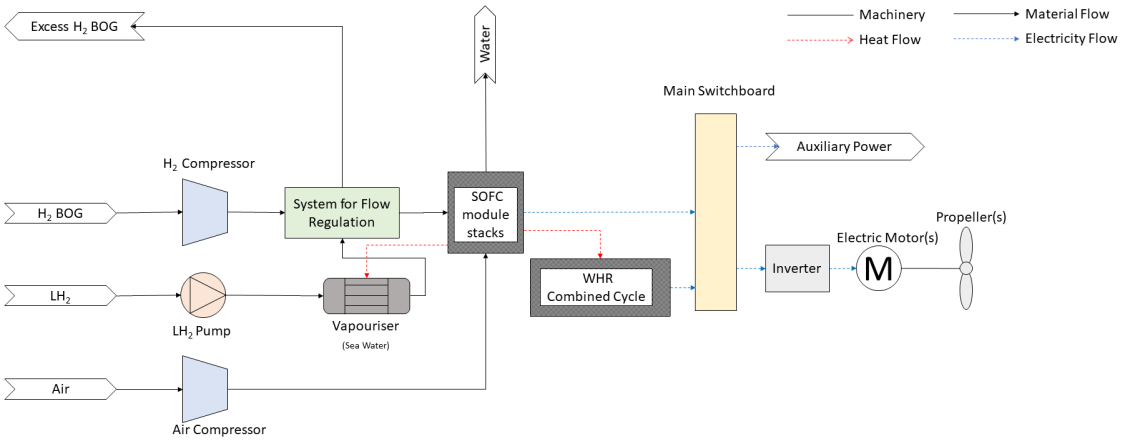

(a) LH_2-SOFC

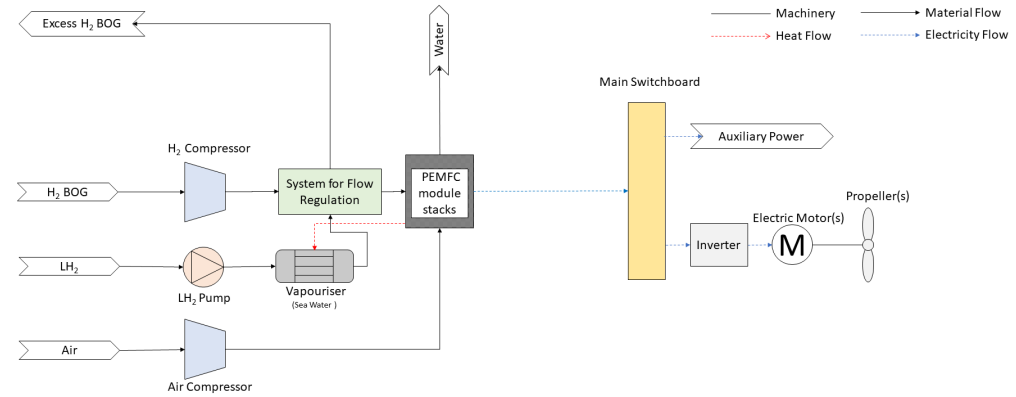

(b) LH_2-PEMFC.

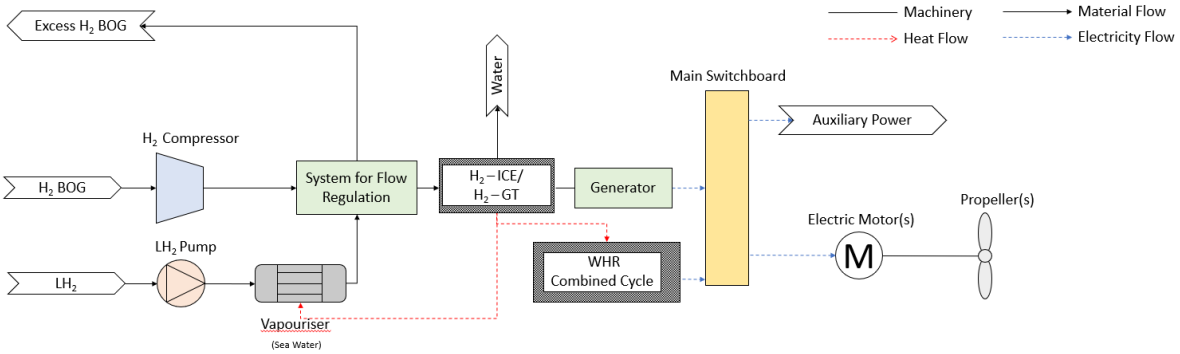

(c) LH_2-ICE/LH_2-GT

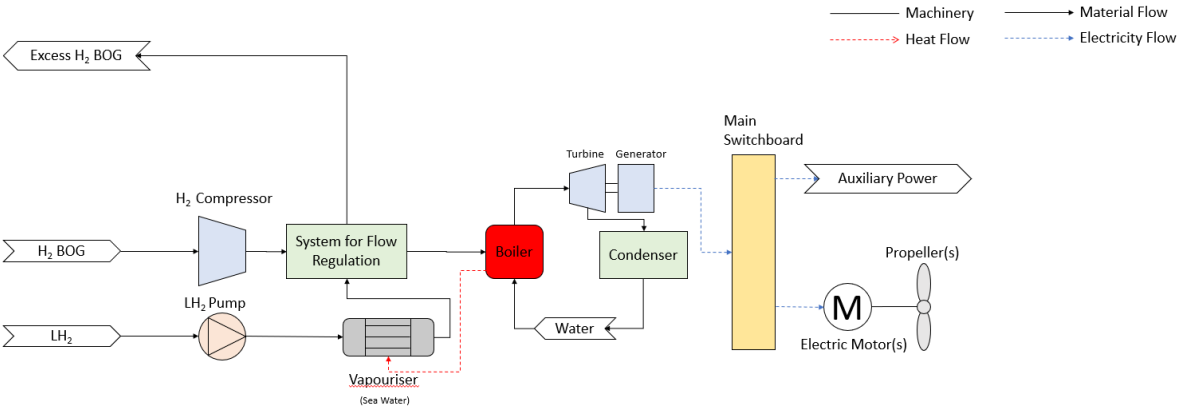

(d) LH_2-ST.

Figure 7.1: Simplified diagram of proposed propulsion systems for LH_2 tanker.

Key Points

- Heat transfer from the energy converter to the LH_2 vapouriser is only necessary during times at which the ambient seawater temperature is very low. The magnitude of heat transfer is generally relatively low, and besides the ambient sea water temperature, it will also depend on the degree

to which BOG covers the ship's power demand.

- In each alternative, a flow regulator is used to match the flow of H_2-BOG with the fuel demand of the vessel power plant. Handling of excess H_2-BOG is covered in Section 7.3.
- The LH_2-SOFC has the potential to achieve the highest final energy conversion efficiency, if integrated with a combined cycle WHR system. Due to the detrimental effect of load cycling on the SOFC, its load should ideally be constant all the way through the voyage. This might necessitate the addition of a battery system for power peak-shaving. An inverter is also needed to deliver a.c. power to the electric motor.
- The LH_2-PEMFC achieves a final energy conversion efficiency of 56%. Unlike the LH_2-SOFC system, the temperature of heat released by the PEMFC system, does not have large potential for WHR. Since PEMFC cells are much more tolerant towards load cycling than SOFCs, there might therefore be no need for a buffer battery system.
- The LH_2-ICE system uses a reciprocating ICE along with a bottoming cycle and generator for electricity production. This system may potentially reach a final energy conversion efficiency of 51%. LH_2-GT uses a hydrogen gas turbine along with a bottoming cycle, achieving a final energy conversion efficiency of 41% (H_2-GT).
- H_2 needs to be compressed before being fed into each energy converter. There are large energy-saving potential in pressurising LH_2 in liquid form, rather than compression in gas form [68]. That is why LH_2 from the cargo tank is pressurised in a pump before vapourisation. H_2-BOG, on the other hand, need to be compressed in a compressor before being fed to each respective energy converter. With reference to Appendix C, this increases the auxiliary power consumption, and reduced the final energy conversion efficiency of each propulsion system.

7.2.3 NH_3 Tanker

Table 7.3 shows different zero-emissions propulsion alternatives for the NH_3 tanker.

Table 7.3: NH_3-fueled ZEV propulsion systems. With respect to efficiencies given in Table 7.1, final conversion efficiencies are lower. Reference is made to Appendix D for details regarding calculation of final energy conversion efficiency.

Propulsion System Name	**Energy Converter**	**WHR System**	**Final Energy Conversion Efficiency**
NH_3-SOFC	SOFC	Combined Cycle	0.73
NH_3-ICE	NH_3-ICE	Combined Cycle Heat transfer to partial cracker	0.52
NH_3-GT	H_2-GT	Combined Cycle	0.38
NH_3-ST	ST	Re-heat	0.38

Figure 7.2 shows different alternatives for the propulsion of the ammonia tanker.

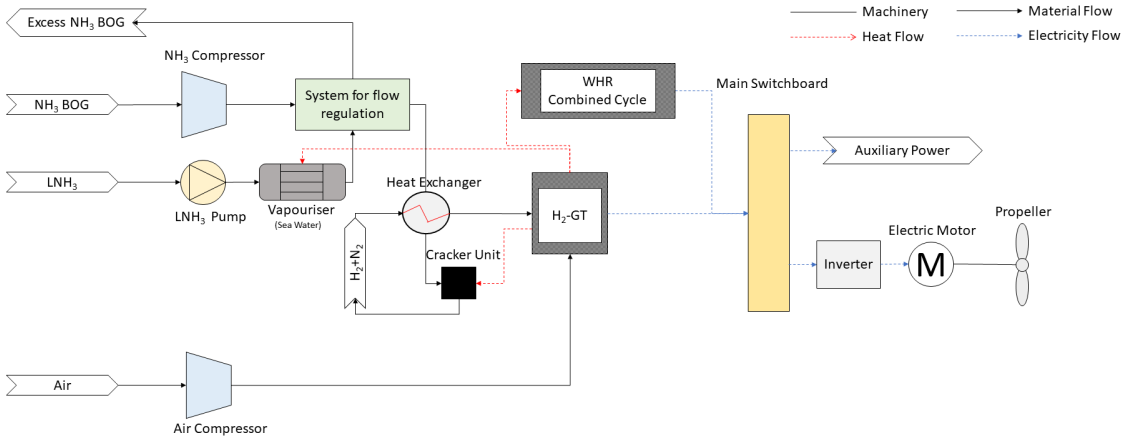

(a) NH_3-GT

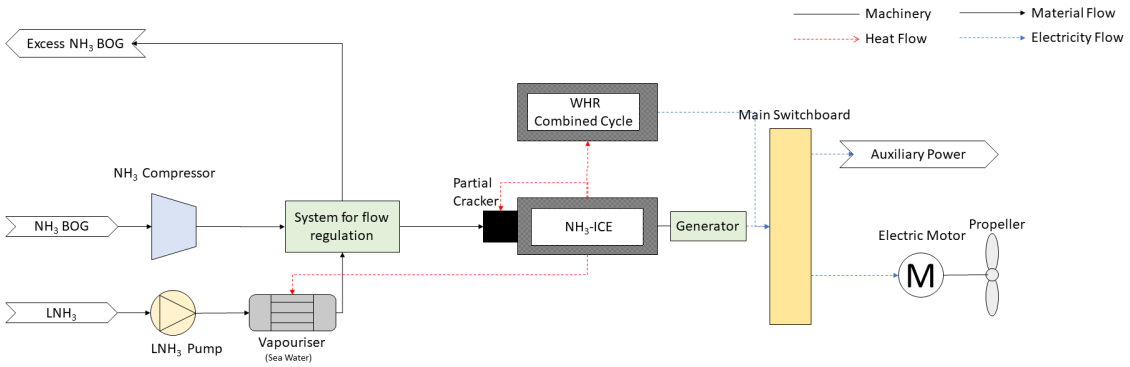

(b) NH_3-ICE.

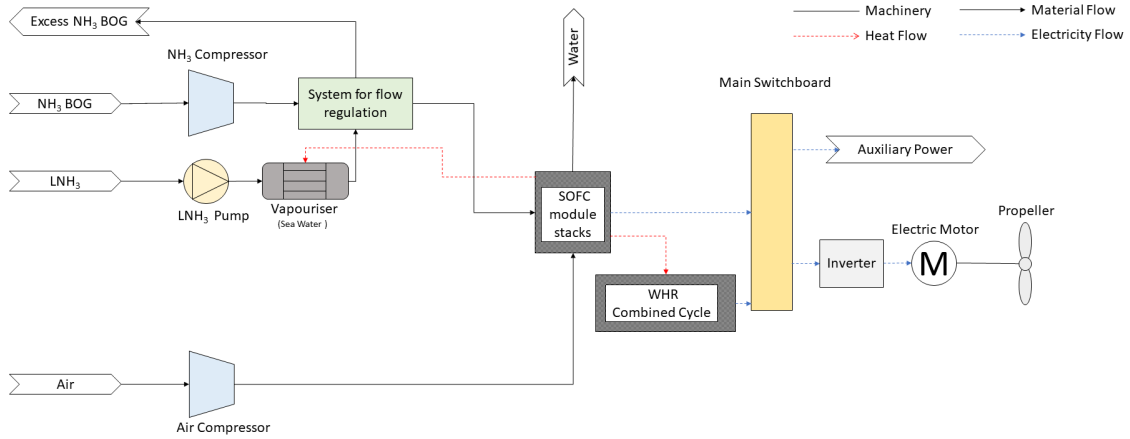

(c) NH_3-SOFC.

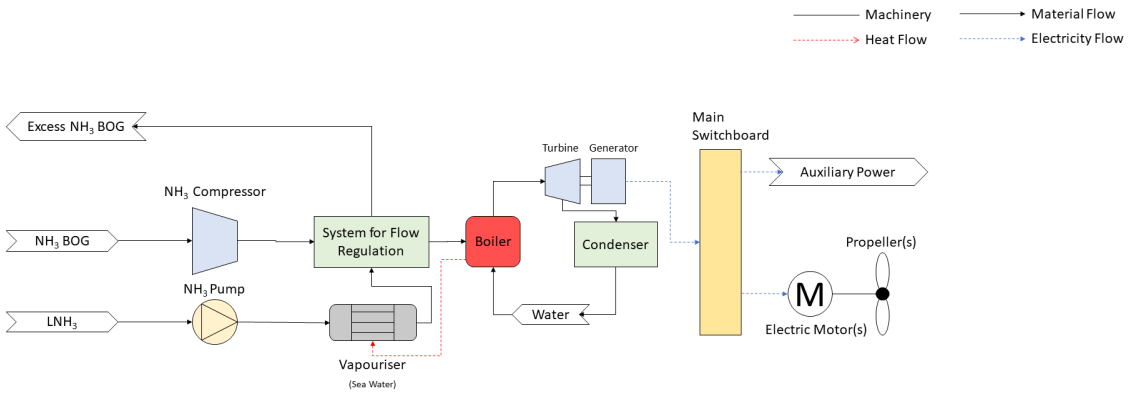

(d) NH_3-ST

Figure 7.2: Simplified diagram of proposed propulsion systems for NH_3 tanker.

Key Points

- For the NH_3-ICE propulsion system, heat transfer to the partial cracker is too insignificant to have a large impact on the final energy conversion efficiency. See Appendix C for details regarding the heat demand of the partial cracker.
- **PEMFCs are not considered as a viable energy converter for NH_3-fueled propulsion systems due to its to sensitiveness to ammonia poisoning**. This could potentially be remedied by the use of a PSA/Metallic membrane purification system, but would add significant complexity to the propulsion system.
- Prospects for direct combustion of ammonia in gas turbines is currently far-fetched[75], leading to its exclusion. The NH_3-GT propulsion system therefore requires complete cracking of ammonia before application in a H_2-GT.
- Experimental results shows that the total thermal efficiency of SOFCs running on NH_3 could reach as high as 0.78, with combined cycles[75]. Final energy conversion efficiency was calculated as 0.73 in Appendix D.
- In all NH_3 propulsion alternatives considered, liquid ammonia (from cargo) needs to be vapourised before use. Similarly to the vapourisation of LH_2 discussed previously, this may be achieved by a sea-water vapouriser with heating of seawater necessary during time at which the seawater temperature is very low. Heating needs for the vapourisation of NH_3 is neglected in the calculation of final energy conversion efficiency.
- The NH_3-ICE propulsion system is based on a reciprocal ICE fueled by a NH_3/H_2 mixture. Due to ammonia's combustion properties, it needs a combustion promoter in order for efficient operation of the engine. This is achieved by the partial cracking of ammonia into a NH_3/H_2 mixture before entering the ICE combustion chamber. Since only a small fraction of ammonia needs to be cracked for efficient engine operation, the required heat transfer from the NH_3-ICE to the partial cracker is relatively low. This allows the addition of a combined cycle WHR system, which brings the system efficiency to 52%.
- For the NH_3-SOFC propulsion alternative, complete cracking of ammonia is required. Due to the high operating temperature of the SOFC, NH_3 cracking is integrated into the fuel cell. SOFC cells are tolerant to any impurities in the H_2 fuel. Any residual NH_3 in the resulting H_2/N_2 mixture will therefore not be a problem.

7.2.4 LOHC Tanker

Table 7.4 shows different zero-emissions propulsion alternatives for the LOHC tanker.

Table 7.4: LOHC-fueled ZEV propulsion systems. With respect to efficiencies given in Table 7.1, final conversion efficiencies are lower. Reference is made to Appendix D for details regarding calculation of final energy conversion efficiency.

Propulsion System Name	**Energy Converter**	**WHR System**	**Final Energy Conversion Efficiency**
LOHC-SOFC	SOFC	Heat transfer to dehydrogenation unit Combined Cycle	0.68
LOHC-PEMFC	PEMFC		0.42
LOHC-ICE	H_2-ICE	Heat transfer to dehydrogenation unit	0.46
LOHC-GT	H_2-GT	Heat transfer to dehydrogenation unit	0.36
LOHC-ST	ST	Heat transfer to dehydrogenation unit	0.32

Figure 7.3 shows the different propulsion alternatives for the LOHC tanker.

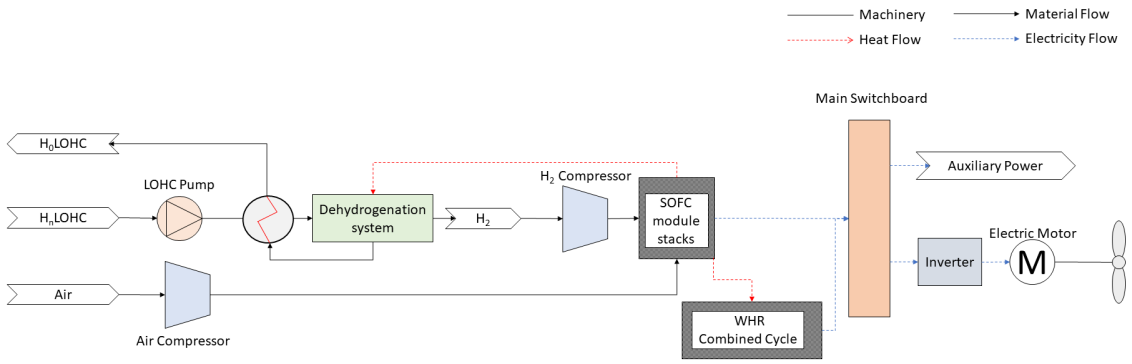

(a) LOHC-SOFC.

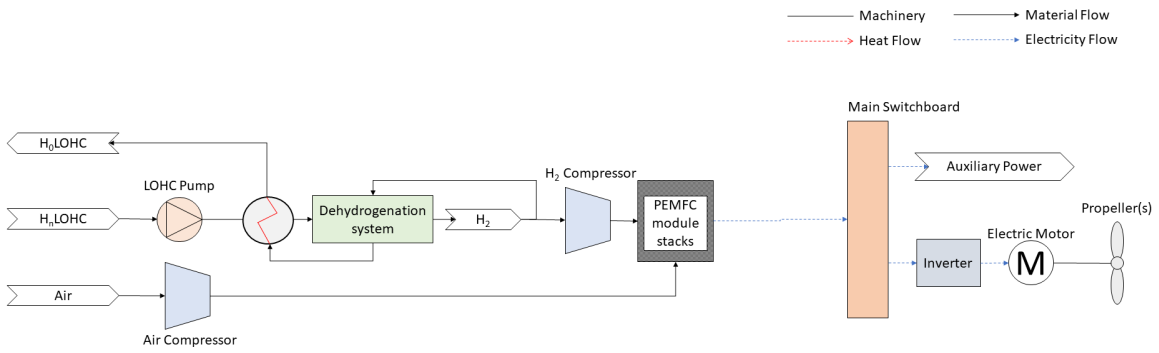

(b) LOHC-PEMFC.

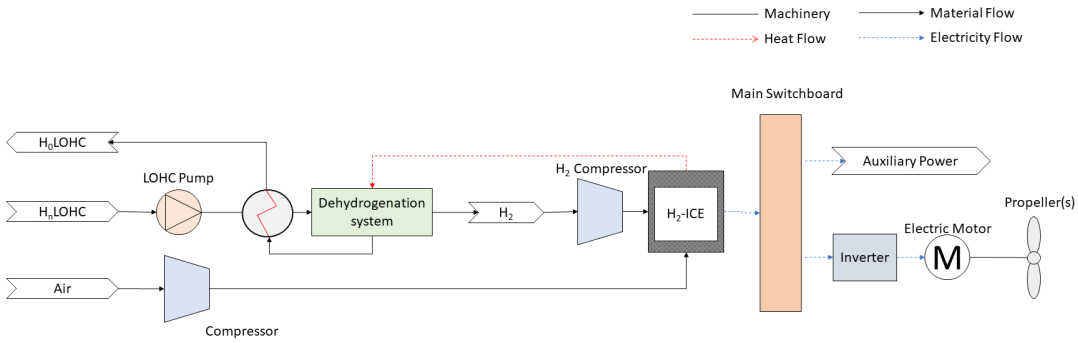

(c) LOHC-ICE.

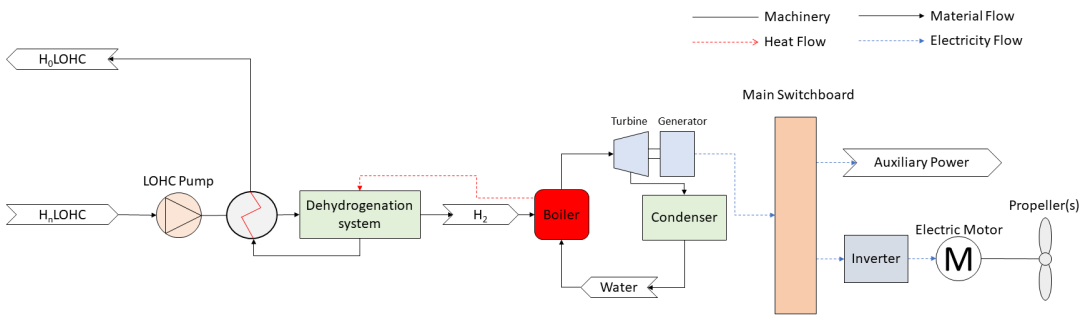

(d) LOHC-ST.

Figure 7.3: Simplified diagram of proposed propulsion systems for LOHC tanker.

Key Points

- All propulsion systems using LOHC as a fuel requires a dehydrogenation unit for H_2 generation. Dehydrogenation is a strongly endothermic process which requires approximately 9.0 kWh/kg H_2 (TOL-LOHC) or 9.4 kWh/kg H_2 (TOL-LOHC) of heat at ≈ 300°C.
- During dehydrogenation, H_2 gas is released from the unloaded LOHC. A separate storage tank for unloaded LOHC is therefore needed on the ship. Ultimately, the need for an additional storage tank may reduce the ship's overall cargo capacity.
- Since hydrogen gas at ambient pressure is released from the dehydrogenation reaction, a compressor is needed to raise the pressure to the inlet pressure of the energy converter. Auxiliary power for raising the pressure of H_2 is estimated in Appendix D and serves to reduce the final energy conversion efficiency of the system.
- The LOHC-SOFC propulsion system consumes waste heat generated in the SOFC for the dehydrogenation reaction. Left-over heat is utilised in a combined cycle steam cycle and raises final energy conversion efficiency to 0.68.
- The LOHC-PEMFC system has a shortcoming compared to the other alternatives when it comes to system efficiency as the PEMFC cell does not release heat with sufficient temperature for the dehydrogenation unit. Therefore, the H_2 gas downstream of the dehydrogenation unit must be partially consumed in order to produce heat for dehydrogenation. This reduces the final energy energy conversion efficiency to 0.42.
- The LOHC-ICE system is assumed to derive part of its heat requirement for dehydrogenation from the H_2-ICE exhaust gas through a heat-to-heat WHR system. With reference to Appendix C.2, product H_2 gas from the dyehydrogenation unit must be partially consumed in order to provide sufficient heat for dehydrogenation. The final energy conversion efficiency is 0.46.
- The LOHC-GT system produces enough waste heat for complete dehydrogenation of LOHC.

7.3 Generation of BOG During Shipping

With reference to Appendix F, boil-off gas (BOG) is inevitably generated inside the cargo-tanks of the NH_3- and LH_2 tanker. The LH_2 tanker will have a more significant boil-off-rate (BOR) than the NH_3 tanker. Table 7.5 shows the assumed boil-off rates for NH_3 tankers and LH_2 tankers.

Table 7.5: Boil-off Rates (BORs) of tankers carrying LH_2 and NH_3.

Type of Cargo	**Boil-off Rate (% of tank volume/day)**	
	Laden Voyage	Ballast Voyage
LH_2	0.3	0.17
NH_3	0.08	0.0045

The following subsections discusses the potential of using BOG as fuel for ship-propulsion. In summary, use of NH_3/H_2-BOG has great potential for supplying a significant amount of the ship's demand for delivered power in the Japan scenario. In the Svalbard scenario, on the other hand, the potential is comparably much lower. This result does not apply to the LOHC tanker, where no BOG is generated inside the cargo tank.

7.3.1 Japan Scenario

Figure 7.4, shows the potential of different propulsion systems to power the ship using BOG for the Japan scenario. At the extreme, the LH_2-SOFC propulsion system could power the LH_2 tanker exclusively using BOG at a speed of approx. 18 knots during laden voyage. This corresponds to a total delivered power of ≈25 MW. Significant power production from BOG is also achieved by the LH_2-PEMFC, LH_2-ICE, LH_2-GT and LH_2-ST. All evaluated propulsion systems for the LH_2 tanker has the potential to use BOG during laden voyage to provide power for speeds below 13 knots. Meanwhile, the potential of utilising BOG to power the ammonia tanker is less than that of the LH_2 tanker, but still significant. This is a result of the comparably lower BOR of NH_3 compared to LH_2. Still, a NH_3-SOFC propulsion system could potentially deliver enough power for a speed of ≈14 knots during laden voyage.

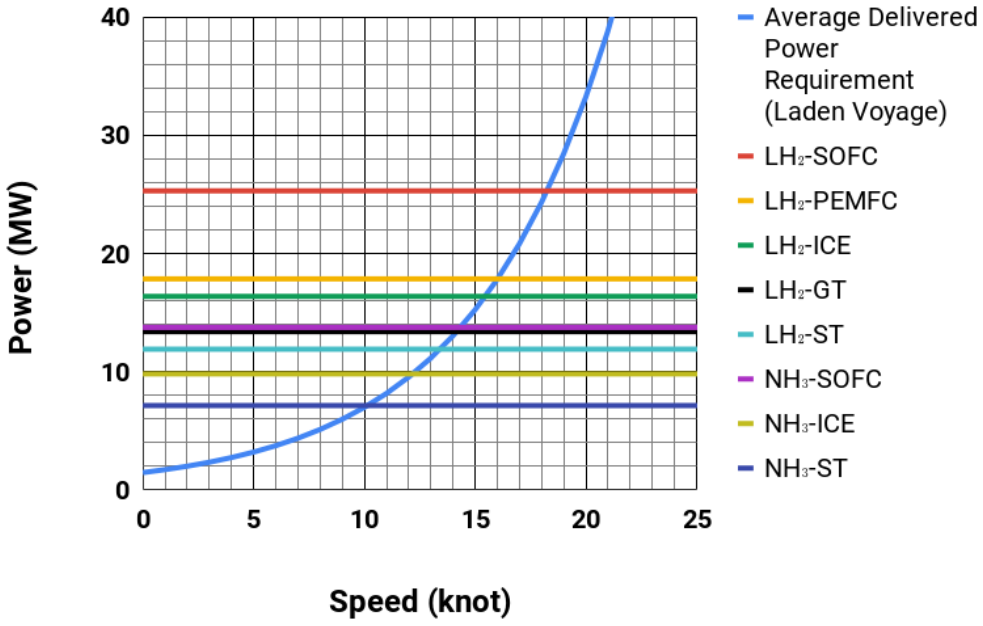

(a) Laden voyage.

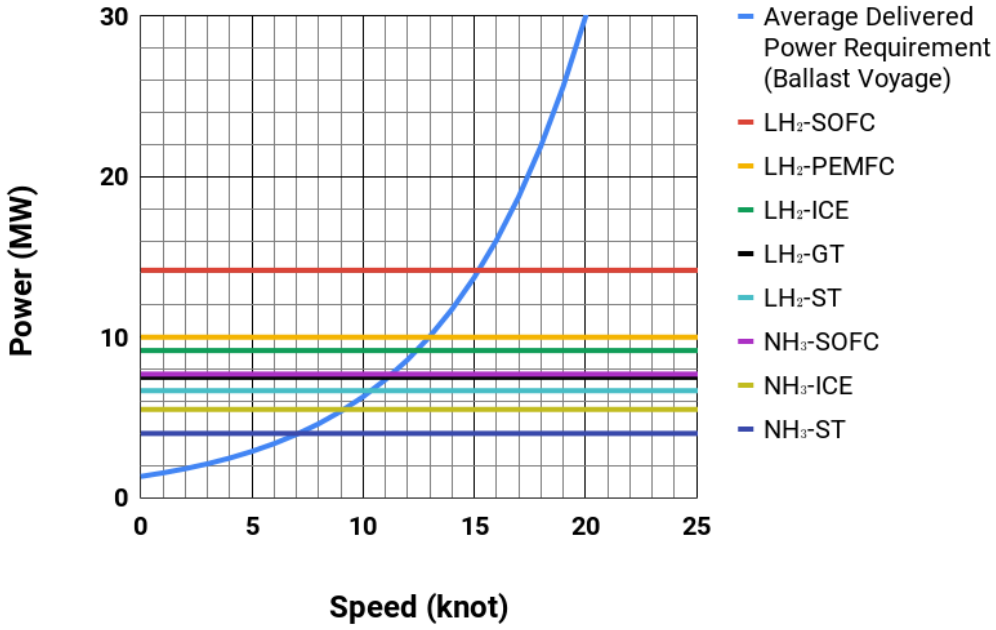

(b) Ballast voyage.

Figure 7.4: Potential of H_2/NH_3-BOG as fuel during laden and ballast voyage for the Japan scenario.

During ballast voyage, the potential for powering the ship with BOG is lower due to reduced BOR. The reduction of BOR is not compensated for by a lower delivered power consumption. Generation of

H_2-BOG is still significant for the LH_2 tanker, with the LH_2-SOFC system delivering enough power for a speed of 15 knots. Generation of NH_3-BOG on the other hand, is lower. Using the NH_3-ICE system exclusively on NH_3-BOG could potentially power the ship for a maximum speed of 9 knots.

7.3.2 Svalbard Scenario

Figure 7.5, shows the potential of different propulsion systems to power the ship using BOG for the Svalbard scenario. As previously mentioned, the 5,000m^3 tanker has an improportionately high power consumption compared to the 160,000^3 tanker, due to a higher resistance per unit length of the ship's LOA. The improportionately high power consumption yields a reduced ability to power the ship by BOG alone - additional means such as using liquid cargo as fuel is necessary. Consequently, at the extreme, a LH_2-SOFC propulsion system may deliver enough power for a speed just under 8 knots during laden voyage, and 6 knots during ballast voyage. The potential of power production by NH_3-BOG is nearly insignificant during laden and ballast voyage.

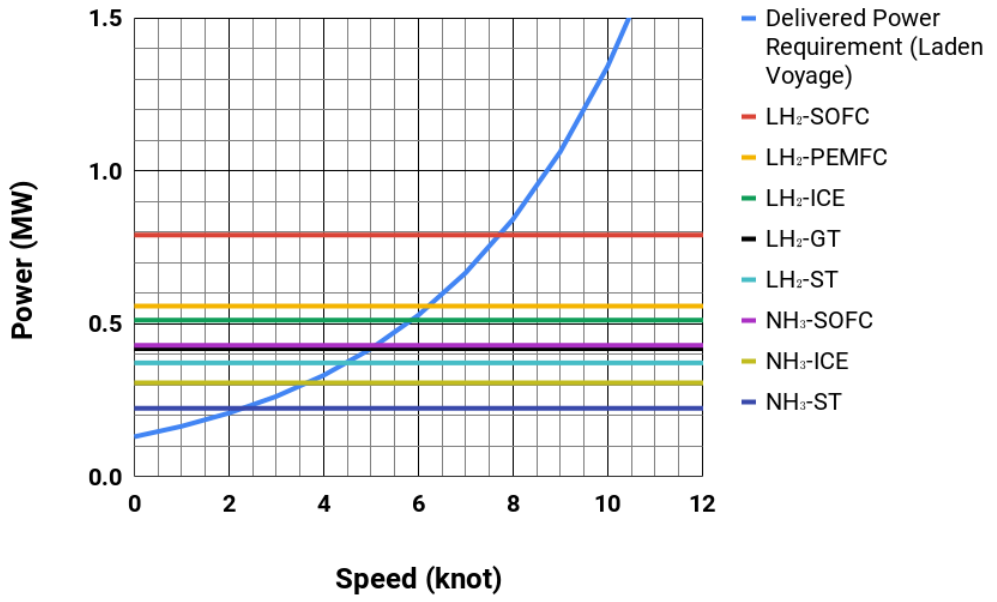

(a) Laden voyage.

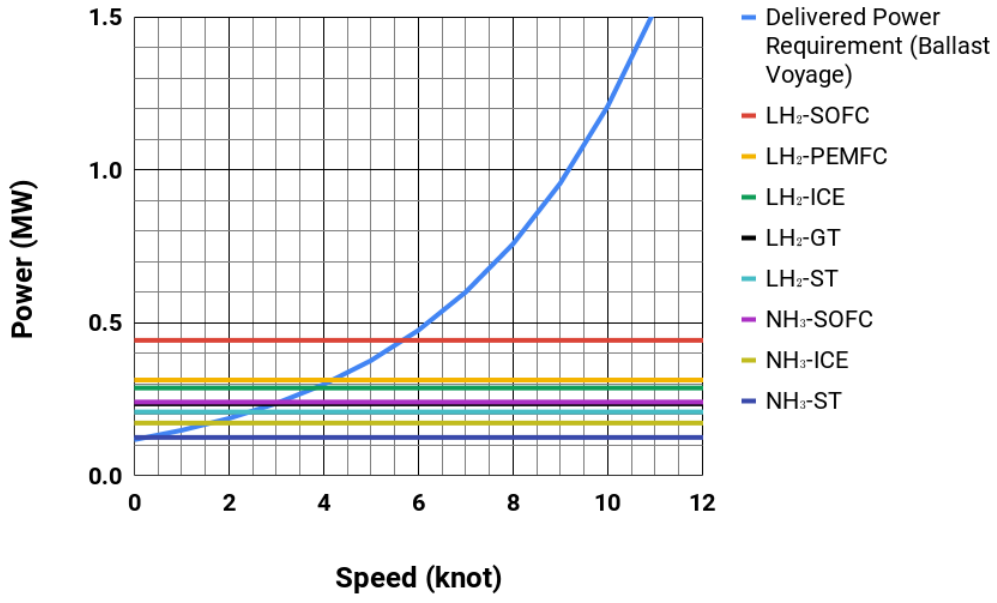

(b) Ballast voyage.

Figure 7.5: Potential of H_2/NH_3-BOG as fuel during laden and ballast voyage in the Svalbard scenario.

7.3.3 Handling Method

As far as boil-off-handling is concerned, there are three primary options:

1. Utilisation as fuel on-board vessel power plant.
2. Re-liquefaction and return to cargo tanks.
3. Combustion in a gas combustion unit (GCU).

Since all the vessels considered are using cargo as fuel for propulsion and auxiliary power generation, the first option is the preferred one. Section 7.3.1 and 7.3.2 showed that there is a great potential for BOG to cover a substantial share of the ship's power consumption - depending on the choice of propulsion machinery. However, given each ship's respective operational profile (given in Appendix B.2), there are times during which the rate of BOG formation exceeds the ship's total delivered power demand. This includes during the operational modes of maneuvering and Suez transit (for the Japan scenario). These instances begs the question: what to do with the excess BOG?

The only remaining options are re-liquefaction and combustion in a GCU. Direct release into the environment is not an option for NH_3-BOG due to pollution concerns and its toxic nature [86]. It is also not considered to be a viable option for H_2-BOG due to danger of ignition. Figure 7.6 shows the different options with regards to handling of BOG.

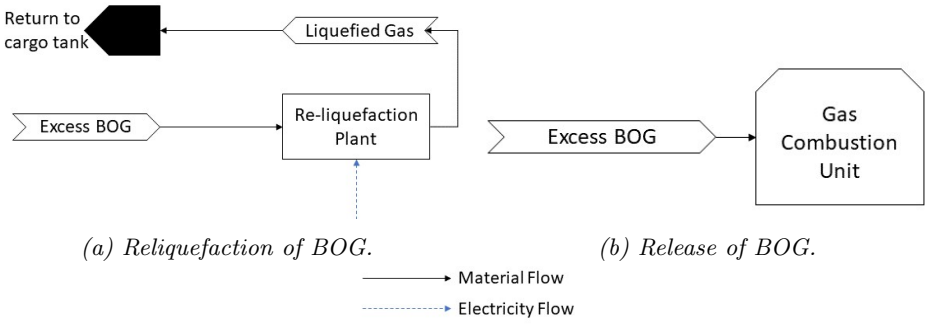

(a) Reliquefaction of BOG. *(b) Release of BOG.*

(c) Legend.

Figure 7.6: Different ways of handling excess BOG.

Re-liquefaction of NH_3-BOG is associated with low energy consumption and re-liquefaction systems are relatively simple with low CAPEX (see process diagram of a simple NH_3 re-liquefaction plant in Appendix A.2.3). Therefore, a natural choice for handling excess NH_3-BOG is by re-liquefaction. Re-liquefaction of LH_2 on the other hand, requires a far more complex and energy-consuming re-liquefaction system. The economic feasibility of re-liquefying excess H_2-BOG versus combustion in a GCU, is a topic which is debatable and worth investigating further. In this thesis however, **it is assumed that both excess NH_3-BOG and H_2-BOG is re-liquefied and returned to the ship's cargo tanks.**

7.4 Modelling of Energy-Consumption During Shipping

The basis for determining speed-power characteristics of each vessel (5,000 m^3 tanker and 160,000 m^3 tanker) is given in Appendix B.1. As evidenced by Figure B.1, there are large variations in the amount of power delivered by the ship propulsion system and the speed of the vessel. Appendix B.2 gives approximations of ship operational profiles for the Japan and Svalbard scenario. Since the operational state of cruising makes up the largest part of each vessel's operational profile (as shown in Table B.2 and B.3), cruising speed therefore has a large impact on the overall energy consumption during voyage. In Appendix B.3, a generic function estimating the total energy consumption of each cargo-ship during a round-trip for both the Japan and Svalbard scenario is given. In principle, the function divides the energy consumption of each cargo-ship into two parts:

1. *Re-liquefaction/refrigeration*: During times at which the energy flow from BOG exceeds the total energy demand of the ship, excess BOG needs to be re-liquefied. Re-liquefaction requires an input of energy; hence re-liquefaction of BOG is associated with energy-loss. The LOHC tanker has liquid cargo at ambient conditions inside the cargo tanks. Therefore there is no need for BOG re-liquefaction in LOHC tankers.

2. *Delivered power for propulsion and auxiliary purposes*: The ship naturally needs energy for propulsion and auxiliary purposes. This energy is derived from BOG from cargo tanks and supplemented by forced vapourisation of cargo if the delivered power demand exceeds that which may be produced from BOG. In the case of the LOHC tanker, the propulsion system exclusively uses H_2 (from dehydrogenated LOHC from the cargo tanks) as fuel.

Figure 7.7 and 7.8 applies functions for the total fuel/energy consumption given in Appendix B.3, and gives the relationship between total fuel consumption of each vessel with variable cruising speed. Fuel consumption is only shown for vessels applying propulsion systems with internal combustion engines (ICEs).

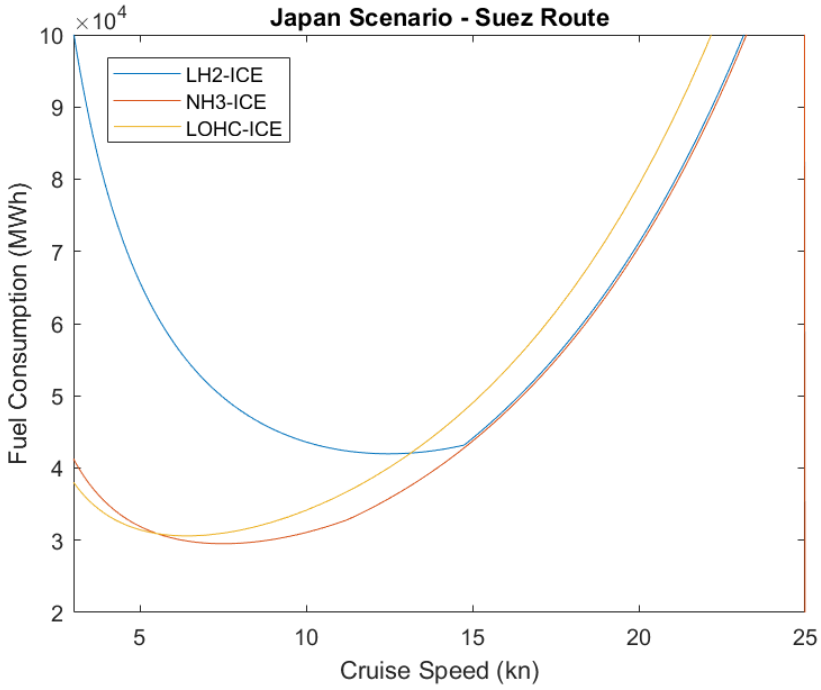

(a) Suez route.

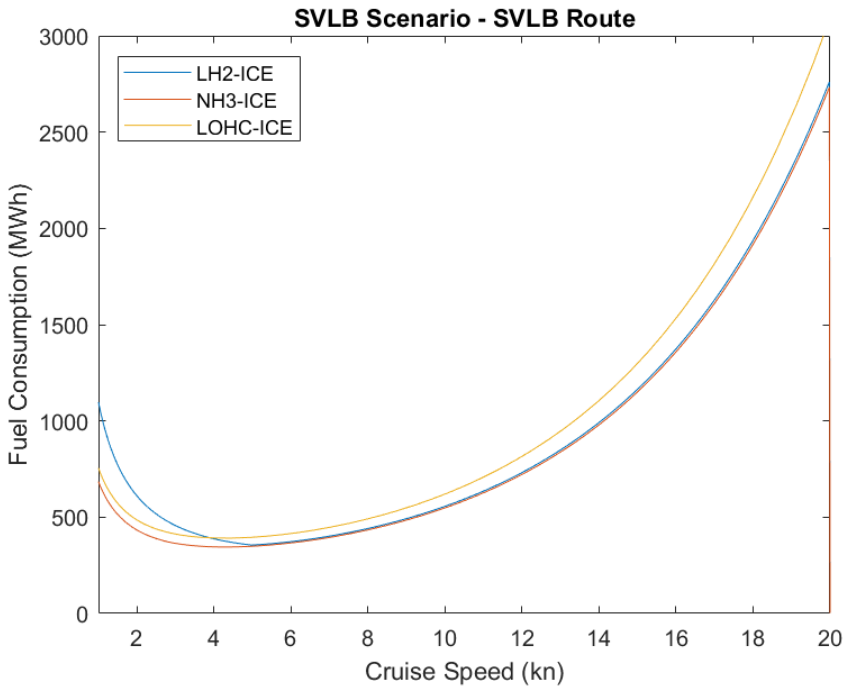

(b) Svalbard.

Figure 7.7: Variation of total fuel consumption (by LHV) during voyage (round-trip) with service speed. The relationship is shown in the figure for propulsion systems based on ICEs.

Key points which may be drawn from Figure 7.7 includes:

- For the Japan scenario, as the cruising speed drops below 15 knots, the re-liquefaction of excess BOG starts consuming substantial amount of energy for the LH_2-ICE ship concept. This effect is much more modest for the NH_3-ICE ship concept, which has to do with the high energy consumption associated with re-liquefaction of H_2-BOG relative to NH_3-BOG. The LH_2 tanker also has a higher BOR than the NH_3 tanker, thus the volume to be re-liquefied in the LH_2 tanker is greater.

- In the Svalbard scenario, the effects of BOG re-liquefaction on the total fuel consumption is far less than for the Japan scenario. This is most likely due to the difference in size between the cargo-vessels operating in the Japan and Svalbard scenario (160,000 m^3 tankers and 5,000 m^3 tankers respectively). This effect was noted in Section 7.3.2.

- In both scenarios, the LOHC-ICE cargo-vessel concept has a higher fuel consumption than the LH_2-ICE and NH_3-ICE concepts except for at very low speeds. This is because of its slightly lower final energy conversion efficiency, when compared to LH_2-ICE and NH_3-ICE. An exception from this is that the LOHC-ICE concept has a lower fuel consumption than the LH_2-ICE tanker for speeds ranging from 0-13 knots in the Japan scenario.

- It is evident that the LH_2 tanker for the Japan scenario should travel with a cruising speed at which a minimal amount of BOG needs to be re-liquefied. If the cruising speed is too low, fuel consumption will reach unsustainable levels.

- Even though cargo-vessels in the Svalbard scenario have an optimum cruising speed (with respect to fuel consumption) at between 4-6 knots, this cruising speed is not realistic. Too low a cruising speed will render the ship difficult to maneuver which pose a threat to safety. Additionally, too low a cruising speed will increase the voyage time to impractical levels.

Figure 7.8 shows the **specific** fuel consumption of ICE-based ship concepts. With reference to Equation B.5, the specific fuel consumption takes into account the maximum hydrogen loading capacity of each hydrogen carrier in the given cargo-vessel.

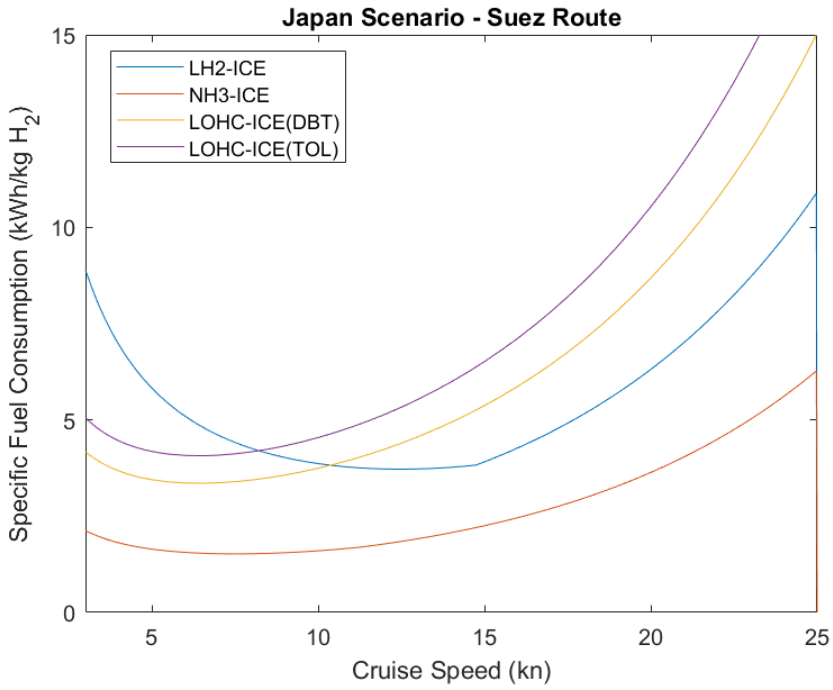

(a) Suez route.

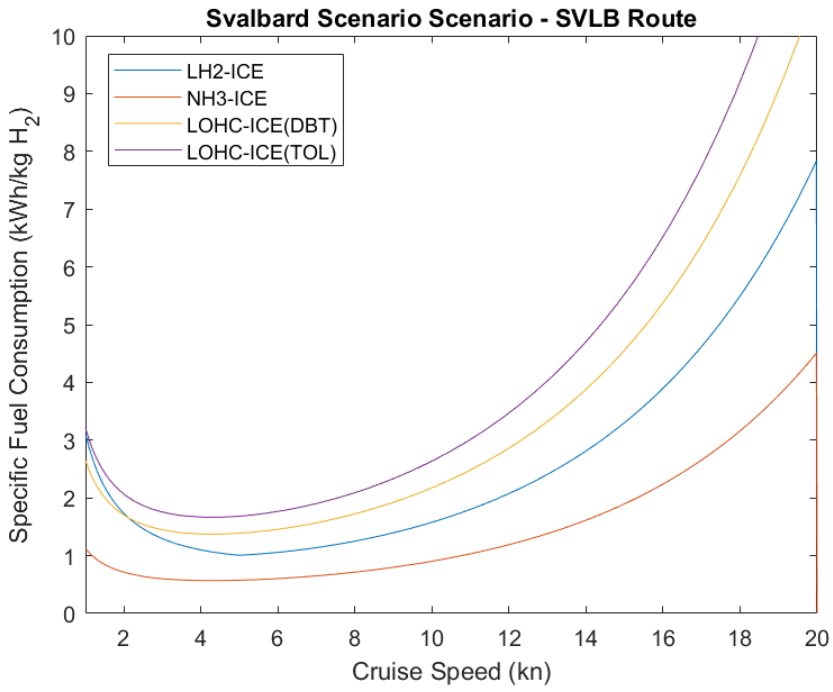

(b) Svalbard.

Figure 7.8: Variation of total fuel consumption (by LHV) during voyage (round-trip) per kilogram H_2 loaded with service speed. The relationship is shown in the Figure for propulsion systems based on ICEs.

From Figure 7.8, the following points may be deduced:

- Shipping hydrogen with NH_3 as the hydrogen carrier is the most energy efficient for both scenarios. This in large part due to the high energy (and hydrogen) density of NH_3 (ref. to Figure 4.2 and 4.1).
- For all practical cruising speeds, shipping of LH_2 is more energy-efficient than TOL/DBT-LOHC. This applies to both the Japan and Svalbard scenario.
- Dibenzyltoluene (DBT) as the LOHC carrier material is more energy efficient than toluene (TOL). This is because of the higher hydrogen density of DBT-LOHC, relative to TOL-LOHC.
- Energy consumption during shipping may significantly be reduced by sailing at a speed lower than the design cruising speed (known as slow steaming) [70]. The average design cruising speed for the two data-sets of ships (used for finding the speed-power characteristics) was ≈14 knots (for 5,000 m^3 cargo-vessels) and ≈19 knots (for the 160,000 m^3 cargo-vessels). Figure 7.8 shows that energy-consumption may be reduced significantly by selecting a cruising speed below 19 knots and 14 knots for the Japan and Svalbard scenario respectively.

While Figure 7.8 and 7.7 shows that substantial fuel savings may be achieved by limiting the cruising speed of each vessel, there will be other implications. By reducing the cruising-speed, one effectively has to increase the number of cargo-ships in operation to deliver an equivalent amount of hydrogen in a given time period. Depending on the type of hydrogen carrier used, each cargo-vessel will exhibit different relationships between fuel consumption and cruising speed. It is therefore not a given that one cruising speed is appropriate for all transportation chains. At present however, **the cruising speed in the Japan and Svalbard scenarios are set to 18.0 knots and 14.0 knots respectively**. This serves to simplify the analysis. The impact of cruising speed on the overall performance of each transportation chain is investigated further in Section 11.3.

7.5 Economic Analysis of Cargo-ship Concepts

Many concepts for the propulsion of cargo-vessel loaded with the hydrogen carriers LH_2, NH_3, and LOHC were proposed and discussed in Section 7.2 from a technical viewpoint. This section investigates the performance of each propulsion concept with respect to economics. A simple economic analysis of the CAPEX and OPEX costs of each ship concept over an operating lifetime of 25 years is conducted.

7.5.1 Dimensioning of Propulsion Power Plant

The design cruising speed and corresponding installed power for both the Japan and Svalbard scenario is given in Table 7.6. Required installed power is estimated based on the required delivered power at design cruising speed. At design cruising speed, each vessel is assumed to operate at 85% of maximum continuous rating (MCR). Total installed power is therefore given as 28,628 kW and 4,114 kW for the Japan and Svalbard scenario respectively.

Table 7.6: Dimensioning of propulsion plant power capacity.

Scenario	**Installed Power (kW)**	**Design Cruising Speed (kn)**	**Cargo Capacity (m^3)**
Japan	28,628	18.0	160,000
Svalbard	4,014	14.0	5,000

7.5.2 Economic Assumptions

Key economic assumptions made when evaluating the economic performance of each ship propulsion concept are given in Table 7.7.

Table 7.7: Key economic assumptions.

Parameter	**Value**	**Unit**
Construction time	2	years
Operating time	25	years
Annual operating days	355	days/year
Discount rate	6	%
Fixed OPEX cost	2.5	%/CAPEX
Internal cost of hydrogen fuel (Japan Scenario)	21	NOK/kg H_2
Internal cost of hydrogen fuel (Svalbard Scenario)	42	NOK/kg H_2

Total OPEX is based on the variable OPEX (fuel consumption costs) and the fixed OPEX as given in Equation 7.1.

$$OPEX_{tot} = OPEX_{Fixed} + OPEX_{Variable} \tag{7.1}$$

All OPEX costs are incurred during the operating time of each vessel from 2030 to 2055.

Economic data used to estimate the CAPEX of each propulsion alternative are given in Appendix G. All CAPEX costs are incurred during the construction time of each vessel, from 2028 to 2029 and is assumed to be evenly distributed. The total CAPEX cost of each ship may be divided into two parts, as shown in Equation 7.2. One part represents the base CAPEX ($CAPEX_{Base}$) of the ship. $CAPEX_{Base}$ is derived from the cost of constructing each ship with the exclusion of its propulsion system. $CAPEX_{Prop}$ represents the CAPEX associated with the chosen propulsion system of the ship.

$$CAPEX_{tot} = CAPEX_{Base} + CAPEX_{Prop} \tag{7.2}$$

Propulsion system CAPEX, $CAPEX_{Prop}$, is based on Table G.1 and depends on the choice of propulsion system.
Base CAPEX, $CAPEX_{Base}$, for each relevant ship-type is given in Table 7.8.

Table 7.8: Base CAPEX assumptions of ships. Cost of conventional propulsion machinery is deducted in accordance to Table G.2.

Type of Cargo-ship	**Size (m^3)**	**Cost (MNOK)**
LH_2 Tanker	160,000	2,400[1]
	5,000	130[1]
NH_3 Tanker	160,000	690[2]
	5,000	60[2]
LOHC Tanker	160,000	340[3]
	5,000	30[4]

[1]Based on new-building price of appropriately sized LNG carrier. The LH_2 tanker is assumed to be twice as expensive as the LNG carrier if CAPEX for its conventional propulsion machinery is deducted.
[2]Based on new-building price of appropriately sized LPG tanker. No LPG tankers currently exist with capacity of 160,000 m^3 to the writer's knowledge. CAPEX is estimated based on CAPEX for an LPG tanker with capacity of 84,000 m^3 and scaled to the appropriate size using the scaling principle in Section 6.5.2.
[3]Based on new-building price of a crude carrier (Suezmax) with cargo capacity of $\approx$ 160,000 m^3.
[4]Based on new-building price of product tanker with capacity 5,000 m^3.

7.5.3 Results

Table 7.9 gives the undiscounted costs for CAPEX and OPEX by each ship concept.

- CAPEX is based on the construction of one ship of the given ship concept, delivered in 2030.

- OPEX is based on the operation of one ship continuously for one year. Each ship follows the operational profile given in Appendix B.2.

Table 7.9: Undiscounted CAPEX and OPEX costs for each ship concept.

Ship Concept	**CAPEX[1] (MNOK)**		**OPEX[2] (MNOK/year)**	
	Japan	Svalbard	Japan	Svalbard
LH_2-SOFC	3,300	280	220	42
LH_2-PEMFC	3,060	240	270	55
LH_2-ICE	2,980	230	286	59
LH_2-GT	3,050	240	334	71
LH_2-ST	3,000	220	365	79
NH_3-SOFC	1,160	150	182	42
NH_3-ICE	930	110	234	56
NH_3-GT	1,080	130	325	79
NH_3-ST	950	100	314	76
LOHC-SOFC	950	140	194	47
LOHC-PEMFC	710	100	282	69
LOHC-ICE	630	90	253	62
LOHC-GT	700	100	323	80
LOHC-ST	650	100	368	92

[1]Includes the construction of the entire vessel, propulsion system included.
[2]FC stack replacement costs are not included.

It is important to note that SOFCs and PEMFCs are assumed to have a lifetime of 50,000 hours and 80,000 hours respectively, as described in Appendix G. Thus, SOFC stacks are to be replaced every 6th year, while PEMFC stacks are replaced every 9th year. The replacement cost of FCs is assumed to be equal to its CAPEX cost, which is a conservative assumption since some parts of the FC system does not need replacement.

The reference year with regards to discounted cash flows is set to 2024. Figure 7.9 shows the net present value (NPV) in 2024 for each ship concept assuming operation of one ship for 25 years (2030 - 2055) and construction time (2028-2029) with delivery in the beginning of 2030.

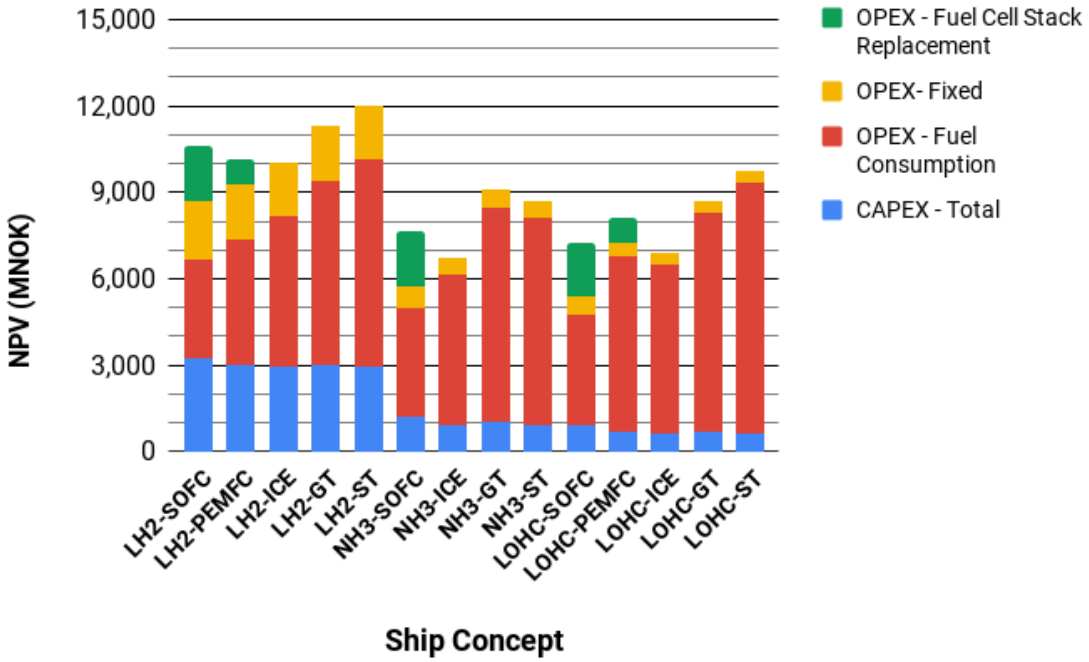

(a) Japan Scenario.

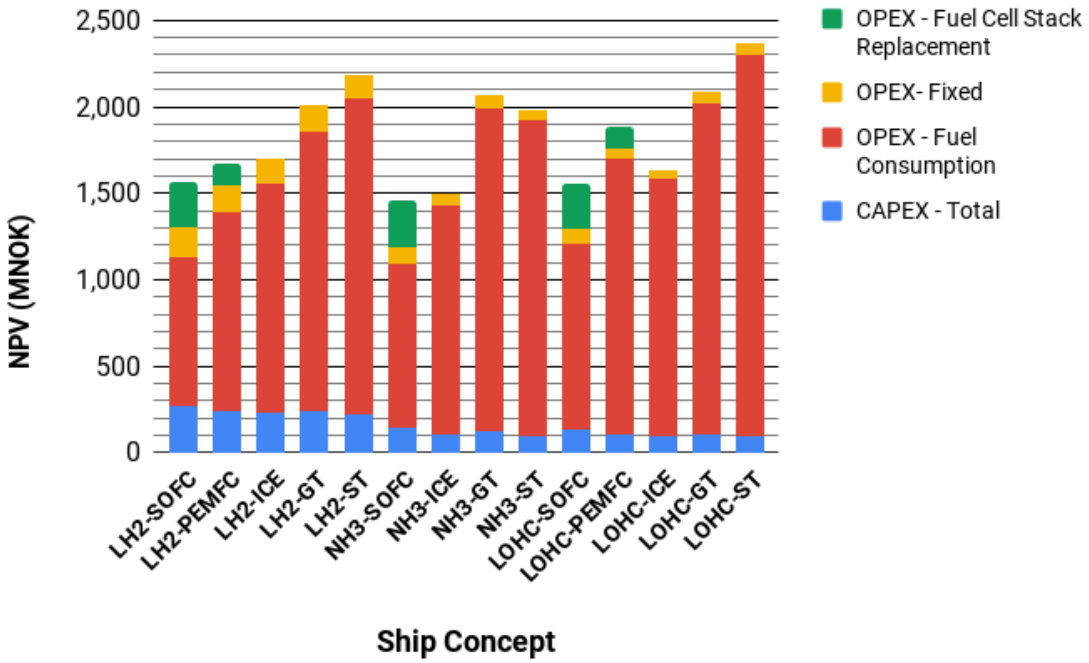

(b) Svalbard Scenario.

Figure 7.9: NPV of cargo-ship concepts. Construction costs for the entire ship and an operational lifetime of 25 years is taken into account.

There are many key points to be drawn from Figure 7.9:

- In the Japan scenario, propulsion options involving use of internal combustion engines consistently has the lowest required NPV for all cargo-ship concepts considered. In the case of the LH_2 tanker, LH_2-ICE is nearly outperformed by LH_2-PEMFC. The results, which indicate that ICEs will still be cost-competitive with FCs in the not too-distant future, is supported by other studies such as one conducted by Lloyd's Register [61]. Even though FCs operate with a higher efficiency, the difference in total fuel costs does not compensate for its relatively high CAPEX and cost of replacing stacks in the Japan scenario. ICEs meanwhile has a low CAPEX, and naturally needs no stack replacements.

- In the Svalbard scenario, fuel consumption costs make up a larger share of the total NPV than for the Japan Scenario. The results suggest that the LH_2-SOFC may have the largest economic potential, regardless of cargo-ship type, slightly outperforming the propulsion options involving PEMFCs and ICEs. An important reason for why fuel consumption is relatively more important for the total NPV of cargo-ships in the Svalbard scenario, compared to the Japan scenario, is the higher price of fuel (as shown in Table 7.7). Generally, it may be stated that SOFCs become more competitive as the cost of fuel increases.

- LH_2 tankers have a significantly higher CAPEX than NH_3 and LOHC tankers. This higher cost is attributed to the cargo containment system, which in the case of LH_2 tankers incurs substantial costs for isolation material (which is also the case for LNG carriers).

- With the exception of the LH_2 tanker in the Japan scenario, propulsion systems involving gas turbines (GTs) and steam turbines (STs) consistently perform worse than the other options. This is not a big surprise, as it is already reflected in the present-day market for propulsion systems - where ICEs dominate, GTs are only used in small nice markets (e.g. navy vessels), and STs have steadily been losing market share for a long time. This is largely because of their relatively high fuel consumption costs. A fairly low CAPEX is not enough to compensate for this.

- For LOHC tankers, propulsion systems based on SOFCs and ICEs are identified as the most promising ones. LOHC-PEMFC systems, though outperforming GTs and STs, have a considerable worse performance than SOFCs and ICEs. This is because of the LOHC-PEMFC propulsion system's relatively low final energy conversion efficiency of 0.42. The root cause being a lack of waste heat energy for LOHC dehydrogenation.

It is important to note that many simplifications were made in the economic analysis:

- *Batteries*: The poor performance of SOFCs with regards to load cycling suggests that it by necessity should be operating at a constant load throughout each voyage. In this case, a large battery system would need to be installed to act as a buffer e.g. at times during which the delivered power by SOFC exceed the ship's demand. CAPEX of batteries is not included in this economic analysis. As a result, the NPV of SOFC systems may be higher in reality. To a lesser extent, the same may be said of PEMFCs.

- *Volume and weight*: No consideration of weight and volume of the different propulsion alternatives has been taken. A report by Sandia National Laboratories, has identified available volume to be a limiting factor with regards to use of FCs and batteries to power large ships [53]. Efforts should be made to evaluate the space-requirements of zero-emission technologies such as FCs on the available space on cargo ships. Potentially, it could have an impact on the cargo capacity of each vessel.

- *Price assumptions*: Assumptions with respect to the CAPEX of different propulsion systems are given in Appendix G.1. These price assumptions are associated with high uncertainty as it is impossible to predict future prices with complete accuracy. This is especially true for the CAPEX cost of FCs, which in this analysis is based on IEA target prices for the period 2025 - 3035[47].

7.6 Selection of Ship Concepts

On a high-level, the different propulsion alternatives have been evaluated from a technical and economical perspective in Section 7.2 and Section 7.5. **Based on the preceding discussion, a decision is made to implement H_2/NH_3 internal combustion engines on each ship, for both the Japan and Svalbard scenario.** The primary two reasons for this includes:

- *Maturity*: Internal combustion engines (ICEs) have a long track-record for maritime applications, compared to other energy converters such as SOFCs and PEMFCs.
- *Economics*: The economic analysis in Section 7.5 showed that propulsion systems based on ICEs are very competitive. In the Japan scenario, vessels with propulsion systems based on ICEs were found to have a lower lifetime cost than all other alternatives for all cargo-types. For the Svalbard scenario, SOFCs were found to be more economic than ICE-based propulsion systems. However, the difference is not that substantial.

Key information about each chosen cargo-ship concept is given below in Table 7.10 7.11, and 7.12. η_{Final} is the final energy conversion efficiency associated with each cargo-vessel with ICE propulsion system.

Table 7.10: Selected cargo-ship concept for the LH_2 transportation chain.

Item	**Scenario**	
	Japan	Svalbard
Propulsion System	LH_2-ICE	
Primary BOG Handling	Utilisation as fuel	
Secondary BOG Handling	Re-liquefaction	
η_{Final}	0.51	

Table 7.11: Selected cargo-ship concept for the NH_3 transportation chain.

Item	**Scenario**	
	Japan	Svalbard
Propulsion System	NH_3-ICE	
Primary BOG Handling	Utilisation as fuel	
Secondary BOG Handling	Re-liquefaction	
η_{Final}	0.52	

Table 7.12: Selected cargo-ship concept for the LOHC transportation chain.

Item	**Scenario**	
	Japan	Svalbard
Propulsion System	LOHC-ICE	
Primary BOG Handling	-	
Secondary BOG Handling	-	
η_{Final}	0.46	

Chapter 8

Technical Analysis of Hydrogen Transportation Chains

This chapter gives a detailed technical analysis of each transportation chain and its associated processes. As such, it gives the basis for all technical input parameters in the model described in Section 6.3. All figures are given on the assumption that all infrastructure has an operation time of 355 days/year.

8.1 Explanation of Terms

Brief explanations of terms which are used used frequently in this chapter are given in Table 8.1.

Table 8.1: Explanation of applied terms.

Term	**Description**
Input mass flow	Mass flow into process.
Output mass flow	Mass flow out of a process.
Electric power consumption	Electric power (drawn from grid) into process. Electric power consumption is represented by blue dashed arrows on each flow chart.
Fuel consumption	For processes in which a heat input is needed, cargo is assumed to be consumed in order to provide heat. Fuel consumption is given as the rate at which energy is provided (on a LHV basis) to each process.
CO_2 emissions	Emissions of CO_2 caused by use of electricity from grid.
Technical maturity	Assessed technical maturity of given technology based on framework given in Table 6.1.
Complexity	Assessed complexity of given process based on framework given in Table 6.2.

8.2 LH_2 Transportation Chain

8.2.1 Overview

Table 8.2 gives an overview of the chosen technology for different processes inherent to the LH_2 transportation chain.

Table 8.2: Overview of technologies chosen for each process.

Process	**Technology**		**Section w/Basis**
	Japan	Svalbard	
Liquefaction	IDEALHY		4.2.1
Ship Propulsion	LH_2-ICE		7.6
Primary BOG Handling	Utilisation as fuel		7.3
Secondary BOG Handling	Re-liquefaction		7.3
Regasification	Open-rack sea water vapouriser	Air vapouriser	4.2.2

8.2.2 Liquefaction

With reference to Section 4.2.1, it is expected that the exergy efficiency of hydrogen liquefaction plants is to improve in the near future. Therefore, the novel design proposed in the IDEALHY project is used as a basis for the modelling of the liquefaction process. Reportedly, an electric energy input of 6.76 kWh_e is required for the liquefaction of one kilogram of H_2. The IDEALHY process has an exergy efficiency of approximately 44% and is shown schematically in Figure 8.1.

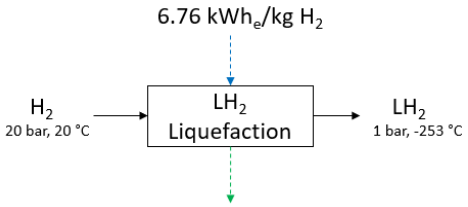

Figure 8.1: Hydrogen liquefaction.

Though an established commercial process, liquefaction of hydrogen gas has never been performed at such high quantities and high efficiency as envisaged in this study. The specific energy consumption of current conventional hydrogen liquefaction plants is signficantly higher than 6.76 kWh_e/kg H_2. As a result, the hydrogen liquefaction process is given a **TRL of 3**. Hydrogen liquefaction requires a very high power inputs, with many process units (ref. to Figure 4.4). Also, special considerations need to be taken in order to safely handle cryogenic hydrogen. Consequently, it is given a **complexity designation of very high**. Table 8.3 shows key technical information about the liquefaction process in the context of the Japan and Svalbard scenario.

Table 8.3: Key technical information about the liquefaction process.

Item	**Value**		**Unit**
	Japan	Svalbard	
Input Mass Flow (H_2)	355,355	4,055	ton/year
Output Mass Flow (H_2)	355,355	4,055	ton/year
Electrical power consumption	282.0	3.22	MW_e
Fuel consumption (LHV)	0.0	0.0	MW
CO_2 emissions	43,240	493	ton/year
Technical Maturity	3		TRL Scale
Complexity	Very high		Complexity designation

8.2.3 Shipping of LH_2

Key information related to the shipping of LH_2 is given in Table 8.4. LH_2-ICE is the ship propulsion concept of choice. More than five LH_2 tankers (5.37) with the operational profile given in Table B.2 is required to transport 300,000 tons of hydrogen to Japan annually.

Table 8.4: Key technical information for LH_2 shipping.

Parameter	**Value**		**Unit**
	Japan	Svalbard	
Input Mass Flow (H_2)	355,355	4,055	ton/year
Output Mass Flow (H_2)	300,360	3,713	ton/year
Electrical power consumption	0.0	0.0	MW_e
Fuel consumption (LHV)	215.2	1.34	MW
CO_2 Emissions	0	0	
Technical Maturity	4		TRL Scale
Complexity	Very high		Complexity designation
Cargo Capacity	160,000	5,000	m^3/ship
Service Speed	18.0	14.0	knot
Propulsion System	LH_2-ICE	LH_2-ICE	-
Primary BOG Handling	Utilisation as fuel	Utilisation as fuel	-
Secondary BOG Handling	Re-liquefaction	Re-liquefaction	-
Required no. of ships	5[1]	0[2]	# no. ships

[1]Rounded to nearest integer.

[2]With reference to Section 3.3, cargo-ships operating in the Svalbard scenario are assumed to be char-

tered.

There are no LH_2 tankers in operation today, though a pilot project undertaken by KHI will see the construction of an LH_2 tanker with capacity of 1250 m^3 by 2020[54]. A full scale 160,000 m^3 LH_2 tanker is planned for 2025. Since shipping of LH_2 has only to a small degree been tested in real-life, with demontrational and industrial pilot projects coming up in a few years, it is given a **TRL of 4**. Because of the cryogenic state of LH_2, many special considerations will need to be taken for shipping. It is therefore assigned a **very high complexity** designation.

8.2.4 Regasification

Regasification may be done in different ways as described in Section 4.2.2. For the scenario with hydrogen export to Japan, regasification by the use of an open-rack seawater vapouriser is deemed to be the most appropriate. For the Svalbard scenario, on the other hand, an open-rack seawater vapouriser may not be used due to the low temperature of seawater near Longyearbyen. The best option is therefore to use an air vapouriser, where heat is transferred from ambient air to the relatively cold LH_2 through air fin heat exchangers. Since the ambient air temperature in Svalbard is relatively cold, an additional heater is needed for bringing the evaporated H_2 gas to the desired temperature. As part of the regasification process, LH_2 is pressurised to 40 bar before regasification. **Regasification was modelled in Hysys, as shown in Appendix A.1.1**. Figure 8.5 shows the regasification process schematically.

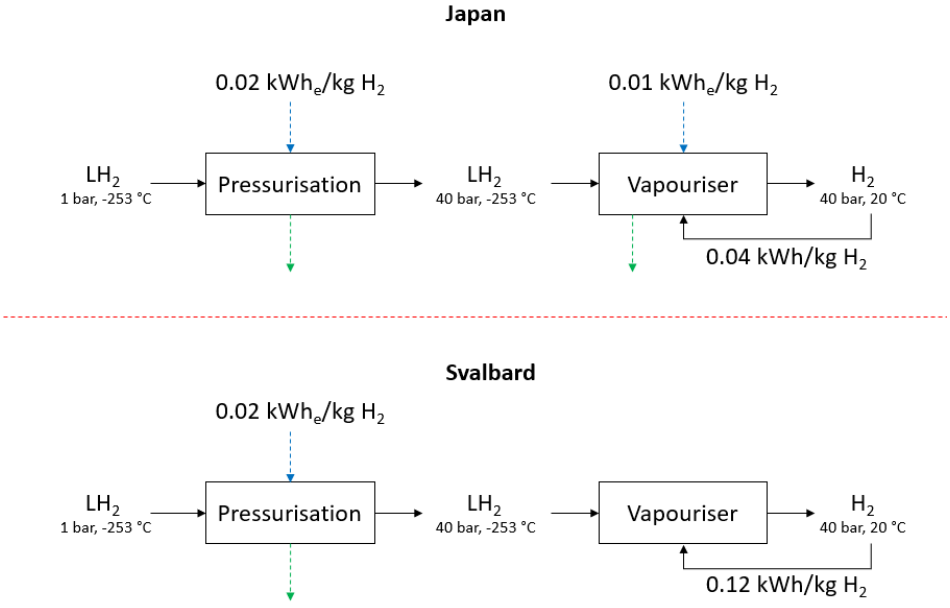

Figure 8.2: H_2 regasification.

There are currently no LH_2 regasification plants in operation. However, a pilot hydrogen handling terminal is planned by Kawasaki in 2020 as part of their LH_2 transport project [54], drawing heavily

on experience with current LNG regasification terminals. The **TRL is determined to be 4**. Regasification of LH_2 is designated with a **moderate complexity**, because relatively few process units is required, and the energy input is also low. Table 8.5 shows key technical information about the regasification process.

Table 8.5: Key technical information for regasification process.

Item	**Value**		**Unit**
	Japan	Svalbard	
Input Mass Flow (H_2)	300,360	3,713	ton/year
Output Mass Flow (H_2)	300,000	3,700	ton/year
Electrical power consumption	0.8	0.01	MW_e
Fuel consumption (LHV)	1.4	0.06	MW
CO_2 Production	1,934	0	ton/year
Technical Maturity	4		TRL Scale
Complexity	Moderate		Complexity designation

8.2.5 Buffer Storage of LH_2 at Export/Import Terminal

During on-shore transit storage, LH_2 will have to be stored in refrigerated tanks. Boil-off-gas (H_2-BOG) will be generated due to ambient heat transfers inside the tanks, as explained in Appendix F. A boil-off rate of 0.1%/day is assumed for on-shore LH_2 buffer tanks. A refrigeration system is needed in order to re-liquefy BOG and keep the vapour pressure inside the tank within design conditions. The refrigeration system is assumed to have an exergy efficiency of 35%, re-liquefying cold BOG from a temperature of -240°C, as shown schematically in Figure 8.3.

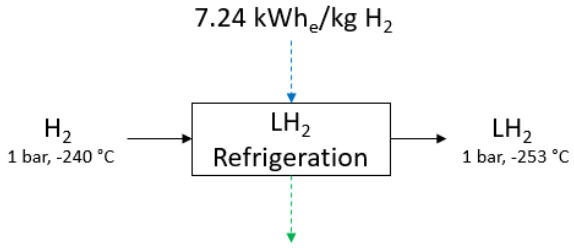

Figure 8.3: LH_2 refrigeration.

Table 8.6 and 8.7 shows key technical information for the refrigeration of LH_2 in both Norway (prior to export), and at the export destination. During loading/offloading of the LH_2 from the LH_2 tanker and on-shore buffer storage tanks, a significant share of the loaded/offloaded LH_2 cargo will evaporate due to ambient heat transfer in piping. It is assumed that 2% of all loaded/offloaded LH_2 is evaporated and turned into H_2-BOG. Using vapour return lines, H_2-BOG is re-liquefied and is therefore not wasted.

LH_2 storage units with capacities ranging up to 3800 m^3 have been built in the past[72], though their niche application in the space industry means only a small number has been built. Storage volumes higher than 100,000 m^3 is however without precedent. Consequently, buffer storage for the Japan scenario is given a **TRL of 4**. For the Svalbard scenario on the other hand, where smaller buffer storage capacities are needed, a **TRL of 8** is given. Re-liquefaction of LH_2 is a relatively complex process, though it is less complex than full liquefaction due to the relatively low temperature of H_2 feed gas. It is given a **complexity designation of high**.

Table 8.6: Key technical information for refrigeration of LH_2 for transit storage in Norway.

Item	**Value**		**Unit**
	Japan	Svalbard	
Storage Capacity	284,000	9,700	m^3
Mass Flow to be Re-liquefied (H_2)[2]	14,245	324	ton/year
Electrical power consumption[1]	12.1	0.28	MW_e
Fuel consumption (LHV)	0.0	0.00	MW
CO_2 Production	1,850	42	ton/year
Technical Maturity	6	8	TRL Scale
Complexity	High		Complexity designation

[1]Given as average. The electric power consumption will be higher during LH_2 tanker loading operations, and correspondingly lower at other times.
[2]Includes total H_2-BOG mass flow during loading operations.

Table 8.7: Key technical information for refrigeration of LH_2 for transit storage in Svalbard/Japan.

Item	**Value**		**Unit**
	Japan	Svalbard	
Storage capacity	240,000	8,900	m^3
Mass Flow to be Re-liquefied (H_2)[2]	12,007	297	ton/year
Electrical power consumption[1]	10.2	0.25	MW_e
Fuel consumption (LHV)	0.0	0.00	MW
CO_2 Production	24,340	0.00	ton/year
Technical Maturity	4	8	TRL Scale
Complexity	High		Complexity designation

[1]Given as average. The electric power consumption will be higher during LH_2 tanker loading operations, and correspondingly lower at other times.
[2]Includes total H_2-BOG mass flow during offloading operations.

8.3 Ammonia Transportation Chain

8.3.1 Overview

Table 8.8 gives an overview of the chosen technology for different processes inherent to the NH_3 transportation chain.

Table 8.8: Technologies chosen for each process.

Process	**Technology**		**Section w/Basis**
	Japan	Svalbard	
Air Separation	Cryogenic		4.3.1
NH_3 Synthesis	Haber-Bosch		4.3.2
Ship Propulsion	LH_2-ICE		7.6
Primary BOG Handling	Utilisation as fuel		7.3
Secondary BOG Handling	Re-liquefaction		7.3
NH_3 Cracking	Catalytic cracking		4.3.3
H_2 Purification	PSA		4.3.3

8.3.2 Air Separation

As outlined in Section 4.3.1, air separation is primarily achieved on a commercial scale by pressure swing adsorption (PSA) and cryogenic air separation. In this study, it is assumed that nitrogen production is being done by cryogenic air separation due to the high capacity requirement of N_2 production. The process is shown schematically in Figure 8.4. Characteristic electric energy consumption in a cryogenic air separation process may be calculated as 0.109 kWh/kg N_2 (or 0.745 kWh/kg H_2) [71]. This includes the compression of N_2 gas to 8 bar. Figure 8.4 shows the air separation process schematically.

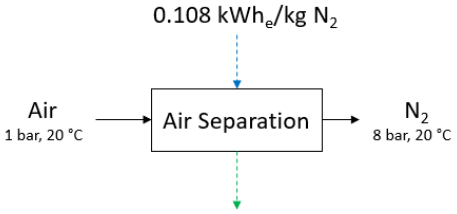

Figure 8.4: Air separation.

Numerous cryogenic air separation plants are in operation, worldwide. As a result, it is given a **TRL of 9**. Cryogenic air separation requires many steps and processing units, though it is simpler than hydrogen liquefaction. It is given a **complexity designation of high**. Table 8.9 shows key technical information for the air separation process.

Table 8.9: Key technical information for air separation process.

Item	Value		Unit
	Japan	Svalbard	
Input Mass Flow (Air)	2,232,520	26,371	ton/year
Output Mass Flow (N_2)	1,743,149	20,590	ton/year
Electrical power consumption	22.1	0.26	MW_e
Fuel consumption (LHV)	0	0	MW
CO_2 Production	3,390	40	ton/year
Technical Maturity	9		TRL Scale
Complexity	High		Complexity designation

8.3.3 Ammonia Synthesis

Different options with respect to ammonia synthesis were outlined in Section 4.3.2. Due to the immaturity of electro-chemical ammonia synthesis, a conventional all-electric Haber-Bosch process was modelled to represent the ammonia synthesis process. Included in the synthesis process is the compression of syngas, and the product is liquid ammonia. **The NH_3-synthesis reaction was modelled using HYSYS (see Appendix A.2.1)**. Data provided by the HYSYS simulation has shown a similar power consumption to that calculated in [99], taking into account different syngas compression. The synthesis process is shown schematically in Figure 8.5.

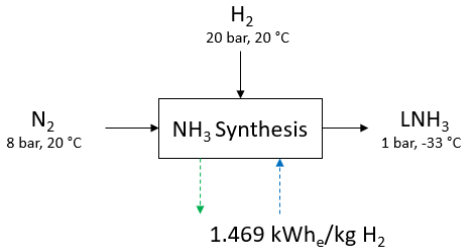

Figure 8.5: All-electric ammonia synthesis.

Owing to ammonia's applications as a fertilizer, numerous ammonia plants are in operation all over the world. The ammonia plant is therefore given a **TRL of 9**. Due to the high pressures and temperature in the synthesis loop, a large number of process units is required and special considerations must be taken for the operation of a NH_3 plant. NH_3 synthesis is therefore given a **high complexity** rating. Table 8.10 shows key technical information about the NH_3 synthesis process.

Table 8.10: Key technical information for the NH_3 synthesis process.

Item	**Value**		**Unit**
	Japan	Svalbard	
Input Mass Flow (H_2)	377,063	4,454	ton/year
Input Mass Flow (N_2)	1,743,150	20,590	ton/year
Output Mass Flow (NH_3)	2,120,212	25,044	ton/year
Electrical power consumption	65.0	0.77	MW_e
Fuel consumption (LHV)	0	0	MW
CO_2 Production	9,970	118	ton/year
Technical Maturity	9		TRL Scale
Complexity	High		Complexity designation

8.3.4 Shipping of NH_3

Key information related to the shipping of NH_3 is given in Table 8.11. NH_3-ICE is the ship propulsion concept of choice. Slightly less than three NH_2 tankers (2.9) with the operational profile given in Table B.2 is required to transport 300,000 tons of hydrogen to Japan annually.

Table 8.11: Key technical information related to the shipping of NH_3.

Parameter	**Value**		**Unit**
	Japan	Svalbard	
Input Mass Flow (NH_3)	2,120,212	25,044	ton/year
Output Mass Flow (NH_3)	1,931,208	23,818	ton/year
Electrical power consumption	0.0	0.0	MW_e
Fuel consumption (LHV)[3]	131.5	0.85	MW
CO_2 Emissions	0	0	
Technical Maturity	8	9	TRL Scale
Complexity	Moderate		Complexity designation
Cargo Capacity	160,000	5,000	m^3/ship
Service Speed	18.0	14.0	knot
Propulsion System	NH_3-ICE	NH_3-ICE	-
Primary BOG Handling	-	-	-
Secondary BOG Handling	-	-	-
Required no. of ships	3[1]	0[2]	# no. ships

[1]Rounded to nearest integer.
[2]With reference to Section 3.3, cargo-ships operating in the Svalbard scenario are assumed to be chartered.
[3]Based on LHV of hydrogen content of NH_3.

NH_3 tankers (also known as VLGCs) with capacities of up to ≈84,000 m^3 are in operation today. NH_3 tankers with cargo capacities in the range of 5,000 [3] is not uncommon either. Thus, for the Svalbard scenario the **TRL is at level 9**. For the Japan scenario, however, a 160,000 m^3 NH_3 tanker is needed for transport. An ammonia tanker of this size is thus far unprecented. Therefore it is given a **TRL of 8**. The NH_3 tankers considered in this thesis keep liquid ammonia cargo at -33°C and 1 bar. This is at a far higher temperature than LH_2(-253°C). Re-liquefaction of NH_3-BOG is a relatively simple process (ref. to Figure A.6). Some consideration does however, need to be taken due to ammonia's toxic nature. NH_3 shipping is assigned a **complexity designation of medium**.

8.3.5 Ammonia Cracking and Hydrogen Purification

A simple ammonia cracking process was modelled in HYSYS, as shown in Appendix A.2.2. Pressurisation of LNH_3 to 40 bar before cracking is included. A total thermal energy consumption of 6.48 kWh/kg H_2 was simulated. However, a more optimised process using heat recycling could have a lower thermal energy consumption of 4.217 kWh/kg H_2[75]. Consequently, 4.217 kWh/kg H_2 is applied as the energy input into the cracking process in the model. Purification of the product H_2 stream is achieved by pressure swing adsorption (PSA) and removal of trace amount of NH_3 by scrubbing. A hydrogen recovery rate of $\approx 90\%$ is assumed for the PSA purification process. Tail-gas containing H_2/N_2 gas mixture and supplementing cracking product gas mixture provide thermal energy for NH_3 cracking. NH_3 cracking and purification is shown schematically in Figure 8.6.

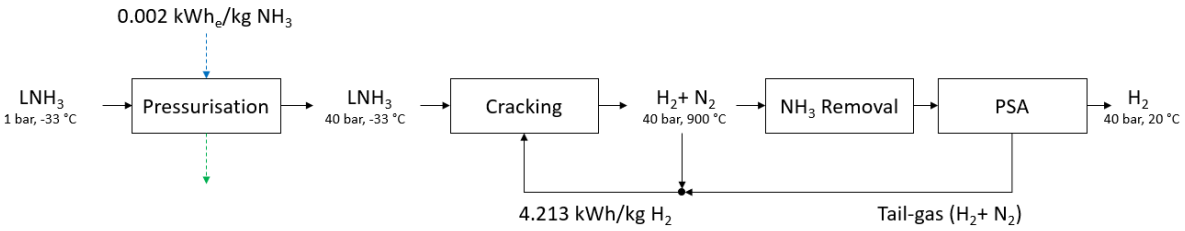

Figure 8.6: NH_3 cracking with integrated scrubbing and purification.

There is one known example of a large scale NH_3 cracker in commercial operation [35], as mentioned in Section 4.3.3. Large-scale cracking of NH_3 is very uncommon. Most operational NH_3 crackers are small-scale and operating at low pressures. Because of this, the cracking process is given a **TRL of 4**. NH_3 cracking requires a high energy input, with high temperatures needed inside the cracking reactor. The cracking plant's integration with a PSA purification system adds complexity to the system. Therefore, the cracking and purification process is given a **high complexity**. Hydrogen purification by PSA is a well-known commercial process and its implementation does not have an impact on the TRL on the combined cracking and purification step. Table 8.12 shows key technical information for the NH_3 cracking and purification process.

Table 8.12: Key technical information for NH_3 cracking and purification.

Item	Value		Unit
	Japan	Svalbard	
Input Mass Flow (NH_3)	1,931,208	23,818	ton/year
Output Mass Flow (H_2)	300,000	3,700	ton/year
Electrical power consumption	0.5	0.01	MW_e
Fuel consumption (LHV)	170.0	2.10	MW
CO_2 Production	1,250	0	ton/year
Technical Maturity	4		TRL Scale
Complexity	High		Complexity designation

8.3.6 Buffer Storage of NH_3 at Export/Import Terminal

Ammonia is kept refrigerated as a liquefied gas during on-shore transit storage. A refrigeration system is required to re-liquefy NH_3-BOG during storage. A boil-off rate of 0.04%/day is assumed for on-shore LNH_3 buffer tanks. **NH_3-BOG re-liquefaction was simulated in HYSYS with two-step compression (ref. to Appendix A.6)**. The refrigeration process is shown schematically in Figure 8.7.

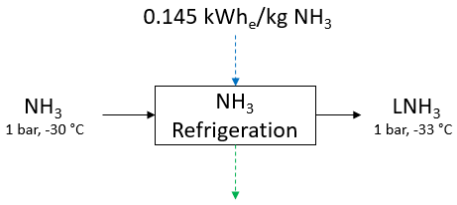

Figure 8.7: NH_3 refrigeration.

Table 8.13 and 8.14 shows key technical information for the refrigeration of NH_3 in both Norway (prior to export), and at the export destination. There are large scale storage units for LNH_3 worldwide. These storage units usually include a refrigeration system which has relatively few process units, and require low power inputs. Consequently, buffer storage of LNH_3 is given a **TRL of 9** and **moderate complexity designation**.

Table 8.13: Key technical information for refrigeration of NH_3 for transit storage in Norway.

Item	**Value**		**Unit**
	Japan	Svalbard	
Storage capacity	175,000	6,200	m^3
Mass Flow to be Re-liquefied (NH_3)	16,962	349	ton/year
Electrical power consumption	0.3	0.01	MW_e
Fuel consumption (LHV)	0.0	0.00	MW
CO_2 Production	15	0	ton/year
Technical Maturity	9		TRL Scale
Complexity	Moderate		Complexity designation

Table 8.14: Key technical information for refrigeration of NH_3 for transit storage in Svalbard/Japan.

Item	**Value**		**Unit**
	Japan	Svalbard	
Storage capacity	160,000	5,900	m^3
Mass Flow to be Re-liquefied (NH_3)	15,450	332	ton/year
Electrical power consumption	0.3	0.01	MW_e
Fuel consumption (LHV)	0.0	0.00	MW
CO_2 Production	214	0	ton/year
Technical Maturity	9		TRL Scale
Complexity	Moderate		Complexity designation

8.4 LOHC Transportation Chain

8.4.1 Overview

Table 8.15 gives an overview of the chosen technology for different processes inherent to the LOHC transportation chain.

Table 8.15: Technologies chosen for each process.

Process	**Technology**		**Section w/Basis**
	Japan	Svalbard	
Hydrogenation	Catalytic		4.4.1
Ship Propulsion	LOHC-ICE		7.6
Primary BOG Handling	-		7.3
Secondary BOG Handling	-		7.3
Dehydrogenation	Catalytic		4.4.2
H_2 Purification	PSA		4.4.2

8.4.2 Hydrogenation

As explained in Section 4.4.1, hydrogenation is an exothermic reaction. Released low-grade heat during hydrogenation is assumed to be wasted. Hydrogenation of DBT incurs an additional energy penalty as it requires a hydrogen feed pressure of 50 bar. Each hydrogenation process is shown schematically in Figure 8.8. Since hydrogenation is exothermic, no heat input is required. Electrical power consumption of auxiliary equipment such as pumps is neglected.

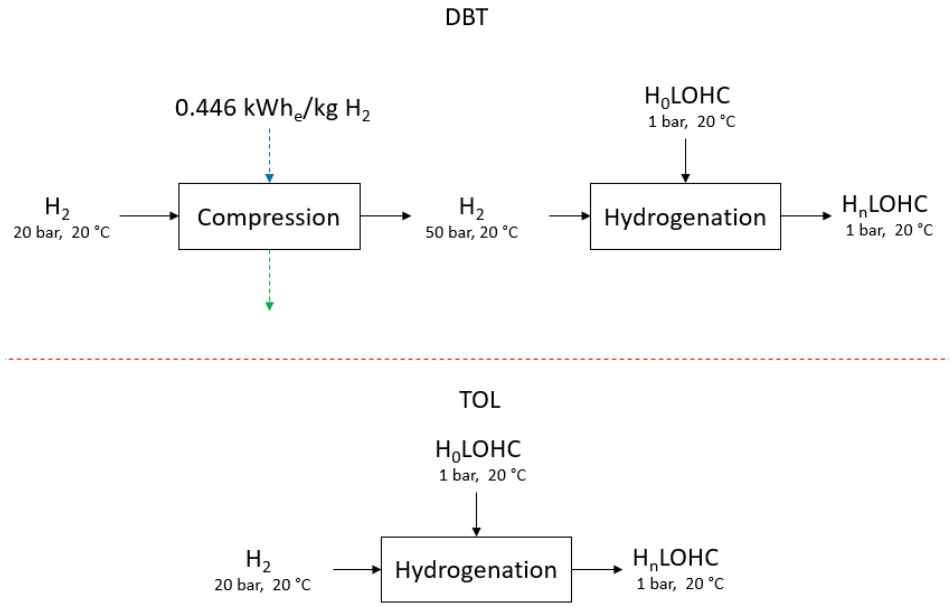

Figure 8.8: LOHC hydrogenation.

It is considered that the hydrogenation process of LOHCs has a **TRL of 4**. It is still in the early stages of development, although it has been tested commercially in small-scale. The complexity is assigned **complexity designation moderate**. Table 8.16 and 8.17 shows key technical information related to the hydrogenation of DBT and TOL respectively.

Table 8.16: Key technical information about hydrogenation of DBT.

Item	**Value**		**Unit**
	Japan	Svalbard	
Input Mass Flow (H_2)	538,605	5,911	ton/year
Output Mass Flow (H_2)	538,605	5,911	ton/year
Electrical power consumption	28.2	0.31	MW_e
Fuel consumption (LHV)	0.0	0.00	MW
CO_2 Production	4,324	47	ton/year
Technical Maturity	4		TRL Scale
Complexity	Moderate		Complexity designation

Table 8.17: Key technical information for hydrogenation of TOL. Hydrogenation of TOL takes place at 20 bar, therefore no H_2 compression is required before the actual hydrogenation process. The process therefore has negligible energy consumption.

Item	**Value**		**Unit**
	Japan	Svalbard	
Input Mass Flow (H_2)	591,544	6,303	ton/year
Output Mass Flow (H_2)	591,544	6,303	ton/year
Electrical power consumption	0.0	0.00	MW_e
Fuel consumption (LHV)	0.0	0.00	MW
CO_2 Production	0	0	ton/year
Technical Maturity	4		TRL Scale
Complexity	Moderate		Complexity designation

8.4.3 Shipping of LOHC

Key information related to the shipping of LOHC is given in Table 8.18 and 8.19. LOHC-ICE is the ship propulsion concept of choice. Slightly more than 7 (7.14) and 9 (9.08) LOHC tankers are needed for transport of DBT-LOHC and TOL-LOHC respectively, in the Japan scenario. That is, assuming the tankers follow the operational profile given in Table B.2.

No dedicated LOHC tankers currently exist. However, LOHC (both TOL-LOHC and DBT-LOHC) exhibit similar properties, with regards to transport, as conventional cargoes such as distilled oils and crude oil. It is therefore expected that there will be few problems (if any) with the shipping of DBT/TOL-LOHC on the seas. Marine transport of DBT/TOL-LOHC is assigned a **TRL of 6** and **low complexity**. More experience in the carriage of LOHC-TOL will be acquired in the upcoming AHEAD project[90], described in Section 5.3.2.

Table 8.18: Key technical information related to shipping of LOHC-DBT.

Parameter	**Value**		**Unit**
	Japan	Svalbard	
Input Mass Flow (H_2)	538,605	5,911	ton/year
Output Mass Flow (H_2)	423,878	5,228	ton/year
Electrical power consumption	0.0	0.00	MW_e
Fuel consumption (LHV)	448.9	2.67	MW
CO_2 Emissions	0	0	
Technical Maturity	8		TRL Scale
Complexity	Low		Complexity designation
Cargo Capacity	160,000	5,000	m^3/ship
Service Speed	18.0	14.0	knot
Propulsion System	LOHC-ICE	LOHC-ICE	-
Primary BOG Handling	-	-	-
Secondary BOG Handling	-	-	-
Required no. of ships	7[1]	0[2]	# no. ships

[1]Rounded to nearest integer.

[2]With reference to Section 3.3, cargo-ships operating in the Svalbard scenario are assumed to be chartered.

Table 8.19: Key technical information related to shipping of LOHC-TOL.

Parameter	**Value**		**Unit**
	Japan	Svalbard	
Input Mass Flow (H_2)	591,544	6,303	ton/year
Output Mass Flow (H_2)	440,020	5,427	ton/year
Electrical power consumption	0.0	0.0	MW_e
Fuel consumption (LHV)	592.8	3.43	MW
CO_2 Emissions	0	0	
Technical Maturity	6		TRL Scale
Complexity	Low		Complexity designation
Cargo Capacity	160,000	5,000	m^3/ship
Service Speed	18.0	14.0	knot
Propulsion System	LOHC-ICE	LOHC-ICE	-
Primary BOG Handling	-	-	-
Secondary BOG Handling	-	-	-
Required no. of ships	9[1]	0[2]	# no. ships

[1]Rounded to nearest integer.

[2]With reference to Section 3.3, cargo-ships operating in the Svalbard scenario are assumed to be chartered.

8.4.4 Dehydrogenation, Purification and Compression

Dehydrogenation is an endothermic reaction and requires heat. A PSA unit working with a recovery rate of $\approx 90\%$ feeds tail-gas into the dehydrogenation process for heat. In addition, heat is provided by the partial consumption of H_2 product from the reaction, to make up for any additional heat demand which is not covered by the tail-gas. Included in the process, is compression of product H_2 gas from 1 bar to 40 bar. Properties of TOL and DBT with regards to dehydrogenation differs slightly, with dehydrogenation of TOL requiring a larger heat input than that of DBT. Additionally, dehydrogenation of DBT achieves a higher conversion fraction of 0.97 compared to 0.95 for TOL. The dehydrogenation process with integrated purification and compression is shown schematically in Figure 8.9.

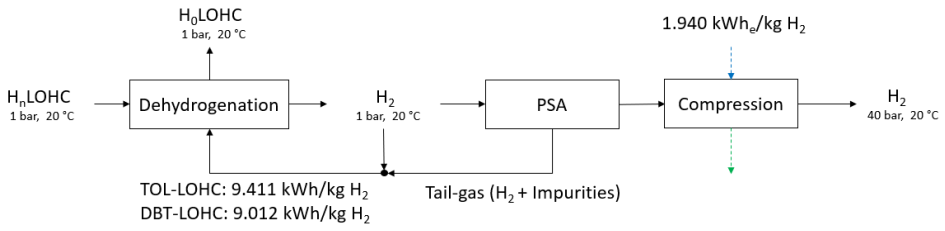

Figure 8.9: LOHC dehydrogenation with integrated purification and compression.

Dehydrogenation plants are still in their early phase of development. Therefore, a **TRL value of 4** is assigned. Furthermore, although dehydrogenation is a very energy-intensive process, relatively few process units are needed. It is given a **moderate complexity**. Table 8.20 and 8.21 shows key technical information related to the dehydrogenation of DBT and TOL respectively.

Table 8.20: Key technical information for dehydrogenation of DBT with integrated purification and compression.

Item	**Value**		**Unit**
	Japan	Svalbard	
Input Mass Flow (H_2)	423,878	5,228	ton/year
Output Mass Flow (H_2)	300,000	3,700	ton/year
Electrical power consumption	68.3	0.84	MW_e
Fuel consumption (LHV)	484.7	5.98	MW
CO_2 Production	162,960	0	ton/year
Technical Maturity	4		TRL Scale
Complexity	Moderate		Complexity designation
Conversion fraction	0.97		-

Table 8.21: Key technical information for dehydrogenation of TOL with integrated purification and compression.

Item	**Value**		**Unit**
	Japan	Svalbard	
Input Mass Flow (H_2)	440,020	5,427	ton/year
Output Mass Flow (H_2)	300,000	3,700	ton/year
Electrical power consumption	68.4	0.84	MW_e
Fuel consumption (LHV)	547.8	6.76	MW
CO_2 Production	162,960	0	ton/year
Technical Maturity	4		TRL Scale
Complexity	Moderate		Complexity designation
Conversion fraction	0.95		-

8.4.5 Buffer Storage of loaded/unloaded LOHC at Export/Import Terminal

Since loaded and unloaded LOHC is kept at ambient conditions, no refrigeration is needed during storage. Since the export/import terminals needs to accommodate the storage of both loaded and unloaded LOHC, the required storage capacity is effectively doubled.

Table 8.22: Key technical information for storage of LOHC-DBT.

Item	**Value**		**Unit**
	Japan	Svalbard	
Unloaded LOHC storage capacity in Norway	532,000	17,500	m^3
Loaded LOHC storage capacity in Norway	532,000	17,500	m^3
Unloaded LOHC storage capacity at export-destination	419,000	15,500	m^3
Loaded LOHC storage capacity at export-destination	419,000	15,500	m^3
Technical Maturity	9		TRL Scale
Complexity	Low		Complexity designation

Table 8.23: Key technical information for storage of LOHC-TOL.

Item	**Value**		**Unit**
	Japan	Svalbard	
Unloaded LOHC storage capacity in Norway	703,000	22,500	m^3
Loaded LOHC storage capacity in Norway	703,000	22,500	m^3
Unloaded LOHC storage capacity at export-destination	523,000	19,400	m^3
Loaded LOHC storage capacity at export-destination	523,000	19,400	m^3
Technical Maturity	9		TRL Scale
Complexity	Low		Complexity designation

Bulk storage of LOHC materials already has prescedent, and conventional tanks may be used. As such, the technical maturity is given as TRL 9. Since there is no refrigeration system needed since both TOL-LOHC and DBT-LOHC is kept at ambient conditions, buffer storage of LOHC is given a low complexity designation.

Chapter 9

Technical Comparison of Hydrogen Transportation Chains

In this chapter, the four transportation chains (LH_2, NH_3, LOHC-DBT, and LOHC-TOL) are analysed and compared technically. The transportation chains are compared on the basis of technical indicators given in Section 6.4, covering areas such as energy, the environment, technical maturity and complexity.

9.1 Energy Consumption

With reference to Section 6.4.1, the total energy consumption in each transportation chain may be categorised into electric and thermal energy. This categorisation is due to the fact that electric energy is associated with higher quality than thermal energy. Thus, thermal and electric energy may not be given equality even though electric energy may be converted into thermal energy.

Figure 9.1 shows the break-down of total electric power consumption for each transportation chain in the Japan and Svalbard scenario.

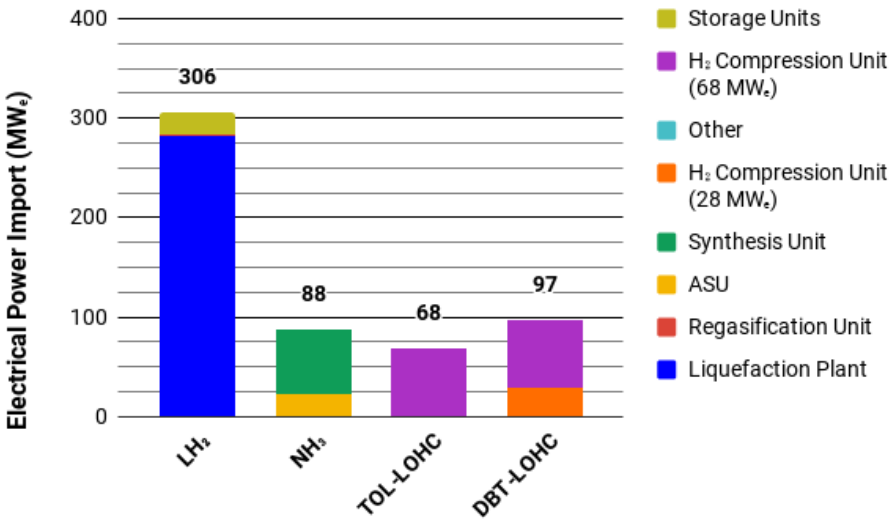

(a) Japan Scenario.

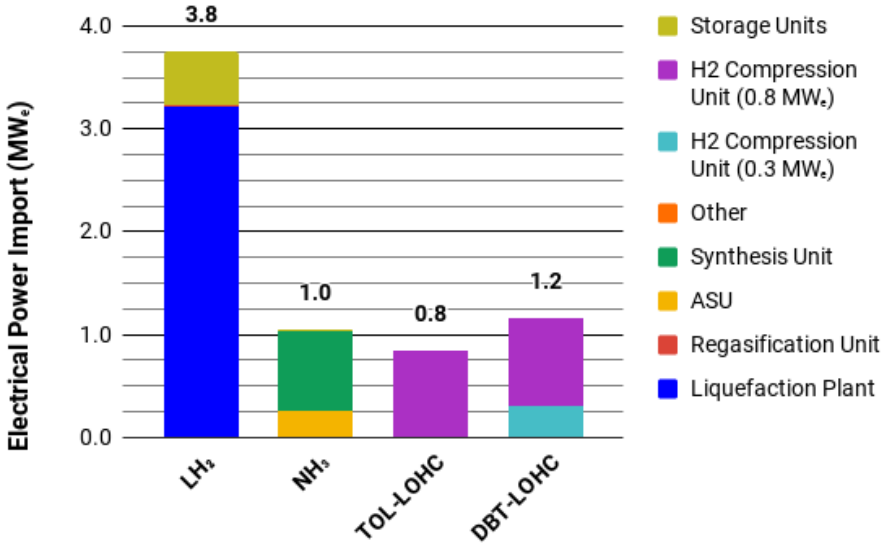

(b) Svalbard Scenario.

Figure 9.1: Break-down of electric energy consumption for each transportation chain. Electric energy is given as a rate with unit MW_e. Subscript e denotes electric energy.

In both scenarios, the LH_2 transportation chain has by far the greatest consumption of electrical power. H_2 liquefaction is a process which demands a large electrical power input. Additionally, refrigeration during buffer-storage on-shore requires a significant amount of electrical energy, due to the re-liquefaction of boil-off gas (BOG) as explained with more detail in Appendix F. At the same time, the NH_3 transportation chain has a sizeable electric power consumption related to ammonia synthesis and the air separation unit (ASU). Both LOHC transportation chains (TOL-LOHC and DBT-LOHC) have relatively low electric power consumptions. In these cases, electric power consumption is restricted

to compression of hydrogen gas after dehydrogenation and before hydrogenation (only applicable to DBT-LOHC). An important aspect of electric power consumption is from which grid electric power is drawn from. Intuitively, it makes more sense that electric power consumption is centered in Norway (the energy exporter) rather than the energy-importer (Japan or Svalbard). Towards this end, the LH_2 transportation cycle is ideal, as electric power consumption is largely concentrated in Norway. Only a small portion of electricity is drawn in Japan/Svalbard due to refrigeration during buffer storage. The same may be said of the NH_3 transportation cycle, where electric power for the ASU and synthesis unit is drawn from the Norwegian grid. The LOHC transportation chains, on the other hand, both require a significant amount of electric power at the export destination. This is due to the fact that the dehydrogenation process has low-pressure hydrogen gas as product. Thus, low-pressure H_2 gas needs to be compressed at the export destination.

One of the key assumptions made during the modelling of each transportation chain was that all fuel consumption is internal in each transportation chain. Fuel consumption is therefore exclusively restricted to the consumption of hydrogen-carrier cargo during transport. Figure 9.2 shows the rate of fuel consumption (on a LHV basis) for each transportation chain in both the Japan and Svalbard scenario.

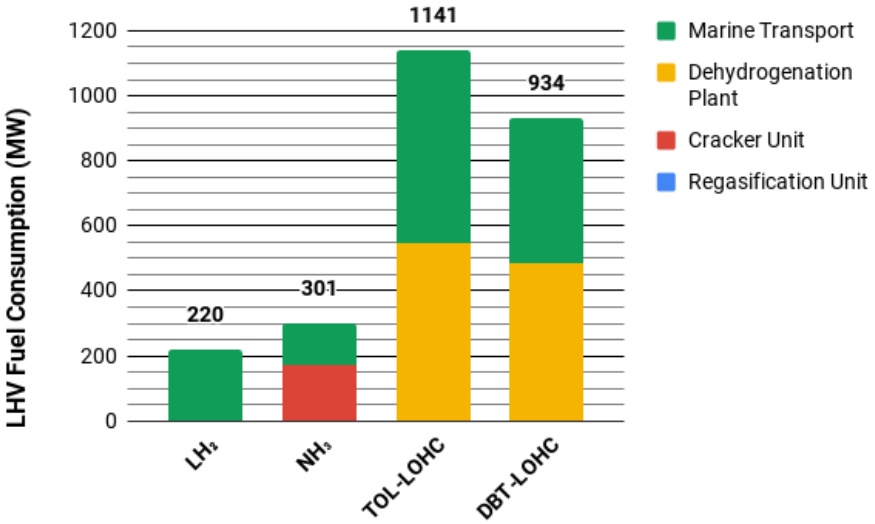

(a) Japan scenario.

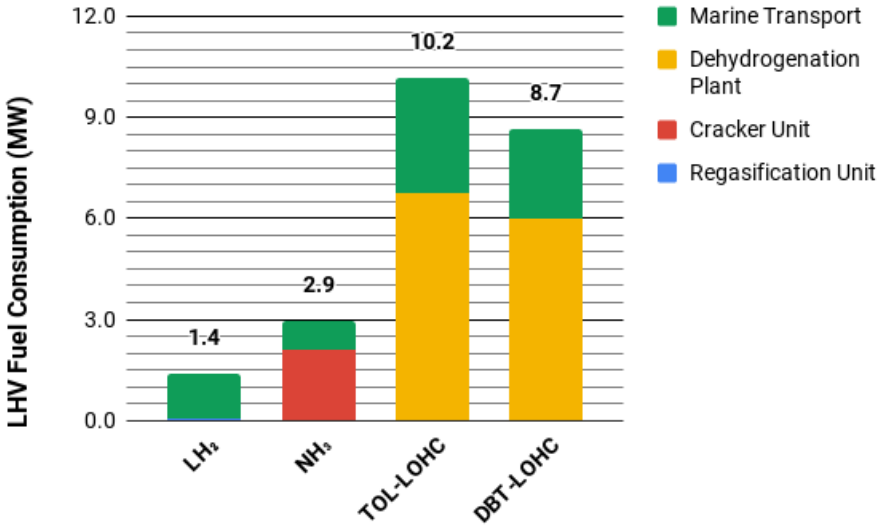

(b) Svalbard scenario.

Figure 9.2: Break-down of fuel consumption for each transportation chain. Fuel consumption is given as a rate on a lower heating value (LHV) basis, with unit MW.

Not surprisingly, fuel for marine shipping of each hydrogen carrier makes up a large portion of the total fuel consumption of each transportation chain. Especially so for the LOHC transportation chains where shipping makes up the majority of all fuel consumption in the Japan scenario. The reason why the LOHC transportation chains require significantly more fuel for shipping when compared to that of LH_2 and NH_3, is in large part due to the relatively low density of hydrogen in loaded LOHC. Therefore, less hydrogen is transported per round-trip than for the LH_2 and NH_3 chains. Another factor for the LOHC chains' large fuel consumption is the fact that a large portion of cargo is consumed at the end-destination in order to provide heat for dehydrogenation. This further increases the fuel

consumption for shipping as more loaded LOHC must be brought over to the export-destination. Ammonia cracking is another energy-intensive process, though not requiring as large a thermal energy input as dehydrogenation. Fuel consumption for the LH_2 transportation chain is almost exclusively concentrated on shipping, with only a fraction of the total fuel consumed during regasification. The TOL-LOHC chain has a signficantly higher fuel consumption than the DBT-LOHC chain. This is mainly due to TOL-LOHC's lower hydrogen density compared to DBT-LOHC.
In Section 6.4.1, Specific Exergy Consumption (SEC) and transportation efficiency are given as technical indicators for energy. Figure 9.3 shows SEC and transportation efficiency for each transportation chain in the Svalbard and Japan scenarios.

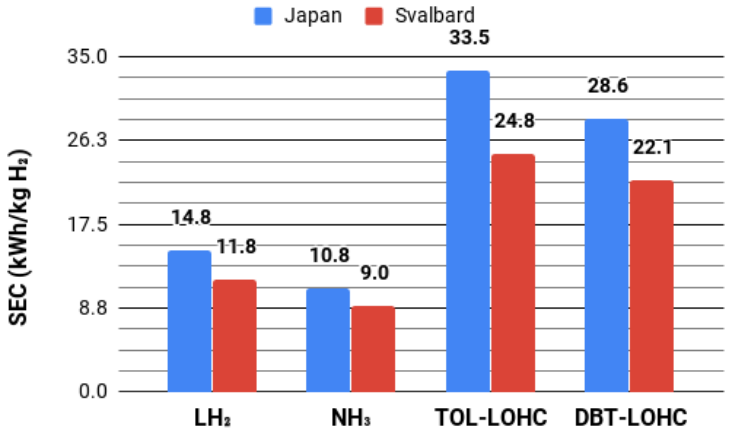

(a) Specific exergy consumption (SEC), given in kWh/kg delivered H_2.

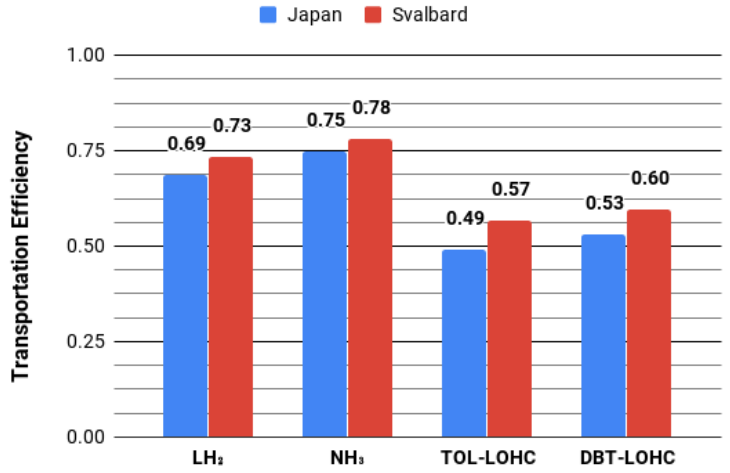

(b) Transportation efficiency.

Figure 9.3: Specific exergy consumption (SEC) and transportation efficiency for each transportation chain.

It is clear that the NH_3 transportation chain has the lowest SEC and highest total transportation

efficiency for both scenarios. NH_3 may therefore be said to be the most energy-efficient hydrogen carrier. Second best, as far as energy efficiency is concerned is LH_2. The TOL-LOHC and DBT-LOHC transportation chains both consume a high amount of energy, especially when it comes to dehydrogenation and shipping. This is underlined by the low transportation efficiency for each LOHC transportation chain in both the Svalbard and Japan scenario. The LH_2 and NH_3 transportation chains achieve a transportation efficiency of 73% and 78% for the Japan scenario. Generally speaking, the SEC is lower (and transportation efficiency higher) for each transportation chain in the Svalbard scenario compared to the Japan scenario. This is primarily due to the fact that in the Japan scenario, shipping makes up a much larger share of the total fuel consumption. This is naturally because of the much larger transportation distance from Norway to Japan as opposed to Norway to Svalbard.

9.2 Environment

With reference to Section 6.4.2, the technical indicators assessing environmental performance of each transportation chain is absolute GHG emissions, and Specific Carbon Emissions (SCE). Absolute GHG emissions (measured in ktonCO_2/year) and SCE are calculated on the basis of electric grid emissions given in Appendix E. Figure 9.4 shows the break-down of absolute GHG emissions for each transportation chain in both the Japan and Svalbard scenario and Figure 9.5 shows the specific carbon emissions (SCE). It is worth bearing in mind that:

- The grid GHG intensity factor of the Svalbard electric grid is set to zero, as one of the assumptions made behind the scenario. Thus, no emissions results from the use of electric power in Svalbard.
- *Zero-Emission Shipping*: Only ship-concepts where zero GHGs are emitted are considered in this thesis. ICEs were chosen as energy converters for shipping in each transportation chain. Consequently, there will inevitably be some emissions of NO_x. Emissions of NO_x is kept to a minimum by the use of selective catalytic reaction (SCR) systems, and is neglected in this thesis.
- Processes which are endothermic (i.e. require heat) such as LOHC dehydrogenation and NH_3 cracking are zero-emission in each scenario. The reason for which is that heat is drawn from the consumption of cargo. Naturally, since the combustion reactions of H_2 or NH_3 produce no GHGs, there will be no CO_2 emissions.

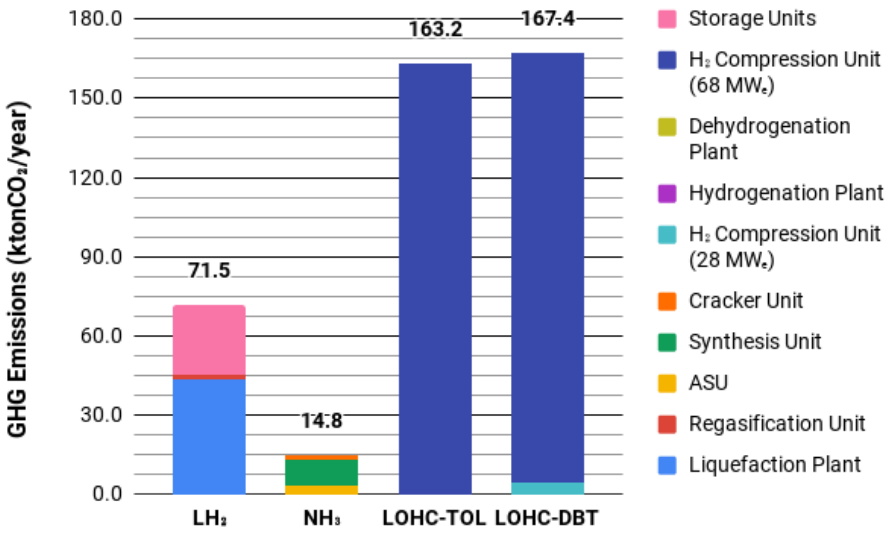

(a) Japan scenario.

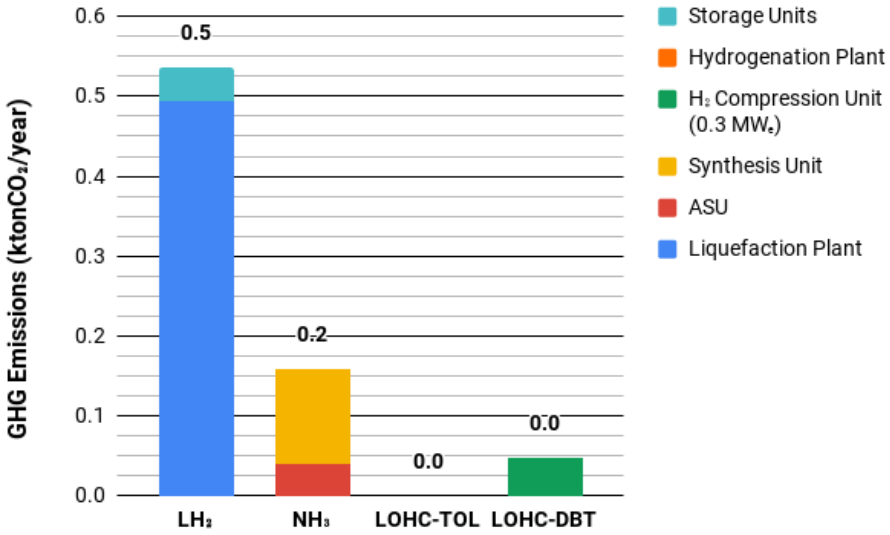

(b) Svalbard scenario.

Figure 9.4: Absolute CO_2 emissions by transportation chain.

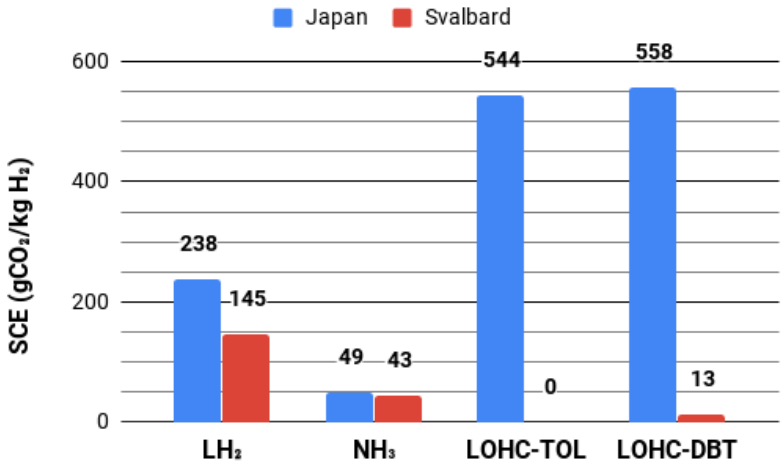

Figure 9.5: Specific Carbon Emissions (SCE) of each transportation chain.

For the Japan scenario, it is evident that the LOHC transportation chains will result in the highest GHG emissions. LOHC-DBT has a slightly worse performance than LOHC-TOL due to the fact that LOHC-DBT needs an additional compression stage prior to hydrogenation in Norway. As shown in Appendix E, the GHG intensity factor of the Japanese grid is assumed to be substantially higher than that of the Norwegian grid (280 gCO_2/kWh and 17 gCO_2/kWh, respectively). As a result, electrical power use in Japan is penalised to a higher degree as far as GHG emissions are concerned, compared to electrical power use in Norway. Both LOHC transportation chains needs a compression stage in Japan, bringing the H_2 pressure from 1 bar to 40 bar, just after dehydrogenation. This compression is power-intensive: hence the high GHG emissions as shown in Figure 9.4. The NH_3 chain achieves the lowest total GHG emissions for the Japan scenario. This is mainly due to the fact that its transportation chain almost exclusively draw power from the Norwegian grid, with only a small electric power demand for the cracking process (0.3 MW_e), mainly in relation to the pressurisation of LNH_3 from 1 bar to 40 bar. The LH_2 chain is by far the transportation chain with the highest consumption of electric power. This is mainly due to the power-intensive liquefaction process. However, since the vast majority of its electric power use is in Norway (where the grid GHG intensity factor is low), total CO_2 production is still low. A sizable electric power use for the LH_2 chain takes place at the export-destination, when LH_2 is kept refrigerated in buffer storage tank at the H_2 import terminal. This results in relatively high GHG emissions in the Japan scenario. However, it is dwarfed by the extent of GHG emissions resulting from H_2 compression (1 bar to 40 bar) in the LOHC transportation chains.

The Svalbard scenario transportation chains have a low SCE compared to the chains in Japan scenario, due to the fact that the GHG intensity of the Svalbard electric grid is assumed to be 0 gCO_2/kWh_e. Consequently, the GHG emissions in the LOHC chains are reduced to insignificant levels (0 and 13 gCO_2/kg H_2 for the TOL-LOHC and DBT-LOHC respectively). The LH_2 transportation chain also has a lower SCE in the Svalbard scenario, compared to the Japan scenario. The main reason for this, is that electricity use tied to re-liquefaction of LH_2 at the import terminal does not cause GHG emissions.

The NH_3 chain, meanwhile, has similar levels of SCE for both the Svalbard and Japan scenario.

An EU certification-scheme called *CertifHY*, defines low-carbon hydrogen as hydrogen produced with an upper GHG emission limit of 4370 $gCO_2/kg\ H_2$[17]. Although, not directly comparable to the given SCE of different transportation chains in Figure 9.5, the *CertiFy* emission limit suggests that all transportation chains evaluated in this thesis have relatively low GHG emissions.

9.3 Technological Maturity and Complexity

Table 9.1 shows the assessed technological maturity and complexity of each step in the LH_2, NH_3, and LOHC transportation chains. The weakest link principle, which states that a chain is only as strong as its weakest link, is applied to determine the overall technical maturity and complexity of the each transportation chain. Technical maturity and complexity is assigned on the basis of the TRL and complexity scale given in Table 6.1 and 6.2 respectively.

Table 9.1: Technical maturity and complexity of all transportation chains for the Japan and Svalbard scenario. No distinction is made between TOL-LOHC and DBT-LOHC.

Item	**Japan Scenario**		**Svalbard Scenario**	
	TRL	Complexity	TRL	Complexity
LH_2 Transportation Chain				
Liquefaction	3	Very high	3	Very high
Shipping	4	Very high	4	Very high
Regasification	4	Moderate	4	Moderate
Buffer Storage	4	High	8	High
Overall	3	Very high	3	Very high
NH_3 Transportation Chain				
Air Separation	9	High	9	High
NH_3 Synthesis	9	High	9	High
Shipping	7	Moderate	9	Moderate
NH_3 Cracking and Purification	4	High	4	High
Buffer Storage	9	Moderate	9	Moderate
Overall	4	High	4	High
LOHC Transportation Chain				
Hydrogenation	4	Medium	4	Medium
Shipping	6	Low	6	Low
Dehydrogenation and compression	4	Moderate	4	Moderate
Buffer Storage	9	Low	9	Low
Overall	4	Moderate	4	Moderate

The LH_2 chain is judged to be the transportation chain with the lowest technological maturity and highest complexity with a TRL of 3, and very high complexity. The LH_2 transportation chain is thought to be in the early stage of its development. Hydrogen liquefaction was identified as the process which is least technically mature in the chain. Large-scale efficient hydrogen liquefaction technology concepts such as IDEALHY needs to be implemented in real-life in order to increase the overall maturity of the LH_2 transportation cycle. Additionally, concepts for large-scale bulk storage of LH_2 (in the same order

of magnitude as in the Japan scenario) needs to materialise in order to increase operational experience. Technical maturity of LH_2 shipping and regasification is likely to increase significantly in the next few years with pilot and demonstrational projects undertaken by Kawasaki[54].

The least mature technology in the ammonia transportation chain is identified as the cracking process. Although NH_3 cracking is taking place commercially, is only doing so at a very limited scale. The use of cracking plants to the extent stipulated by the ammonia transportation chains in this thesis, would require a drastic upscaling of current cracking technology. Higher pressure NH_3 cracking would also be necessary, to keep H_2 compression needs to a minimum. Although cracking is given a relatively low TRL, the cracking process uses equipment which is similar to reforming units applied in the petroleum industry. Apart from cracking, all processes taking place in the ammonia transportation chain are deemed to be relatively mature, though the construction of a 160,000 m^3 ammonia tanker is currently without unprecedent. The NH_3 transportation chain is deemed to have a high complexity. Processes such as cryogenic air separation, NH_3 synthesis, and NH_3 cracking are relatively complex, with many process units and high power requirements. Cryogenic air separation and NH_3 synthesis are however proven processes, and many ASUs and NH_3 synthesis plants exist with much operational experience. If the cracking process was to be emitted from the NH_3 transportation chain, the overall TRL would be significantly improved to a value of 7 or 9 for the Japan and Svalbard scenarios, respectively. This could be achieved if NH_3 was to be consumed directly in devices such as NH_3-ICEs, SOFCs, and in the long-term NH_3 gas turbines.

The LOHC transportation chains are considered to have a TRL of 4 with moderate complexity. The two most technically immature processes in the LOHC chain are hydrogenation and dehydrogenation, which have only been taking place at a very small scale commercially up until now. As these processes are implemented in large-scale plants, the technical maturity should increase. More experience in use of TOL-LOHC as a hydrogen carrier will materialise in the upcoming demonstrational AHEAD project, where TOL-LOHC is transported by ship from Brunei to Japan. This may serve to increase the overall TRL of the LOHC transportation chain. As far as complexity is concerned, the LOHC chains are given an overall moderate complexity designation. This entails that the LOHC transportation chain is considered to have a lower complexity than that of NH_3 and LH_2.

Chapter 10

Economic Analysis and Comparison of Hydrogen Transportation Chains

This chapter contains an economic analysis of all transportation chains. The methodology applied is described in Section 6.5.

10.1 General

All transportation chains are evaluated over a project lifetime of 30 years; 5 years of construction and 25 years operating time. Construction is assumed to start in 2025. Thus, construction finds place from 2025 -2029, while each transportation chain operates from 2030 - 2055. Some of the key parameters and assumptions are given in Table 10.1. Table 10.2 gives projected exchange rates assumed to be valid for the time period 2025-2055.

Table 10.1: Key economic assumptions.

Parameter	Value	Unit
Construction Period	5	years
Operating Time	25	years
Discount Rate	6	%
Annual operating days	355	days/year

Table 10.2: Projected exchange rates(2030)[75].

Exchange Rates
9.0 NOK/EUR
7.0 NOK/US$
10.5 NOK/GBP

10.2 CAPEX

Capital Expenditure (CAPEX) is funds used to buy or improve capital assets such as ships, processing plants and equipment. In this study, capital expenditure includes construction and installation costs, and is assumed to be evenly distributed during all years of construction. More information about CAPEX is given in Section 6.5.2. Table 10.3 and 10.4 shows the estimated CAPEX costs for the Japan and Svalbard scenario respectively. The cost-estimates are based on the given CAPEX data in Appendix H and scaled using the scaling-principle described in Section 6.5.2, if not stated otherwise.

Table 10.3: Assumed CAPEX costs for transport infrastructure of each hydrogen carrier in the Japan Scenario. When applicable, the capacities given relates to the output mass flow. The costs are assumed to apply for the time period 2025-2029.

Item	**Capacity**	**Cost (MNOK)**
LH_2 Transportation Chain		
LH_2 Liquefaction Plant	1000 tpd H_2	14,050
LH_2 Regasification Plant	850 tpd H_2	1,340
LH_2 Storage Unit	37,259 ton (525,000 m^3)	11,290[1]
LH_2 Tankers	160,000 m^3	2500 × 5
NH_3 Transportation Chain		
Air Separation Unit	5970 tpd NH_3	2,850
NH_3 Storage Units	228190 tons NH_3	1,930
NH_3 Synthesis Unit	5,970 tpd NH_3	6,250
NH_3 Cracker Unit	5,440 tpd NH_3	3,860
PSA Unit	440,140 Nm^3/h H_2	1,170
NH_3 Tankers	160,000 m^3	800 × 3
DBT-LOHC Transportation Chain		
LOHC Storage Unit	1,900,000 m^3	2,850[1]
H_2 Compression Unit (20 bar to 50 bar)	28 MW_e	1,510
LOHC Hydrogenation Unit	1,520 tpd H_2	1,120
LOHC Dehydrogenation Unit	850 tpd H_2	560
H_2 Compression Unit (1 bar to 40 bar)	68 MW_e	2,800
LOHC Tankers	160,000 m^3	800 × 7
PSA Unit	440,140 Nm^3/h H_2	1,170
TOL-LOHC Transportation Chain		
LOHC Storage Units	2,450,000 m^3	3,680
LOHC Hydrogenation Unit	1,670 tpd H_2	1,200
LOHC Dehydrogenation Unit	850 tpd H_2	560
H_2 Compression Unit (1 bar to 40 bar)	68 MW_e	2,8000
PSA Unit	440,140 Nm^3/h H_2	1,170
LOHC Tankers	160,000 m^3	800 × 9
General		
Port Facilities	160,000 m^3 Ship	1,710

[1]Based on linear scaling.

Table 10.4: Assumed CAPEX costs for transport infrastructure of each hydrogen carrier in the Svalbard Scenario. When applicable, the capacities given relates to the output mass flow. The costs are assumed to apply for the time period 2025-2029.

Item	**Capacity**	**Cost (MNOK)**
LH_2 Transportation Chain		
LH_2 Liquefaction Plant	11 tpd H_2	250
LH_2 Regasification Plant	10 tpd H_2	60
LH_2 Storage Unit	1,320 tons (19,000 m^3)	410[1]
NH_3 Transportation Chain		
Air Separation Unit	71 tpd NH_3	130
NH_3 Storage Units	8260 tons NH_2	70
NH_3 Synthesis Unit	71 tpd NH_3	280
NH_3 Cracker Unit	67 tpd NH_3	180
PSA Unit	5430 Nm^3/h H_2	50
DBT-LOHC Transportation Chain		
LOHC Storage Unit	66,000 m^3	100[1]
H_2 Compression Unit (20 bar to 50 bar)	0.3 MW_e	60
LOHC Hydrogenation Unit	17 tpd H_2	50
LOHC Dehydrogenation Unit	10 tpd H_2	30
H_2 Compression Unit (1 bar to 40 bar)	0.8 MW_e	130
PSA Unit	5430 Nm^3/h H_2	50
TOL-LOHC Transportation Chain		
LOHC Storage Units	84,000 m^3	130[1]
LOHC Hydrogenation Unit	18 tpd H_2	50
LOHC Dehydrogenation Unit	10 tpd H_2	25
H_2 Compression Unit (1 bar to 40 bar)	0.8 MW_e	130
PSA Unit	5430 Nm^3/h H_2	50
General		
Port Facilities	5,000 m^3 Ship	150

[1]Based on linear scaling.

Note that the CAPEX cost of cargo vessels are not included in Table 10.4, which applies to the Svalbard scenario. The reason for which is that cargo vessels are assumed to be chartered, and thus only counts as an OPEX cost. LOHC materials (TOL and DBT) are assumed purchased externally at the prices given in Table H.2. The break-down of CAPEX for the Japan and Svalbard scenarios are shown graphically in Figure 10.1.

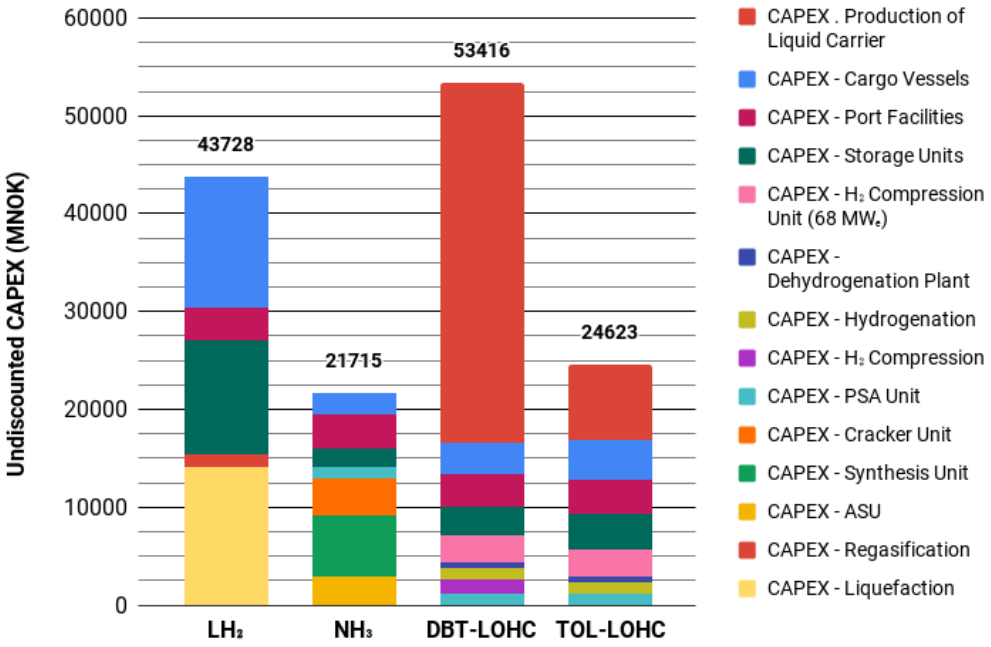

(a) Japan scenario.

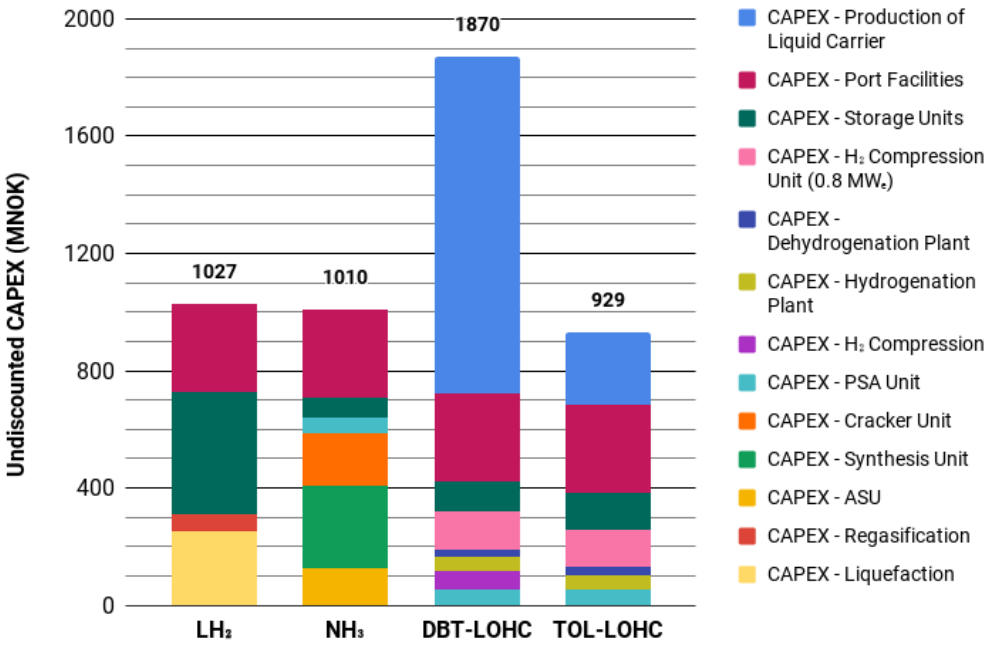

(b) Svalbard scenario.

Figure 10.1: Break-down of total undiscounted CAPEX.

In the Japan scenario, DBT-LOHC has the highest CAPEX. This is in large part due to the high cost

of purchasing the LOHC material dibenzyltoluene (DBT). The LH_2 chain, meanwhile has the second largest CAPEX. The cost of the H_2 liquefaction plant, LH_2 cargo vessels and storage units make up the vast majority of CAPEX in the chain. TOL-LOHC has a much lower CAPEX than both the LH_2 and DBT-LOHC chains. Its largest CAPEX items are the production of toluene (TOL), and cost of port facilities. The lowest CAPEX is incurred for the NH_3 chain. Its largest single CAPEX item is the NH_3 synthesis plant.

The CAPEX break-down of the Svalbard scenario shows similarities to that of the Japan scenario. However, one major difference is that the CAPEX of cargo vessels is not included. The total CAPEX of the LH_2, NH_3 and TOL-LOHC chains are at a very similar total CAPEX level.

It should be noted that the DBT-LOHC transportation chains look to perform poorly CAPEX-wise due to the high cost of purchasing dibenzyltoluene (DBT). The price given in Table H.2 for DBT is based on present-day prices. However, the price of DBT may very well decrease in the future, as production volumes are increased. This development is addressed in Section 11.2.

10.3 OPEX

OPEX is divided into fixed OPEX and variable OPEX. Fixed OPEX is set to 2.5% of CAPEX annually, whereas variable OPEX depends on the consumption of fuel and energy.

Table 10.5 gives the assumed cost of using hydrogen as a fuel in each scenario. As mentioned in Section 3.2, the Japanese government has set target hydrogen price of approximately 21 NOK/kg H_2 in 2030 - reflected in the cost given in Table 10.5. Since the the Svalbard scenario represents a much smaller scale of hydrogen transport and consumption, compared to that in the Japan scenario, its cost of hydrogen is set to 42 NOK/kg H_2 - which is twice compared to that in the Japan scenario.

The cost of electricity given in Table 10.6 are based on current prices of electricity in Norway and Japan. Price parity is assumed between the Norwegian mainland electric grid and the grid in Svalbard (Longyearbyen).

Table 10.5: Internal cost of hydrogen as fuel.

Scenario	**Cost (NOK/kg H_2)**
Japan	21
Svalbard	42

Table 10.6: Assumed cost of electricity.

Grid	**Cost (NOK/kWh$_e$)**
Norway (mainland)	0.7
Japan	1.2
Svalbard (Longyearbyen)	0.7

Table 10.7 shows general OPEX assumptions made in the economic analysis. An important point of notice is that the fixed OPEX only applies to assets which incurs costs such as direct labour costs, administrative costs, operating and maintenance costs, insurance, and taxes. LOHC materials (TOL and DBT) do not fall under this category. Therefore, production of TOL and DBT are not associated with any fixed OPEX cost. However, replenishment of LOHC material is a cost which incurs repeatedly during the operating time of each LOHC transportation chain. Consequently, it is classified as a variable OPEX in the model. 0.1%wt of LOHC material is assumed to be lost each cycle of loading/releasing H_2 in the TOL-LOHC and DBT-LOHC transportation chains[73].

Table 10.7: General OPEX assumptions.

Item	**Value**	**Unit**
Chartering Rate (Svalbard Scenario)[1]	15	% of CAPEX/year
Fixed OPEX[2]	2.5	% of CAPEX
LOHC material loss	0.1	%mass/cycle

[1]The chartering rate for the Svalbard scenario is an approximation of typical relationships between current chartering rates for different ship-types with respect to their total CAPEX cost. For convenience, the chartering rate is given as an annual rate, rather than a daily rate which is convention.
[2]Does not apply to production cost of LOHC material.

Figure 10.2 shows the undiscounted OPEX costs for each transportation chain in the Japan and Svalbard scenario.

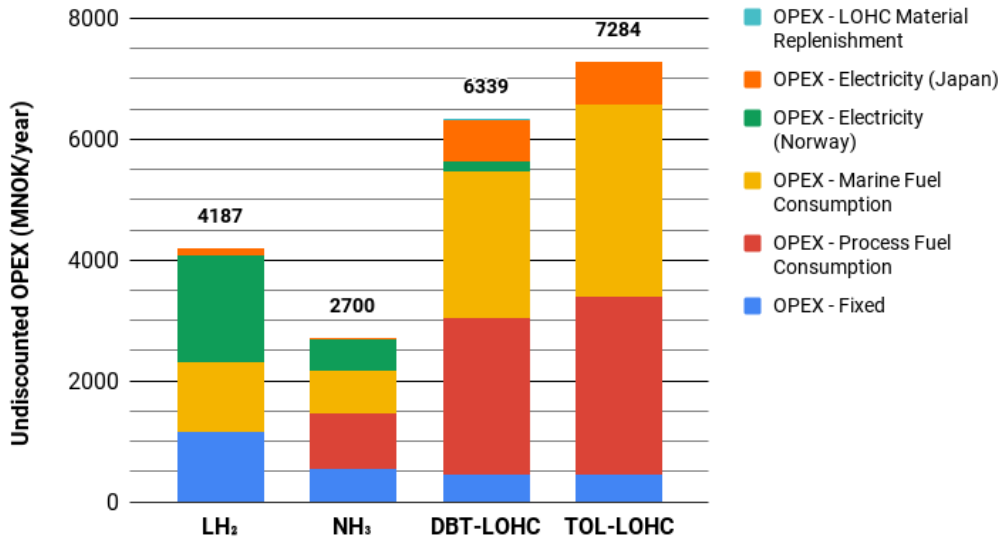

(a) Japan scenario.

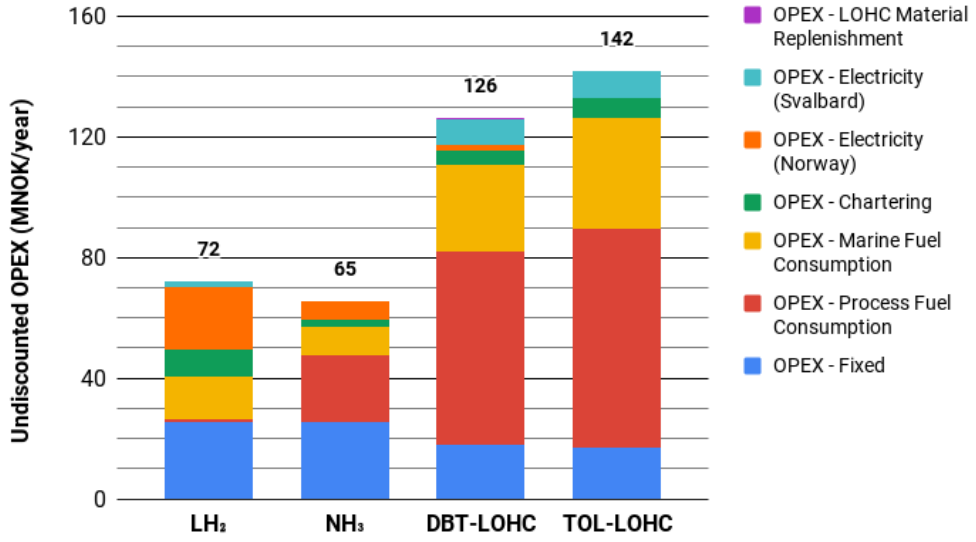

(b) Svalbard scenario.

Figure 10.2: Break-down of total undiscounted OPEX per year.

In both the Japan and Svalbard scenario, the NH_3 transportation chain has the lowest undiscounted annual OPEX costs. This is in part due to its relatively low marine fuel consumption; a cause of which is the high hydrogen density in NH_3 which reduces the no. of round-trips needed for transportation of 300,000 tons H_2/year. Cost of electricity is a large component of the undiscounted OPEX break-down

of the LH_2 transportation chain, whereas process fuel consumption is the single largest OPEX item for both the DBT-LOHC and TOL-LOHC chains. The chartering cost incurred by each transportation chain makes up a relatively small part of the total undiscounted OPEX of the Svalbard scenario.

10.4 Levelised Cost

The CAPEX and OPEX given in Section 10.2 and 10.3, respectively, present two different aspects of the economic analysis of hydrogen transportation chains. In order to give a single economic indicator (in which both are considered simultaneously) the Levelised Cost of Hydrogen Transport (LCoHT) was formulated in Section 6.5.3. LCoHT takes into account the total CAPEX and OPEX of each hydrogen transportation chain over its lifetime, and expresses the cost per kg delivered H_2. Figure 10.3 gives the break-down of LCoHT in each transportation chain for both the Japan and Svalbard scenario.

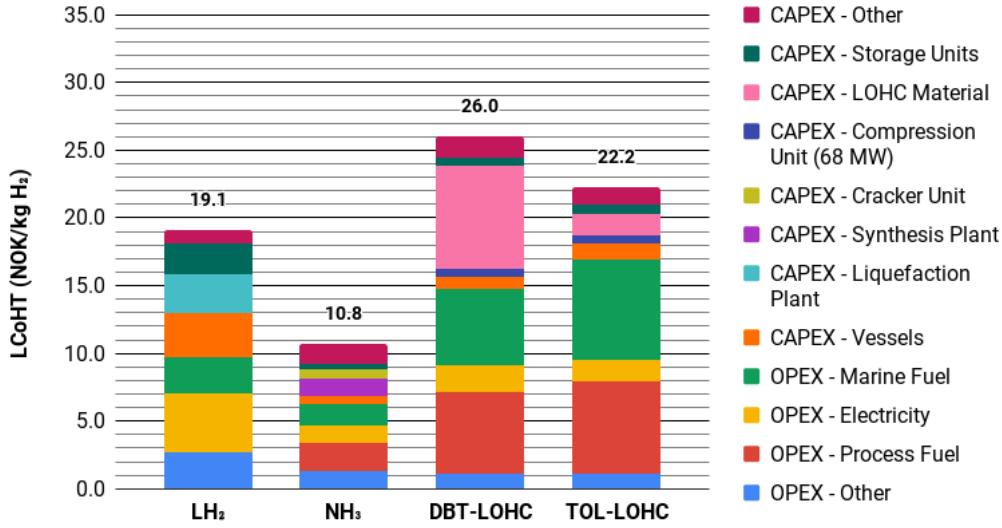

(a) Japan scenario.

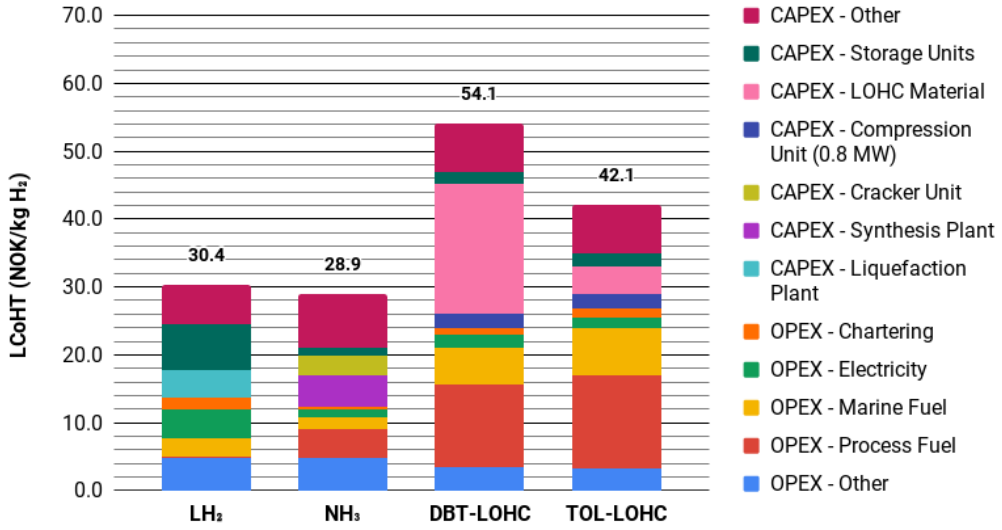

(b) Svalbard scenario.

Figure 10.3: Levelised Cost of Hydrogen Transport (LCoHT).

For the Japan scenario, the NH_3 transportation chain is found to have a significantly lower cost per kg delivered H_2 than the other transportation chains. This is in part due to its low marine fuel consumption, lowest among all transportation chains. The LOHC transportation chains have very high costs associated with fuel consumption, when compared to the LH_2 and NH_3 chain. This is largely due to the energy-consuming dehydrogenation process and high marine fuel consumption.

Due to a higher cost of hydrogen fuel in the Svalbard scenario, as shown in Table 10.6, all transportation chains are more heavily penalised for consumption of hydrogen cargo. Consequently, OPEX cost of marine fuel (per kg H_2 delivered) is higher in the Svalbard scenario even though the transportation distance (and associated energy consumption during shipping) is lower.

Typical transportation cost for LNG shipping from Norway to Japan is approximately 21 NOK/MBtu (3$/MBtu)[75]. This figure only takes into account shipping. Liquefaction, buffer storage and regasification (which are all processes part of the LNG value chain) are not taken into account. In Figure 10.3, the break-down of Levelised Cost of Marine Energy Transport (LCoMET) for each hydrogen transportation chain is given. All stages of each respective hydrogen carrier's transportation chain, apart from shipping, is left out.

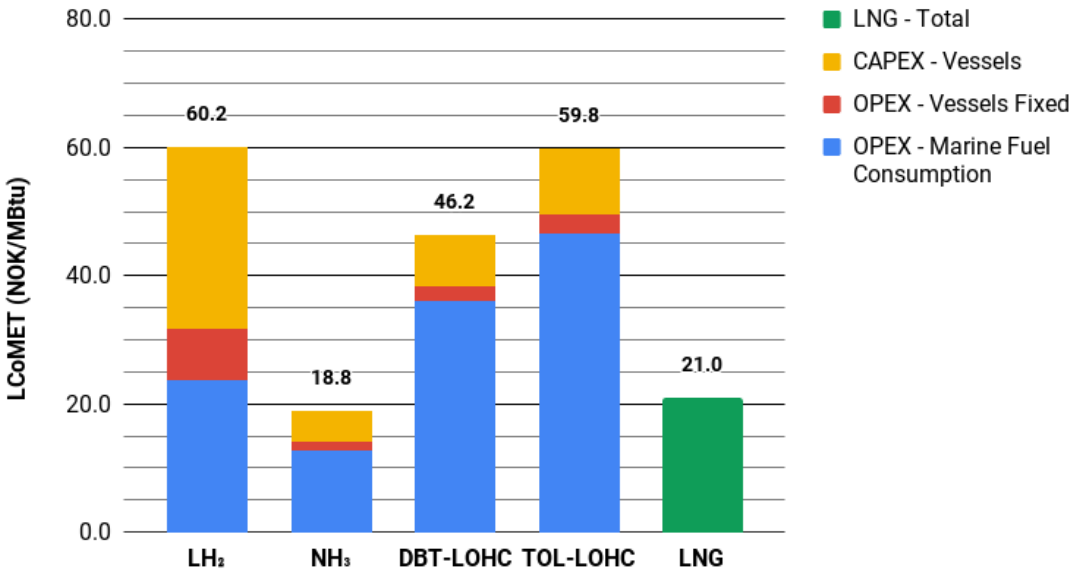

Figure 10.4: Levelised Cost of Marine Energy Transport (LCoMET) for the Japan scenario. Given on a million british thermal unit (MBtu) basis. The LCoMET is given for shipping, isolated. All other stages of each hydrogen carriers' transportation chain is not accounted for.

It is interesting to note that the NH_3 chain has a slightly lower cost of transportation when compared to the cost of LNG-shipping from Norway to Japan. Meanwhile, LH_2, DBT-LOHC and TOL-LOHC has a significantly higher LCoMET of transportation. DBT-LOHC has a significantly lower LCoMET of shipping compared to the LH_2 chain. It is also interesting to see from Figure 10.4 the distribution

of CAPEX and OPEX. For the LH_2 chain, the vessel CAPEX constitutes a larger component of the total LCoMET than for the other hydrogen carriers. This is a result of the high costs associated with construction of LH_2 tankers, as noted in Section 7.5. For the LOHC chains, on the other hand, OPEX on fuel consumption, is the largest single element of the LCoMET. Despite high OPEX on fuel consumption, both LOHC transportation chains achieve a lower LCoMET than the LH_2 chain. Most notably, the DBT-LOHC has a LCoMET which is lower by ≈14 NOK/MBtu.

Chapter 11

Analysis of Sensitivities

The results presented in Chapter 9 and 10 are prone to various sensitivities in the input-parameters used for modelling. This chapter aims to further investigate a few selected sensitivities which are deemed to have a large impact on the result. Only results which is directly related to each given sensitivity is shown in the following discussions.

11.1 Availability of Waste Heat at Export Destination

11.1.1 Background

Depending on circumstances, there could be many sources of waste heat at the export-destination. These waste heat sources may be integrated with the dehydrogenation process of the LOHC transportation chain which requires relatively low-grade heat. Broadly speaking, different sources of waste heat may be categorised as follows:

1. *Industrial processes*: Many industrial processes (unrelated to hydrogen) produce waste heat of sufficient grade and magnitude for LOHC dehydrogenation.

2. *Hydrogen utilisation*: Power-producing processes such as combustion of hydrogen in a gas turbine or H_2 consumption in a solid oxide fuel cell (SOFC), produce waste heat which may be applied to LOHC dehydrogenation.

Irregardless of the source, waste heat is assumed to cover all energy demands for dehydrogenation in this sensitivity study.

11.1.2 Technical Analysis

In effect, availability of waste heat at the export destination eliminates the need to use fuel for providing heat for the dehydrogenation process. This is shown in Figure 11.1.

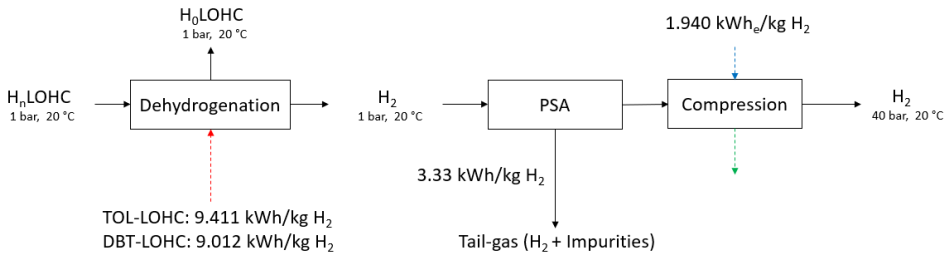

Figure 11.1: LOHC dehydrogenation using waste heat at export-destination. The PSA unit is assumed to have a recovery rate of 90%. See Figure 8.9, for comparison with the case when waste heat is not available.

Since the PSA unit is assumed to have an efficiency of 90%, 10% hydrogen (in the PSA tail-gas) is effectively lost. In the main analysis, PSA tail-gas is consumed for dehydrogenation and did therefore not impact the energy-balance. Since waste heat is used for dehydrogenation in this sensitivity, however, PSA tail-gas does impact the energy-balance.

11.1.3 Results

Figure 11.2 shows the impact of available waste heat for dehydrogenation, on the total fuel consumption of the TOL-LOHC and DBT-LOHC transportation chains.

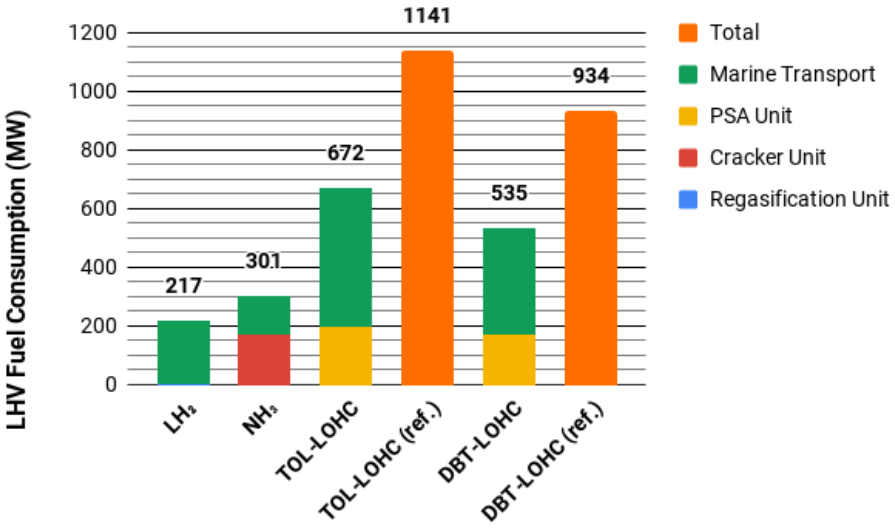

(a) Japan scenario.

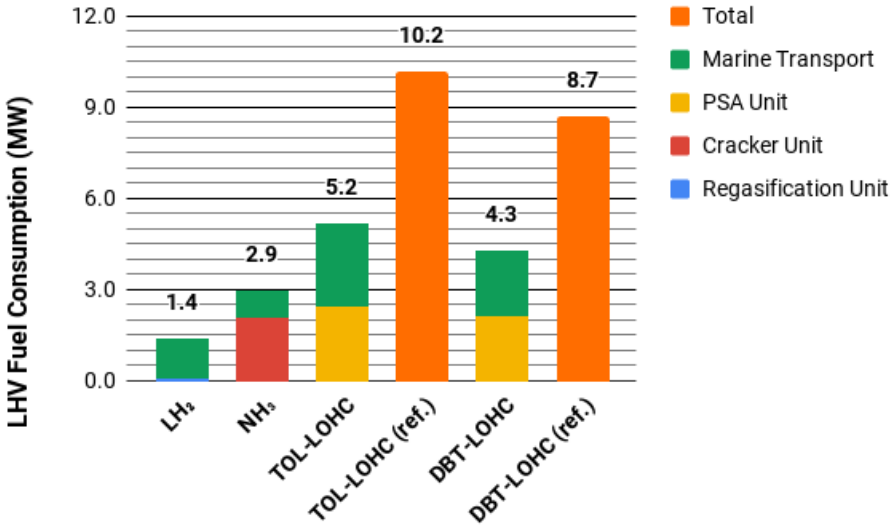

(b) Svalbard scenario.

Figure 11.2: Break-down of fuel consumption (on a LHV basis) when dehydrogenation energy requirement is covered by waste heat. DBT-LOHC (ref.) and TOL-LOHC (ref.) are the fuel consumption applicable for when waste heat is not available.

Total fuel consumption for the LOHC transportation chains is almost cut in half when waste heat is available at the export-destination. Despite this, total fuel consumption is still higher for the LOHC chains compared to the LH_2 and NH_3 transportation chains. Figure 11.3 shows the break-down of LCoHT for each transportation chain.

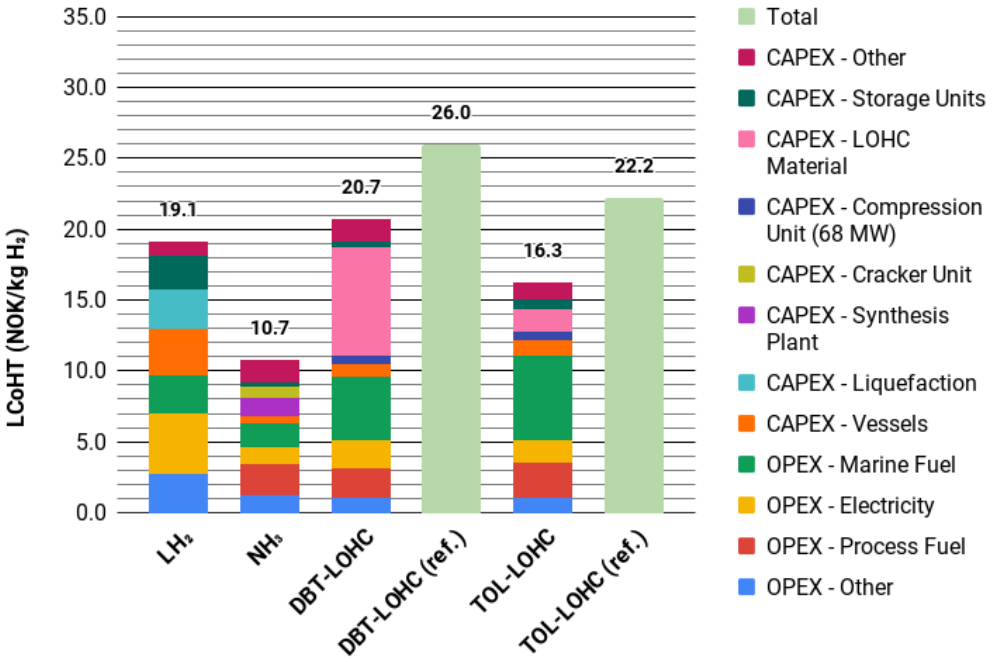

(a) Japan scenario.

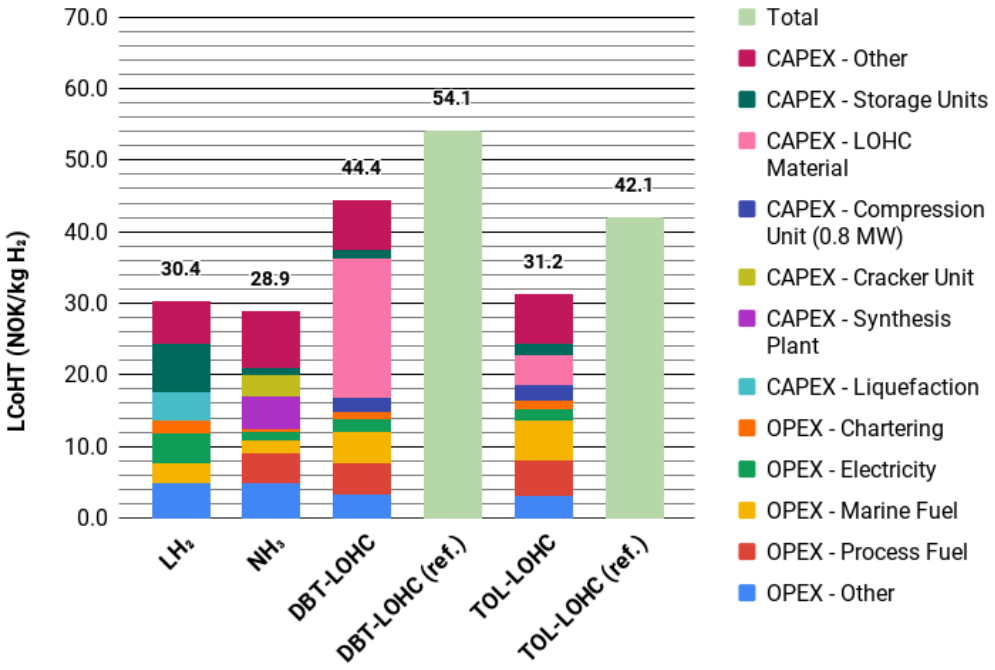

(b) Svalbard scenario.

Figure 11.3: Break-down of Levelised Cost of Hydrogen Transport (LCoHT) when dehydrogenation energy requirement is covered by waste heat. DBT-LOHC (ref.) and TOL-LOHC (ref.) are reference LCoHTs for applicable for when waste heat is not available.

The reduction in fuel consumption has a great effect on the transportation cost for the LOHC chains. The LCoHT of the LH_2 transportation chain is now more than 17% higher than that of the TOL-LOHC chain for the Japan scenario. The DBT-LOHC chain still, however, has the highest LCoHT, despite a large improvement from the case where no waste heat for dehydrogenation is available. The high cost of DBT is the single largest transportation cost. In the Svalbard scenario, both LOHC chains have higher LCoHTs relative to the other chains despite the availability of waste heat for dehydrogenation. This is because the LOHC chains still have a high fuel consumption, and are penalised by the high cost of fuel in the Svalbard scenario.

11.2 Cost of Dibenzyltoluene

The cost of dibenzyltoluene was set to be 36 NOK/kg DBT in the main analysis. However, as production volumes of DBT increase, it is expected that the cost of DBT will be significantly reduced from today's level. Figure 11.4 shows the impact of changes in the cost of DBT on the LCoHT of each transportation chain.

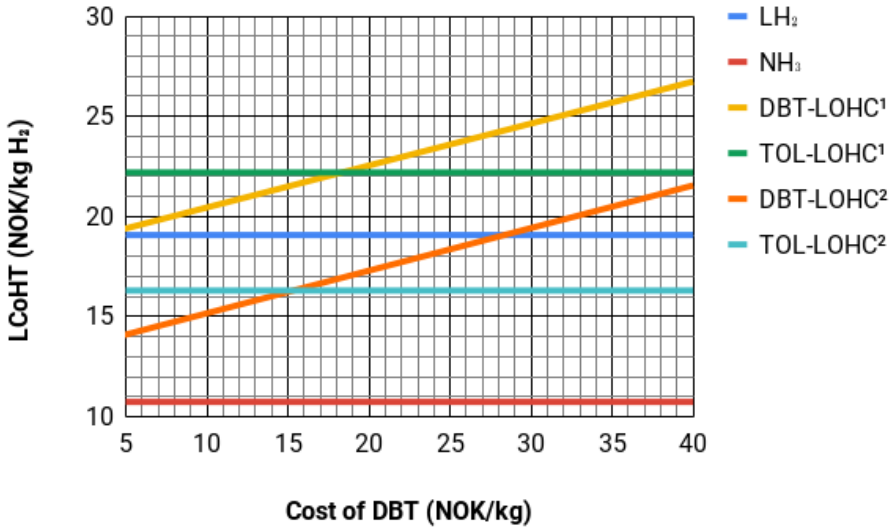

(a) Japan scenario.

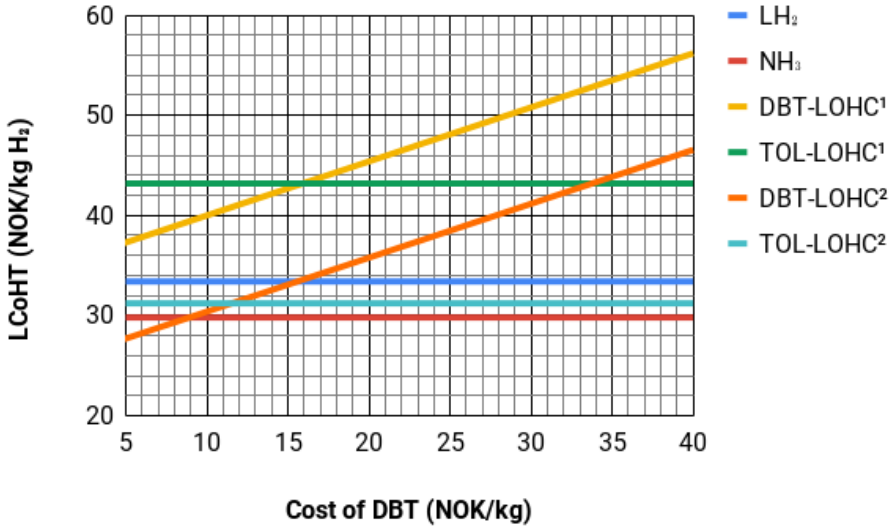

(b) Svalbard scenario.

Figure 11.4: Levelised Cost of Hydrogen Transport (LCoHT) vs. cost of DBT for each transportation chain. The LCoHT of LOHC transportation chains were waste heat is assumed to be available for dehydrogenation, is also shown.

[1]No available waste-heat for dehydrogenation at export-destination.
[2]Available waste-heat for dehydrogenation at export-destination. Reference to sensitivity-study in Section 11.1.

Varying the cost of dibenzyltoluene has a large impact on the DBT-LOHC transportation chain, as evidenced by the relatively steep gradient of the LCoHT for the DBT-LOHC chains in Figure 11.4. In the Svalbard scenario, the DBT-LOHC chain (given that waste heat for dehydrogenation is available at the export-destination) becomes competitive with the NH_3 chain at a cost of 9 NOK/kg DBT. This is one of the few circumstances, where any of the transportation chains has a lower transportation cost than the NH_3 chain. In the Japan scenario, DBT-LOHC has lower transportation cost than TOL-LOHC when the cost of DBT is less than 15 NOK/kg and waste heat for dehydrogenation is available. In both scenarios, the LOHC chains have a lower transportation costs than the LH_2 chains, given that waste heat for dehydrogenation is available and the cost of DBT is less than 16 NOK/kg.

11.3 Cruising Speed

Cruising speed was chosen in the main analysis to be 18.0 kn and 14.0 kn for the Japan and Svalbard scenario respectively. Section 7.4, showed that the choice of cruising-speed had a large impact on the total fuel-consumption of each vessel during voyage. Figure 11.5 shows the impact of varying cruising speed on the LCoHT of each transportation chain.

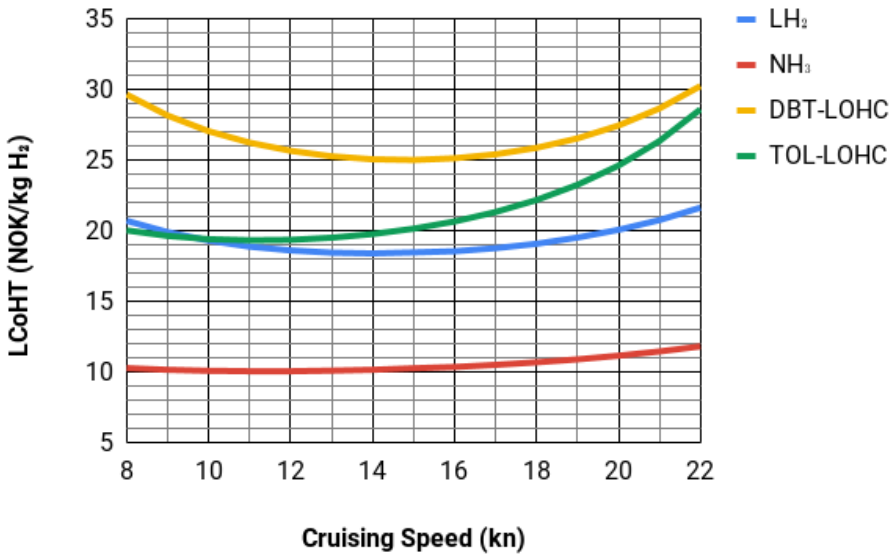

(a) Japan scenario.

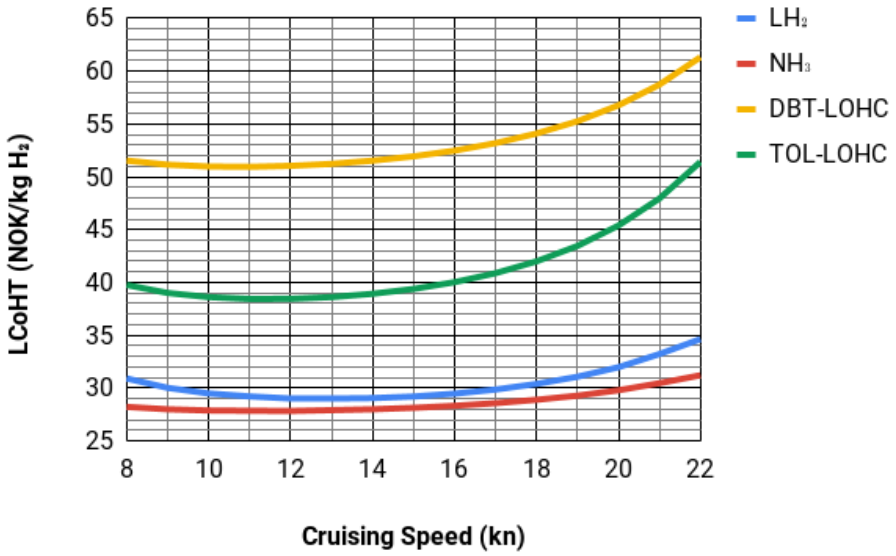

(b) Svalbard scenario.

Figure 11.5: Levelised Cost of Hydrogen Transport (LCoHT) vs. cruising speed of each transportation chain.

As evidenced by Figure 11.5, each transportation chain has different responses to changes in cruising speed. DBT-LOHC, TOL-LOHC, and the LH_2 transportation chains are relatively sensitive to changes in cruising speed, when compared to the NH_3 transportation chain. All transportation chains have an optimum cruising speed which is below 18 kn and 14 kn for the Japan and Svalbard scenario, respectively. The optimal cruising speed is dependent on a trade-off between two important factors: fuel consumption and CAPEX cost for cargo-ships. As shown in Figure 7.8, significant amounts of fuel is saved by adopting low cruising speeds. On the other hand, lower cruising speeds necessitates the construction of more cargo-ships to facilitate transportation. In the case of LOHC systems, there is a significant additional factor - the cost of LOHC material (DBT and TOL). A low cruising speed, necessitates the purchase of more LOHC material in order to fill the capacities of more ships. Since the cost of DBT is higher than that of TOL (36 NOK/kg vs 7.2NOK/kg), the effect is is more pronounced for the DBT-LOHC transportation chain.

11.4 Grid GHG Intensity in Japan

Grid GHG intensities were calculated in Appendix E. The Japanese GHG grid intensity was calculated on the basis of a 50% reduction relative to 2015. There is, however, a lot of uncertainty attached to the assumed Japanese GHG grid intensity. Therefore, it is useful to investigate the sensitiveness of Japanese GHG grid intensity on the total transportation chain GHG emissions, as shown in Figure 11.6.

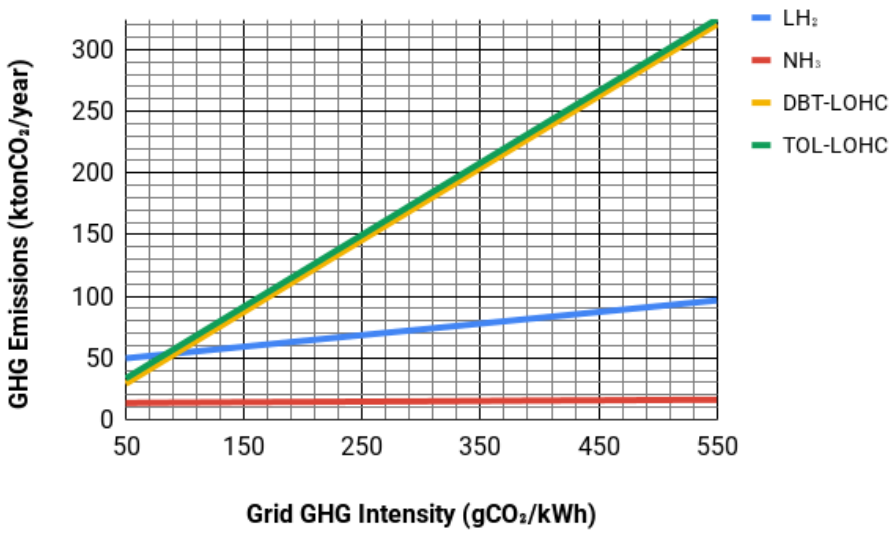

Figure 11.6: Total transportation chain GHG emissions versus grid GHG intensity at the Japanese grid. This figure only applies to the Japan scenario. In the main analysis, the GHG intensity of the Japanese grid was set to 280 gCO_2/kWh_e.

The LOHC transportation chains are very sensitive to GHG grid intensity in Japan, compared to the NH_3 and LH_2 transportation chain. For grid GHG intensities of less than $\approx$ 90 gCO_2/kWh_e, the DBT/TOL-LOHC transportation chains emit less CO_2 than the LH_2 chain. Regardless of Japanese grid GHG intensity, however, the NH_3 chain is likely to have the lowest overall GHG emissions in the Japan scenario.

11.5 Discount Rate

Depending on the application, economic analyses of different projects use different discount rates. In the public sector, a relatively low discount rate is used (also known as social discount rate), whereas a higher discount rate is used in the private sector. The difference in discount rate between the private and public sectors is tied to unequal requirements with regards to profitability and valuation of future benefits. Figure 11.7 shows the impact of changing the discount rate for both the Svalbard and Japan scenario.

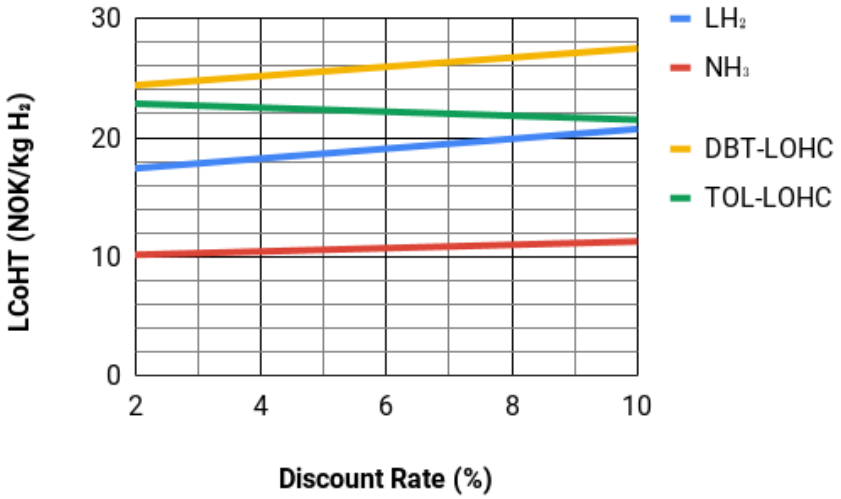

(a) Japan scenario.

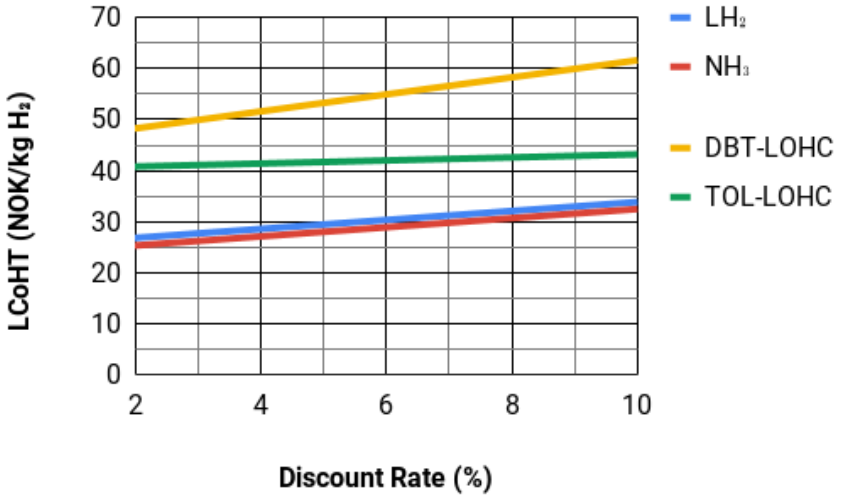

(b) Svalbard scenario.

Figure 11.7: Levelised Cost of Hydrogen Transport (LCoHT) vs. discount rate. In the two main case scenarios, discount rate is set to 6%.

The given discount rate affects the degree to which future cash flows have an impact on the net present value. Increasing it, reduces the effect of future values. With reference to Section 6.5.3, LCoHT is given as the ratio between the total discounted lifetime costs and total discounted lifetime H_2 mass output associated with each transportation chain. Both components, are discounted according to the given discount rate. The results indicate that the transportation cost generally increase, as discount rate increases. Therefore, generally, as the discount rate increases, the rate at which the total discounted mass flow decreases is higher than the rate at which the total discounted lifetime cost decreases. The exception to this, is the TOL-LOHC chain in the Japan scenario. The reason for this, is that the Japan TOL-LOHC chain has by far the highest OPEX component of LCoHT compared the other chains - especially so in the Japan scenario as shown in Figure 10.3. This implies that most of the costs incurred by the TOL-LOHC chain occurs in the future.

11.6 Price of Electricity

The cost of electricity in Norway may change in the future. Figure 11.8 shows how changes in the cost of electricity in the Norwegian grid affects the LCoHT of each hydrogen transportation chain.

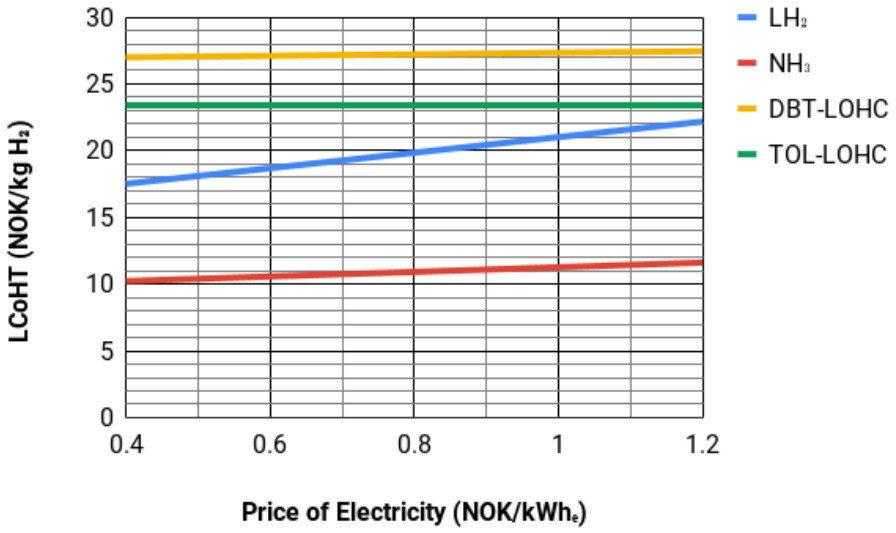

(a) Japan scenario.

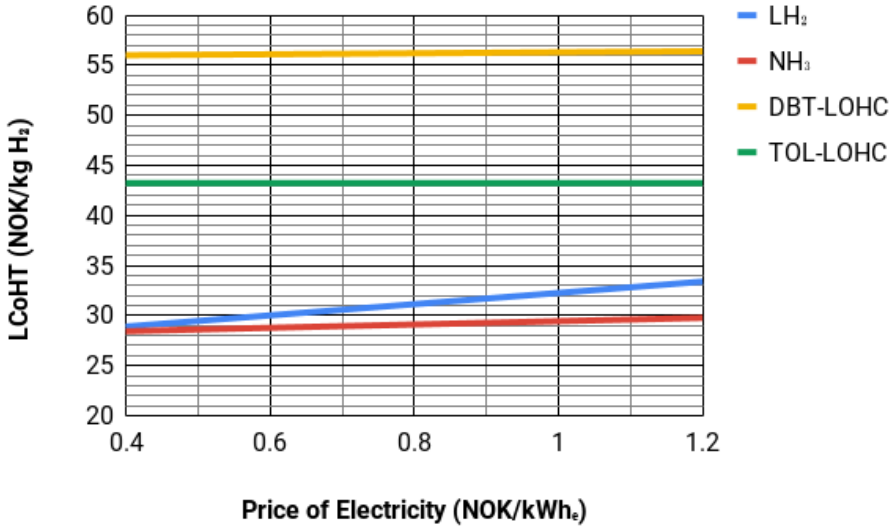

(b) Svalbard scenario.

Figure 11.8: Levelised Cost of Hydrogen Transport (LCoHT) vs. price of electricity in the Norwegian mainland. In the two main case scenarios, price of electricity is set to 0.7 NOK/kWh$_e$.

As Figure 11.8 shows, the LH_2 transportation chain is sensitive towards changes in the price of electricity, as evidenced by the relatively steep gradient of the LH_2 line. The other transportation chains

are not very sensitive to changes in the cost of electricity in Norway. In the Svalbard scenario, the LCoHT of LH_2 approaches that of NH_3 for an electricity cost of $\approx$0.4 NOK/kWh$_e$.

11.7 Internal Cost of Hydrogen as Fuel

All of the transportation chains consume fuel for shipping and energy-conversion processes such as NH_3 cracking and dehydrogenation. Figure 11.9 shows the impact of changes in the cost of fuel on the LCoHT of each transportation chain.

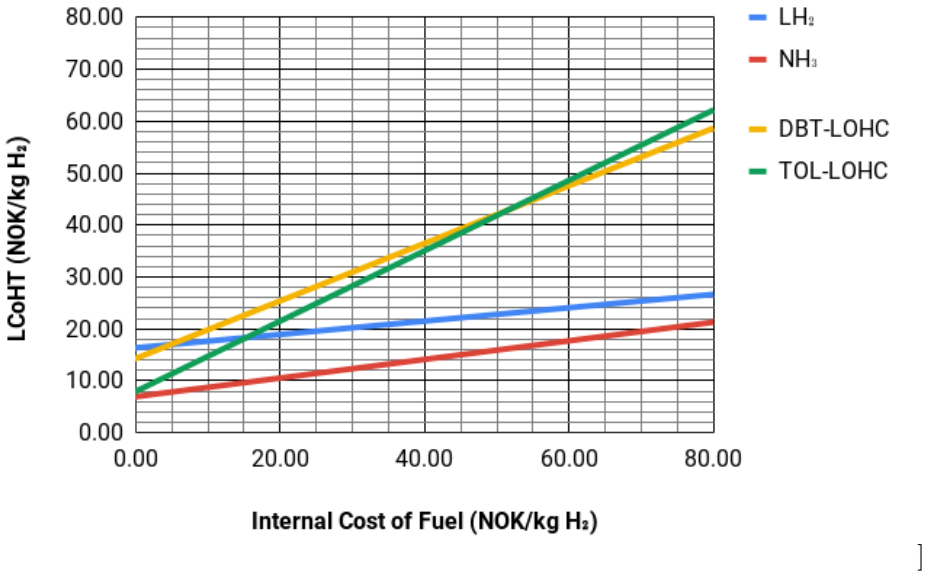

(a) Japan scenario.

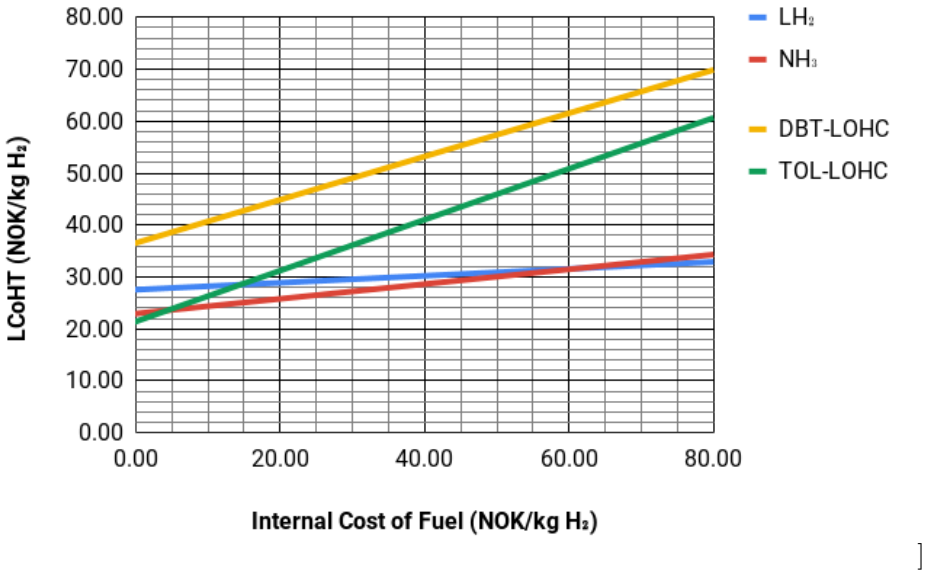

(b) Svalbard scenario.

Figure 11.9: Levelised Cost of Hydrogen Transport (LCoHT) versus internal cost of fuel. In the two main case scenarios, the internal cost of fuel is set to 21 NOK/kg H_2 and 42 NOK/kg H_2 for the Japan and Svalbard scenario respectively.

All transportation chains exhibit a strong sensitivity towards the internal cost of fuel. This is especially true for DBT-LOHC and TOL-LOHC, owing to their high fuel-consumption. In the Japan scenario, the TOL-LOHC chain has a lower LCoHT than the LH_2 chain for a fuel cost of $\approx$ 17 NOK/kg H_2. Irregardless of the fuel cost, however, the NH_3 transportation chain remains the most economically competitive in the Japan scenario. In the Svalbard scenario, the LH_2 transportation chain is the most competitive for fuel prices above $\approx$65 NOK/kg H_2. Moreover, the TOL-LOHC transportation chain has a lower LCoHT than LH_2 for fuel costs below $\approx$15 NOK/kg H_2.

Chapter 12

Discussion of Key Findings

Different performance aspects of each hydrogen carrier transportation chain has so far been presented. A model was developed to make comparisons in areas such as energy, the environment, and economics of each transportation chain. Discussion points found in this chapter, are based on results presented in Chapter 9, 10 and 11.

- Using LH_2 as a hydrogen carrier for long-distance transport requires significant amounts of electric power for on-shore buffer storage, and most importantly, hydrogen liquefaction. Electricity consumption is to a large degree concentrated on the site of export, which potentially necessitates grid infrastructure upgrades depending on the magnitude of electric power drawn. Dependence on electric power from the grid, implies that the profitability of the LH_2 transportation chain is to a large degree dependent on the price of electricity in the country of export. To a lesser extent, the same might be said of the NH_3 transportation chain which draws significant amount of electric power for air separation and NH_3 synthesis at the country of export.

- A potential drawback for the LOHC transportation chains is that dehydrogenation only has the potential to produce low-pressure hydrogen in gas phase. Since low-pressure hydrogen is difficult to store, and power-producing processes usually require higher pressure hydrogen, a high electric power use for compression of H_2 gas is needed at the export-destination. The use of large amounts of electric power at the export destination is counter-intuitive since energy is supposed to be transferred to the export-destination, not consumed from. This has a large impact for the LOHC transportation chains in electric grid systems which are associated with relatively high GHG intensity (such as that in Japan), as electric power use will lead to emissions of CO_2. This effect is eliminated if the export-destination grid is carbon-neutral (such as the projected Svalbard grid). Another effect of this is economic; the price of electricity in the export-destination is likely to be high as it is based on import of energy. Thus, ideally, all electric energy use should be limited to country where hydrogen is exported from.

- Magnitude of energy consumption during shipping is different for each hydrogen carrier. This is due to two major reasons:

1. *Hydrogen density*: Since LNH_3 has by far the highest hydrogen density, a higher amount of hydrogen (by mass) is transported during each round-trip of shipping.
2. *Post-shipping consumption of hydrogen*: The LOHC and NH_3 transportation chains both have a large consumption of hydrogen-fuel post-shipping due to the processes of dehydrogenation and NH_3 cracking. Since hydrogen cargo is consumed for these processes, more hydrogen must be shipped to the export-destination in order to compensate. Since dehydrogenation is a more energy-demanding process than NH_3 cracking, the LOHC transportation systems are the most affected by this. Assuming that thermal energy-demand for dehydrogenation is covered by waste heat at the export-destination, fuel consumption of the LOHC transportation chains is substantially reduced.

- The NH_3 transportation chain has the highest total energy chain efficiency in both the Svalbard and Japan scenario, achieving an efficiency of 0.78 and 0.75 respectively. The LH_2 chain, meanwhile, performs second best, with the LOHC chains performing worst. As far as energy consumption is concerned, the largest difference between the Svalbard and Japan scenario is the length at which hydrogen is transported. That is why the hydrogen transportation chains in the Svalbard scenario consistently has a higher efficiency than in the Japan scenario. Looking at the difference in efficiency between the Svalbard scenario and Japan scenario for each hydrogen transportation chain, one may conclude that the NH_3 chain copes best with increasing range of hydrogen transport. The NH_3 chain has a 3% reduction in the Japan scenario relative to the Svalbard scenario. Equivalent figures for the LH_2, TOL-LOHC, and DBT-LOHC chains are 4%, 8% and 7% respectively.

- The environmental performance of each hydrogen transportation chain is to a very large extent affected by grid CO_2 intensity of the grids from which electric power is used. In the Japan scenario, the LH_2 and NH_3 chains have the lowest overall GHG emissions. Conversely, for the Svalbard scenario, TOL-LOHC and DBT-LOHC have the lowest GHG emissions - TOL-LOHC is even found to have negligible CO_2 emissions.

- The least overall technically mature hydrogen transportation chain was found to be the LH_2 chain. The reason for which, is that the liquefaction process needs large improvements in both efficiency and scale (relative to present-day liquefaction plants). The weakest link, as far as TRL is concerned, of the NH_3 chain is the cracking process which require large upscales in technology. Dehydrogenation and hydrogenation processes in the LOHC chain also needs to be scaled up for adoption in large-scale energy transport. If cracking was to be disregarded from the NH_3 transportation chain, due to the direct application of NH_3 as fuel, its overall technical maturity would see a significant rise.

- The LH_2 transportation chain is found to be the most technologically complex. This is primarily due to the high technical requirements of the liquefaction process and shipping. The NH_3 chain is overall designated with a high complexity. Especially the air separation process, NH_3 synthesis, and NH_3 cracking has a high complexity. The LOHC transportation chains are associated with overall moderate complexity. In this regard, the LOHC transport chains has an edge over the NH_3 and LH_2.

- The NH_3 transportation chain is by far the most cost competitive economically for the Japan scenario, with a Levelised Cost of Hydrogen Transport (LCoHT) at 10.8 NOK/kg H_2. The NH_3 transportation chain is associated with relatively low OPEX than the other transportation chains. This is evident by the fact that fuel and electricity consumption only makes up approximately 6 NOK/kg H_2 of its LCoHT, compared to 14 NOK/kg H_2 for the DBT-LOHC chain. The main reason for why DBT-LOHC and TOL-LOHC both have higher LCoHTs than LH_2 and NH_3 chains in both scenarios, is their high OPEX to marine and process fuel consumption. A root cause for the high marine fuel consumption is the relatively low density of hydrogen in LOHCs, as seen in Figure 4.1. This necessitates a high no. of round-trips for cargo ships in order to transport the same amount of hydrogen annually as the other transportation chains.

- The LCoHT for the Svalbard scenario is consistently higher for all transportation chains than in the Japan Scenario. This is the case for two primary reasons:

    1. *Higher internal hydrogen fuel price*: The price of internal hydrogen fuel is 42 NOK/kg H_2 in the Svalbard scenario, as opposed to 21 NOK/kg $_2$ in the Japan scenario. This naturally leads to increased OPEX cost for marine fuel and process fuel.
    2. *Small-scale*: CAPEX costs for on-shore plants are more dominant in the Svalbard-scenario. This is because of the much smaller scale of hydrogen transport, as opposed to the Japan scenario. CAPEX costs per unit of output are hence, higher. This is reflected in the CAPEX scaling-principle shown in the Equation 6.5.

- Figure 10.4 gives the Levelised Cost of Marine Energy Transport (LCoMET) for each transportation chain in the Japan scenario, and compares it with that of LNG. The figure indicates that NH_3 has a lower cost than LNG-shipping per energy unit of transport. The reason for which could be the fact that LNH_3 tankers have a significantly lower CAPEX cost than LNG tankers. In this thesis, the CAPEX of a 160,000 m^3 ammonia tanker was estimated to be ≈800 MNOK. In comparison, a 160,000 m^3 LNG tanker is valued at ≈1300 MNOK. On the contrary, Figure 4.1 shows that LNG has a higher LHV energy density than LNH_3. Therefore, it would be reasonable to assume LNG transport from Norway to Japan is associated with lower fuel-costs as fewer voyage round-trips are required to transport any given amount of energy. Furthermore, the results imply that if one considers shipping isolated, transportation of LH_2 is almost three times as expensive as transporting LNG from Norway to Japan, per energy unit.

The model developed for evaluating each transportation chain may relatively easily be adapted to accommodate different case definitions, or investigating the sensitivity of key parameters. The sensitivity studies in Chapter 11 led to the uncovering of the following key points:

- Availability of waste heat at the end-destination for dehydrogenation has a large impact on the fuel consumption of each LOHC transportation chain. Total fuel consumption is reduced by approximately 40% and 50% for the DBT-LOHC and TOL-LOHC transportation chains in the Japan and Svalbard scenario respectively. In turn, this improves the cost-effectiveness of each LOHC transportation chain. In both the Japan and Svalbard scenario, TOL-LOHC has a lower transportation cost than LH_2 if waste heat is available for dehydrogenation. For the DBT-LOHC

chain however, availablity of waste heat is not enough to increase its competitiveness. The cost of DBT must also be significantly reduced from its current level of 36 NOK/kg DBT, if DBT-LOHC is to be an economical alternative relative to LH_2 and TOL-LOHC.

- Each transportation chain has different optimal cruising speeds, and the LH_2, DBT-LOHC and TOL-LOHC transportation chains are all relatively sensitive to cruising speed. For instance, by reducing the cruising speed from 18 kn to 12 kn in the Japan scenario, the TOL-LOHC may see a reduction of approx. 13% in hydrogen transportation costs. It is therefore important for marine transportation networks to optimise cruising speed, in order to minimise costs.

- LOHC transportation chains are sensitive to changes in the grid GHG intensity of the Japanese electric grid. The main reason is that both LOHC transportation chains require a large electric power input in Japan for compression. The NH_3 and LH_2 chains are meanwhile less sensitive, due to low electric power use at the export-destination. The implication of this, for an environmental perspective, is that the LOHC transportation chains are less suitable for export of clean energy to countries where the grid GHG intensity is high.

- The LH_2 transportation chain is sensitive towards changes in the cost of electricity in the Norwegian mainland grid. A low cost of electricity, boosts the competitiveness of the LH_2 chain relative to the other transportation chains.

- All transportation chains were found to have a strong sensitivity towards the internal cost of hydrogen-fuel. Especially so for the DBT-LOHC and TOL-LOHC chains which have a high fuel consumption for energy-conversion processes and shipping. The LH_2 chain, being the transportation chain with lowest total fuel consumption, is not as sensitive to fuel cost as the other chains. An important point is that for sufficiently high costs of fuel in the Svalbard scenario ($\approx$65 NOK/kg H_2), the LH_2 transportation chain has a lower transportation cost than the NH_3 chain.

Bibliography

[1] R Agarwal et al. "LNG Regasification Terminals: The Role of Geography and Meteorology on Technology Choices". English. In: *Energies* 10.12 (2017). ISSN: 1996-1073.

[2] Air Liquide. *Air Liquide to build first world scale liquid hydrogen production plant dedicated to the supply of Hydrogen energy markets*. Nov. 2018. URL: https://energies.airliquide.com/air-liquide-build-first-world-scale-liquid-hydrogen-production-plant-dedicated-supply-hydrogen.

[3] Alexander Seidel. *Refuelling of fuel cell vehicles by hydrogen from the LOHC process*. 2019. URL: https://www.gas-for-energy.com/fileadmin/G4E/pdf_Datein/2019/Fachbericht_Seidel_Hydrogenious/gfe1_19_fb_Seidel_V3.pdf.

[4] Alfa Lavel. *Exhaust gas heat recovery boiler*. URL: https://www.alfalaval.com/globalassets/images/products/heat-transfer/boilers/exhaust-gas-economizer/aalborg-av-6n-heat-recovery-boiler.pdf.

[5] Alfa Lavel. *Waste Heat Recovery Unit after gas turbines*. URL: https://www.alfalaval.com/globalassets/documents/industries/energy/power/pee00363-waste-heat-recovery-unit-after-gas-turbines.pdf.

[6] Alvar Mjelde (DNV GL). *Written correspondance*. 2019.

[7] Riccardo Amirante et al. "Effects of lubricant oil on particulate emissions from port-fuel and direct-injection spark-ignition engines". In: *International Journal of Engine Research* 18.5-6 (2017), pp. 606–620. DOI: 10.1177/1468087417706602. eprint: https://doi.org/10.1177/1468087417706602. URL: https://doi.org/10.1177/1468087417706602.

[8] Muhammad Aziz, Takuya Oda, and Takao Kashiwagi. "Comparison of liquid hydrogen, methylcyclohexane and ammonia on energy efficiency and economy (Book review)". eng. In: *Energy Procedia* 158 (2019), pp. 4086–4091. ISSN: 18766102.

[9] Francesco Baldi. *Modelling, analysis and optimisation of ship energy systems*. URL: http://www.transportportal.se/energieffektivitet/etapp2/Baldi-avhandligen.pdf.

[10] Jeffrey Ralph Bartels. "A feasibility study of implementing an Ammonia Economy". MA thesis. Jan. 2008.

[11] Battelle. *Manufacturing Cost Analysis of 100 and 250 kW Fuel Cell Systems for Primary Power and Combined Heat and Power Applications*. 2017. URL: https://www.energy.gov/sites/prod/files/2018/02/f49/fcto_battelle_mfg_cost_analysis_100_250kw_pp_chp_fc_systems_jan2017.pdf.

[12] Trevor Brown. *Pilot project: an ammonia tanker fueled by its own cargo*. URL: https://www.ammoniaenergy.org/bunker-ammonia-new-report-quantifies-ammonia-as-the-most-competitive-fuel-for-zero-emission-maritime-vessels-in-2030/.

[13] Selma Brynolf et al. "Electrofuels for the transport sector: A review of production costs". eng. In: *Renewable and Sustainable Energy Reviews* 81.P2 (2018), pp. 1887–1905. ISSN: 1364-0321.

[14] U. Cardella, L. Decker, and H. Klein. "Roadmap to economically viable hydrogen liquefaction". eng. In: *International Journal of Hydrogen Energy* 42.19 (2017), pp. 13329–13338. ISSN: 0360-3199.

[15] Carlo Raucci. *The potential of hydrogen to fuel international shipping*. 2017. URL: http://discovery.ucl.ac.uk/1539941/1/PhD%5C%20Thesis%5C%20Carlo%5C%20Raucci%5C%20Final.pdf.

[16] W.F Castle. "Air separation and liquefaction: recent developments and prospects for the beginning of the new millennium". eng. In: *International Journal of Refrigeration* 25.1 (2002), pp. 158–172. ISSN: 0140-7007.

[17] CertifHy. *CertifHy-SD Hydrogen Criteria*. 2019. URL: https://www.certifhy.eu/images/media/files/CertifHy_2_deliverables/CertifHy_H2-criteria-definition_V1-1_2019-03-13_clean_endorsed.pdf.

[18] "Chapter 5 - Natural Gas Liquefaction Cycle Enhancements and Optimization". eng. In: *Handbook of Liquefied Natural Gas*. 2014, pp. 229–257. ISBN: 978-0-12-404585-9.

[19] C-Job. *Ammonia as ship's fuel: C-Job's future-proof way of thinking*. URL: https://c-job.com/ammonia-as-ships-fuel-c-jobs-future-proof-way-of-thinking/.

[20] L.M. Das. "7 - Hydrogen-fueled internal combustion engines". eng. In: *Compendium of Hydrogen Energy*. 2016, pp. 177–217. ISBN: 978-1-78242-363-8.

[21] Rob Dekkers. *Applied Systems Theory*. eng. 2015th ed. Cham: Springer International Publishing, 2015. ISBN: 9783319108452.

[22] DNV GL. *Energy Transition Outlook 2018*. June 2018. URL: https://eto.dnvgl.com/2018/.

[23] DNV GL. *Maritime Forecast to 2050: Energy transition outlook 2018*. Jan. 2018. URL: https://eto.dnvgl.com/2018/maritime.

[24] Dr. Dmitri Kopeliovich. *Ammonia cracker*. 2017. URL: http://www.substech.com/dokuwiki/doku.php?id=ammonia_cracker.

[25] EDF Group. *HySiLabs: the alternative hydrogen supply*. 2018. URL: https://www.edf.fr/en/hysilabs-liquid-hydrogen#how-does-it-work.

[26] Egyptian International Shipping Agencies & Services. *EISAS Guide to Suez Canal Convoy*. URL: http://www.eisgroup.info/wp-content/uploads/2017/04/suez-canal-Transit-Guide-Formal-document.pdf.

[27] EMSA, DNV GL. *STUDY ON THE USE OF FUEL CELLS IN SHIPPING*. Jan. 2017. URL: www.emsa.europa.eu/emsa-documents/download/4545/2921/23.html.

[28] Energy Sector Management Assistance Program (ESMAP). *Study of Equipment Prices in the Power Sector*. 2009. URL: https://esmap.org/sites/default/files/esmap-files/TR122-09_GBL_Study_of_Equipment_Prices_in_the_Power_Sector.pdf.

[29] European Environment Agency. *Overview of electricity production and use in Europe*. 2018. URL: https://www.eea.europa.eu/data-and-maps/indicators/overview-of-the-electricity-production-2/assessment-4.

[30] Stefano Frigo and Roberto Gentili. "Analysis of the behaviour of a 4-stroke Si engine fuelled with ammonia and hydrogen". English. In: *International Journal of Hydrogen Energy* 38.3 (2013). ISSN: 0360-3199.

[31] Ioannis Garagounis et al. "Electrochemical Synthesis of Ammonia in Solid Electrolyte Cells". In: *Frontiers in Energy Research* 2 (Jan. 2014). DOI: 10.3389/fenrg.2014.00001.

[32] S. Giddey et al. "Ammonia as a Renewable Energy Transportation Media". In: *ACS Sustainable Chemistry & Engineering* 5.11 (2017), pp. 10231–10239. DOI: 10.1021/acssuschemeng.7b02219. eprint: https://doi.org/10.1021/acssuschemeng.7b02219. URL: https://doi.org/10.1021/acssuschemeng.7b02219.

[33] Global maritime energy efficiency partnerships (GloMEEP). *WASTE HEAT RECOVERY SYSTEMS*. 2016. URL: https://glomeep.imo.org/technology/waste-heat-recovery-systems/.

[34] Agata Godula-Jopek. *Hydrogen storage technologies : new materials, transport, and infrastructure*. eng. 2nd ed. Weinheim: Wiley-VCH Verlag GmbH & Co. KGaA, 2012. ISBN: 3-527-64994-8.

[35] H21 North of England. *H21 NoE Report 2018*. 2018. URL: https://northerngasnetworks.co.uk/h21-noe/H21-NoE-23Nov18-v1.0.pdf.

[36] René Heindl et al. "New and Innovative Combustion Systems for the H2-ICE: Compression Ignition and Combined Processes". eng. In: *SAE International Journal of Engines* 2.1 (2009), pp. 1231–1250. ISSN: 1946-3944.

[37] Steffen Møller Holst et al. *Hydrogen verdikjeder og potensial*. URL: https://www.sintef.no/contentassets/cd105affc9d64e09a7b6e822203c5b0d/underlagsnotat_hydrogen_sintef.pdf.

[38] Honeywell UOP. *50 Years of PSA Technology for H2 Purification*. URL: https://www.uop.com/?document=psa-50-paper&download=1.

[39] Horizon 2020 - EU. "HORIZON 2020 – WORK PROGRAMME 2014-2015". In: (Jan. 2014). URL: https://ec.europa.eu/research/participants/data/ref/h2020/wp/2014_2015/annexes/h2020-wp1415-annex-g-trl_en.pdf.

[40] Hydrogen Council. *Hydrogen Scaling Up: A Sustainable pathway for the global energy transition.* Oct. 2017. URL: http://hydrogencouncil.com/wp-content/uploads/2017/11/Hydrogen-Scaling-up_Hydrogen-Council_2017.compressed.pdf.

[41] Hydrogenious. *Hydrogenious Technologies' ReleaseUNIT - products for hydrogen release.* URL: https://www.hydrogenious.net/index.php/en/products/thereleaseunit/.

[42] Hydrogenious. *Hydrogenious Technologies' StorageUNIT - Products for hydrogen storage.* URL: https://www.hydrogenious.net/index.php/en/products/thestorageunit/.

[43] Institut Francais des Relations Internationales. *Japan's Hydrogen Strategy and Its Economic and Geopolitical Implications.* 2018. URL: https://www.ifri.org/en/publications/etudes-de-lifri/japans-hydrogen-strategy-and-its-economic-and-geopolitical-implications.

[44] International Energy Agency(IEA). *Costs and benefits of emergency stockholding.* 2018. URL: https://webstore.iea.org/insights-series-2018-costs-and-benefits-of-%20emergency-stockholding.

[45] International Energy Agency(IEA). *ENERGY POLICIES OF IEA COUNTRIES:Japan.* 2016. URL: https://webstore.iea.org/energy-policies-of-iea-countries-japan-2016-review.

[46] International Energy Agency(IEA). *ENERGY POLICIES OF IEA COUNTRIES:Norway.* 2017. URL: https://www.regjeringen.no/contentassets/b6abc54c8d034fc39755f10005392b0d/iea-rapport-idr_2017_norway_web-final.pdf.

[47] International Energy Agency(IEA). *Technology Roadmap Hydrogen and Fuel Cells.* URL: https://www.iea.org/publications/freepublications/publication/TechnologyRoadmap%20HydrogenandFuelCells.pdf.

[48] International Maritime Organization (IMO). *Second IMO GHG Study 2009.* Jan. 2009. URL: http://www.imo.org/en/OurWork/Environment/PollutionPrevention/AirPollution/Documents/SecondIMOGHGStudy2009.pdf.

[49] International Maritime Organization (IMO). *UN body adopts climate change strategy for shipping.* Apr. 2018. URL: http://www.imo.org/en/mediacentre/pressbriefings/pages/06ghginitialstrategy.aspx.

[50] International Renewable Energy Agency (IRENA). *Hydrogen from Renewable Power: Technology Outlook for the Energy Transition.* Sept. 2018. URL: https://www.irena.org/publications/2018/Sep/Hydrogen-from-renewable-power.

[51] Japan Ministry of Economy, Trade and Industry (METI). *Japan's Energy: 20 Questions to understand the current energy situation.* URL: http://www.enecho.meti.go.jp/en/category/brochures/pdf/japan_energy_2017.pdf.

[52] Japan Ministry of Economy, Trade and Industry (METI). *The Basic Hydrogen Strategy.* 2017. URL: http://www.meti.go.jp/english/press/2017/1226_003.html.

[53] John J. Minnehan and Joseph W. Pratt, Sandia National Laboratories. *Practical Application Limits of Fuel Cells and Batteries for Zero Emission Vessels.* 2017. URL: https://energy.sandia.gov/wp-content/uploads/2017/12/SAND2017-12665.pdf.

[54] Shoji Kamiya, Motohiko Nishimura, and Eichi Harada. "Study on Introduction of CO2 Free Energy to Japan with Liquid Hydrogen". eng. In: *Physics Procedia* 67 (2015), pp. 11–19. ISSN: 1875-3892.

[55] Jeanette Berge Knutsen. "Near zero emission energy export and electric power supply based on natural gas". MA thesis. 2018.

[56] Hideaki Kobayashi et al. "Science and technology of ammonia combustion". eng. In: *Proceedings of the Combustion Institute* 37.1 (2019), pp. 109–133. ISSN: 1540-7489.

[57] Hideaki Kobayashi et al. "Science and technology of ammonia combustion". eng. In: *Proceedings of the Combustion Institute* 37.1 (2019), pp. 109–133. ISSN: 1540-7489.

[58] Songwut Krasae-in, Jacob H. Stang, and Petter Neksa. "Development of large-scale hydrogen liquefaction processes from 1898 to 2009". eng. In: *International Journal of Hydrogen Energy* 35.10 (2010), pp. 4524–4533. ISSN: 0360-3199.

[59] A. Kumar and M. Sehgal. "Hydrogen Fuel Cell Technology for a Sustainable Future: A Review". In: vol. 2018-. SAE International, 2018.

[60] Ahmed Laouir. "Performance analysis of open-loop cycles for LH2 regasification". eng. In: *International Journal of Hydrogen Energy* (2019). ISSN: 0360-3199.

[61] Lloyd's Register Marine and UMAS (University Maritime Advisory Services. *Zero-Emission Vessels 2030. How do we get there?* 2017. URL: http://www.lrs.or.jp/news/pdf/LR_Zero_Emission_Vessels_2030.pdf.

[62] MAN B&W. *Diesel-electric Propulsion Plants - A brief guideline how to engineer a diesel-electric propulsion systems.* 2012. URL: https://marine.mandieselturbo.com/docs/librariesprovider6/marine-broschures/diesel-electric-drives-guideline.pdf.

[63] Man Diesel SE. *LNG Carrier Power.* 2008. URL: https://marine.mandieselturbo.com/docs/librariesprovider6/technical-papers/lng-carrier-power.pdf?sfvrsn=6.

[64] MAN Diesel & Turbo. *Ship Operation Using LPG and Ammonia As Fuel on MAN B&W Dual Fuel ME-LGIP Engines.* eng. 2019. URL: https://nh3fuelassociation.org/2018/12/07/ship-operation-using-lpg-and-ammonia-as-fuel-on-man-bw-dual-fuel-me-lgip-engines/.

[65] MAN Diesel & Turbo. *Two-stroke Low Speed Diesel Engines for Independent Power Producers and Captive Power Plants.* 2013. URL: https://www.mandieselturbo.com/docs/default-source/shopwaredocumentsarchive/two-stroke-low-speed-diesel-engines.p.

[66] MAN Diesel & Turbo. *Waste Heat Recovery System (WHRS) for Reduction of Fuel Consumption, Emissions and EEDI.* 2014. URL: https://mandieselturbo.com/docs/librariesprovider6/technical-papers/waste-heat-recovery-system.pdf.

[67] Marek Dzida, Wojciech Olszewski. "THE SYSTEM COMBINED OF LOW-SPEED MARINE DIESEL ENGINE AND STEAM TURBINE IN SHIP PROPULSION APPLICATIONS". In: 2011. URL: http://www.polishcimeeac.pl/Papers1/2011/005.pdf.

[68] MariGreen Project - MARIKO, FME, Institute for Combustion Engines (Aachen University). *Perspectives for the Use of Hydrogen as Fuel in Inland Shipping*. 2018. URL: http://marigreen.eu/wordpress_marigreen/wp-content/uploads/2018/11/Hydrogen-Feasibility-Study-MariGreen.pdf.

[69] Mitsubishi Heavy Industries, Ltd. *Development of High Efficiency Marine Propulsion Plant (Ultra Steam Turbine)*. 2007. URL: https://www.mhi.co.jp/technology/review/pdf/e443/e443015.pdf.

[70] Anthony F. Molland. *The Maritime Engineering Reference Book*. eng. Butterworth-Heinemann, 2008. ISBN: 9780080560090.

[71] Eric R. Morgan. "Techno-Economic Feasibility Study of Ammonia Plants Powered by Offshore Wind". eng. In: (2013). URL: https://scholarworks.umass.edu/cgi/viewcontent.cgi?article=1704&context=open_access_dissertations.

[72] NCE Maritime Cleantech. *Norwegian future value chains for liquid hydrogen*. 2016. URL: https://maritimecleantech.no/wp-content/uploads/2016/11/Report-liquid-hydrogen.pdf.

[73] M. Niermann et al. "Liquid organic hydrogen carriers (LOHCs) techno-economic analysis of LOHCs in a defined process chain". In: *Energy & Environmental Science* 12.1 (2019), pp. 290–307. ISSN: 1754-5692.

[74] Norsk Oljemuseum. *Kollsnes processing plant*. June 2018. URL: https://www.norskolje.museum.no/en/kollsnes-processing-plant/.

[75] Jostein Pettersen. *Verbal communication, supervisor*. 2019.

[76] M. Pochet et al. "Ammonia-Hydrogen Blends in Homogeneous-Charge Compression-Ignition Engine". In: vol. 2017-. September. SAE International, 2017.

[77] Oil&Gas Portal. *LNG R&D for the Liquefaction and Regasification Processes*. Mar. 2016. URL: http://www.oil-gasportal.com/lng-rd-for-the-liquefaction-and-regasification-processes/.

[78] M. Reuß et al. "Seasonal storage and alternative carriers: A flexible hydrogen supply chain model". eng. In: *Applied Energy* 200 (2017), pp. 290–302. ISSN: 0306-2619.

[79] Royal Academy of Engineering. *Future Ship Powering Options Exploring alternative methods of ship propulsion*. July 2013. URL: http://www.imo.org/en/OurWork/Environment/PollutionPrevention/AirPollution/Documents/Air%5C%20pollution/Future_ship_powering_options_report.pdf.

[80] Lyndon Ruff and Alasdair Bruce. *Carbon Intensity API*. URL: https://carbonintensity.org.uk/.

[81] F. Schüth et al. "Ammonia as a possible element in an energy infrastructure: catalysts for ammonia decomposition". In: *Energy Environ. Sci.* 5 (4 2012), pp. 6278–6289. DOI: 10.1039/C2EE02865D. URL: http://dx.doi.org/10.1039/C2EE02865D.

[82] G. Shu et al. "A review of waste heat recovery on two-stroke IC engine aboard ships". In: *Renewable and Sustainable Energy Reviews* 19 (2013), pp. 385–401. ISSN: 13640321.

[83] Singh et al. *Prospects of Alternative Transportation Fuels*. eng. Singapore, 2018.

[84] SINTEF, Petter Nekså and Dabid Berstad. *Large Scale Hydrogen Production and Liquefaction*. URL: http://injapan.no/wp-content/uploads/2017/02/10-SINTEF-Large-Scale-H2-Production.pdf.

[85] Dylan Slater. *A hydrogen storage and logistics system is launched as part of Anglo American Platinum's investment*. URL: http://www.engineeringnews.co.za/article/a-hydrogen-storage-and-logistics-system-is-launched-as-part-of-anglo-american-platinums-investment-2016-05-13/rep_id:4136.

[86] Claire Stam. *Vella: Ammonia emissions is an 'enormous' problem that needs to be tackled*. 2018. URL: https://www.euractiv.com/section/agriculture-food/news/vella-ammonia-emissions-is-an-enormous-problem-that-needs-to-be-tackled/.

[87] Statkraft, Sintef, and Nordic Zoning. *Fornybar energiforsyning til Svalbard – Longyearbyen*. Nov. 2018. URL: https://www.statkraft.com/globalassets/explained/svalbard_rapport_0911_final.pdf.

[88] K. Stolzenburg and R. Mubbala. *Integrated Design for Demonstration of Efficient Liquefaction of Hydrogen (IDEALHY)*. Dec. 2013. URL: https://www.idealhy.eu/uploads/documents/IDEALHY_D3-16_Liquefaction_Report_web.pdf.

[89] Tadashi Tanuma. *Advances in steam turbines for modern power plants*. eng. Waltham, MA, 2017.

[90] The Advanced Hydrogen Energy Chain Association for Technology Development (AHEAD). *The Advanced Hydrogen Energy Chain Association for Technology Development (AHEAD)*. URL: https://www.ahead.or.jp/en/research.html.

[91] The Commonwealth Scientific and Industrial Research Organisation, CSIRO. *Delivering Clean Hydrogen Fuel from Ammonia Using Metal Membranes*. Nov. 2017. URL: https://nh3fuelassociation.org/2017/10/01/delivering-clean-hydrogen-fuel-from-ammonia-using-metal-membranes/.

[92] The International Association for Catalytic Control of Ship Emissions to Air (IACCSEA). *MARINE SCR*. 2016. URL: https://www.iaccsea.com/marine-scr/.

[93] The Linde Group. *Hydrogen Recovery by Pressure Swing Adsorption*. URL: https://www.linde-engineering.com/en/images/HA_H_1_1_e_09_150dpi_NB_tcm19-6130.pdf.

[94] The Maritime Executive. *Liquefied Hydrogen Bunker Vessel Designed*. URL: https://www.maritime-executive.com/article/liquefied-hydrogen-bunker-vessel-designed.

[95] The Maritime Executive. *World's First Hydrogen-Powered Cruise Ship Scheduled*. 2017. URL: https://www.maritime-executive.com/article/worlds-first-hydrogen-powered-cruise-ship-scheduled.

[96] THEMA and Multiconsult. *Alternativer for framtidig energiforsyning på Svalbard*. June 2018. URL: https://www.thema.no/wp-content/uploads/2018/08/THEMA-og-Multiconsult-Energiforsyningen-p%C3%A5-Svalbard_final-1-1.pdf.

[97] Peter Tubaas. *How hydrogen can revolutionize maritime transport – NCE Maritime CleanTech*. Jan. 2019. URL: https://maritimecleantech.no/2019/01/16/how-hydrogen-can-revolutionize-maritime-transport/.

[98] U.K. Government Office for Science. *Future of the Sea: Implications from Opening Arctic Sea Routes*. July 2017. URL: https://assets.publishing.service.gov.uk/government/uploads/system/uploads/attachment_data/file/634437/Future_of_the_sea_-_implications_from_opening_arctic_sea_routes_final.pdf.

[99] University of Oxford. *Analysis of Islanded Ammonia-based Energy Storage Systems*. Sept. 2015. URL: http://www2.eng.ox.ac.uk/systemseng/publications/Ammonia-based_ESS.pdf.

[100] U.S. Department of Eenrgy. *Combined Heat and Power Technology Fact Sheet Series*. 2016. URL: https://www.energy.gov/sites/prod/files/2016/09/f33/CHP-Steam%5C%20Turbine.pdf.

[101] A Valera-Medina et al. "Ammonia for power". eng. In: *Progress in Energy and Combustion Science* 69 (2018), pp. 63–102. ISSN: 0360-1285.

[102] Alan Welch et al. *Challenges in Developing Hydrogen Direct Injection Technology for Internal Combustion Engines*. eng. 2008. URL: https://saemobilus.sae.org/content/2008-01-2379.

[103] Winterthur Gas&Diesel (WinGD). *Low- and high-pressure dual-fuel Technology Evaluation Process; Case Studies for LNG Carriers and Merchant Vessel*. 2015. URL: https://www.wingd.com/en/documents/general/papers/dual-fuel-technology-selection-(d-stroedecke)/.

[104] Staff Writer. *Hydrogen import hub seen to further diversify fuel supply*. Jan. 2016. URL: https://asia.nikkei.com/Business/Hydrogen-import-hub-seen-to-further-diversify-fuel-supply.

[105] Christina Wulf and Petra Zapp. "Assessment of system variations for hydrogen transport by liquid organic hydrogen carriers". eng. In: *International Journal of Hydrogen Energy* 43.26 (2018), pp. 11884–11895. ISSN: 0360-3199.

[106] S.F. Yin et al. "A mini-review on ammonia decomposition catalysts for on-site generation of hydrogen for fuel cell applications". eng. In: *Applied Catalysis A, General* 277.1 (2004), pp. 1–9. ISSN: 0926-860X.

[107] Jin Zhong Zhang. *Hydrogen generation, storage, and utilization*. eng. 2014. ISBN: 1-5231-1082-1.

Appendix A

Simulations of Energy-Conversion Processes

In order to estimate technical input-parameters for the model, many of the energy-conversion steps in each transportation chain was simulated in Aspen HYSYS. Process flow diagrams for each of the energy-conversion processes simulated are given in this appendix.

A.1 LH_2

A.1.1 Regasification

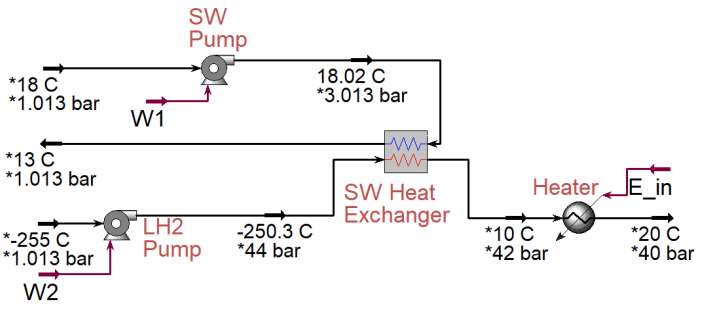

Figure A.1: Process flow diagram of the LH_2 sea water regasification process.

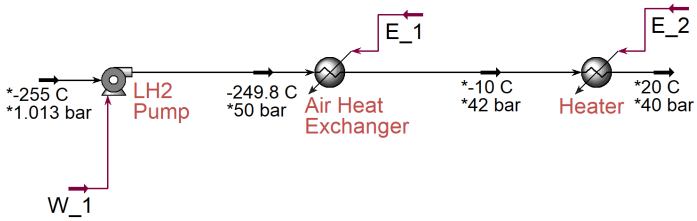

Figure A.2: Process flow diagram of the LH_2 air regasification process.

A.2 Ammonia

A.2.1 Ammonia Synthesis

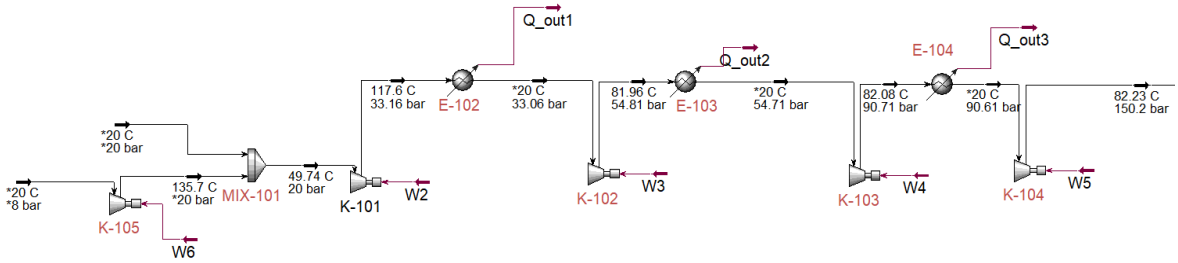

Figure A.3: Process flow diagram of the 4-stage compression of H_2/N_2 syngas w/ intercooling.

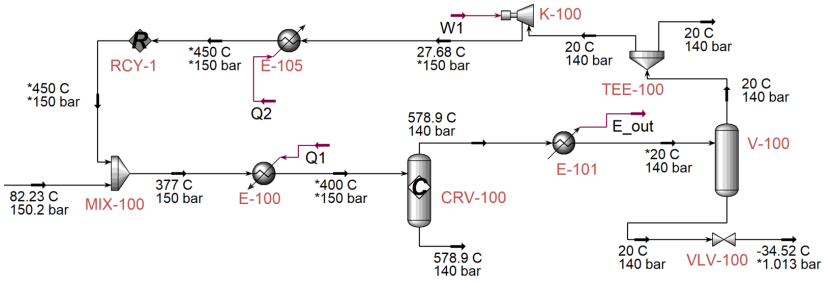

Figure A.4: Process flow diagram of the Haber-Bosch loop.

A.2.2 Ammonia Cracking

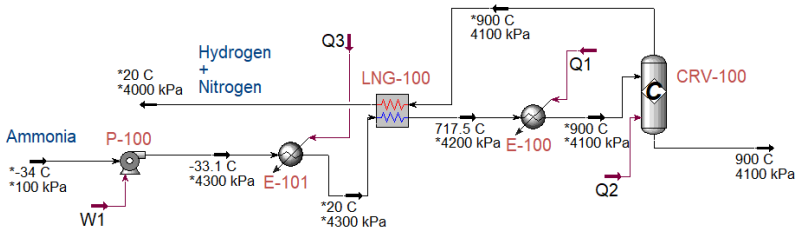

Figure A.5: Process flow diagram of NH_3 cracking.

A.2.3 Ammonia Refrigeration

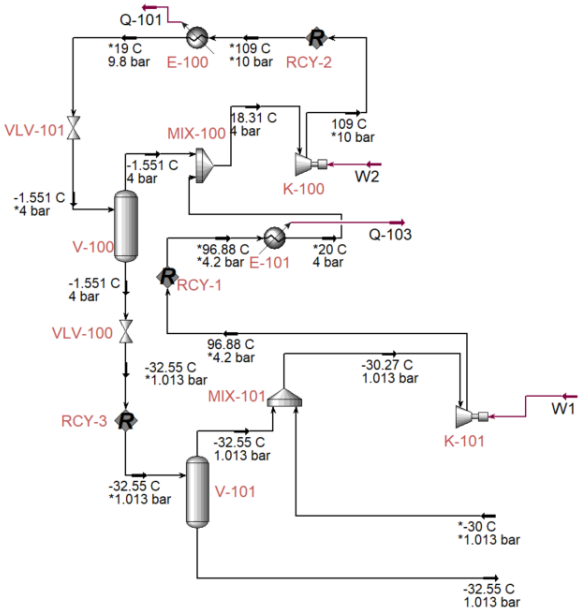

Figure A.6: Process flow diagram of NH_3 refrigeration. Courtesy of Jostein Pettersen[75].

A.3 LOHC

A.3.1 Hydrogenation

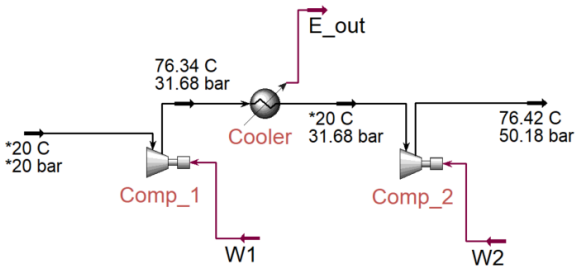

Figure A.7: Process flow diagram of compression of H_2 from 20 bar to 50 bar for hydrogenation of DBT.

A.3.2 Dehydrogenation

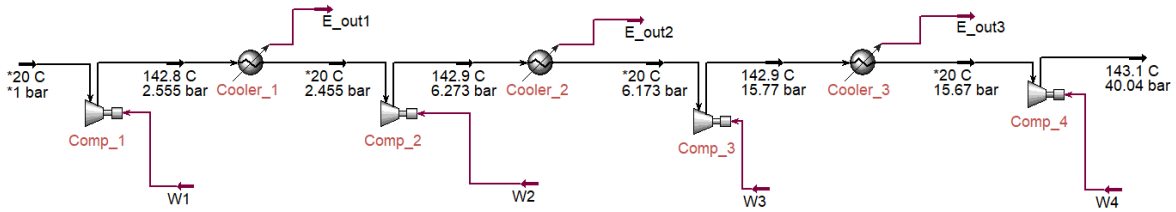

Figure A.8: Process flow diagram of 4-stage compression w/ intercooling of H_2 from 1 bar to 40 bar post-dehydrogenation.

Appendix B

Cargo-Vessel Power Consumption and Operational Profile

This appendix gives the basis on which the total energy-consumption of each vessel in the Japan and Svalbard scenario is calculated.

B.1 Vessel Power Requirement

Calculation of the energy usage during marine transportation of hydrogen with respect to the cases described in Chapter 3, necessitates determining the power-characteristics of each vessel. The power-characteristics of a vessel depends to a large degree on the size of ship. Real-life automatic identification system (AIS) data for a set of two different vessel-sizes were used to determine the power-characteristics of each ship. AIS-data was provided by DNV GL[6]. By using AIS-data, the speed and corresponding fuel consumption could be calculated. Thus, an exponential power-to-speed relationship could be deduced for each cargo-ship. The underlying assumption is that the power-speed relationship of each vessel is dictated by its size, and not its type of cargo i.e. LH_2, NH_3, or LOHC.

Assuming that each vessel has a Service Continuous Rating (SCR) at design cruising speed which is 85% of its Maximum Continuous Rating (MCR), the total thermal efficiency of the ship power-plant is determined as in Equation B.1. The effective delivered power by the ship machinery is then calculated by applying Equation B.2.

$$\eta_{overall} = \frac{W_{installed} \cdot SCR/MCR}{LHV_{fuel} \cdot \dot{m}_{fuel,service}} \tag{B.1}$$

$$W_{delivered} = \eta_{overall} \cdot LHV_{fuel} \cdot \dot{m}_{fuel,s} \tag{B.2}$$

$\eta_{overall}$ = Thermal efficiency of propulsion machinery.
SCR = Service Continuous Rating (MW).
MCR = Maximum Continuous Rating (MW).
LHV_{fuel} = Lower heating value of fuel (MJ/kg).
$\dot{m}_{fuel,service}$ = Mass flow of fuel at service speed (kg/s).
$\dot{m}_{fuel,s}$ = Mass flow of fuel at speed s (kg/s).
$W_{installed}$ = Total installed power on ship (MW).
$W_{delivered}$ = Total delivered power by ship machinery(MW).

An important assumption is that the cargo-vessel has a constant thermal efficiency for all speeds. The power characteristics shown in Figure B.1 are based on AIS-data for a set of 27 LNG tankers and 33 LPG tankers with cargo-capacities ≈160,000m^3 and ≈5,000m^3 respectively. The average design cruising speeds of the ships from the two data-sets is ≈19 knots (LNG tankers) and ≈14 (LPG tankers).

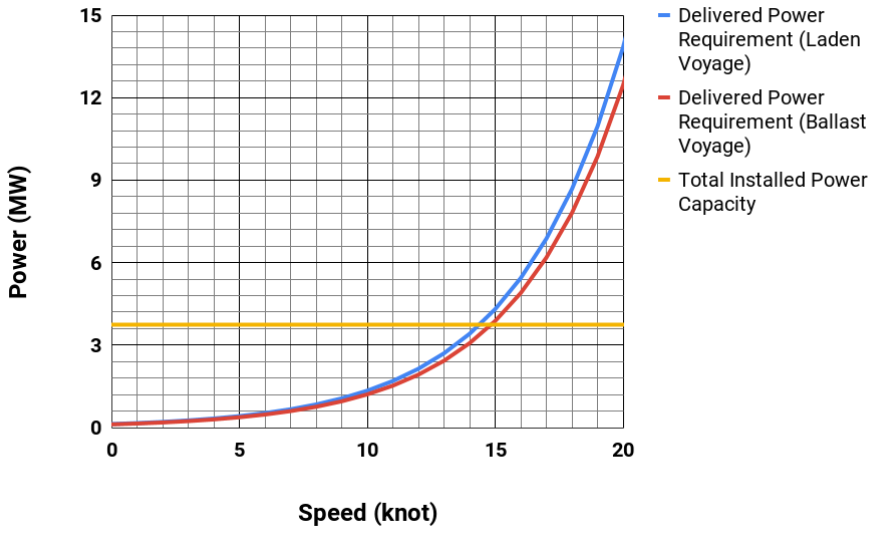

(a) Vessel with cargo-capacity 5,000m^3.

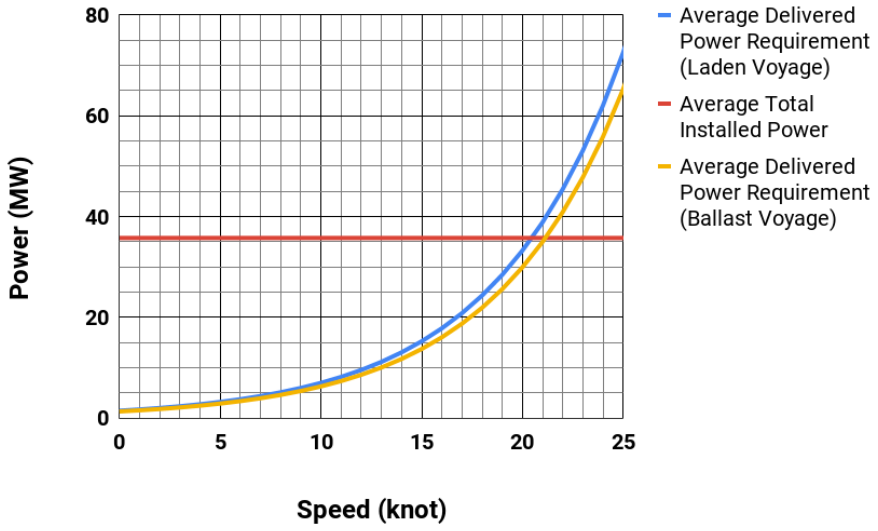

(b) Vessel with cargo-capacity 160,000m^3.

Figure B.1: Power-speed characteristics. During ballast voyage, it is assumed that each ship consumes 90% of the delivered power requirement with respect to laden voyage.

All the cargo-ships for which AIS-data was used were built in 2018. The total power requirement of the ship is given as the delivered power by the ship power plant - for both propulsion and auxiliary purposes. The useable mechanical power to sustain the ship's movement through the water will be less due to various losses in the shaftline and propulsor[9].

As shown in Figure B.1, the power plant of the vessel with cargo-capacity 5,000m^3 is dimensioned for lower speeds than the vessel with cargo-capacity 160,000m^3. Moreover, for a speed of 15 knot, the 160,000m^3 cargo-ship requires a delivered power of ≈15.2 MW, compared to 4.3 MW for the 5,000m^3 cargo-ship. Hence, despite carrying 32 times the amount of cargo, the larger cargo-ship only consumes ≈3.5 times the delivered engine power at a speed of 15 knots. This is to a large degree explained by the fact that by increasing the length overall (LOA) of a ship, reduces its wave-making resistance per unit length[70]. Consequently, the larger cargo-ship has an improportionately lower delivered power consumption compared to the smaller cargoship.

B.2 Operational Profiles

Depending on the route taken for hydrogen cargo delivery, vessels will operate with different operational profiles. Table B.1 summarises how vessel-size relates to each scenario described in Section 3.

Table B.1: Key information about shipping.

Scenario	**Ship Cargo Capacity (m^3)**	**Route**
Japan	160,000	Suez
Svalbard	5,000	Svalbard

Different operational profiles corresponding to each route is given below. The operational profile of each ship is based on the voyage-distance. Time spent loading, discharging and idle are based on typical values based on ship-size. These operational profiles are approximations and do not take into account factors such as maintenance work or dry-docking of ships. Delivered power consumption during loading and offloading is based on typical values applicable to LNG carriers[63].

B.2.1 Suez Route

The Suez route is the current preferred route for the vast majority of cargo ships transporting goods from Europe to East-Asia. The maximum speed-limit for tankers while traversing the Suez canal is approx. 7.5 knot [26]. Table B.2 shows the operational conditions for a ship operating on the Suez route (round-trip).

Table B.2: Operational mode and corresponding speed and ship power consumption for a round-trip.

Operational Mode	**Speed (knots)**	**Time (hrs)**	**Total Delivered Power (MW)**	
			Laden	Ballast
Cruising	18	1263	24.3	21.9
Suez Canal transit	7.5	27	4.4	3.9
Manoeuvring	5	134	3.2	2.9
In port (loading)	0	24	-	4
In port (discharging)	0	24	7.5	-
Idle	0	24	1.5	1.5
Total	-	1,455	-	-

Figure B.2 shows the time spent in each operational mode during a round-trip graphically.

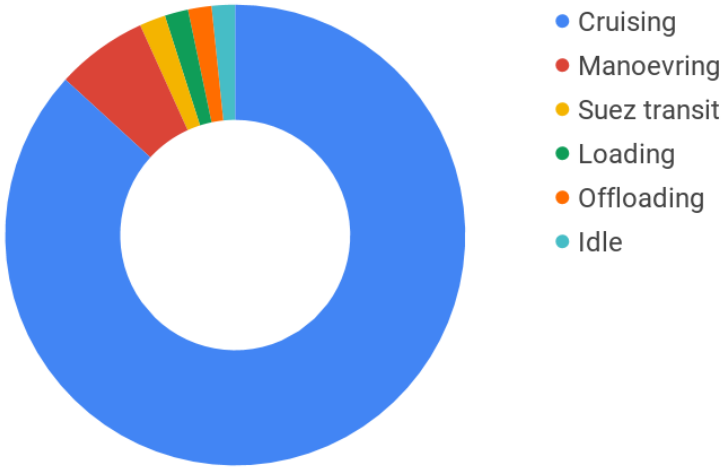

Figure B.2: Operational profile of vessel operating on the sea-route from Norway to Japan via the Suez canal.

B.2.2 Svalbard Route

The route to Svalbard from Kollsnes, Norway, is assumed to be navigable by ships without ice-breaking capabilities all-year round. Table B.3 shows the operational conditions for a ship operating on the route to Svalbard (round-trip).

Table B.3: Operational mode and corresponding speed and ship power consumption for a round-trip.

Operational Mode	**Speed (knots)**	**Time (hrs)**	**Total Delivered Power (MW)**	
			Laden	Ballast
Cruising	14	144	3.41	3.07
Manoeuvring	5	9	0.42	0.38
In port (loading)	0	4	-	0.50
In port (discharging)	0	4	0.3	-
Idle	0	24	0.06	0.06
Total	-	195	-	-

Figure B.3 shows the time spent in each operational mode during a round-trip graphically.

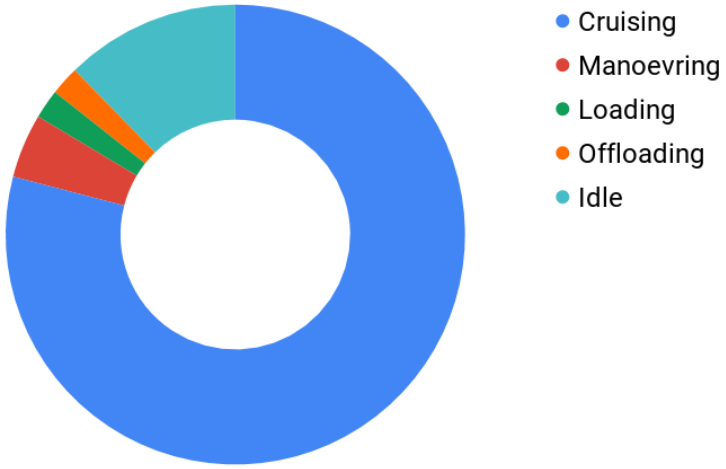

Figure B.3: Operational profile of vessel operating on the sea-route from Norway to Svalbard.

B.3 Modelling of Total Energy Consumption During Shipping

Estimating the total energy consumption of cargo-ships loaded with the hydrogen carriers LH_2, LNH_3, DBT-LOHC and TOL-LOHC is important for the totality of each hydrogen transportation chain. Based on operational profiles given in Appendix B.2, and the speed-power characteristics in Appendix B.1, Equation B.4 gives a generic function for the total energy consumption of each cargo vessel during a round-trip.

$$E_{ref}(v_{cr}) = \frac{\sum_{s=1}^{2}\left[\left(\eta_f \cdot BOG_{ther,s} - P_{cr,s}(v_{cr})\right)^{+} \cdot \frac{d_{cr}}{v_{cr}} + \sum_{o=1}^{n}\left(\eta_f \cdot BOG_{ther,s} - P_{o,s} \cdot t_o\right)^{+}\right] \cdot \eta_{ref}}{\eta_f^2} \tag{B.3}$$

$$E_{tot}(v_{cr}) = E_{ref} + \frac{\sum_{s=1}^{2}\left[P_{cr,s}(v_{cr}) \cdot \frac{d_{cr}}{v_{cr}} + \sum_{o=1}^{n} P_{o,s} \cdot t_o\right]}{\eta_{Final}} \tag{B.4}$$

$$e_{sec} = \frac{E_{tot}(v_{cr})}{m_{load}} \tag{B.5}$$

z^{+} denotes $max\{z, 0\}$.

E_{ref} = Round-trip fuel consumption of re-liquefaction plant, given on a LHV basis (MWh).
v_{cr} = Cruising speed (kn).
s = State of cargo-ship (Ballast or laden voyage).
$P_{cr,s}$ = Delivered power consumption of ship during cruising, at state s (MW).
d_{cr} = Cruising distance (nm).
o = Operational mode of ship.
$P_{o,s}$ = Delivered power consumption of ship during operation mode, o, in state, s (MW).
n = No. of operational modes.
t_o = Time spent in operation mode (single trip) (hrs).
η_{ref} = LHV efficiency of cargo refrigeration/re-liquefaction system.
η_f = Final energy conversion efficiency of ship propulsion system.
E_{tot} = Total round-trip fuel consumption of cargo-ship, given on a LHV basis (MWh).
e_{sec} = Total specific round-trip fuel consumption of cargo-ship, given on a LHV basis (MWh/kg loaded H_2).
m_{load} = Total loaded mass of hydrogen in cargo-vessel (kg).

The re-liquefaction efficiency, η_{ref}, depends on whether the BOG gas subject to re-liquefaction is NH_3-BOG or H_2-BOG. The assumed LHV efficiency of the NH_3-BOG re-liquefaction plant is based on the simple two-step refrigeration cycle shown in Appendix A.2.3, with a LHV efficiency of ≈4.7%. The H_2-BOG re-liquefaction plant is assumed to have an exergy efficiency of 35% (lower than the IDEALHY liquefaction process with an exergy efficiency of ≈ 45%) in bringing H_2-BOG from a temperature of -240°C to liquid state at -253°C. This corresponds to an LHV efficiency of 21.7%.

Appendix C

Waste Heat Recovery for Ship Propulsion

This appendix discusses the potential of using waste heat from different energy converters to provide energy for NH_3 cracking and LOHC dehydrogenation. All is written in the context of the different propulsion alternatives proposed in Section 7.2.

C.1 Heat Sources

Table C.1 gives typical values for the temperature of waste heat sources for different energy converters.

Table C.1: Temperature of waste heat sources from different energy converters. Based on information from [5], [67], [27], [4], [9], [66], [89], and [48].

Energy Converter	**Waste Heat Temperature(°C)**	**Share of Total Energy(%)**	**Heat Source**
SOFC	∼900	∼40	Cooling air
PEMFC	∼90	∼40	Cooling water
GT	∼600	∼60	Exhaust gas
H_2-ICE/NH_3-ICE[1]	∼400	∼25	Exhaust gas
ST	∼500	∼60	Exhaust gas (from boiler) and low-pressure steam

[1]H_2-ICEs and NH_3-ICEs are assumed to exhibit similar properties as current natural gas fuelled engines [48].

C.2 Heat-to-heat WHR

Heat-to-heat WHR processes are important for the application of LNH_3 and loaded LOHC as fuel onboard vessels. This stems from the fact that both LNH_3 and loaded LOHC undergoes endothermic

processes in order to release/produce H_2 gas. Table C.2 shows the heat demand for the endothermic processes of NH_3 cracking and LOHC dehydrogenation.

Table C.2: Heat requirement for endothermic processes.

Endothermic Process	**Temperature (°C)**	**Heat (kWh/kg H_2)**
Dehydrogenation (TOL/DBT-LOHC)	∼300	∼9.0
Complete NH_3 Cracking	∼900	∼4.2
Partial NH_3 Cracking (5% H_2)	n.a.	∼0.2

In Section 7.2, three propulsion alternatives pre-conditions the cracking of NH_3. In NH_3-SOFC, NH_3 is assumed to be completely cracked when entering the anode of the solid oxide fuel cell. For NH_3-GT, ammonia is assumed to be fully cracked before entering the gas turbine. Finally, in the NH_3-ICE system, partial cracking of NH_3 is assumed before entry to the combustion chamber. These assumptions should hold because:

- NH_3-SOFC: For 1 kg of H_2, the SOFC produce ∼ 13 kWh of heat at ∼ 900°C. This is more than suffcient to cover the 4.2 kWh/kg H_2 required by the cracking process. Excess heat could be used in a heat-to-power WHR system.
- NH_3-ICE: Figure 4.14 shows the equilibrium conversion of NH_3 into H_2 and N_2. Even though gas engines produce waste heat of relatively modest temperatures (∼400 °C), high temperature heat is not required for partial cracking. With reference to Section 5.1.2, only small percentages of H_2 (∼ 3% by mass) are required to keep an NH_3 engine running smoothly [30]. If one assumes that 5% hydrogen (by mass) is needed for the NH_3-ICE, a modest heat requirement of 0.2 kWh/kg H_2 is needed for cracking. This heat demand has little impact on the NH_3-ICE system's ability to produce electric power in a heat-to-power WHR system.
- NH_3-GT: Gas turbines produce waste heat in the order of magnitude ∼20kWh/kg H_2 at 600°C. This is sufficient to the heat demand of NH_3-cracking. Excess heat may also be used to produce power.
- NH_3-ST: Steam turbines apply NH_3 as fuel directly. Therefore there is no need for NH_3 cracking.

Although dehydrogenation requires heat at a lower temperature than NH_3 cracking, the magnitude is greater (9 kWh/kg H_2 vs 4.2 kWh/kg H_2). In Section 7.2, five propulsion systems using loaded LOHC as fuel are evaluated.

- LOHC-SOFC: For 1 kg of H_2, the SOFC should produce ∼ 13 kWh of heat at ∼ 900°C. This is more than suffcient to cover the ∼9 kWh/kg H_2 required by the dehydrogenation process. Excess heat could be used in a heat-to-power WHR system.
- LOHC-PEMFC: Even though the PEMFC produces a significant magnitude of heat, it is very low grade. It is therefore not suitable for providing thermal energy for dehydrogenation, and dehydrogenation must be achieved by the combustion of product H_2 gas.

- LOHC-ICE: A gas engine typically supplies waste heat at ∼400°C and in the order of magnitude ∼8 kWh/kg H_2. An additional heat source of ∼1 kWh/kg H_2 is needed to fulfill the heat demands of the dehydrogenation process. This may be achieved by the combustion of product H_2 gas.
- LOHC-GT: A gas turbine typically supplies waste heat at ∼600°C and in the order of magnitude ∼20 kWh/kg H_2. This is more than sufficient to cover heat demands for dehydrogenation. Excess heat may be used in a heat-to-power WHR system.
- LOHC-ST: A steam typically supplies waste heat at ∼500°C and in the order of magnitude ∼20 kWh/kg H_2. This is more than sufficient to cover heat demands for dehydrogenation. Excess heat may be used for steam re-heat.

Appendix D

Calculation of Final Energy Conversion Efficiencies for Propulsion Systems

This appendix gives details regarding the calculation of final energy conversion efficiency for each of the propulsion systems proposed in Section 7.2.

D.1 Auxiliary Power to Fuel Supply System

Depending on the propulsion system, the auxiliary power requirement of the fuel supply system could have an impact on the overall system efficiency. Each energy converter requires a certain inlet pressure, given in Table D.1.

Table D.1: Assumed inlet pressure of fuel for different energy converters.

Energy Converter	**Inlet Fuel Pressure (bar)**
SOFC	1
PEMFC	1
H_2-ICE/NH_3-ICE	5
GT	40
ST	1

In order to deliver fuel at a given pressure to each energy converter, the fuel supply system needs to compress/pressurise the fuel. This is achieved through a series of pumps and compressors. From an energy point of view, increasing the pressure of the fuel in liquid state is preferred to compression in gaseous state. However, due to the formation of boil-off gas in NH_3/LH_2 tankers, the fuel supply system needs to increase the pressure of the fuel in both liquid (when pumped from cargo tank) and

gaseous state. Table D.2 shows an estimated electricity consumption for fuel supply equipment in each propulsion alternative. Auxiliary power requirements was estimated using Aspen HYSYS.

Table D.2: Auxiliary power demand for fuel supply system. Estimated using HYSYS, with a pressure loss of 1 bar assumed for all piping systems.

Propulsion System Name	**Auxiliary Power (kWh/kg H_2)**	
	BOG Fuel	Liquid Fuel from Cargo
LH_2-SOFC	0.3	0.0
LH_2-PEMFC	0.3	0.0
LH_2-ICE	0.9	0.0
LH_2-GT	1.9	0.0
LH_2-ST	0.3	0.0
NH_3-SOFC	0.2	0.0
NH_3-ICE	0.5	0.0
NH_3-GT	1.1	0.0
NH_3-ST	0.2	0.0
LOHC-SOFC	-	0.3
LOHC-PEMFC	-	0.3
LOHC-ICE	-	0.9
LOHC-GT	-	1.9
LOHC-ST	-	0.3

Key Points

- When using NH_3-BOG or H_2-BOG as fuel, auxiliary power demand increases relative to using LNH_3 or LH_2 from cargo tanks. The reason for which is that pressurisation of liquid phase fuel is less energy-consuming than compression of gaseous fuel.
- It was found that negligible power is necessary for pressurising fuel in liquid state.
- NH_3 cracking may take place at a pressure of 40 bar. Performing the cracking process at a pressure of 40 bar is ideal because compression of NH_3 requires less energy (kWh/kg H_2) than compression of H_2 gas.
- Since dehydrogenation may only take place at a pressure of ∼1 bar, hydrogen gas needs to be compressed to its given energy converter inlet pressure for each propulsion alternative. This imposes an additional auxiliary fuel supply system power demand on LOHC tankers.

D.2 Final Energy Conversion Efficiency

Taking into account electricity consumption in the auxiliary fuel supply system and heat demand for endothermic reactions (dehydrogenation and cracking), Equation D.1 gives the conversion efficiency of each propulsion system. The conversion efficiency will be different depending on whether or not

the fuel is BOG or liquid, due to different requirements for auxiliary power. Up until this point, peak energy conversion efficiencies have been used. In order to account for variations of energy conversion efficiency with partial loads, each efficiency is reduced by 5%, by the imposition of η_{Adj} in Equation D.1.

Equation D.2 gives the final energy conversion efficiency, taking into account the relative contribution of both BOG and liquid fuel to the ship's total energy consumption.

$$\eta_{sys} = \left(\eta_{base} + \eta_{WHR} \cdot (1 - \frac{Q_{out}}{Q_{demand}})\right) \cdot \left(1 - \frac{W_{aux}}{LHV_{H_2}}\right) \cdot \left(1 - \frac{Q_{comb}}{LHV_{H_2}}\right) \cdot \eta_{adj} \tag{D.1}$$

$$\eta_{Final} = \eta_{sys} \cdot r_{BOG} \tag{D.2}$$

η_{sys} = Conversion efficiency of system.
η_{base} = Electrical/thermal efficiency of energy converter.
η_{WHR} = Potential increase in electrical/thermal efficiency of energy converter using heat-to-power WHR system.
Q_{out} = Waste heat used for either H_nLOHC dehydrogenation or NH_3 cracking(kWh/kg H_2).
Q_{demand} = Heat demand for endothermic process (H_nLOHC dehydrogenation or NH_3 cracking)(kWh/kg H_2).
W_{aux} = Electricity required for auxiliary fuel supply system(kWh/kg H_2).
LHV_{H_2} = Lower heating value of hydrogen(kWh/kg H_2).
Q_{comb} = Partial consumption of H_2 to produce thermal energy for endothermic processes(kWh/kg H_2).
η_{adj} = Adjustment factor for final combined energy conversion efficiency. $\eta_{Adj} = 0.95$.
r_{BOG} = Factor quantifying contribution of BOG to total energy consumption of ship.
η_{final} = Final energy conversion efficiency of propulsion system.

Equation D.1 is applied in Table D.3 in order to calculate the system conversion efficiency of each propulsion system.

Table D.3: System conversion efficiency, η_{sys}.

Propulsion System Name	η_{sys}	
	BOG Fuel	Liquid Phase Fuel
LH_2-SOFC	0.80	0.81
LH_2-PEMFC	0.56	0.57
LH_2-ICE	0.51	0.52
LH_2-GT	0.40	0.43
LH_2-ST	0.37	0.38
NH_3-SOFC	0.73	0.73
NH_3-ICE	0.51	0.55
NH_3-GT	0.38	0.39
NH_3-ST	0.38	0.4
LOHC-SOFC	-	0.68
LOHC-PEMFC	-	0.42
LOHC-ICE	-	0.46
LOHC-GT	-	0.36
LOHC-ST	-	0.32

Table D.4 gives the final energy conversion efficiency for each evaluated propulsion system.

Table D.4: Final energy conversion efficiency, η_{Final}.

Propulsion System Name	η_{Final}	
	Japan	Svalbard
LH_2-SOFC	0.80	0.80
LH_2-PEMFC	0.56	0.56
LH_2-ICE	0.51	0.51
LH_2-GT	0.41	0.41
LH_2-ST	0.38	0.38
NH_3-SOFC	0.73	0.73
NH_3-ICE	0.52	0.52
NH_3-GT	0.38	0.38
NH_3-ST	0.38	0.38
LOHC-SOFC	0.68	0.68
LOHC-PEMFC	0.42	0.42
LOHC-ICE	0.46	0.46
LOHC-GT	0.36	0.36
LOHC-ST	0.32	0.32

Table D.4 shows that there is a minimal difference in final energy conversion efficiency between the

Svalbard and Japan scenario. Consequently, the same efficiency is used irregardless of scenario.

Appendix E

Basis for GHG Grid Intensity

The basis for calculating the GHG intensity factors of the electric grids in Japan, the Norwegian mainland and Svalbard(Longyearbyen) is given in this appendix.

E.1 GHG Intensity by Fuel Type

Table E.1 shows GHG intensity factors for power-stations based on different fuel types.

Table E.1: GHG intensity factors for each fuel type[80].

Fuel type	**GHG Intensity (gCO_2/kWh_e)**
Biomass	120
Coal	937
Oil	935
Gas (Combined Cycle)	394
Gas (Open Cycle)	651
Nuclear	0
Hydro	0
Wind	0
Solar	0
Geothermal	0

E.2 Electricity Generation Mix

Table E.2 and E.3 shows the electricity generation mix of Japan and Norway respectively.

Table E.2: Japanese electricity generation mix (2015)[45].

Fuel type	**Share of total electricity generation mix (%)**
Coal	34.0
Oil	9.0
Gas (Combined Cycle)	39.2
Nuclear	0.9
Hydro	8.4
Wind	0.5
Solar	3.6
Geothermal	0.3
Biomass	4.1

Table E.3: Norwegian electricity generation mix (2017)[46].

Fuel type	**Share of total electricity generation mix (%)**
Coal	0.1
Oil	0.02
Gas (Combined Cycle)	1.8
Nuclear	0.0
Hydro	95.8
Wind	1.7
Solar	0.0
Geothermal	0.2
Biomass	0.3

The electricity generation mix in Svalbard (Longyearbyen) is assumed to be exclusively based on hydrogen.

E.3 Calculation of Grid GHG Intensity

Based on data from Table E.3, the GHG intensity factor for the Norwegian grid may be calculated as $\sim$10 gCO_2/kWh_e. However, Norway imported 7.4 TWh from EU countries in 2015[46], which is equivalent to $\sim$5% of Norway's annual electricity generation. The EU electricity grid had a GHG intensity factor of $\sim$300 gCO_2/kWh_e in 2016[29]. Since the EU grid GHG intensity is set to fall in the future, a 50% reduction is assumed relative to 2016. This brings the figure down to $\sim$150 gCO_2/kWh_e. Factoring in import of electricity generated in the EU into the Norwegian electricity mix, the GHG intensity of the Norwegian grid increases to approximately $\sim$17 gCO_2/kWh_e.

Based on data from Table E.2 and E.1, the grid GHG intensity factor may be calculated as ∼560 gCO_2/kWh_e in Japan. However, in order to reflect the fact that the emissions tied to power-generation in Japan is likely to fall in the near future, a reduction of 50% (relative to 2015) is assumed.

The GHG grid intensity in Svalbard is zero, assuming that electricity generation is hydrogen-based.

Table E.4 gives the assumed grid GHG intensity factor for electricity grids in Norway (mainland), Svalbard and Japan.

Table E.4: GHG grid intensity.

Place	**GHG Intensity (gCO_2/kWh_e)**
Norway(mainland)	17
Svalbard	0
Japan	280

Appendix F

Generation of Boil-off Gas from Liquefied Gases

Due to ambient heat transfers, liquefied gases generate boil-off gas (BOG) during storage. Since LH_2 and LNH_3 are liquefied gas at -253.0°C and -33.3°C respectively, BOG is inevitably generated inside the storage tank. The BOG phenomenon has been studied extensively in order to facilitate the global LNG trade. It is therefore natural to compare BOG properties of LH_2 and LNH_3 with that of methane, as shown in Table F.1. A way of handling BOG must be deviced in order to keep the vapour pressure inside the tank within safe limits.

Table F.1: Comparison of physical properties of hydrogen, ammonia and methane.

Physical Property	**NH_3**	**H_2**	**Methane**	**Unit**
Boiling temperature	-33.3	-252.9	-161.6	°C
Liquid density (at ambient pressure)	679.8	70.8	422.5	kg/m^3
Gas density	0.71	0.084	0.668	kg/m^3
Heat of vapourisation	1.37	0.45	0.51	MJ/kg
Volumetric heat of vapourisation	932.1	31.77	215.64	MJ/m^3

LNH_3, LH_2 and LNG (methane), have significantly different BOG properties as shown in Table F.1. LH_2 is by far the liquefied gas for which the required heat of vapourisation is lowest. This implies that LH_2 is more easily evaporated by ambient heat transfers than LNH_3 and LNG. Moreover, on a volumetric basis; for the same volume of liquefied gas, LH_2 requires only 1/7th the amount heat for evaporation, compared to LNG. This has large implications for the boil-off-rate (BOR) of each liquefied gas during storage. LNH_3 is less easily evaporated as a liquid gas, requiring more heat on both a mass and volumetric basis than LNG and LH_2.

Sloshing is defined as the movement of liquid inside a container which is also typically undergoing motion, and is commonplace inside the cargo tank of a ship carrying liquids. Since sloshing leads

to friction-induced heat inside the tank, it leads to an increased rate of formation of BOG inside the ship's cargo tank. Consequently, the BOR of liquefied gases inside ship cargo tanks, is typically greater compared to inside on-shore storage tanks.

Table F.2 shows the assumed BOR for both on-shore storage tanks and ship cargo tanks for both LNH_3 and LH_2.

Table F.2: Boil-off rates for LNH_3 and LH_2. BOR of LNH_3 is based on [71].

Liquefied Gas	**Boil-off Rate (% of tank volume/day)**	
	On-shore	Cargo-ship (laden/ballast)
LNH_3	0.04	0.08/0.0045
LH_2	0.1	0.30/0.1700

The characteristic relationship between laden and ballast voyage BORs for typical LNG tankers is that the BOR during ballast voyage is usually ≈55% of that during the laden voyage[63]. The same relationship is adopted for the LNH_3 tanker and the LH_2 tanker.

It is standard practice in the LNG shipping industry to leave behind a relatively small amount of cargo in the cargo-tanks for the ballast voyage (return journey). This small amount of cargo is called heel, and usually amounts to approximately 5% of the total cargo capacity of the ship [63]. The same practice is assumed to be the case for LH_2 and NH_3 shipping in this thesis.

Appendix G

CAPEX Data for Cargo-Vessels

Table G.1: CAPEX assumptions propulsion systems onboard ships. Unless otherwise stated, power units refer to the installed power of the vessel.

Item	**Unit**	**Cost**	**Source**
Energy Converters			
H_2-ICE/NH_3-ICE (inc. generator)	NOK/kW	3500	Own assumption[8]
Gas Turbine (CC inc. generator and SCR)	NOK/kW	6300	[28]
SOFC	NOK/kW	14000[1]	[47]
PEMFC	NOK/kW	5600[2]	[47]
Steam Turbine (w/ re-heat inc. generator)	NOK/kW	4500	[100]
Electric motor	NOK/kW	800	[15]
Auxiliary Equipment			
Fuel handling system (LH_2 tanker)	NOK/kW	1600	Own assumption[10]
Fuel handling system (NH_3 tanker)	NOK/kW	400	Own assumption[9]
SCR	NOK/kW	400	[92]
Heat-to-power WHR (160,000 m^3 Cargo-ship)	MNOK	35	[33]
Heat-to-power WHR (5,000 m^3 Cargo-ship)	MNOK	10	[33]
Dehydrogenation Unit (160,000 m^3 Cargo-ship)	MNOK	120	Own assumption[3]
Dehydrogenation Unit (5,000 m^3 Cargo-ship)	MNOK	20	Own assumption[4]
NH_3 Cracker (160,000 m^3 Cargo-ship)	MNOK	80	Own assumption[3]
NH_3 Cracker (5,000 m^3 Cargo-ship)	MNOK	10	Own assumption[4]
Inverter	NOK/kW	1000	[11]
LH_2 Re-liquefaction System (160,000m^3 tanker)	MNOK	370	Own assumption[5]
LH_2 Re-liquefaction System (5,000m^3 tanker)	MNOK	10	Own assumption[6]
NH_3 Re-liquefaction System (160,000m^3 tanker)	MNOK	50	Own assumption[7]
NH_3 Re-liquefaction System (5,000m^3 tanker)	MNOK	1	Own assumption[7]

[1]Based on price-target in the period 2025-2035 by IEA[47]. Lifetime:80,000 hours.

[2]Based on price-target in the period 2025-2035 by IEA[47]. Lifetime:50,000 hours.
[3]Based on CAPEX for land-based unit with capacity of 0.4 kg H_2/s (48 MW by LHV). Final cost is multiplied by two to reflect small-scale.
[4]Based on CAPEX for land-based unit with capacity of 0.08 kg H_2/s (8 MW by LHV). Final cost is multiplied by 2 to reflect small-scale.
[5]Based on forecasted low-efficiency ((12 kWh_e/kg H_2)) liquefaction plant CAPEX by US DoE [72]. Assumed liquefaction capacity of 0.26 kg H_2/s which is sufficient for complete re-liquefaction of excess BOG.
[6]Based on forecasted low-efficiency ((12 kWh_e/kg H_2)) liquefaction plant CAPEX by US DoE [72]. Assumed liquefaction capacity of 0.009 kg H_2/s which is sufficient for complete re-liquefaction of excess BOG.
[7]Based on the assumption that a two-step LNH_3 re-liquefaction plant has a CAPEX of 0.1 MNOK/kW [75], where the given power is the power consumption of the liquefaction process.
[8]H_2-ICE/NH_3-ICE are assumed to have comparable prices with conventional reciprocating diesel engine-generator plants[28]. The given price includes the addition of a generator for electricity-generation.
[9]Price reduction of 75% relative to a low-pressure fuel-handling system of an LNG carrier[103].
[10]Based on price of a low-pressure fuel-handling system of an LNG carrier[103].

The CAPEX of conventional propulsion machinery (which was deducted from the cost in Table 7.8) is based on data shown in Table G.2.

Table G.2: CAPEX assumptions for conventional propulsion systems for each type of cargo-ship. Data is based on [103].

Type of Cargo-ship	**Cost (NOK/kW)**
LH_2 Tanker	4600
NH_3 Tanker LOHC Tanker	2700

Appendix H

CAPEX Data for Land-Based Processing Units

CAPEX data for land-based facilities in each transportation chain are given in Table H.1. In addition, assumed costs for the purchase of LOHC carrier materials (toluene and dibenzyltoluene) are given in Table H.2.

Table H.1: CAPEX assumptions for transport infrastructure of each hydrogen carrier.

Item	**Capacity**	**Cost (MNOK)**	**Source**
LH_2 Transportation Chain			
LH_2 Liquefaction Plant	50 tpd	945	[88]
LH_2 Regasification Plant	1,220 tpd	1,733	[35]
LH_2 Storage Unit[2]	1 ton	0.315	[72]
NH_3 Transportation Chain			
Air Separation Unit	400 tpd NH_3	430	[10]
NH_3 Storage Unit	276 000 tons NH_3	2,331	[35]
NH_3 Synthesis Unit	4,600 tpd NH_3	5,208	[35]
NH_3 Cracker Unit	9,200 tpd NH_3	5,555	[35]
PSA Unit	313,000 Nm^3/h H_2	924	[35]
LOHC Transportation Chain[3]			
LOHC Storage Unit	1000 m^3	1.5	[44]
LOHC Hydrogenation Unit	300 tpd H_2	360	[78]
LOHC Dehydrogenation Unit	300 tpd H_2	270	[78]
H_2 Compression Unit[1]	3.5 MW_e	350	[75]
PSA Unit	313,000 Nm^3/h H_2	924	[35]
General			
Port Facilities	80,000 m^3 Ship	1050	[35]

[1]Based on cost and capacity of 6-step CO_2 compressor with intercooling.

[2]Based on characteristic prices for LNG storage tanks, with the assumption that LH_2 tanks are 50% more expensive than LNG tanks of similar volume capacities[72].

[3]All capital costs the TOL-LOHC and DBT-LOHC transportation chains are assumed to be at a similar level.

Table H.2: Assumed cost of LOHC materials. Based on current prices [73].

Material	**Cost (NOK/kg)**
Toluene (TOL)	7.2
Dibenzyltoluene (DBT)	36

Øyvind Sekkesæter

NTNU
Norwegian University of
Science and Technology